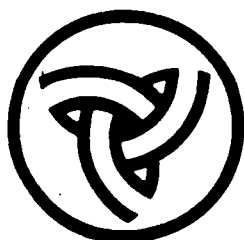


# **Evaluating Pavement Design Features - Five Year Performance Evaluation of FA 401 and FA 409**

**Physical Research Report No. 112  
February 1993**



**Illinois Department of Transportation**  
Bureau of Materials and Physical Research

EVALUATING PAVEMENT DESIGN FEATURES -  
FIVE YEAR PERFORMANCE EVALUATION OF  
FA 401 AND FA 409

BY

CHRISTINE M. REED, P.E.  
AMY M. SCHUTZBACH, P.E.

ILLINOIS DEPARTMENT OF TRANSPORTATION  
DIVISION OF HIGHWAYS  
BUREAU OF MATERIALS AND PHYSICAL RESEARCH

FEBRUARY 1993

1. Report No. FHWA /IL/PR-112		2. Government Accession No.		3. Recipient's Catalog No.	
4. Title and Subtitle Evaluating Pavement Design Features-Five Year Performance Evaluation of FA 401 and FA 409				5. Report Date February 1993	
				6. Performing Organization Code	
7. Author(s) Christine M. Reed & Amy M. Schutzbach				8. Performing Organization Report No. Physical Research No. 112	
9. Performing Organization Name and Address Illinois Department of Transportation Bureau of Materials and Physical Research 126 East Ash Street Springfield, Illinois 62704-4766				10. Work Unit No.	
				11. Contract or Grant No.	
12. Sponsoring Agency Name and Address Illinois Department of Transportation Bureau of Materials and Physical Research 126 East Ash Street Springfield, Illinois 62704-4766				13. Type of Report and Period Covered Final Report May 1986 - February 1993	
				14. Sponsoring Agency Code	
15. Supplementary Notes IL 85-07 A through F: Evaluating Pavement Design Features. This study conducted in cooperation with the U.S. Department of Transportation, Federal Highway Administration					
16. Abstract <p>In the summer of 1986, the Illinois Department of Transportation began the construction of four demonstration projects which focused on evaluating proposed mechanistically-based asphalt concrete (AC) and portland cement concrete (PCC) pavement design procedures and determining the effects of pavement design variables on pavement performance. The demonstration projects were proposed in an experimental features work plan entitled "Evaluating Pavement Design Procedures". This report details the construction and performance monitoring of the demonstration projects.</p> <p>The construction sections of this report describes the pavement locations, cross sections, instrumentation, and construction details. Of particular interest is the subsection on instrumentation, which details the types of monitoring equipment and gauges installed in the demonstration projects.</p> <p>The performance monitoring section of this report describes in detail the extensive monitoring performed to date on the demonstration projects. The performance monitoring included condition surveys, structural response monitoring, moisture monitoring, surface response monitoring, and maintenance. The condition surveys included Condition Rating Survey reviews, distress surveys, patching efforts, moisture damage study results, and rutting surveys. The structural response monitoring included full-depth AC pavement deflection testing, and PCC pavement deflection testing, strain gauge measurements, and hinge joint movements. The moisture monitoring included underdrain outflow, subgrade moisture, and frost depth data. The surface response monitoring included ride quality and friction testing. In general, most of these performance indicators showed the demonstration projects were performing as the proposed mechanistically-based design procedures had predicted.</p>					
17. Key Words full-depth asphalt concrete pavement, hinge-jointed pavement, continuously reinforced concrete pavement, strain gauges, underdrain outflows, pavement performance monitoring			18. Distribution Statement No restrictions. This document is available to the public through the National Technical Information Service, Springfield, Virginia 22161.		
19. Security Classif. (of this report) Unclassified		20. Security Classif. (of this page) Unclassified		21. No. of Pages 197	22. Price

## TABLE OF CONTENTS

CONTENTS	PAGE
EXECUTIVE SUMMARY	i
INTRODUCTION	1
OBJECTIVES	1
HISTORICAL PERSPECTIVE	1
CONSTRUCTION	2
Location	2
Cross Sections	3
Instrumentation	4
Construction Details	5
PERFORMANCE MONITORING	8
Condition Surveys	8
Structural Response Monitoring	12
Moisture Monitoring	28
Surface Response Monitoring	34
Maintenance	34
COSTS	35
ANALYSIS	35
Objective 1	35
Objective 2	40
Objectives 3 and 4	43
FUTURE MONITORING	43
SUMMARY	43
Full-Depth AC Pavement	45
PCC Pavement	46
REFERENCES	48
DISCLAIMER	50
ACKNOWLEDGEMENTS	50
TABLES	
FIGURES	

## List of Tables

Table 1A:	Design ESALs for Projects 1 and 2
Table 1B:	Design ESALs for Projects 3 and 4
Table 2:	Asphalt Concrete Surface Mixture Design Data for Project 1
Table 3:	Asphalt Concrete Binder Mixture Design Data for Project 1
Table 4:	Asphalt Concrete Surface Mixture Design Data for Project 3
Table 5:	Asphalt Concrete Binder Mixture Design Data for Project 3
Table 6:	Design vs. Average Production Values for Asphalt Concrete for Project 1
Table 7:	Design vs. Average Production Values for Asphalt Concrete for Project 3 (Clinton County)
Table 8:	Design vs. Average Production Values for Asphalt Concrete for Project 3 (St. Clair County)
Table 9:	PCC Mix Design for Project 2
Table 10:	PCC Mix Design for Project 4
Table 11:	PCC Daily Material Property Tests for Project 2
Table 12:	CRCP Daily Material Property Tests for Project 4
Table 13:	Jointed PCC Daily Material Property Tests for Project 4
Table 14A:	1990 Distress Summary for Project 1
Table 14B:	1992 Distress Summary for Project 1
Table 15A:	1990 Distress Summary for Project 3
Table 15B:	1992 Distress Summary for Project 3
Table 16A:	1990 Distress Summary for Project 2
Table 16B:	1992 Distress Summary for Project 2
Table 17A:	1990 Distress Summary for Project 4
Table 17B:	1992 Distress Summary for Project 4
Table 18:	Summary of Full-Depth Repaired Areas on Project 3
Table 19:	1989 Core Data Summary for Projects 1 and 3
Table 20:	Hand-Measured Rut Depth Data History for Project 1
Table 21A:	1988 Hand-Measured Rut Depth Data for Project 3
Table 21B:	1989 Hand-Measured Rut Depth Data for Project 3
Table 21C:	1990 Hand-Measured Rut Depth Data for Project 3
Table 21D:	1992 Hand-Measured Rut Depth Data for Project 3
Table 22A:	Summary of Road Profiler Rut Depths for Project 1
Table 22B:	Summary of Road Profiler Rut Depths for Project 3
Table 23:	FWD Statistics for Deflections for Project 1
Table 24A:	FWD Statistics for Deflections for 5/87 for Project 3
Table 24B:	FWD Statistics for Deflections for 9/87 for Project 3
Table 24C:	FWD Statistics for Deflections for 5/88 for Project 3
Table 24D:	FWD Statistics for Deflections for 5/89 for Project 3
Table 24E:	FWD Statistics for Deflections for 10/89 for Project 3
Table 24F:	FWD Statistics for Deflections for 8/90 for Project 3
Table 24G:	FWD Statistics for Deflections for 8/91 for Project 3
Table 25:	FWD Note Summary
Table 26:	Comparison of Core Split Tensile Strengths from Project 3
Table 27A:	FWD Statistics for Hinge and Dowel Joint Deflections and Areas for Project 2
Table 27B:	FWD Statistics for Hinge and Dowel Joint Load Transfer Efficiency (LTE) for Project 2
Table 28A:	FWD Statistics for Hinge and Dowel Joint Deflections and Areas for Project 4

## List of Tables (cont.)

- Table 28B: FWD Statistics for Hinge and Dowel Joint Load Transfer Efficiency (LTE) for Project 4
- Table 28C: FWD Statistics for Pavement/Shoulder Joint Load Transfer Efficiency (LTE) for Project 4
- Table 29: Underdrain Outflow Data for Projects 3 and 4
- Table 30: Moisture Gauge Locations for Projects 3 and 4
- Table 31: Frost Measurements from Winter Months 1988-1990 for Project 3
- Table 32: Ride Quality Data (Roadometer) for Projects 1, 2, 3, and 4
- Table 33A: Ride Quality Data (Road Profiler) for Project 1
- Table 33B: Ride Quality Data (Road Profiler) for Project 2
- Table 33C: Ride Quality Data (Road Profiler) for Project 3
- Table 33D: Ride Quality Data (Road Profiler) for Project 4
- Table 34: Summary of Treaded Tire Friction Data
- Table 35: Summary of Smooth Tire Friction Data
- Table 36: Final Construction Costs
- Table 37: Effect of Underdrains on  $E_{rj}$
- Table 38: Project 3 Rut Depth Comparison by AC Type (Road Profiler Measurements)
- Table 39: JRCF Crack Survey Summary for Project 4
- Table 40: JPCF Crack Survey Summary for Project 4

## List of Figures

- Figure 1: Projects 1, 2, 3 and 4 Location Map
- Figure 2: Project 1 Test Section Layout
- Figure 3: Hinge-Jointed Panel Design
- Figure 4: Project 2 Test Section Layout
- Figure 5: Tied PCC Shoulder Design Detail
- Figure 6: Project 3 Test Section Layout
- Figure 7: Project 4 Test Section Layout
- Figure 8: Project 4 Instrumentation Site Locations
- Figure 9: Project 3 Instrumentation Site Locations
- Figure 10: Hinge-Jointed Panel Crack Locations on Project 4
- Figure 11: Deflection Basin Area
- Figure 12: Project 3 Pavement Temperature Profile
- Figure 13: Project 3 FWD Data from May 1987
- Figure 14: Project 3 FWD Data from September 1987
- Figure 15: Project 3 FWD Data from May 1988
- Figure 16: Project 3 FWD Data from May 1989
- Figure 17: Project 3 FWD Data from October 1989
- Figure 18: Project 3 FWD Data from August 1990
- Figure 19: Project 3 FWD Data from August 1991
- Figure 20: Design  $E_{ac}$  vs. Design Pavement Temperature
- Figure 21: Backcalculated  $E_{ac}$  at 82° F vs. Pavement Age
- Figure 22: Project 2 Strain Gauge Location Diagrams
- Figure 23: Project 4 Strain Gauge Location Diagrams
- Figure 24A: Sample Static Strain Gauge Data for Longitudinal Edge Gauges
- Figure 24B: Sample Static Strain Gauge Data for Transverse Edge Gauges
- Figure 25A: Dynamic Strain Gauge Data Test Speed Comparison - Mid-Slab Longitudinal Gauges
- Figure 25B: Dynamic Strain Gauge Data Test Speed Comparison - Transverse Gauges
- Figure 26A: Typical 1986 Strain Gauge Dynamic Test Data
- Figure 26B: Typical 1989 Strain Gauge Dynamic Test Data
- Figure 27A: Static vs. Dynamic Data Comparison for Longitudinal Gauges
- Figure 27B: Static vs. Dynamic Data Comparison for Transverse Gauges
- Figure 28: Gauge Depth Effects on Theoretical Strain Values
- Figure 29: Increased  $E_{pcc}$  and  $k$  Effects on Theoretical Strain Values
- Figure 30: Load Transfer Effects on Theoretical Strain Values
- Figure 31: Bonding Effects on Theoretical Strain Values
- Figure 32A: Strain Data for Mid-slab Gauges in 10-inch Jointed PCC
- Figure 32B: Strain Data for Mid-slab Gauges in 9.5-inch Jointed PCC
- Figure 32C: Strain Data for Mid-slab Gauges in 7.5-inch Jointed PCC
- Figure 33A: Strain Data for Quarter-slab Gauges in 10-inch Jointed PCC
- Figure 33B: Strain Data for Quarter-slab Gauges in 9.5-inch Jointed PCC
- Figure 33C: Strain Data for Quarter-slab Gauges in 7.5-inch Jointed PCC
- Figure 34A: Strain Data for Corner Gauges in 10-inch Jointed PCC
- Figure 34B: Strain Data for Corner Gauges in 7.5-inch Jointed PCC
- Figure 34C: Strain Data for Transverse Edge Gauges in 10-inch Jointed PCC
- Figure 34D: Strain Data for Transverse Edge Gauges in 10-inch Jointed PCC
- Figure 35: Effect of CRCP Crack Spacing on Longitudinal Strain Gauges
- Figure 36: Effect of CRCP Crack Spacing on Transverse Strain Gauges
- Figure 37A: Strain Data for Longitudinal Edge Gauges in 7-inch CRCP
- Figure 37B: Strain Data for Longitudinal Edge Gauges in 9-inch CRCP
- Figure 37C: Strain Data for Longitudinal Edge Gauges in 7-inch CRCP

Figure 38A: Strain Data for Transverse Edge Gauges in 7-inch CRCP  
Figure 38B: Strain Data for Transverse Edge Gauges in 9-inch CRCP  
Figure 38C: Strain Data for Transverse Edge Gauges in 9-inch CRCP  
Figure 39A: Dowel Joint Opening vs. Air Temperature  
Figure 39B: Hinge Joint Opening vs. Air Temperature  
Figure 40A: Dowel Joint Opening vs. Pavement Mid-Depth Temperature  
Figure 40B: Hinge Joint Opening vs. Pavement Mid-Depth Temperature  
Figure 41: Graphs of Subdrainage Outflow for 20-foot Jointed PCC Test Sections - July 1988  
Figure 42: Graphs of Subdrainage Outflow for 20-foot Jointed PCC Test Sections - March 1989  
Figure 43: Graphs of Subdrainage Outflow for 40-foot Jointed PCC Test Sections  
Figure 44: Graphs of Subdrainage Outflow for 8-inch CRCP Test Sections  
Figure 45: Graphs of Subdrainage Outflow for Full-Depth AC Test Sections  
Figure 46: Moisture Access Tube Installation Diagram  
Figure 47A: Centerline Subgrade Moisture Data for Jointed PCC with Underdrains  
Figure 47B: Outer Wheelpath Subgrade Moisture Data for Jointed PCC with Underdrains  
Figure 47C: Edge Subgrade Moisture Data for Jointed PCC with Underdrains  
Figure 47D: Shoulder Subgrade Moisture Data for Jointed PCC with Underdrains  
Figure 48A: Centerline Subgrade Moisture Data for Jointed PCC without Underdrains  
Figure 48B: Outer Wheelpath Subgrade Moisture Data for Jointed PCC without Underdrains  
Figure 48C: Edge Subgrade Moisture Data for Jointed PCC without Underdrains  
Figure 48D: Shoulder Subgrade Moisture Data for Jointed PCC without Underdrains  
Figure 49A: Inner Wheelpath Subgrade Moisture Data for Full-Depth AC with Underdrains  
Figure 49B: Outer Wheelpath Subgrade Moisture Data for Full-Depth AC with Underdrains  
Figure 49C: Shoulder Subgrade Moisture Data for Full-Depth AC with Underdrains  
Figure 50A: Inner Wheelpath Subgrade Moisture Data for Full-Depth AC without Underdrains  
Figure 50B: Outer Wheelpath Subgrade Moisture Data for Full-Depth AC without Underdrains  
Figure 50C: Shoulder Subgrade Moisture Data for Full-Depth AC without Underdrains  
Figure 51: Subgrade Moisture Data Comparison of Unsealed Jointed PCC with and without Underdrains  
Figure 52: Subgrade Moisture Data Comparison of Sealed Jointed PCC with and without Underdrains  
Figure 53: Subgrade Moisture Data Comparison for 12.5-inch Full-Depth AC with and without Underdrains  
Figure 54: Subgrade Moisture Data Comparison for 9.5-inch Full-Depth AC with and without Underdrains  
Figure 55: Effect of Sealant on Subgrade Moisture for Jointed PCC Without Underdrains  
Figure 56: Effect of Sealant on Subgrade Moisture for Jointed PCC With Underdrains  
Figure 57: Frost Gauge Installation Diagram



## EXECUTIVE SUMMARY

The American Association of State and Highway Officials (AASHO) Road Test was conducted in 1959 and 1960 in Ottawa, Illinois. The main objective of the Road Test was to relate pavement performance to structural design and traffic loadings. One of the principle results of the road test was an empirically-based pavement design procedure. For several years, the Illinois Department of Transportation (IDOT) based its pavement design on the concepts developed at the Road Test. By the early 1980's, however, several inherent limitations to this design process became apparent, and research efforts were initiated to review potential pavement design options. The results of this research yielded proposed mechanistically-based design procedures.

In the summer of 1986, IDOT began the construction of four demonstration projects, which focused on evaluating the proposed mechanistically-based pavement design procedures and determining the effects of pavement design variables on pavement performance. The demonstration projects were proposed in an experimental features work plan entitled "Evaluating Pavement Design Procedures". This report details the construction and performance monitoring of the demonstration projects, in accordance with the experimental features work plan.

The construction section of this report describes the pavement location, cross section, instrumentation, and construction details. Of particular interest is the subsection on instrumentation, which details the types of monitoring equipment and gauges installed in the demonstration projects.

The performance monitoring section of this report describes in detail the extensive monitoring performed to date on the demonstration projects. The performance monitoring included condition surveys, structural response monitoring, moisture monitoring, surface response monitoring, and maintenance. The condition surveys included Condition Rating Survey reviews, distress surveys, patching efforts, a moisture damage study, and rutting surveys. The structural response monitoring included full-depth asphalt concrete pavement deflection testing, and portland cement concrete pavement deflection testing, strain gauge measurements, and hinge joint movements. The moisture monitoring included underdrain outflow, subgrade moisture, and frost depth data. The surface response monitoring included ride quality and friction testing. In general, most of these performance indicators showed the demonstration projects were performing as the proposed mechanistically-based design procedures had predicted.

The performance data, in conjunction with maintenance activity data, will provide valuable information on the performance of the pavements and the validity of the mechanistically-based design procedures.

## INTRODUCTION

In the summer of 1986, the Illinois Department of Transportation (IDOT) began the construction of four demonstration projects. The focus of the demonstration projects was to evaluate proposed mechanistically-based pavement design procedures under development by the University of Illinois (1,2) and to determine the effects of variable design inputs on pavement performance. These demonstration projects were proposed in an experimental features work plan entitled, "Evaluating Pavement Design Features". This report details the construction and performance monitoring of these four demonstration projects, in accordance with the experimental features work plan.

## OBJECTIVES

The specific objectives outlined in the experimental features work plan were:

1. The comparison of measured load-deflection responses of full-depth asphalt concrete (AC) pavements to those predicted by the proposed design principles. This objective included the evaluation of various AC thicknesses, the utilization of underdrains, and the benefit of lime-modified subgrade on pavement performance.
2. The comparison of measured responses (strains and deflections) in the portland cement concrete (PCC) pavements with tied concrete shoulders to those predicted by the theories used to develop the mechanistically-based design procedures. This objective included the evaluation of various slab thicknesses, the utilization of underdrains, and the benefit of joint sealant on pavement performance.
3. The evaluation of asphalt cement viscosity grades AC-10 and AC-20 on the performance of full-depth AC pavements.
4. The evaluation of 40-, 20-, and 15-foot joint spacings on the performance of PCC pavements with tied concrete shoulders. This objective included the evaluation of a hinge-jointed design.

## HISTORICAL PERSPECTIVE

The American Association of State Highway Officials (AASHO, which was changed in later years to AASHTO, the American Association of State Highway and Transportation Officials) Road Test was conducted in Ottawa, Illinois between 1959 and 1960. The purpose of the AASHO Road Test was to relate pavement performance to structural design and traffic loadings. Both AC and PCC test sections were built and evaluated. The AASHO Road Test used repeated applications of known truck loads to determine a rate of damage and a deterioration rate of ride quality. These trends of pavement serviceability over time were subsequently used to define pavement performance.

Through the years, Illinois' empirically-based design (3) was modified as technology advanced. Over time, however, several inherent limitations became apparent as the design principles were applied to pavement systems, paving materials, environments, and service conditions other than those that existed at the AASHTO Road Test. By the early 1980's, vehicle weights and traffic factors had increased in such a manner that the current AASHTO-based design procedures could not keep pace; therefore, research efforts were initiated to review potential pavement design options. The results of this research yielded a proposed mechanistically-based design which allowed for several pavement cross section design evaluations.

To validate these mechanistically-based design concepts, IDOT instrumented four demonstration projects with extensive monitoring systems. The four projects were constructed in 1986, two on FA 401 (U.S. 20) in northern Illinois and two on FA 409 (U.S. 50) in south central Illinois. Since 1986, FA 401 has been redesignated FA 301 and FA 409 has been redesignated FA 327; however, for consistency, they will be referred to as FA 401 and FA 409 in this report. Demonstration Project 1 is a full-depth AC pavement on FA 401, and demonstration Project 2 is a jointed PCC pavement on FA 401. Demonstration Project 3 is a full-depth AC pavement on FA 409. Demonstration Project 4 has both jointed and continuously reinforced PCC pavements and is also on FA 409. This report details the construction and performance monitoring of these four demonstration projects.

## CONSTRUCTION

### Location

Demonstration Project 1 is part of FA 401 (U.S. 20) northeast of Freeport, Illinois in Stephenson County. It consists of 3.8 miles of full-depth AC pavement built under Contract 40463 and designated Section 177-3&4. Demonstration Project 2 is an adjacent 2.8 miles of rigid pavement built under Contract 40455 and designated Section 177-4-1. The location of these projects is shown in Figure 1.

Demonstration Project 3 is part of FA 409 (U.S. 50) between Lebanon, Illinois and the Sugar Creek Bridge in St. Clair and Clinton Counties. It consists of 7.5 miles of full-depth AC pavement, which were built under Contracts 40448 (St. Clair County) and 40315 (Clinton County) and designated Sections 82-11 and 14-12, respectively. Demonstration Project 4 is 9.7 miles of rigid pavement on FA 409 (U.S. 50) between the St. Rose Road intersection and the IL 127 intersection. Project 4 consists of segments of continuously reinforced concrete pavement (CRCP), jointed reinforced concrete pavement (JRCP), jointed plain concrete pavement (JPCP), and hinge-jointed concrete pavement. The CRCP segment of Project 4 was built under Contract 40317 and designated Section 14-14, and all of the jointed concrete pavement segments were built under Contract 40456 and designated Sections 14-15, 14-16x. The exact locations of these projects are also shown in Figure 1.

## Cross Sections

### Design Information for Projects 1 and 2

The cross-sectional design of Project 1 was a 13-inch full-depth AC pavement. To evaluate the influence of asphalt cement viscosity on pavement thermal cracking, rutting, and overall performance, test sections were constructed using both AC-10 and AC-20 grade asphalt concrete mixes. The layout of the individual test sections is included in Figure 2.

All of the test sections of the adjacent rigid pavement, Project 2, were constructed with a 10-inch thick slab on a 4-inch thick Cement Aggregate Mixture II (CAM II, or econocrete) subbase. The pavement included sections with 40-foot mesh-reinforced jointed, 15-foot and 20-foot non-reinforced jointed, and hinge-jointed pavements. The hinge joint design used both doweled and tied joints to construct longer effective pavement slabs. The hinge joint design required dowel-reinforced joints every 40 feet. In between the doweled joints, sawed cracks were made in locations with tie bar reinforcing. This design allowed for longer effective slab lengths with controlled panel cracks. Details of the hinge-jointed panel designs are included in Figure 3. Design A1 had dowels every 40 feet and tied saw cracks in the middle of the slab. Design A2 was the same as A1, except that A2 included 7-foot long, full-width pavement fabric for reinforcement. Design B featured 40-foot doweled panels with two tied saw cracks 13.3 feet apart. The layout for all of the test sections included in Project 2 are presented in Figure 4.

The IDOT PCC pavement design standard in effect at that time had to be modified to account for the inclusion of tied concrete shoulders. Tied concrete shoulders were included in the cross-sectional design because they were the standard for the proposed mechanistically-based design cross section. The shoulders started with the same thickness as the adjacent 10-inch mainline PCC slab and tapered to an outside edge of 6 inches. A female keyway in the mainline slab and #5 deformed bars were used to tie the pavement/shoulder joint. Surface treatments of the shoulders included tining and rumble strips. Additionally, transverse joints were sawed in the shoulder to match the joint spacing in the mainline slab. The shoulder design detail is included in Figure 5.

Design Equivalent Single Axle Loads (ESALs) were backcalculated for each of the test sections using the individual cross section variables and the mechanistically-based design procedure (4). These numbers are given in Table 1A. All calculations assumed "poor" subgrade conditions ( $K = 50$  or  $E_{pi} = 2$  ksi) and a high reliability.

Due to the geographic characteristics of the area, both projects were partially built through rock cuts. No longitudinal edge drains were used in the sections through the rock cuts, but they were used in the sections with a soil foundation. Lime modification of the subgrade was not necessary on either project.

## Design Information for Projects 3 and 4

Project 3 was built with cross section thicknesses of 9.5, 11, and 12.5 inches of full-depth AC pavement to evaluate the effects of AC thickness on pavement performance. The primary cross-sectional design for Project 3 consisted of an 11-inch AC layer, with underdrains and a lime-modified subgrade. To evaluate the significance of each component of the primary design, test sections with and without a lime-modified subgrade, sections with and without longitudinal underdrains, and sections with an AC-10 instead of an AC-20 mix were incorporated into the project. The layout for all of the test sites within Project 3 is included in Figure 6.

Directly east of Project 3 is 3.9 miles of CRCP which was constructed in 1980. East of that section is Project 4. Project 4 consists of 4.0 miles of CRCP and an adjacent 5.7 miles of jointed PCC pavement, all on a 4-inch thick CAM II subbase. Slab thicknesses of 7, 8, and 9 inches for the CRCP sections and 7.5, 8.5, and 9.5 inches for the jointed PCC sections were constructed. Mesh-reinforced sections with 40-foot joints, non-reinforced sections with 20-foot joints, and hinge-jointed sections were incorporated into the jointed concrete pavement segment of Project 4. The hinge joint designs used in Project 4 were the same as those used in Project 2 and are shown in Figure 3. As with Project 3, the original cross section parameters were varied to include several experiments within the project. These variations included test sections with and without longitudinal underdrains, test sections with and without a lime-modified subgrade, and test sections with and without a sealed pavement/shoulder joint. The layout for all of the test sections within Project 4 is included in Figure 7. The shoulders in Project 4 were constructed similarly to those described in Project 2, only a male keyway, instead of a female keyway, was paved in the mainline.

The backcalculated design ESALs for each of the test sections are included in Table 1B. The backcalculated design ESALs were calculated for each test section based on the individual cross section variables. All calculations assumed "poor" subgrade support ( $k = 50$  or  $E_{p1} = 2\text{ksi}$ ) and a high reliability (4).

## **Instrumentation**

All of the demonstration projects were instrumented to assist in the performance evaluation of each of the test sections. One of the key elements in the evaluation of the proposed mechanistically-based design procedures rested on the ability to measure the actual strains within the pavement. A literature search found that fairly reliable strain measurements in PCC pavements could be recorded. Strain measurements in AC pavements, however, were considered unreliable. For this reason, only the PCC projects were instrumented with strain gauges. In the CRCP segment of Project 4, strain gauges were placed in the pavement and on the reinforcing steel. In the jointed PCC sections of Projects 2 and 4, strain gauges were placed in the pavement. The exact locations for the strain gauges are included in Figure 4 for Project 2 and Figure 8 for Project 4.

In addition to the strain gauges, several different types of monitoring gauges were installed on Projects 3 and 4 to measure climatic effects. Thermocouples were installed in all of the projects to provide information on internal pavement temperatures during deflection testing. Frost gauges were installed in Project 4 to record the depth of frost penetration. Capped holes were installed in both projects to allow the subgrade moisture to be read by a nuclear moisture gauge. Outflow meters were installed on the underdrain outlets to determine the effectiveness of the different cross-sectional variations in preventing water infiltration in the pavement system. Finally, a rain gauge was purchased in 1989 and placed at various locations on FA 409 to provide more accurate data in the evaluation of the underdrain outflow and subgrade moisture data. The exact locations for the various types of gauges installed are shown in Figures 8 and 9. A thorough explanation of the selection and installation processes of all of the instrumentation used on the demonstration projects, with particular attention to the selection and installation processes of the strain gauges, has been published elsewhere (5).

## Construction Details

### Quality Tests

Prior to construction, in-depth soil surveys were made on all of the projects. Particular care was taken with the soil borings in the instrumented test sections prior to construction. In addition to the routine soil classification tests, Illinois Bearing Ratio (similar to the California Bearing Ratio) and/or resilient modulus tests were performed on these samples. In-place subgrade density was also measured using a nuclear density gauge.

On both of the full-depth AC sections (Projects 1 and 3), the asphalt binder and surface course mixtures complied with IDOT's Class I Specifications for Bituminous Concrete Overlays on Interstate Highways (6). This type of construction was known as "full-depth, full-quality." Previous experience with flexible pavement cross sections had been limited to projects designed with granular layers and low strength binders in the bottom lifts. It was believed the new "full-depth, full-quality" pavements would substantially increase the overall strength of the pavement and increase the life expectancy of the pavement. The bituminous mix designs for the surface and binder mixtures for Project 1 are included in Tables 2 and 3. The bituminous mixture designs for the surface and binder courses used in the construction of Project 3 are included in Tables 4 and 5.

The standard quality control programs were augmented with additional material sampling and testing. Routine Marshall stability and extraction tests were conducted periodically on samples collected from the haul trucks. All of the test results were weighted on the total production that day. If two or more tests were conducted during the same day, the test results were weighted evenly by dividing the total tonnage for the day by the number of tests conducted that day.

Table 6 contains a comparison of the design vs. average production values for the asphalt concrete used in the construction of Project 1. The only production results that were not within the specified design parameters were the air voids on the AC-20 surface mix. These air void values were

determined from Marshall test results. The average air void content for production was 2.3 percent. The problem with air voids was not evident until the last day of production; therefore, the problem was not identified until production was complete. Cores taken during the production of Project 1 indicated the air voids were in the acceptable range.

Tables 7 and 8 contain comparisons of design vs. average production values for the asphalt concrete test results obtained from samples collected from the construction of Project 3. As with Project 1, cores were used to determine total and individual lift thicknesses. From Table 8 it is clear that the average asphalt cement contents of the binder mixes used in St. Clair County were substantially less than the design asphalt cement contents. This lower average could be attributed to the fact that the samples tested for asphalt content were taken from the haul trucks. This type of sampling is prone to segregated samples. The tests with low asphalt contents were also out of the specified gradation range on the #8 sieve, on the coarse side. Since the sampling technique allowed for segregated, coarse samples, it follows that the asphalt content of the coarse samples would have been low. The average field density for this mix was 94.6 percent, which was in the acceptable range. Thus, the field densities did not indicate that there were significant problems with the mix.

Tables 7 and 8 also indicate the air voids in the AC-20 surface mix were high. The individual Marshall test results show the air voids ranged from 3.9 to 8.1 percent. This range suggests that the mix itself was variable. In addition to the variability of the mix, the average dust content (minus #200 sieve material) was less than the design formula specified. Logically, since the dust content was low, the void content would be high.

The PCC mixture design for Project 2 is included in Table 9, and the PCC mixture design for Project 4 is included in Table 10. In these sections, 3-, 7-, 28-, and 90-day flexural strengths were determined for the pavement panels instrumented with the strain gauges, in addition to the routine air content, slump, and 14-day flexural tests. A comparison of the test results to the standard specifications and design criteria show that, although a few individual tests were out of the specified acceptable range, the average production values were well within the specified ranges. These comparisons can be found in Tables 11 through 13.

### Construction Problems

The construction phase of Projects 1 and 2 went well with no major complications. The earthwork and pavement were constructed in accordance with IDOT's Standard Specifications for Road and Bridge Construction (7). The pregrade work was completed in the fall of 1985. Prior to paving in the spring of 1986, the pregrade contractor was called back to the job to do some minor repair work. Final construction was completed, and the road was opened to traffic in the fall of 1986.

The construction of Projects 3 and 4 had several complications worth noting. The pregrade work was divided into three separate projects. In 1980, the pregrade was completed from IL 160, Section N, to west of CH 14, Section R.

In 1985, the pregrade work on the other two contracts was nearly completed, with a small part of the pregrade work for Project 3 completed in the early spring of 1986. Lime modification of the subgrade began in the spring of 1986. A few test sections that were originally designated as no-lime sections were changed to lime-modified sections because of poor subgrade conditions.

The paving of the full-depth AC in Project 3 began in the late spring of 1986. During the paving of Section N, it became apparent that there were structural problems. Deflection testing outlined 1,200 feet of weak subgrade support. The pavement, which had already been placed, was milled off. The weak subgrade material was removed to a depth of three feet and replaced with a clean aggregate, which had a top size of 6 inches. The milled material was repaved on the aggregate and construction continued from there without further subgrade problems.

As paving operations continued, a number of "fat" spots appeared in the top layer of the asphalt binder in Section B. "Fat" spots are pockets of asphalt cement in the asphalt concrete surface. A motorgrade was used to grade off the "fat" spots. Even so, some of the "fat" spots have continued to come through to the surface of the pavement. The exact cause of these "fat" spots has never been determined, but they do not appear to have affected the performance of this section.

Paving of the rigid pavement sections on Project 4 also began in the late spring of 1986. At the request of the contractor, the paver was modified to construct a male keyway in the mainline, instead of the standard female keyway. Maintaining this keyway shape was a continuous problem as the keyway had a strong tendency to chip and break off as the shoulder tie bars were being straightened.

As the concrete set, the sawing of the contraction joints became critical. In jointed PCC Sections MA, OA, and PA, uncontrolled transverse cracking did occur. Most of the panels were reconstructed in accordance with the Standard Specifications for Road and Bridge Construction (7); however, some of the cracks were patched and some were sealed with an epoxy grout instead. At the present time, none of the sealed cracks have required maintenance even though the epoxy grout failed prematurely.

On selected sections in Project 4, the longitudinal pavement/shoulder joint was sawed and sealed. The unforeseen problem was locating the exact place of the pavement/shoulder joint. The mainline pavement had edge slump in many places, but was within the acceptable tolerances. During the paving of the shoulder, the strike-off plate rested on the mainline pavement. In locations of edge slump, this placement technique allowed the shoulder material to be placed on top of the mainline pavement. After the initial set, the saw cut was made along the obvious pavement/shoulder seam; however, the true pavement/shoulder joint eventually reflected through. Thus, the sawing of the longitudinal pavement/shoulder joint only created a slot in the pavement or shoulder. It was only after the section had been opened to traffic that this discrepancy became noticeable.

Finally, the strain gauges required significantly more time to install than was originally anticipated. The gauges in the bottom of the pavement were mounted on steel chairs, approximately one inch off of the CAM II base, prior to paving. There was nothing, however, to attach the surface gauges to. A limited amount of surface gauges were used in Project 2, and they were



installed by simply floating them into place in the wet concrete. On Project 4, there were significantly more gauges to be placed in the top of the pavement. Two alternative installation methods were used. The first was to saw cut the hardened concrete and sand grout the gauges and connecting wires into place. The other method was to insert wooden forms in the wet concrete in the locations where gauges were to be placed. The wooden forms were removed after the concrete had set-up, a saw cut was made in the hardened concrete to place the connecting wires in, and gauges and wires were installed and sealed with epoxy. Although accurate depth placement is the most difficult with floating the gauges in the fresh concrete, this would be the recommended procedure for any future installations.

## PERFORMANCE MONITORING

### Condition Surveys

#### Condition Rating Survey (CRS)

The biennial Condition Rating Survey (CRS) is a visual inspection of pavements performed by a trained panel of raters (8). The assigned CRS value is a visual measurement of the current pavement condition with values ranging from 1.0 for a failed pavement to 9.0 for a pavement in excellent condition. If a pavement is critically deficient - in need of immediate improvement - it is assigned a CRS of 4.5 or less. If the pavement is approaching a condition that will likely necessitate improvement over the short term, the pavement is assigned a CRS value of 4.6 to 6.0. A CRS value of 6.1 to 7.5 is assigned to pavements in acceptable to good condition, and a high quality pavement is assigned a CRS value of 7.6 to 9.0.

During the 1992 field review, Project 1 was given a CRS rating of 8.0, and Project 2 rated a CRS of 8.2. The overall rating for Project 3 was 7.5 and 8.2 for Project 4. All of these CRS ratings indicate the projects are performing in the good to excellent range.

#### Distress Surveys

Detailed distress surveys are necessary in order to characterize distress development in a pavement. In June of 1989 all four projects were photologged by PASCO U.S.A., Inc. PASCO specializes in automated distress collection. PASCO uses a high-speed photologging system to photograph the pavement surface. During March of 1990, a walking field survey was conducted on all of the projects to verify the PASCO surveys. Again in April of 1992, a walking field survey was conducted on all of the projects. Both these surveys mapped out distress locations and severity levels. Summaries of the distresses recorded are included in Tables 14A through 17B.

The summaries of the 1990 and 1992 crack surveys for Projects 1 and 3 are included in Tables 14A, 14B, 15A, and 15B. Transverse cracking, alligator cracking, and rutting are key performance indicators for full-depth AC pavements. Rut-depth measurements were taken every 2,000 feet during the 1990 and 1992 walking surveys and are discussed in detail later in this report. The 1990 distress survey summary for Project 1, shown in Table 14A, lists

raveling and weathering, longitudinal cracking, alligator cracking, transverse cracking, asphalt bleeding, and centerline cracking distresses. At the time of the 1990 survey, Project 1 had received approximately 90,000 ESALs. All of the traffic estimates included in this report are based on Weigh-In-Motion (WIM) data and IDOT equivalency factors. These rough estimates will be refined as more data become available. As of the 1992 survey, summarized in Table 14B, Project 1 had received 200,000 ESALs. The transverse cracking and alligator cracking distresses were still only in limited locations and were of minor significance. In 1992, block cracking and center of lane cracking were added to the list of distresses. Although showing localized signs of distress, overall Project 1 is performing well.

The 1990 distress survey summary for Project 3, shown in Table 15A, lists asphalt bleeding, centerline cracking, alligator cracking, permanent patching, longitudinal cracking, and transverse cracking distresses. At the time of the 1990 survey, the eastbound driving lane on Project 3 had received 180,000 ESALs, and the westbound had received 130,000 ESALs. In 1992, corrugation or shoving, localized distress, and block cracking were added to the list of distresses summarized in Table 15B. The summaries of the survey data for Project 3 show only minimal occurrences of transverse cracking in five of the fifteen test sections. Section A has one transverse crack, Sections N, O, and P each have two transverse cracks, and Section M1 has seven. When considering the entire project length, these few cracks are of minor consequence.

Six of the fifteen test sections on Project 3 have some alligator cracking, usually a serious example of fatigue-related distress. Of these six, Sections K, M, and M1 have required extensive patching. This problem has been the focus of an in-depth study to determine its cause, as discussed later in this report. The majority of the the alligator cracking not in Sections K, M, and M1 is contained in Section P, near entrance and exit ramps. These ramps were used during construction as access locations for the haul trucks, and it is possible that the early loadings accelerated the fatigue mechanisms in these areas. The remaining alligator cracking in Section P is located in the two-lane section and is more accurately described as surficial cracking that is interconnecting. This cracking is not fatigue-related; however, the distress has a pattern similar to alligator cracking.

Block cracking is usually an example of age-related distress. All of the block cracking is contained in Sections O and P. This block cracking is definitely low severity. Like the interconnecting cracking in the two-lane section of Section P, this block cracking is a surface distress which is patterning itself in blocks. At the time of the 1992 survey, the eastbound driving lane of Project 3 had received 280,000 ESALs, and the westbound driving lane had received 230,000 ESALs.

The summaries of the 1990 and 1992 crack surveys for Projects 2 and 4 are included in Tables 16A, 16B, 17A, and 17B. At the time of the 1990 survey, Project 2 had received 140,000 ESALs, which increased to 370,000 ESALs by the 1992 survey. At the time of the 1990 survey, Project 4 had received 260,000 ESALs on the eastbound driving lane and 210,000 ESALs on the westbound driving lane. By the time of the 1992 survey, the traffic on the eastbound driving lane had increased to 430,000 ESALs and 390,000 ESALs on the westbound driving lane.

The summaries of the crack survey data for Projects 2 and 4 show that most of the cracks in the PCC sections were limited to Sections MA and PA in Project 4 and the 40-foot JRCP sections. Sections MA, OA, and PA in Project 4 are the sections which experienced construction problems (as noted in detail earlier in the **Construction** section of this report). The majority of the rest of the transverse cracking is in the 40-foot JRCP sections. Nearly all of the 40-foot JRCP panels cracked in the middle of the slab. Of these mid-slab cracks, the majority of them were still low severity in 1992; however, a notable number were at the medium severity level. The 40-foot panels are reinforced with mesh to minimize distresses associated with the cracks and to assist in keeping the cracks tight.

The hinge-jointed test sections DA, DB, and DC on Project 4 are located in an intersection. In order to facilitate left turn lanes, additional tapered hinge-jointed panels were added, as shown in Figure 10. Some of the outside panels have cracked in Section DB. It is believed these cracks are due to the lack of attention to joint details and not the actual hinge joint design. These cracks were first detected by PASCO in 1989. These cracks were not recorded on the 1990 distress survey because the survey included only the complete interior panels. This was also the case with the 1992 distress surveys; however, field reviews in June and August of 1992 did record the cracks in the outside panels.

In addition to these transverse cracks, random longitudinal cracks were found in the outside panels in 1987. These cracks were tight and short, approximately 6 to 24 inches long. The cracks could be found between stations 3266+00 and 3270+00 with the pattern most visible between stations 3267+50 and 3269+00. During the August 1992 field review, these cracks were recorded, although they were still very short, tight, and random.

### Patching Efforts

Patch locations and sizes were also recorded on the distress survey sheets. Projects 1 and 2 have never been patched; however, both Projects 3 and 4 have been patched in limited areas. Most of the patching within Project 4 is limited to Section OA. (Figure 7 contains the site descriptions for this section.) This section developed plastic shrinkage cracking before the joints were sawed, as discussed in detail in the **Construction** section of this report.

The patching in Project 3 is significant. In August 1988, two years after construction, four areas in Sections K and M required "skin" patches. "Skin" patching is a simple method of repair which entails placing a thin overlay over distressed sections to fill in depressed and rutted areas. In July and August of 1989, the areas which were "skin" patched in 1988 were again severely rutted and humped. In addition, other areas in Sections M and M1 required patching. These locations are listed in Table 18. All of these test sections were originally constructed of 9.5 inches of AC-20 asphalt concrete. All but one of the distressed areas were repaired by completely removing the pavement and replacing it with a full-depth patch. Construction of the full-depth patches entailed placing crushed stone in the bottom of the patch to level the base area to the bottom of the pavement. The crushed stone

was then compacted and primed. The patches were completed by placing 9.5 inches of asphalt concrete in lifts and compacting the individual lifts to the existing surface. All of the repairs were allowed to cool prior to reopening the area to traffic.

At station 602+50, a different type of patch was tried. The lower 3 to 4 inches of the patch were filled in with crushed stone, which was compacted and primed as before. Subsequently, 5 to 6 inches of asphalt concrete was placed in lifts and compacted to the surface. This patch was also allowed to cool prior to reopening the area to traffic. Patching in Sections K, M, and M1 was again required in July 1990 and June 1991 as detailed in Table 18. In July 1990, the partial-depth patch at station 602+50 had failed, and so was removed and replaced with a full-depth AC patch.

### Moisture Damage

During the 1989 patching efforts in Sections K, M, and M1, evidence of moisture damage was detected. Moisture damage is the loss of asphalt film from individual aggregate particles, which can result in a significant reduction in strength. The presence of moisture damage in AC samples taken from the patched areas raised concerns about the possible presence of moisture damage in all of the test sections in Projects 1 and 3. To assess the potential extent of moisture damage, full-depth AC cores were collected from all of the test pavement cross sections on Projects 1 and 3. The cores were cut dry (no water was used during the coring process) so as to minimize additional moisture damage to the material. The cores were shipped to the Central Bureau of Materials and Physical Research's Bituminous Laboratory for testing.

The cores were split into binder lifts. Indirect split tensile tests at 77°F were run on the unconditioned cores, which were then visually surveyed for signs of moisture damage. The testing procedure used was the same as the one currently specified by IDOT for evaluating the effectiveness of anti-strip additives (9).

Cores taken from Project 1 showed little signs of moisture damage. The 77°F tensile strengths of cores taken from the AC-10 sections averaged 156 psi, and the 77°F tensile strengths of cores taken from the AC-20 sections averaged 183 psi. These data are summarized in Table 19. These higher tensile strengths coupled with no apparent moisture damage agreed with the visual distress surveys, which indicated no real structural damage.

Cores taken from Project 3 showed signs of moisture damage ranging from slight to severe. Tensile strengths at 77°F of the Project 3 cores are summarized in Table 19. The 77°F tensile strengths of cores taken from the AC-10 sections averaged 78 psi, and the 77°F tensile strengths of cores taken from the AC-20 sections averaged 103 psi. These tensile strengths are considerably lower than the tensile strengths found on Project 1, and appear to be a result of moisture damage. The visual distress surveys showed fatigue-related distress in the areas that were patched, which would be consistent with materials weakened by moisture damage.

## Rutting Surveys

The 1990 and 1992 distress surveys recorded rut depth measurements at 2,000-foot intervals. Along with these measurements, independent manual rut surveys were conducted on Project 1 in July 1988 and Project 3 in both June 1988 and August 1989. The independent manual rut surveys recorded rut depths in 100-foot intervals. Both surveys measured the rut depths by placing a 6-foot straight edge over half a lane width and sliding a "measuring shoe" under the straight edge in several places to locate the point of maximum rut. A summary of the hand-measured rut histories can be found in Tables 20 and 21A through 21D. Relative traffic levels are included on each of these tables.

Hand-measured rut depths taken on Project 1 in 1992 ranged from an average 0.06-inch depth in the eastbound driving lane in Section B to an average 0.14-inch depth in the westbound driving lane in Section A. These are relatively minor rut depths. In comparison, the hand-measured 1992 rut depths on Project 3 ranged from 0.00 inches to an average 0.64-inch depth in the eastbound driving lane in Section K. Since the readings were taken every 2,000 feet, the data are quite variable. Additional readings were taken in areas of visible rutting. The higher rut depths on Project 3 reflect the increased amount of maintenance that has been performed as compared to Project 1.

The road profiler, used to measure ride quality since 1990 in Illinois, also records average rut depths. The manual rut gauge and the road profiler "read" rut depths differently, but can be expected to illustrate the same general trends, if not the same measurements (10). The road profiler rut depths are summarized in Tables 22A and 22B. The relative traffic levels at the time of testing are also included in these tables.

## **Structural Response Monitoring**

### Full-Depth AC Deflection Testing

#### Project 1

Deflection testing with IDOT's Dynatest 8002 Falling Weight Deflectometer (FWD) has been conducted annually on Project 1 since construction. Tests were taken in the outer wheelpath in both directions. The data were normalized to a 9,000-pound load. Deflection basin area values were backcalculated using concepts and algorithms developed by Professor Marshall Thompson of the University of Illinois (11). Area values are an indication of the pavement's structural integrity, and are calculated by determining the area of the deflection basin, as shown in Figure 11. Algorithms developed by Professor Thompson to backcalculate subgrade resilient modulus ( $E_{Ri}$ ) values and asphalt concrete modulus ( $E_{AC}$ ) values from FWD data were not appropriate for use with Project 1, since the pavement was constructed on a rock foundation.

Temperature data were collected during FWD testing on Project 1. Pavement temperatures were taken at a nominal 4-inch depth at the beginning and end of each FWD testing sequence. Holes were drilled in the pavement, filled with oil, and a thermometer inserted. Pavement temperatures were assumed to vary at a constant rate throughout the sequence. The data were broken into ranges based on temperature fluctuations. The pavement temperatures are included in the FWD data summary in Table 23.

Average deflections and deflection basin areas for each FWD test date are summarized by asphalt cement type for Project 1 in Table 23. Deflections under the load averaged between 3.4 and 11.5 mils (0.001-inch) in the AC-10 sections and between 3.3 and 15.2 mils in the AC-20 sections. Deflection basin areas averaged between 17.8 and 26.4 inches in the AC-10 sections and between 19.8 and 27.2 in the AC-20 sections. The numbers show both the AC-10 and AC-20 sections to be sound, full-depth AC pavements, a finding that is supported by the visual distress survey data.

### Project 3

Deflection testing with the FWD has been conducted annually on Project 3 since construction. Tests were taken in the outer wheelpath in the driving lane in both directions. The data were normalized to a 9,000-pound load. Deflection basin areas and  $E_{Ri}$  values were backcalculated using concepts and algorithms developed at the University of Illinois (11). Average  $E_{AC}$  values were also backcalculated using an algorithm developed at the University of Illinois (M. R. Thompson, unpublished data).

The  $E_{Ri}$  and  $E_{AC}$  algorithms were developed from a matrix of computer runs using ILLI-PAVE, a stress-dependent, finite element pavement model (12). The  $E_{Ri}$  algorithm is valid for full-depth AC thicknesses ranging from 4 to 16 inches,  $E_{Ri}$  values ranging from 1 to 12.3 ksi, and  $E_{AC}$  values ranging from 200 to 2,000 ksi (11). The  $E_{AC}$  algorithm is valid for full-depth AC thicknesses ranging from 9.5 to 18 inches,  $E_{Ri}$  values ranging from 1 to 12.3 ksi, and  $E_{AC}$  values ranging from 100 to 1,000 ksi (M. R. Thompson, unpublished data).

Temperature data were collected during FWD testing on Project 3. Thermocouples were placed in Section E at depths of 0.5, 1.5, 3.25, 6.5, and 12 inches from the top of the 12.5-inch thick AC layer. A sample profile showing pavement temperature as a function of time of day is shown in Figure 12. The temperature at a depth of  $0.35 \times$  (AC layer thickness) was used as the "effective temperature" corresponding to an "effective  $E_{AC}$ ". The time of day a given section was tested with the FWD was noted, and the time of day corresponding to the mid-point of the section's testing was the time at which the effective temperature was read off of the temperature profile. For the AC layer thicknesses on Project 3, 9.5 inches, 11.0 inches, and 12.5 inches, the depths corresponding to  $0.35 \times$  (AC layer thickness) were 3.3 inches, 3.8 inches, and 4.4 inches, respectively.

"Effective  $E_{AC}$ " is the modulus of a theoretical layer of constant stiffness AC that behaves similarly to the actual full-depth AC comprised of layers of variable stiffness. The concepts of effective temperature and effective  $E_{AC}$  are discussed elsewhere (13).

Effective temperatures, deflections, deflection basin areas, effective  $E_{AC}$ , and  $E_{Ri}$  values were averaged for each pavement test section and are summarized in Tables 24A through 24G. Table 25 contains all the reference data for Tables 23 and 24A through 24G. In general, Section E showed the lowest deflections and Sections K and M the highest deflections. Sections O and K most frequently had the lowest deflection basin areas, while Section E consistently had the highest deflection basin areas, indicating a higher degree of structural integrity. The data are quite variable, however, depending upon the test temperature.

Figures 13 through 19 illustrate the effect temperature has on  $E_{AC}$ . Effective pavement temperature versus  $E_{AC}$  data backcalculated from FWD testing were plotted for each FWD testing date. Three sets of data are shown on each graph: all the AC-10 sections, all the AC-20 sections, and the AC-20 sections minus Sections K, M, and M1. The algorithms designed to backcalculate  $E_{AC}$  from FWD testing were developed assuming "fully intact" and structurally sound pavements. Sections K, M, and M1 have all shown structural distress and have required patching as discussed previously, and so can no longer be considered "fully intact." For this reason, Sections K, M, and M1 were removed from the AC-20 data.

The equations of the best-fit line and the corresponding coefficient of determination ( $R^2$ ) are shown on each figure. Eliminating Sections K, M, and M1 usually improved the  $R^2$  values for the remaining AC-20 sections. In general, when a range of temperature data were collected on the given FWD testing date, the data show reasonable  $R^2$  values. On certain test dates, the temperature spread was quite small, and the effective temperature versus backcalculated  $E_{AC}$  relationship yielded a very low  $R^2$ . The AC-20 data on May 1988 and May 1989, the AC-10 data on May 1989, and all data on August 1990 and August 1991 had  $R^2$  values less than 0.50. During the August 1991 FWD testing, for example, only a 2°F spread was recorded. The FWD testing was conducted in the rain, and as no thermocouple data was available, manual pavement temperatures were taken instead.

In general, the data exhibited the expected behavior. Backcalculated  $E_{AC}$  values decreased as the effective pavement temperature increased. The AC-10 decrease in backcalculated  $E_{AC}$  for a given increase in effective temperature roughly paralleled the same trends in the AC-20 sections. On the earlier test dates, notably May 1987 and September 1987, when the  $R^2$  of all the data were 0.65 or better, the AC-10/AC-20 trend resembled typical  $E_{AC}$ -AC pavement temperature relationships shown in Figure 20 that were previously developed for IDOT's mechanistically-based AC pavement design (4).

The presence of stripping on Project 3, as discovered during the 1989 maintenance patching efforts and the subsequent core stripping study, may have affected the  $E_{AC}$ -AC pavement temperature relationship. Previous research by IDOT has shown that backcalculated  $E_{AC}$  values can be affected by the presence of stripping (14). To determine the variation of  $E_{AC}$  over time, Figure 21 was prepared. In the current IDOT full-depth AC mechanistically-based design process, the design pavement temperature for Project 3 is 82°F (4). From Figures 13 through 19, the  $E_{AC}$  value corresponding to 82°F was selected from the regression lines for the AC-10 sections, all the AC-20 sections, and the AC-20 sections minus Sections K, M, and M1. These 82°F values were plotted as a function of the pavement's age at the time of the FWD testing in Figure 21.

The  $R^2$  of the regression lines plotted in Figure 21 are quite low. The general data trends are informative, however. The backcalculated  $E_{AC}$  values show a general decrease over time. Typical  $E_{AC}$  values should show an increase over time, reflecting the stiffening of the AC mixture as a result of the aging process. Since the expected trend of stiffening over time was not apparent, it is possible that the presence of stripping adversely affected the backcalculated  $E_{AC}$  of the sections on Project 3.

The algorithms designed to backcalculate  $E_{AC}$  from FWD testing were developed assuming uniform AC layer thickness and materials of consistent quality. Misleading backcalculated  $E_{AC}$  values could thus result if the algorithms were used on AC layers of variable thickness and material quality. Sections K, M, and M1 were eliminated from the other AC-20 sections in Figures 13 to 19 and Figure 21 because of known structural failures that affected both material quality and effective AC layer thickness. Moisture damage was identified on Project 3 during the 1989 core investigation, so it is reasonable to assume that variations in effective AC layer thickness and material quality may exist in other sections on Project 3 as well. Because of these factors, it was thought that a measure of the AC material quality obtained from laboratory  $E_{AC}$  and split tensile strength testing would be more accurate.

Immediately after the construction of Project 3 in 1986, IDOT had obtained full-depth cores from the various pavement cross sections. The University of Illinois had conducted indirect split tensile and laboratory instantaneous AC resilient modulus testing on the binder lifts of the cores. Regression analyses were made, and relationships between laboratory  $E_{AC}$  values and split tensile strengths were developed (13). In September 1991, IDOT again obtained cores from the various pavement cross sections on Project 3, and the University of Illinois again conducted indirect split tensile and laboratory instantaneous AC resilient modulus testing on the binder lifts. A new series of regression analyses were made and relationships between laboratory  $E_{AC}$  values and split tensile strengths developed from the 1991 cores (M. R. Thompson, unpublished data). Table 26 shows both the 1986 construction core and 1991 core indirect tensile strengths. A comparison of the 1986 construction core and 1991 core  $E_{AC}$ -tensile strength relationships for both AC-10 and AC-20 cores is presented below:

#### 1986 CONSTRUCTION CORE ANALYSIS

##### ALL AC-10

$$E_{AC} = -183 + 5.87(St) \quad (\text{Equation 1})$$

R = 0.976  
SEE = 38.2 ksi  
n = 20 tests

##### ALL AC-20

$$E_{AC} = -173 + 6.07 (St) \quad (\text{Equation 2})$$

R = 0.801  
SEE = 110 ksi  
n = 63 tests

#### 1991 CORE ANALYSIS

##### ALL AC-10

$$E_{AC} = -389 + 7.95 (St) \quad (\text{Equation 3})$$

R = 0.803  
SEE = 171 ksi  
n = 26 tests



ALL AC-20

$$E_{AC} = -177 + 5.56 (St) \quad (\text{Equation 4})$$

$$R = 0.740$$

$$SEE = 123 \text{ ksi}$$

$$n = 52 \text{ tests}$$

where:

$E_{AC}$  = laboratory instantaneous resilient modulus of asphalt concrete at 77°F, ksi  
 $St$  = tensile strength at 77°F, psi

From Table 26, the average 77°F tensile strength obtained from the 1986 AC-10 binder construction cores was 98 psi, and the average 77°F tensile strength for the 1986 AC-20 binder construction cores was 125 psi. The September 1991 AC-10 binder cores had an average 142 psi tensile strength at 77°F and the AC-20 binder cores had an average 160 psi tensile strength at 77°F. Substituting these average tensile strengths into equations 1 through 4 yields the following results:

#### 1986 CONSTRUCTION CORES

ALL AC-10

$$E_{AC} = -183 + 5.87(98)$$

$$E_{AC} = \underline{392 \text{ KSI}}$$

ALL AC-20

$$E_{AC} = -173 + 6.07(125)$$

$$E_{AC} = \underline{586 \text{ KSI}}$$

#### 1991 CORES

ALL AC-10

$$E_{AC} = -389 + 7.95(142)$$

$$E_{AC} = \underline{740 \text{ KSI}}$$

ALL AC-20

$$E_{AC} = -177 + 5.56(160)$$

$$E_{AC} = \underline{713 \text{ KSI}}$$

These relationships show an average increase in AC-10  $E_{AC}$  from 392 ksi to 740 ksi between construction and September 1991, and an average increase in AC-20  $E_{AC}$  from 586 ksi to 713 ksi during the same time period. These values exhibit the expected trend of increased asphalt concrete stiffness as a function of the aging process that was not apparent from the  $E_{AC}$  values backcalculated from the FWD data.

These laboratory  $E_{AC}$ -tensile strength relationships were developed specifically for Project 3. The laboratory-derived relationships more truly represent the actual  $E_{AC}$  values than the  $E_{AC}$  values backcalculated from the FWD data. The backcalculation model assumed uniform AC layer thickness and material quality, assumptions that were invalidated due to the presence of moisture damage and the need for patching. Although these assumptions may not be entirely correct, the backcalculated data from FWD testing are still useful. A large amount of data can be collected quickly with FWD testing, and the backcalculated values by pavement section for a given test date can be informative relative to the other pavement sections and to other test dates.

As discussed previously, binder split tensile strengths were obtained from cores taken in 1986 after construction, cores taken in August 1989 as part of the moisture damage study, and cores taken in September 1991. Table 26 summarizes the tensile strengths. The split tensile strengths show an overall strength increase from 98 to 142 psi for the AC-10 binder cores and from 125 to 160 psi for the AC-20 binder cores from construction to September 1991. Again, this is compatible with the expected trend of increased stiffness as a function of the aging process.

The August 1989 cores, however, had lower tensile strengths than those obtained immediately after construction or in September 1991. Although both the August 1989 and September 1991 cores showed signs of moisture damage, the August 1989 cores exhibited greater moisture damage, which is a possible explanation for the lower tensile strengths. The cores taken in August 1989 were taken during a period of hot, wet weather, whereas the cores taken in September 1991 were taken during a cooler, drier period. It is possible that the effects of moisture damage - lower tensile strengths and corresponding lower  $E_{AC}$  values - become manifest in a cyclic pattern in response to climatic variations. The need for the patching done in Sections K, M, and M1 became evident during periods of hot, wet weather. At the time of the September 1991 coring, the pavement may have been in a less saturated state and a correspondingly stronger condition. Additional research is needed to investigate this phenomenon.

### PCC Deflection Testing

#### Project 2

A limited amount of deflection testing was conducted on the concrete sections on Project 2. The deflection testing was limited to Sections G1, G2, and G3, the hinge-jointed sections. The Department's FWD was used to make a series of drops of 4,000, 8,000, and 12,000 pounds in both the eastbound and westbound directions. These drops were normalized to a standard 9,000-pound load during analysis. The tests were made on the leave sides of both dowel and hinge joints in the outer wheelpath to determine the load transfer efficiency (LTE) of the joints.

The data are summarized in Tables 27A and 27B. The average deflections under the load at the hinge and dowel joints ranged from 2.8 to 4.2 mils as shown in Table 27A. As would be expected of a properly performing joint in a sound concrete pavement, these deflections were quite low. Average deflection basin areas calculated from the joint deflection testing ranged from 25.3 to

28.4 inches. Area values are an indication of the pavement's rigidity, and are calculated by determining the area of the deflection basin, as shown in Figure 11. Area values are generally calculated from deflections taken in the center of a panel, away from joints or cracks. A very limited number of center panel tests were taken on Project 2, too few for the results to be statistically significant. The area values calculated from the joint deflections are probably slightly lower than areas obtained from center panel testing due to slab geometry, but nonetheless are representative of a sound concrete pavement.

The LTE of the joints was calculated by dividing the deflection, on the unloaded side of the joint, by the deflection directly beneath the loaded plate. Table 27B shows that, in Section G1, the hinge joints had an average 92 percent LTE and the dowel joints an average 91 percent LTE; in Section G2, the hinge joints had an average 92 percent LTE and the dowel joints an average 91 percent LTE; and in Section G3, the hinge joints had an average 91 percent LTE and the dowel joints an average 90 percent LTE. These values indicate good load transfer at both the dowel and hinge joints. During warmer weather, slightly better LTEs were found. As the concrete expands and the joint closes, aggregate interlock contributes to the LTE. At this point, there is little difference in the LTE of the hinge and dowel joints, and both types of joints are performing as expected. There is little apparent difference in joint LTE between the sections, with all three designs performing equally well.

#### Project 4

A limited amount of deflection testing was conducted on the concrete sections on Project 4. The deflection testing was limited to Sections DA, DB, and DC, the hinge-jointed sections. The Department's FWD was used to make a series of drops of 4,000, 8,000, and 12,000 pounds in both the eastbound and westbound directions. These drops were normalized to a standard 9,000-pound load for analysis. The tests were made on the leave sides of both dowel and hinge joints in the outer wheelpath to determine the LTE of the joints. Early in the life of the pavement, before it was opened to traffic, a limited number of tests were made of the LTE of the pavement/shoulder joint. Nominal 8,000-pound drops were made at the edge of the pavement, with sensors recording deflections on both the pavement and the shoulder.

The data are summarized in Tables 28A, 28B, and 28C. The average deflections under the load at the hinge and dowel joints ranged from 6.0 to 8.3 mils, as shown in Table 28A. These deflections are at an acceptable level. Average deflection basin areas calculated from the joint deflection testing ranged from 24.9 to 26.7 inches. Area values are an indication of the pavement's rigidity and are calculated by determining the area of the deflection basin, as shown in Figure 11. Area values are generally calculated from deflections taken in the center of a panel, away from joints or cracks. A very limited number of center panel tests were taken on Project 4, too few for the results to be statistically significant. The area values calculated from the joint deflections are probably slightly lower than areas obtained from center panel testing due to slab geometry, but are still representative of a sound concrete pavement.

The LTE of the hinge and dowel joints was calculated by dividing the deflection, on the unloaded side of the joint, by the deflection directly beneath the loaded plate. Table 28B summarizes the LTE for the hinge and dowel joints. In Section DA, the hinge joints had an average 90 percent LTE and the dowel joints had an average 92 percent LTE; in Section DB, the hinge joints had an average 83 percent LTE and the dowel joints had an average 89 percent LTE; and in Section DC, the hinge joints had an average 90 percent LTE and the dowel joints had an average 86 percent LTE. These values indicate good load transfer at both the dowel and hinge joints. In Sections DA and DB, the dowel joints appear to have marginally better LTE than the hinge joints, while in Section DC, the hinge joints show marginally better LTE. The LTEs of both the hinge and dowel joints are good. The differences in LTE between the hinge and dowel joints are too small to comment on. All three designs appear to be performing in a reasonably similar fashion.

The LTEs of the pavement/shoulder joints shown in Table 28C were good, averaging 83 to 93 percent. Since these tests were taken when the pavement was new, it is reasonable to expect that the pavement/shoulder LTEs will decrease over time. Variability between individual pavement/shoulder LTE tests is to be expected. Shoulders were tied to the mainline pavement using #5 tie bars spaced at 30-inch centers. The FWD drops may have been made over a tie bar, which would have yielded good LTEs, or between tie bars, which would have yielded somewhat lower LTEs.

### Strain Gauge Measurements

As discussed earlier in this report, deflection testing and distress surveys were conducted to assist in the short-term evaluation of Projects 2 and 4. In addition, the theoretical strains due to wheel loads could also be verified in the short term with the use of the strain gauges. Gauges were installed in 5 sections of CRCP and 22 sections of JPCP and JRCP. Sixteen different cross sections were instrumented in all. Tests were conducted with an 18-kip single axle, dual tire wheel load from 1986 to 1989. Diagrams of the strain gauge locations for each of the different cross sections are included in Figures 22 and 23 for Projects 2 and 4, respectively. Corner, mid-panel, and quarter-panel gauges were installed in the JPCP and JRCP sections approximately 6 inches in from the edge of the pavement. In the CRCP sections, gauges were installed 6, 36, and 72 inches in from the edge of the pavement. It is important to note that, over time, some of the strain gauges could not be read because they could not be balanced. This problem could be attributed to many things, such as the fact that the electrical circuit between the gauge and the recording equipment could not be completed, the gauge had been strained beyond yield and therefore overstressed, or the gauge had been subjected to moisture damage.

With assistance from the University of Illinois, two different testing techniques were used with the strain gauges. The first technique applied a static load to the gauges, which allowed the maximum strain for each gauge to be recorded. The second technique applied a dynamic load to the strain gauges, which allowed the pavement's responses to moving loads to be recorded.

## Static Tests

The testing process for conducting the static tests was simple. An initial zero load reading of the gauges was taken manually. Then an 18-kip single axle load was placed directly over the gauge; after the gauge reached a maximum deflection, a second reading was recorded. Finally, the load was removed and the gauge was read one last time in the zero load condition. Portable SR-4 Strain Indicators (Type N) were used to read the voltage changes in the strain gauges. This testing sequence was repeated four times for each gauge. The change in strain for each gauge for each test was then calculated. It is important to note that under the static load condition only one gauge reading in the loaded condition was recorded. If the load was shifted, either laterally or longitudinally, and not centered directly over the gauge when the reading was taken, the absolute maximum strain for that gauge was not obtained. Although care was exercised when conducting the tests, this potential human error must be considered.

Along with the potential human error, other error factors must also be considered. The primary factors which influence a pavement's response to a static stress include effective LTE, temperature, and time of day. The effective LTE to the shoulder is important because the pavement will not strain as much under good LTE conditions as it does under poor LTE conditions. In addition, the consistency of this type of testing is dependent on the temperature at which the test is conducted. The temperature at which the gauges were installed is called the baseline temperature. Any testing conducted at a temperature different than this temperature will be affected by thermal expansion or contraction. The farther the testing temperature is from the baseline temperature, the greater this effect will be. Finally, the time of day the testing is conducted is important because the curling stresses in a pavement in the morning are very different from the curling stresses in the same pavement in the late afternoon, even though the air temperature at the time of both tests is the same.

Secondary factors influencing the static test results include the bond of the gauge with the concrete and the bond of the pavement with the subbase. All of these factors, in combination with one another, made the static data variable.

For this reason, the static data will only be discussed briefly. The static data included in this summary have been selected for presentation because both the initial zero load reading and final zero load reading were the same. Fifty to 75 percent of the data recorded for each gauge met this criterion. Due to the questionable reliability of the static data, only a couple of typical sections are presented for review. These samples of the static data are shown in Figures 24A and 24B. From Figures 24A and 24B, it is clear that although the static data are variable, they can be close to the theoretical maximum strains predicted by ILLISLAB, the finite element computer model developed by the University of Illinois (15, 16).

## Dynamic Tests

The second type of testing, the dynamic testing, applied a moving load to the strain gauges and used a portable computer to read and record the

effects of the moving load on the strain gauges. Dynamic tests were conducted with an 18-kip single axle load passing over the gauges at 3 mph and 40 mph. A comparison of the data collected at both 3 mph and 40 mph is contained in Figures 25A and 25B. From this comparison, it is clear that the differences between the data collection at 3 mph and 40 mph are negligible; therefore, there will be no distinction between them in this report.

The dynamic data were recorded as voltage changes in millivolts from the strain gauges in the field. For analysis, the data had to be converted to microstrain. To do this, prior to conducting any dynamic testing, all of the gauges were calibrated. The calibration test consisted of recording the change in voltage each gauge experienced when subjected to a known increment of resistance. By calibrating each gauge independently, the need for a gauge factor correction was eliminated.

During the subsequent dynamic tests, 400 readings per second per gauge for the 40 mph tests and 100 readings per second per gauge for the 3 mph tests were recorded by the computer in ASCII files. For analysis, the ASCII files were then imported into worksheets and the following relationship was used to convert the data from millivolts to microstrain:

$$S = \frac{FS \times R}{C} \quad (\text{Equation 5})$$

where:

- S = Gauge Strain, microstrain
- FS = Field Strain, millivolts
- R = Increment of Known Resistance, microstrain
- C = Calibration Step Size, millivolts

The simplest method of comparing the theoretical strains to the dynamic strains recorded in the field was to compare their respective maximum change in strain values; therefore, the final step of the data reduction was to select the maximum change in strain recorded by each gauge for each test. After the data were converted to microstrain, the average gauge reading when no external loads were applied was approximately 450 microstrain. In order to calculate the maximum changes in strain, the average zero load reading was subtracted from all of the readings for each individual test. This resulted in wheel pulses or maximum changes in strain of approximately 40 microstrain. What is important about this procedure is the fact that the average zero load strain was subtracted from all readings for each gauge for each individual test. The average zero load reading was the strain due to curling stress and warping stress and even resistance of the wires connecting the gauges to the monitoring equipment. With these elements factored out, the field-measured strain changes are pure strains due to wheel loads on the pavement.

Perhaps the most difficult aspect of the dynamic tests was minimizing the interference from outside electronic noise. Electronic noise can come from high tension wires and radio signals and even from automobile ignition sparks (17). It was originally believed that high quality lead wires, connectors, and plugs would keep the outside noise problem to a minimum. Unfortunately, this was not the case. Instead, the early test data were covered with outside

noise and were virtually useless, as demonstrated in Figure 26A. Trends in strain increases could be distinguished from these data, but in-depth analyses were impossible. Eventually, the equipment was reground and high frequency filters were installed. These changes significantly improved the quality of the data, practically eliminating the interference from outside noise, as shown in Figure 26B. These improvements were not made until 1989, the last year testing was conducted. As a result, the only data presented and discussed in this report are the data collected in 1989.

The clarity of the measurements of the field strains was important to ensure that the strain selected for analysis was actually the maximum strain. Unlike the static data, the sheer volume of data recorded by this technique virtually guaranteed that the maximum strain was recorded. Figures 27A and 27B show both the dynamic and static field data. From these graphs it is clear that the static and dynamic data show the same general trends although they differ slightly in magnitude.

### Jointed PCC Data

Several factors must be considered when comparing the theoretical strains to the actual strains. First of all, it is important to note that under dynamic loading conditions, the modulus of the concrete pavement changes with respect to the dynamic load; however, ILLISLAB, the finite element computer model developed by the University of Illinois, is a static model.

In the field, the position of the applied load was critical to measuring the maximum strain during the dynamic tests. Logically, the maximum strain the pavement experiences is directly under the load; therefore, it follows that the load must pass directly over the gauge for the maximum strain to be recorded. Along with load location, the gauge location is also important. For the ILLISLAB theoretical values, it was assumed the strain gauges were one inch away from the top and bottom of the pavement. As discussed in the construction phase of this report, few top gauges were installed in Project 2, and the top gauges installed in Project 4 were installed by three different methods. Due to this fact, it is highly unlikely that the top gauges were all placed exactly one inch from the surface; however, the bottom gauges were placed on chairs exactly one inch off the subbase. By using chairs, the exact position of the bottom gauge was known. To minimize the potential for error in the analysis, the data recorded from the top gauges were not included in this analysis. Figure 28 contains a comparison of how vertical gauge location alone can affect the theoretical strains predicted by ILLISLAB.

The conditions of the pavement itself can also greatly influence the field data. Unfortunately, establishing values for the material properties is difficult. The concrete modulus of elasticity ( $E_{pcc}$ ) value for the pavement being tested had to be assumed as no direct measurements were taken at the time of strain gauge testing. For this analysis, the  $E_{pcc}$  of the pavement was assumed to be  $3.8 \times 10^6$  psi. A measurement of  $E_{pcc}$  for Project 2 was made in July of 1990 and for Project 4 in November of 1989. The  $E_{pcc}$  for Project 2 ( $5.8 \times 10^6$  psi) was significantly higher than the  $E_{pcc}$  for Project 4 ( $3.8 \times 10^6$  psi). Usually, the  $E_{pcc}$  is assumed to be approximately  $4 \times 10^6$  psi (17). From Figure 29, it is clear that the difference in

the two  $E_{pcc}$  values on the theoretical strain values is minimal, approximately 4 microstrain; therefore, the analysis for this report used an  $E_{pcc}$  of  $3.8 \times 10^6$  psi for both Projects 2 and 4.

In addition, the conditions of LTE between the mainline pavement and the tied concrete shoulder influence the predicted ILLISLAB strains. For this analysis, the LTE was assumed to be a conservative 60 percent. From the FWD data presented in Table 28C, the LTE at the time of construction was 80 percent or better. It is important to note that the better the LTE, the lower the theoretical strains will be. This relationship is shown in Figure 30.

The conditions surrounding the pavement also influence the field-recorded strains. As with the  $E_{pcc}$  for the pavement, the modulus of subgrade reaction ( $k$ ) must be assumed. The effect of the subgrade  $k$  values on the ILLISLAB theoretical values is depicted in Figure 29. For the following analysis, the  $k$  value was assumed to be 100 pci for both Projects 2 and 4. This value is in line with testing conducted during the construction of Project 4 (17). As discussed in the construction phase of this report, some of the sections on Project 2 were through rock cuts, which can significantly alter the subgrade characteristics. From Figure 29, however, it is clear that the value of  $k$  can be doubled to 200 pci with only a minimal impact on the theoretical strain values. By doubling the  $k$  value, the predicted maximum strain decreases only four microstrain.

Not only is it important to know the subgrade conditions, but the subbase also plays a major role in determining the shape of the theoretical strain graph. If the subbase is cracked at the joints, the slab will react much differently to applied loads than if it is not. In addition, if the subbase is bonded to the slab, the theoretical strains from ILLISLAB are greatly reduced, as depicted in Figure 31. The actual degree of bonding between the slab and the subbase was not known. For the theoretical calculation purposes, no bond was assumed, as this assumption was the most conservative. The modulus of elasticity ( $E$ ) of the subbase was assumed to be  $1 \times 10^6$  psi, since no actual test data were available.

Each of these variables alone has an effect on the theoretical strains; in combination, the variables have an undetermined effect on the theoretical strains. Different variable inputs will produce different theoretical strains. Because of this fact, the closeness of the measured field data and the theoretical strains depend on the ability of the modeler to define as accurately as possible the input variables. Although the exact values of these variables and the relationships between them are not known, educated estimates can be made which do yield reasonable results. It is important to note that, when faced with a choice, the conservative alternative was always selected for the theoretical calculations. If less conservative values for the LTE, pavement and subbase  $E$ , subgrade  $k$ , and extent of bonding conditions had been selected, the theoretical strain values would decrease. With the static data, unmodelable variables included temperature, time of day (curling stress), and degree of bonding of the gauge with the concrete. Although these variables are also unmodelable for the dynamic data analysis, they were factored out of consideration when the zero load strain was subtracted from the data.



## Jointed PCC Analysis

As discussed in the distress survey phase of this report, nearly all of the 40-foot JRCF panels cracked at mid-slab, resulting in an effective slab length of 20 feet. This illustrates the advantage of the hinge joint design because an inherent assumption of the hinge joint design is that the 40-foot slabs will crack. Tie bars are required in the hinge joint design to hold the cracks together. Because all of the 40-foot slabs cracked, the testing conducted in 1989 centered around the 20- and 15-foot JPCF sections. Other researchers have tested the 40-foot JRCF slabs in cooperation with IDOT and compared the measured strains to those predicted by ILLISLAB (18). In their analysis, the 40-foot JRCF slab was modeled as two 20-foot slabs with a weak joint. The researchers were successful in obtaining similar values for the measured field and theoretical ILLISLAB data.

For the analysis in this report, several ILLISLAB-generated strain measurements were calculated for the different thicknesses of the JPCF sections. Strain measurements for slab lengths of 13.3, 15, and 20 feet for both hinge and dowel joints were graphed together. The LTE inputs into ILLISLAB were assumed to be the same for both the hinge and dowel joints. This is a valid assumption because the FWD-measured LTE for both joint types were virtually identical, as discussed previously and presented in Tables 27B and 28B for Projects 2 and 4, respectively. The following summary highlights the results of the analysis.

### Mid-Slab Gauges

Figures 32A through 32C contain the comparisons of the predicted theoretical strains to the measured field strains for the mid-slab gauges for slab thicknesses of 10, 9.5, and 7.5 inches, respectively. These gauges are located in the middle of the slab, between the joints as shown in Figures 22 and 23. All of the theoretical strains are greater than the measured field strains. The strains recorded in the field for the loads applied 18 inches away from the edge of pavement are consistently closer to the theoretical strains than those located on the edge of the pavement because the effect of LTE diminishes as the load is moved away from the shoulder. Figure 30 demonstrates the effect of LTE on the theoretical edge strains as a function of pavement position.

### Quarter-Slab Gauges

Figures 33A through 33C contain the comparisons of the theoretical strains to the field-measured strains for the quarter-slab gauges for slab thicknesses of 10, 9.5, and 7.5 inches, respectively. These gauges are located one-quarter of a slab length away from the leave side of the slab. For both the 9.5- and 7.5-inch thick slabs, only data from the 20-foot slab sections were available because the quarter-slab gauges for both the 13.3- and 15-foot JPCF sections could not be stabilized. The theoretical values for the quarter-slab gauges are slightly less than those for the mid-slab gauges since the

quarter-slab gauges are closer to the joint, where there is additional structural support. Albeit minor, the field data appears to mirror this slight decrease in strain.

### Hinge Joint Gauges

Graphs of the data from the gauges located on joints are included in Figures 34A through 34D. Both the theoretical and measured strains shown in these graphs are significantly lower than the measured strains at the quarter-slab and mid-slab locations because they are located within 6 inches of a joint. Figures 34A and 34B contain the data for the gauges located on the corners of the slabs. The data in Figures 34C and 34D are the data for the gauges installed on the hinge joint, but 6 and 36 inches away from the edge of the pavement.

### CRCP Data

Most of the same factors that affected the field data of the JPCP sections also affected the data recorded in the CRCP sections. These factors included load location, gauge location, subgrade k value, pavement and subbase E values, percent of load transfer, and degree of subbase bonding. Along with these variables, the CRCP field data were also dependent on aggregate interlock, crack spacings, and gauge distance from cracks. For the analysis included in this report, aggregate interlock values of  $10^2$  (less than 5 percent LTE) and  $10^6$  (98 percent LTE) are presented on all CRCP strain comparisons. These two values were chosen because it is impossible to measure the degree of aggregate interlock accurately, and, logically, the field data should fall somewhere between these two values.

The importance of crack spacing is depicted in Figures 35 and 36. Figure 35 depicts the effect crack spacing has on the strains measured by the longitudinal strain gauges, and Figure 36 depicts the effect crack spacing has on the strains measured by the transverse gauges. An average aggregate interlock of  $10^4$  (60 percent LTE) was used in generating the theoretical values included in these graphs.

In conjunction with the crack spacing, the distance between the gauge and the closest crack is important. If a gauge is directly between two cracks it will strain differently than a gauge located within a few inches of a crack. Gauges within a few inches of a crack will show only minimal signs of strain, similar to those gauges located on a joint. Conversely, if the gauge is located between two cracks, it will experience strains similar to the gauges located in the middle of a slab on a jointed PCC pavement.

### CRCP Analysis

Several ILLISLAB-generated strain measurements were calculated for the different thicknesses of the CRCP sections. The following summary highlights the results of the analysis.

### Longitudinal Edge Gauges

Figures 37A through 37C contain the comparisons of the theoretical strains to the field strains for the longitudinal edge gauges. The longitudinal gauges were located a few inches in from the pavement/shoulder joint and were parallel to the pavement/shoulder joint. Depending on the degree of aggregate interlock and crack spacing, the data correlate anywhere from fair to good with the theoretical data. Due to the number of pavement condition possibilities, it is very difficult to analyze these data accurately. For the longitudinal edge gauges, the effective slab size is more important to the accurate predictions of strains than the degree of aggregate interlock. The field strains were closer to the theoretical strains generated for a 2-foot crack spacing than for the 4- or 6-foot crack spacings.

### Transverse Gauges, 36 Inches from the Edge of Pavement

Figures 38A through 38C contain the comparisons of the theoretical strains to the field-measured strains for the transverse gauges. The transverse gauges are located 36 inches from the edge of pavement and are perpendicular to the edge of pavement. Pavement sections containing these gauges have the potential to act as cantilevered sections; therefore, some of the theoretical values can be negative strain. As with the pavement sections containing longitudinal gauges, these sections have a number of pavement condition possibilities; therefore, it is difficult to do an in-depth analysis or comparison to theoretical values. However, the field-measured strains do appear to mirror the theoretical strains.

### Hinge Joint Movements

Three hinge joint PCC pavement cross sections, as shown in Figure 3, were constructed on Projects 2 and 4. The purpose of these designs was to control the mid-panel cracking of PCC slabs. A number of states have adopted the policy of requiring short slab lengths of less than 20 feet. This controls mid-panel cracking, but results in more contraction joints, which can lead to maintenance and ride quality problems. Hinge-jointed pavements employ dowel joints to relieve stresses from contraction and expansion and at the same time provide load transfer. To provide longer spacing between the doweled contraction joints, yet control the panel cracks, the hinge joint designs induce cracks at either mid-slab or at third points with saw cuts one-third the thickness of the slab. Thirty-six-inch long #6 epoxy coated tie bars are spaced on 18-inch centers to provide extra reinforcement at these induced cracks, which are known as hinge joints. The saw-induced crack is uniform and can easily be sealed.

Early investigations of the hinge-jointed sections were limited to visual inspections for panel cracks. After 2.5 years, a few cracks in Project 4 were observed in Section DB. As discussed in the **Distress Survey** section of this report, these cracks were attributed to the lack of attention to joint details in an intersecting PCC pavement and not the hinge joint design.

In order to monitor the slab movements in the hinge joint sections better, a simple joint opening measuring system was used on the sections on Project 2. Due to the cracked panels and potential traffic control problems in the intersection, Project 4 was not monitored. As part of the monitoring equipment, small brass plugs were grouted into drilled holes on both sides of the dowel and hinge joints in Sections G1, G2, and G3. A Whittmore gauge, which can be read to 0.0001-inch, was used to measure the distance between the plugs. Readings of both dowel and hinge joint openings were taken in May, August, and December of 1989. Periodically during testing, pavement surface temperature readings were made with an infrared temperature gun. Pavement temperatures 1 inch from the top and bottom of the slab were recorded from thermocouples installed in the slab. Air temperatures were also measured periodically during testing.

Figures 39A and 39B are plots of air temperature versus joint opening for dowel and hinge joints, respectively. Figure 39A shows approximately a 0.10-inch difference in dowel joint opening widths between the summer and winter measurements. Although the dowel joint openings are quite small, it is nonetheless apparent that the dowel joints are freely moving, opening and closing in response to the slab's thermal contractions and expansions. Figure 39B shows approximately a 0.01-inch difference in hinge joint opening widths between the summer and winter measurements. The hinge joints experience much smaller variations in joint openings than dowel joints over the same temperature span. This is to be expected since the tie bars at the hinge joint restrain slab expansion and contraction, whereas the dowels at the dowel joint permit expansion and contraction. Variations in joint opening at hinge joints reflect the curling stresses and strains that develop in the slab as a result of temperature differentials between the top and bottom of the slab.

The slope of the lines on the air temperature versus dowel joint opening graph becomes flatter at higher temperatures, as shown in Figure 39A. Smaller movements are noted at the higher temperatures since slab expansion has caused the joint to close, thereby creating compression in the slab.

Figures 40A and 40B are plots of the pavement mid-depth temperature versus joint opening for dowel and hinge joints, respectively. The pavement surface temperature, obtained with an infrared temperature gun, and the pavement temperatures 1 inch from the top and bottom of the slab, obtained from thermocouples, were plotted as a function of slab depth. The temperature corresponding to the 5-inch depth was calculated and used as the pavement mid-depth temperature. Concrete slabs experience temperature gradients, so a plot of air temperature versus joint opening can be somewhat misleading. The pavement mid-depth temperature is a more consistent value during temperature fluctuations than the air temperature. Figures 40A and 40B mirror the trends noted for Figures 39A and 39B, but the movements are somewhat more pronounced since they occur over a smaller temperature range. This is especially evident on Figure 40A, since the dowel joints experience more movement than the hinge joints.

Dowel and hinge joint movements will continue to be monitored. Future plots of temperature versus joint opening that resemble the baseline graphs shown in Figures 39A through 40B will indicate that the dowel and hinge joints are performing as expected. Dowel joints that in the future show little movement over a range of temperatures will be an indication of frozen joints.

The hinge joints that start to show a wider range of movement over a range of temperatures will be an indication that the tie bars have failed and the "controlled crack" hinge joints have developed into working cracks.

## Moisture Monitoring

### Underdrain Outflow

The monitoring of the outflow from the underdrain systems was confined to Projects 3 and 4. A total of four different cross sections, with grades of 0.4 percent or less, were studied. The study in the PCC sections centered around the effectiveness of the longitudinal joint sealant. Data was collected on 7.5-inch and 8.5-inch thick, 20-foot and 40-foot jointed PCC pavement sections (Sections CA, EA, LA, and MA) and 8-inch thick CRCP sections (Sections S and T).

For the full-depth AC sections, the study focused on AC thickness and the use of a lime-modified subgrade. The control section for this experiment was 12.5 inches of full-depth AC on a lime-modified subgrade (Section I) while the test section was 9.5 inches of full-depth AC on an untreated subgrade (Section K).

Two pairs of outflow meters were used to monitor the test sections. One pair was used on the full-depth AC sections and one pair was used on the PCC sections. The tipping bucket outflow meters were first installed on the 20-foot JPCP and full-depth AC sections in April 1987. Originally, the intent was to collect the outflow data at the site and compare it to the rainfall data collected at the Belleville and Carlyle weather stations. Unfortunately, this rainfall data was too general for a detailed analysis because the weather stations were several miles away from the test sites; therefore, a rain gauge was installed on Project 4 in April 1989. The rain gauge allowed researchers to precisely determine the time between the start of a rainfall and the start of underdrain outflow, which is called the lag time.

At the same time the rain gauge was installed, a survey of the condition of the edge joint sealant in the 20-foot JPCP test section was conducted. More than 25 percent of the test section edge joint sealant failed prematurely, as discussed earlier in the **Construction** section of this report. No other suitable sections could be found to continue the evaluation of the 20-foot JPCP section, thus the outflow meters were moved to the 40-foot JRCP test sections. After recording several rainfalls in June 1989, the outflow meters were moved to the CRCP test sections. The equipment was left there until adequate data for evaluation had been collected. In September 1989, the rain gauge was moved to the full-depth AC section that had been monitored with outflow meters since April 1987.

The total amount of rainfall and outflow data collected was extensive. The data have been reduced to the maximum outflow, average lag time, and average recovery time for each site in Table 29. From Table 29 it is clear that there is only a minimal difference between the outflows in the two 20-foot JPCP sections. A comparison of the effectiveness of using edge joint sealant cannot be made from the data collected in the 20-foot JPCP section because of the improper construction. There is reason to suspect that the sealed section acted like the unsealed section because there were many areas

of sealant failure. Figures 41 and 42 contain typical graphs of outflows from the 20-foot JPCP sections.

A fair comparison of the data collected from the 40-foot JRCP sections was possible. Typical data for these sections are included in Figure 43. After the rain gauge was installed, nine rainfalls were recorded. Usually, there was an hour lag time from the start of a rainfall until water flowed from the underdrains. The peak outflow from the two sections was always recorded in the same hour. The sealed section, however, always recovered to 0.5 gallon per hour outflow or less 24 hours prior to the unsealed section. Hourly and total outflow volumes from the sealed section were approximately one-half the volume of the unsealed section outflow.

The data collected in the CRCP test sections ranged in total rainfall from 0.04 to 1.99 inches. With all but the lowest rainfall intensities, peak outflows occurred in the same hour for both the sealed and unsealed sections. As with the 40-foot JRCP sections, there was a 1-hour lag time from the start of the rain to the start of outflow from the underdrains. The sealed section outflows always recovered to 0.5 gallon per hour or less in 24 hours or less, while the unsealed section took 24 to 36 hours. Total outflows from the sealed test section were approximately 70 percent the volume of the unsealed section outflows. Figure 44 contains typical data for these sections.

Simultaneous testing was not carried out between the CRCP, 20-foot JPCP, and 40-foot JRCP sections. Even so, it was apparent that for a given rainfall intensity, less water flowed out from the CRCP section underdrains than the 20-foot JPCP or 40-foot JRCP section underdrains. Along the same lines, the outflow from the 40-foot JRCP section was less than the 20-foot JPCP. Although all of the transverse joints were sealed, these observations indicated the sealed joints were not entirely impermeable to water.

The full-depth AC sections were the only sections that were monitored continuously from April 1987 to November 1989. The most significant observation that can be made from these data is that the outflows decreased over time. The maximum outflow was 409 gallons of water in one hour and was recorded in the 12.5-inch lime-modified section in 1987. The maximum outflow in 1989 was 69 gallons in the same section. Since the rain gauge was not installed until 1989, it is impossible to compare the rainfall intensities for these dates; however, an additional 14 readings over 300 gallons of water in one hour were also recorded in 1987. It is theorized that the diminishing outflows over the last few years are a result of either the action of traffic sealing the surface of the asphalt concrete pavement, the sealing of the pavement/subgrade interface, or the clogging of the underdrain fabric wrap. Most likely, the answer lies in a combination of these.

A comparison of the 12.5-inch thick AC on lime-modified subgrade section to the 9.5-inch thick AC on untreated subgrade section shows that the 12.5-inch section always had a higher peak outflow than the 9.5-inch section. In addition, the 12.5-inch section always stopped flowing water prior to the 9.5-inch section. Even though the 9.5-inch section flowed slower, in the long run it consistently flowed more water. During the summer months, the 9.5-inch section continued to have outflows weeks after the last rainfall. The 12.5-inch section also followed this pattern though to a much lesser degree. Figure 45 contains typical data for the full-depth AC sections.

## Subgrade Moisture

A nuclear moisture gauge was used to measure seasonal subgrade moisture variations at selected sites on Projects 3 and 4. Table 30 lists these gauge locations and site descriptions. For the first year, moisture data was collected at three-month intervals, and annually in the spring thereafter. A complete explanation as to the operation of the nuclear moisture gauge is included elsewhere (5) and will not be discussed in this report.

Once paving operations were completed, the holes for the access tubes, from which the moisture readings would be made, were constructed by coring through the pavement and driving Shelby tubes into the subgrade. The access tubes consisted of 2-inch thin wall standard galvanized steel tubing, which extended 10 feet under the pavement surface. Prior to installation, the lower end of the access tube was capped with a metal plug and sealed with a silicone sealant. Since the tubing provided a tight fit with the existing soil, no backfill material was required. The tubing was grouted in-place in the pavement. To provide a watertight non-obstructive covering for the access tube, a rubber stopper was inserted into the top of the tubes and a removable standard cast iron sewer clean-out was screwed into the top of the tube with petroleum jelly applied as a water repellent. Figure 46 shows a cross section of a moisture access tube installation.

To obtain readings, the cast iron cap and rubber stopper were removed, and the probe was lowered into the access tube to the desired depth. Cable stops were marked on the gauge such that readings could be made at the following depths from the pavement surface: 19.5, 25.5, 31.5, 37.5, 43.5, 49.5, 61.5, 79.5, 97.5, and 115.5 inches. Readings of one minute in length were taken at these depths to establish a pavement moisture profile for the various cross sections.

The nuclear moisture gauge used on FA 409 was primarily designed for agriculture use; therefore, it read volumetric water content. Volumetric water content is defined as:

$$\theta = (V_w/V_t) \times 100 \quad (\text{Equation 6})$$

where:

$\theta$  = Volumetric water content, %

$V_w$  = Volume of water in sample

$V_t$  = Total volume of sample

Most civil engineers are more familiar with gravimetric water contents. The two are related by this equation:

$$\theta = (Y_d / Y_w) \times \omega \quad (\text{Equation 7})$$

where

$\theta$  = Volumetric water content, %

$Y_d$  = Dry unit weight of soil

$Y_w$  = Unit weight of water

$\omega$  = Gravimetric water content, %

The early moisture readings were suspect because there was only minimal variation in moisture contents in relationship to depth and season at a given location. The moisture gauge was rechecked by the manufacturer and was found to be in good working order. Further investigations revealed that the gauge had been calibrated using a sandy soil containing no significant minerals or organic material. The soils reports for both projects showed that the soil type was not sandy, but a silty clay; thus, it was decided to perform a field calibration.

The field calibration process took place in the fall of 1987. Two cores were taken for new moisture tube locations, one in the 12.5-inch full-depth AC pavement section and one in the 7.5-inch jointed PCC pavement section. Shelby tubes were driven in these cored locations and the samples were tested in the laboratory for moisture content. The laboratory-determined moisture contents were compared to the nuclear gauge readings taken in the field, and a new calibration was developed from the results for both the full-depth AC and the jointed PCC pavement sections. The field calibrations differed significantly from the laboratory-determined calibration. Using the new field calibrations, the subsequent readings demonstrated the expected moisture profiles. The readings recorded prior to recalibration were revised using the field calibrations.

At any access tube location in the jointed PCC and full-depth AC sections, moisture changes with depth appeared to be fairly uniform with the seasons. The general shapes of the moisture-depth curves were the same from season to season. At two sets of locations in the jointed PCC and full-depth AC pavement sections, multiple access tubes were installed across the pavement. At the jointed PCC test sites, access tubes were installed at the centerline, in the outer wheelpath, at the pavement/shoulder joint, and in the shoulder of the westbound lane. At the full-depth AC test sites, access tubes were installed in both the inner and outer wheelpaths as well as the shoulder of the westbound lane. The variation of moisture readings across the pavement is summarized below.

#### 8.5-inch JPCP, underdrains, unsealed edge joint

The outer wheelpath was consistently the wettest to a depth of 40 to 45 inches below the pavement surface. Below that point, no clear trends were apparent. The largest difference in volumetric water contents across the pavement was only 3.5 percentage points. These two trends are shown in Figures 47A to 47D.

#### 8.5-inch JPCP, no underdrains, unsealed edge joint

The readings taken at the edge and in the outer wheelpath were consistently the wettest readings recorded at virtually all depths. Slightly more



variation in moisture content across the pavement was noticed in the section without underdrains than in the previous section with underdrains. Figures 48A to 48D show these trends.

#### 12.5-inch full-depth AC, underdrains, lime-modified subgrade

The inner wheelpath was consistently the wettest area in this test section to a depth of 19.5 inches. No pattern is discernible below that depth. The maximum variation in volumetric water contents across the pavement occurred at a depth of 31.5 inches. Beyond this depth, the moisture readings across the pavement show a much smaller spread, as is shown in Figures 49A, 49B, and 49C.

#### 12.5-inch full-depth AC, no underdrains, lime-modified subgrade

No trend in moisture content across the pavement was noted in this cross section. Maximum variations in volumetric water contents across the pavement ranged from 5.1 to 8.6 percentage points, and occurred at depths of 25.5 to 49.5 inches below the pavement surface. These relationships are shown in Figures 50A, 50B, and 50C.

Overall, the full-depth AC sections demonstrated wider variations in moisture contents across the pavement than the jointed PCC sections. This may have been a result of the relatively permeable nature of an asphalt concrete surface as compared to a PCC surface. There was no single location across the pavement in the full-depth AC sections that was uniformly the wettest; however, in the jointed PCC sections, the outer wheelpath and edge locations were predominantly wetter than the centerline or shoulder locations. This is probably due to the unsealed pavement/shoulder joints.

The subgrade moisture readings also provided information on the effectiveness of the longitudinal edge drains. A comparison of locations, varying only by the presence or absence of longitudinal underdrains, is discussed below:

#### 8.5-inch JPCP unsealed edge joint (edge of pavement location)

The section without underdrains had volumetric water contents 1 to 3.5 percentage points greater than the section with underdrains to a depth of 43.5 inches. Below that point, the section with underdrains was slightly wetter, as shown in Figure 51.

#### 8.5-inch JPCP sealed edge joint (edge of pavement location)

The section with underdrains had volumetric water contents as much as 18 percent greater than the section without underdrains to a depth of 49.5 to 61.5 inches. Below this point the section without underdrains was slightly wetter, as shown in Figure 52.

12.5-inch full-depth AC lime-modified subgrade (outer wheelpath location)

Volumetric water content readings 19.5 inches below the pavement surface were 3.5 to 11.5 percentage points wetter for the section without underdrains than the section with underdrains. Below this point, the moisture contents varied between the underdrain and no underdrain sections by 0.3 to 5.5 percentage points, as shown in Figure 53.

9.5-inch full-depth AC, lime-modified subgrade (outer wheelpath location)

The section with underdrains had volumetric water contents as much as 31 percentage points wetter than the section without underdrains for 70 to 80 percent of the readings, as shown in Figure 54.

The results of the effectiveness of underdrains on controlling subgrade moisture were mixed. From this study, there is no conclusive evidence that longitudinal underdrains were successful in removing water from beneath the pavement with any degree of consistency.

The moisture content readings also assisted in evaluating the effectiveness of the pavement/shoulder sealant. The following comparisons were made for the PCC sections.

8.5-inch JPCP, no underdrains (edge of pavement location)

The section without the pavement/shoulder sealant was uniformly wetter than the section with sealant to a depth of 55 inches. The difference in the volumetric water contents was as much as 8 to 16 percentage points at the maximum point. Below this point, there was no distinguishable difference. This relationship is shown in Figure 55.

8.5-inch JPCP, underdrains (edge of pavement location)

The results from this comparison were mixed. The general shape of the moisture-depth curves were consistent over the range of test dates; however, on any given test date, the sealed section was sometimes wetter and sometimes drier than the unsealed section. This variation depended on the depth of the reading, as shown in Figure 56. The inconsistency in the readings was most likely the result of poor sealing techniques as discussed in detail previously.

In general, the proper use of a pavement/shoulder edge joint sealant does seem to have a positive effect on controlling the moisture content of the subgrade.

Frost Depth Data

To determine the influence of AC layer thickness, subgrade lime-modification, and underdrains on frost penetration, a simple experiment was developed. Near the completion of construction of Project 3, access tubes for frost gauges were installed in the outer wheelpath, 50 feet from moisture

access tube locations. The frost gauge installation is shown in Figure 57. Two gauges were installed in the 9.5-inch full-depth AC pavement and two in the 12.5-inch full-depth AC pavement.

The gauges were placed in the access tubes for the first time on November 20, 1986. The frost penetration below the top of the pavement was periodically recorded. All of the collected data are summarized in Table 31. Due to an unusually mild winter, no readings were taken during the winter of 1986-1987.

From the limited data collected on Project 3, no significant distinction between pavement cross sections versus frost penetration can be made.

## Surface Response Monitoring

### Ride Quality

The ride quality indexes of all four projects have been monitored since construction was complete. Early ride quality measurements were taken with the Department's Roadometer, which was patterned after the Bureau of Public Roads Roadometer. In 1990, the Department started using a road profiler patterned after South Dakota's Road Profiler to measure roughness. Both devices measure surface roughness in inches per mile, but they use different scales to determine the adjective rating. All test results corresponded to an adjective rating of smooth to very smooth. There has been no indication of a significant decrease in the overall ride quality of any of the projects. Summaries of the projects' average roughness indexes are included in Tables 32 and 33A through 33D. The results immediately after construction compare favorably with statewide averages for like pavements constructed between 1977 and 1987 (19).

### Friction

Both treaded and smooth tire friction tests have been performed periodically on all four projects. All of the projects and individual test sections continue to provide adequate frictional resistance to skidding. The results are shown in Tables 34 and 35. The average treaded tire friction number for Projects 1, 2, 3, and 4 have been 52, 63, 50, and 64, respectively. The average smooth tire friction number for Projects 1, 2, 3, and 4 have been 40, 62, 34, and 59, respectively. These numbers compare favorably with conventional pavements of similar age constructed between 1980 and 1986 (20).

## Maintenance

The major maintenance performed to date has been the full-depth AC patching in Sections K, M, and MI that was detailed previously under **Patching Efforts**. It was IDOT's intent to keep detailed maintenance activity records on Projects 1, 2, 3, and 4. The various pavement sections have been signed in the field for use with IDOT's Maintenance Management Information System (MMIS). This system enables the Bureau of Maintenance to collect maintenance needs, develop an annual work program, provide annual and monthly work plans, report performance and costs, and evaluate work accomplished. At this time, however, detailed reports of maintenance performed on Projects 1, 2, 3, and 4 were not available.

## COSTS

The final construction costs are included in Table 36. An economic analysis of each project was not included as part of this study because the main purpose of this study was to evaluate the proposed mechanistically-based design procedures for both full-depth AC pavements and PCC pavements with tied shoulders. It would be erroneous to compare these completion costs with the costs of a typical pavement constructed in 1986 due to the extensive instrumentation placed within each project.

## ANALYSIS

There were four main objectives detailed in the work plan for this experimental features study. The first objective was to compare measured load-deflection responses of full-depth AC pavements to those predicted by the proposed mechanistically-based design procedure developed by the University of Illinois (1). In conjunction with this objective, the effects of various AC thicknesses, the utilization of underdrains, and the benefits of a lime-modified subgrade on pavement performance were also to be determined. The second objective was to compare measured strains and deflections of PCC pavements with tied shoulders to those predicted by the proposed mechanistically-based design procedure developed by the University of Illinois (2). In conjunction with this objective, the effects of various slab thicknesses, the utilization of underdrains, and the benefits of joint sealant on pavement performance were to be determined.

The third objective was to evaluate the effect of asphalt cement viscosity grades AC-10 and AC-20 on the performance of full-depth AC pavements. The fourth objective was to evaluate the effect of joint spacings of 40, 20, and 15 feet and 3 hinge joint designs on the performance of PCC pavements with tied shoulders. The instrumentation and the performance monitoring efforts described previously were undertaken to meet these four objectives. The following analyses address the objectives and how they were met.

### Objective 1

The original intent of the experimental features study was to compare measured load-deflection responses in full-depth AC pavements to responses predicted by the proposed mechanistically-based design procedure (1). However, these demonstration projects were not instrumented in such a fashion as to be able to document such a claim. Low voltage transformers (LVT) would have been required to be placed in the pavement structure to determine the measured load-deflection responses. The two main design variables in the proposed procedure are AC thickness and  $E_{AC}$ . The ability of these two variables to relate to the design model is more critical than measured load-deflection responses. The analysis of Objective 1 will therefore concentrate on the effects of AC thickness, utilization of underdrains, and the benefits of lime-modified subgrade on pavement performance. The effect of  $E_{AC}$  will also be addressed.

### AC Thickness

Project 3 was the only project on which variations in AC thickness were included; therefore, this analysis will concentrate only on Project 3. Two thicknesses, 9.5 and 12.5 inches, of AC-10 pavement were constructed, and three thicknesses, 9.5, 11, and 12.5 inches, of AC-20 pavement were constructed.

Thermal cracking, fatigue cracking, and rutting are key indicators of full-depth AC pavement performance. Deflection testing with the FWD also provides an indication of performance. An examination of Table 15B, which summarizes the results of the 1992 distress survey, shows that Sections A and B, the 9.5-inch AC-10 sections, are exhibiting more transverse cracking than Sections C and D, the 12.5-inch AC-10 sections. Neither the 9.5-inch nor 12.5-inch AC-10 sections are exhibiting fatigue cracking at this time. The rut depths for these sections, shown in Tables 21A through 21D and 22B, have been consistently comparable. Deflection data from Tables 24A through 24G show slightly higher deflections under the load and slightly lower deflection basin areas in the 9.5-inch AC-10 sections. Although the 9.5-inch and 12.5-inch AC-10 sections are all performing quite well, these findings display the expected trend of increased structural performance with increased AC thickness.

The AC-20 sections show similar trends. The 12.5-inch thick sections, E, H, and I, showed no signs of transverse or alligator cracking in the 1992 distress survey. The 11-inch thick Section P had a nominal amount of transverse cracking and a small percentage of alligator cracking. The 9.5-inch thick sections, J, K, L, M, M1, N, and O, showed more transverse and alligator cracking, some of which required maintenance patching as discussed previously. The rut depths for the 11- and 12.5-inch sections have been consistently comparable, averaging 0.21-inch for the 11-inch sections and 0.25-inch for the 12.5-inch sections in 1992. The average rut depth for the 9.5-inch thick sections was 0.30-inch in 1992. The deflection data showed that the 12.5-inch sections consistently had the lowest deflections under the load and the highest deflection basin areas, indicators of better pavement performance. The 9.5-inch sections consistently had the highest deflections under the load. The 9.5-inch sections consistently had lower deflection basin areas than the 12.5-inch sections; however, the 11-inch sections had lower deflection basin areas than the 9.5-inch sections. Although these findings generally display the expected trend of increased structural performance with increased AC thickness, one important qualification should be noted.

All of the AC-10 sections and all of the 11-inch and 12.5-inch thick AC-20 sections were constructed on lime-modified subgrade, but approximately 50 percent of the 9.5-inch AC-20 sections were constructed on untreated subgrades. Increased fatigue cracking and rutting in the 9.5-inch AC-20 sections may well be a function of the untreated subgrade. The quality of construction on a lime-modified subgrade is higher than the quality of construction on an untreated subgrade. Without lime-modifying the subgrade, the structural integrity of the full-depth AC layer can be diminished during construction. The effect of AC thickness on pavement performance is not as clear in the AC-20 sections due to the obscuring effect of the untreated subgrades.

## Underdrains

Project 1 used underdrains in areas of soil foundation and not in areas of rock cuts. Since their use was irregular throughout the project, this analysis concentrated on Project 3 to determine the effect of underdrains on pavement performance. Figure 6 details the test section layout of Project 3 and identifies the sections which had underdrains. The presence of underdrains should result in less subgrade moisture and a corresponding higher  $E_{Ri}$ .

Two types of data were analyzed to determine the effect of underdrains on pavement performance: FWD data and subgrade moisture measurements. Table 37 compares FWD backcalculated  $E_{Ri}$  values for Project 3 sections with and without underdrains. The average spring  $E_{Ri}$  value for sections with underdrains was 6.35 ksi, compared to 6.27 ksi for sections without underdrains. The average fall  $E_{Ri}$  value for sections with underdrains was 7.59 ksi, and the average fall  $E_{Ri}$  value for sections without underdrains was 6.99 ksi. These data suggest that underdrains have little effect on  $E_{Ri}$ .

The subgrade moisture readings also provided information on the effectiveness of underdrains, although the results were mixed. In the 12.5-inch thick sections, the volumetric water contents directly below the pavement surface were higher in the section without underdrains, indicating that the underdrains were successfully removing water from the subgrade. In the 9.5-inch thick sections, however, the volumetric water contents were much lower in the section without underdrains. Based on these results, there was no conclusive evidence that underdrains were successful in removing water from beneath the pavement with any degree of consistency.

Sections exhibiting fatigue cracking in the 1992 distress survey were K, M, M1, N, O, and P; Sections K, N, and P had underdrains, while M, M1, and O did not. The presence of fatigue cracking in these sections seemed to be more a function of AC layer thickness and lack of lime-modified subgrade, as described previously, rather than a function of the presence or absence of underdrains.

Since the data did not indicate that underdrains were consistently successful in removing water from beneath the pavement or in improving the  $E_{Ri}$ , it did not appear that underdrains had a measurable effect on pavement performance.

## Asphalt Cement Viscosity Grades

Both Projects 1 and 3 used AC-10 and AC-20 grades of asphalt cement. Since an AC-10, by definition, has a lower viscosity than an AC-20, an AC-10 should provide increased protection against thermal cracking. An AC-20 should provide increased resistance to rutting since it is a stiffer grade of asphalt cement.

After six years of service, both Section A (AC-10) and Section B (AC-20) on Project 1 showed little signs of thermal cracking. The hand-measured 1992 rut depth data showed approximately twice the amount of rutting in the AC-10 sections as the AC-20 sections. Although these data exhibited the expected increased viscosity/decreased rutting trend, two points must be noted: 1) the 1992 hand-measured rut depth data were a very small sampling, and 2) the rut depths all averaged less than 0.15-inch. The 1992 rut depths collected by the

road profiler all averaged less than 0.10-inch and showed little variation between the AC-10 and AC-20 sections. The data indicated that after six years of service, little difference in pavement performance between the AC-10 and AC-20 sections on Project 1 could be noted.

A comparison of pavement performance between AC-10 and AC-20 sections on Project 3 was somewhat more illustrative. On Project 3, Sections A, B, C, and D were constructed with an AC-10, and Sections E, H, I, J, K, L, M, M1, N, O, and P with an AC-20. The 1992 distress summary shown in Table 15B noted considerably more transverse cracking per lane-mile in the AC-20 sections than in the AC-10 sections. The average 1992 hand-measured rut depth in the AC-10 sections was 0.17-inch and in the AC-20 sections was 0.27-inch, contradictory to the expected trend of increased viscosity and decreased rutting. The hand measurements were taken with greater frequency in areas of noticeable rutting, however, so the data were somewhat skewed. The average 1992 road profiler rut depth in both the AC-10 and AC-20 sections was 0.24-inch, as shown in Table 38. These data would suggest little difference in rutting potential as a function of asphalt cement viscosity.

A more probable explanation for the increase in transverse cracking in the AC-20 sections and the apparent similarity in rutting potential between the AC-10 and AC-20 sections is the presence of failed pavement in the AC-20 sections. The full-depth patching required in the AC-20 Sections K, M, and M1, as summarized in Table 18, manifested itself in the form of increased cracking and rutting. Field surveys have indicated the potential need for additional patching in these sections because of cracking and rutting. The poor performance of these sections is less a function of the grade of asphalt cement used than a function of moisture damage and soft subgrades. Long-term monitoring will be required to determine if asphalt cement viscosity has an effect on the performance of these projects.

### Lime-Modified Subgrade

Lime-modified subgrades were not used on Project 1, so this analysis was limited to Project 3. All of the AC-10 sections were constructed on lime-modified subgrade. Of the AC-20 sections, only 2 sections were constructed on untreated subgrades. Sections K and M1 were constructed of 9.5 inches of full-depth AC on an untreated subgrade. Sections K and M1 both exhibited transverse and alligator cracking in the 1992 distress survey. The 1992 profiler rut depths averaged 0.32 inch in Section K and 0.21 inch in Section M1; Section K was above the overall AC-20 average rut depth of 0.24 inch. The beneficial effect of lime-modified subgrade is probably best illustrated by the fact that 2 of the 3 sections requiring patching were constructed on untreated subgrades. The decreased level of performance in Sections K and M1 cannot solely be linked to the absence of lime-modified subgrade since Sections M, N, O, and P also showed signs of transverse and alligator cracking and rutting in spite of having a lime-modified subgrade.

The quality of the subgrade, whether lime-modified or not, has a large impact on pavement performance. Soft subgrades provide a poor construction platform on which to compact full-depth AC, and can lead to increased subgrade

deformations and decreased pavement performance. A survey of the FWD data for Project 3, summarized in Tables 24A through 24G, showed that Sections B, K, L, and M consistently had the lowest backcalculated  $E_{ri}$ . Sections B and K were among the sections with the highest amount of rutting. Sections K and M both had alligator cracking and required patching. Section L did not show any cracking or significant rutting as of the 1992 survey. Based on these relatively short-term results, the importance of adequate subgrade support has been shown. Pavements constructed on lime-modified subgrade did develop rutting and alligator cracking, as in Sections B, M, N, O, and P. However, the lime-modified subgrade usually has a higher modulus than an untreated subgrade, which provides a stable construction platform on which to compact full-depth AC pavements. Better compaction during construction decreases the potential for permanent subgrade deformations.

### EAC

As discussed previously in the **Full-Depth AC Deflection Testing** section of this report,  $E_{AC}$  values could not be backcalculated on Project 1 due to the presence of a rock foundation. The accuracy of backcalculated  $E_{AC}$  values from FWD testing on Project 3 was questionable due to the presence of moisture damage and patched pavement. A plot of  $E_{AC}$  backcalculated from FWD testing as a function of pavement age was shown in Figure 21. The data were normalized to the 82°F design temperature. The data showed a slight decrease in  $E_{AC}$  over time, indicating a weakening of the asphalt concrete. However, the algorithms designed to backcalculate  $E_{AC}$  from FWD testing were developed assuming uniform AC thickness and quality. The presence of moisture damage and patched areas made the backcalculated  $E_{AC}$  values questionable. More reliable  $E_{AC}$  data were obtained from laboratory testing performed by the University of Illinois on cores from Project 3. A comparison of  $E_{AC}$  values predicted by the 1986 construction core and 1991 core  $E_{AC}$ -tensile strength relationships was made previously. It showed an average increase in AC-10  $E_{AC}$  from 392 ksi to 740 ksi and an average increase in AC-20  $E_{AC}$  from 586 ksi to 713 ksi between construction and September 1991. These data suggested that stiffening of the AC had occurred, a typical occurrence in the aging process.

The laboratory-calculated  $E_{AC}$  values were actual measurements, and as such, were more representative than the  $E_{AC}$  values backcalculated from FWD testing. The FWD data were still useful, however. A large amount of data were collected quickly, and the backcalculated values by pavement section for a given test date were informative relative to the other pavement sections and other test dates. One such comparison that could be made was the effect of  $E_{AC}$  on pavement performance. Test temperature had a large impact on  $E_{AC}$ . Although temperature was not directly accounted for, it was noted that, in general, Sections K and M had the lowest  $E_{AC}$  backcalculated from FWD testing as shown in Tables 24A through 24G. This observation was in direct agreement with the increased amount of rutting, cracking, and patching noted in these sections.



## Objective 2

Slab cracking is the most critical distress in portland cement concrete (PCC) pavements which affects the performance of the pavement (17). The proposed mechanistically-based design procedure (2) determines the slab thickness by analyzing the structural responses to loads which will induce slab cracking. The design procedure must be capable of accurately modeling the stresses which cause slab cracking. The primary focus of this objective was to compare measured strains and deflections of PCC pavements with tied concrete shoulders to those predicted by the proposed mechanistically-based design procedure. Since deflections are not a critical component of the design, the analysis included in this report is limited to the strains measured from the strain gauges.

As discussed in the **Strain Gauge Measurements** portion of this report, comparisons of strains recorded in the field to those predicted by the proposed mechanistically-based design procedure are included in Figures 24A and 24B, 32A through 34D, and 37A through 38C. Generally, the strains measured in the field are lower than those predicted by the proposed mechanistically-based design procedure. Although this appears to indicate the proposed mechanistically-based design procedure is conservative, there are several factors, which are either difficult to model or too variable to quantify, that affect the strains recorded in the field. These factors were discussed in detail in the **Strain Gauge Measurements** portion of this report and will not be evaluated again here. All of these factors act in various combinations with each other. Essentially, the strains recorded in the field are close to those predicted by the proposed mechanistically-based design procedure; however, the field strains are too undependable to be used in an in-depth evaluation of the proposed mechanistically-based design procedures. Such an evaluation would be invalid. The analysis of Objective 2 will therefore concentrate on the effects of slab thickness, utilization of underdrains, utilization of joint sealants, and joint spacings.

### Slab Thickness

Project 4 was the only project which included variations in PCC slab thickness, therefore, this part of the analysis will focus on data collected from the test sections on Project 4. Three CRC slab thicknesses, 7, 8, and 9 inches, were constructed, and three JRCP and JPCP slab thicknesses, 7.5, 8.5, and 9.5 inches, were constructed. The distress surveys and strain gauge measurements can be used as early indicators of the effect slab thickness has on performance.

Table 17B, which summarizes the 1992 distress survey information for Project 4, shows that only one transverse crack had deteriorated to a notable level of distress in all of the CRCP test sections. The only other distress listed for any of the CRCP sections was construction joint deterioration. Construction joints are a function of construction and not pavement performance, thus all of the CRCP test sections are essentially performing at the same level to date.

Table 17B also contains the 1992 distress survey information for the JRCP test sections. All of the JRCP test sections have 40-foot joint spacings. As

mentioned previously, the major distress for PCC pavements is cracking, and nearly all of the 40-foot long panels did crack transversely at least once. Table 39 contains a summary of the transverse cracks for the various slab thicknesses for the JRCF test sections. The 9.5-inch thick test section contains a lower percentage of low severity and more medium severity cracks than the 8.5- and 7.5-inch thick sections. This statistic may be skewed due to the fact that there are four times as many 8.5- and 7.5-inch panels as 9.5-inch panels. Since the project is only five years old, this statistic may reverse itself as the test sections age.

Table 17B listed the distresses for the JPCP test sections as of the 1992 distress survey as well. All of the JPCP test sections on Project 4 have a 20-foot joint spacing. Table 40 contains a summary of the transverse cracks for the various slab thicknesses for the JPCP test sections. From Table 40, the 9.5-inch thick section, AA, is displaying no signs of distress, but both the 8.5- and 7.5-inch thick test sections have minimal distresses. Of these distresses, the 7.5-inch pavement test Sections MA and NA have more cracking than the 8.5-inch thick test Sections, IA, JA, KA, and LA. With time, these trends will probably continue.

The strain gauge data can also be used to investigate the effect different slab thicknesses have on pavement performance. There is a notable difference in the strains between the 9.5-inch thick test sections and the 7.5-inch thick test sections. Figures 32B and 32C show that mid-panel gauges in the 9.5-inch thick sections recorded notably lower strains than the 7.5-inch thick sections. Figures 33B and 33C show that the quarter-panel gauges in the 9.5-inch thick sections have lower strains than those recorded in the 7.5-inch thick sections. The CRCP test sections with various pavement thicknesses also demonstrate this trend. Figures 37A and 37B show that the strains decreased as the slab thickness increased.

### Underdrains

The effect of underdrains on pavement performance is a difficult phenomenon to investigate without long-term performance data available. The best indication of the effectiveness of underdrains was the subgrade moisture tests which were conducted on Project 4. In the **Subgrade Moisture** portion of this report, the procedure used to measure seasonal subgrade moisture variations was detailed.

The test sections with underdrains in the 8.5-inch JPCP with an unsealed edge joint were drier than those without underdrains. The test sections without underdrains in the 8.5-inch JPCP with a sealed edge joint were drier than those with underdrains. The findings of the subgrade moisture tests were inconclusive, as there was no convincing evidence that longitudinal underdrains were successful in removing water from beneath the pavement with any degree of consistency.

### Joint Sealant

The pavement/shoulder joint was sealed in some of the test sections on Project 4 to prevent water from infiltrating the pavement. Both the subgrade moisture readings and the underdrain outflow readings can be used as indicators of the effectiveness of the joint sealant.

In the JPCP sections without underdrains, the section without the joint sealant uniformly had wetter subgrade moisture readings than the section with the sealant to a depth of 55 inches. This relationship is shown in Figure 55. In the 8.5-inch JPCP sections with underdrains, the sealed section was sometimes wetter and sometimes drier than the unsealed section. This relationship is shown in Figure 56. The inconsistency in the readings for this area was most likely the result of poor sealing techniques, as discussed in the **Underdrain Outflow** portion of this report. In general, the proper use of an edge sealant did seem to have a positive effect on controlling the moisture content of the subgrade.

In the **Underdrain Outflow** portion of this report, comparisons were made between the outflows from the CRCP, JPCP, and JRCP test sections with the pavement/shoulder joint sealed to identical test sections without the pavement/shoulder joint sealed. From Table 29 and Figures 41 and 42, it is clear that there is only a minimal difference between the outflows in the two 20-foot JPCP sections. An evaluation of the effectiveness of using an edge joint sealant should not be made from the data collected in these sections because of improper construction as outlined previously.

A comparison of the data collected from the 40-foot JRCP sections was possible. The sealed and unsealed sections usually reached a peak outflow in the same hour; however, the sealed section recovered to 0.5 gallon per hour outflow or less 24 hours prior to the unsealed section. Hourly and total outflow volumes from the sealed section were approximately 50 percent the volume of the unsealed section.

In the CRCP sections, the sealed and unsealed sections usually reached a peak outflow in the same time. The sealed section always recovered to 0.5 gallons per hour or less in less than 24 hours. The unsealed section, however, took between 24 and 36 hours. The total outflows from the sealed section were approximately 70 percent the volume of the unsealed section.

Both the subgrade moisture and the underdrain outflow test results indicate that the proper use of edge joint sealant does seem to have a positive effect on controlling the moisture content of the subgrade.

### Joint Spacing

After six years of performance monitoring, it is clear that joint spacings play an important role in pavement performance. On Project 2, 15-, 20-, and 40-foot joint spacings were used. From Table 16B, there are no distresses in either of the 15-foot JPCP sections, E and H. The 20-foot JPCP sections, C and F, contain only two transverse cracks in 272 panels. In the 40-foot JRCP sections, D and G4, all of the panels have cracked, at least once.

On Project 2, Sections G1, G2, and G3 were designed with hinge-jointed panels. None of these panels are showing any signs of distress. The fact that all of the 40-foot JRCP panels cracked validates the hinge joint design procedure, which advocates the use of hinge joints to control cracking in longer slabs. As part of the evaluation of this design, these sections were tested for deflections. Tables 27A and 27B contain the results from these tests. The load transfer efficiencies (LTEs) indicate all of the sections are performing well, with the hinge joints averaging LTEs of 92, 92, and 91 for

Sections G1, G2, and G3, respectively. The dowel joints are averaging LTEs of 91, 91, and 90 for Sections G1, G2, and G3, respectively.

Project 4 contains 20-foot and 40-foot jointed PCC pavements. Sections AA, IA, JA, KA, LA, MA, and NA all have a 20-foot joint spacing. Sections BA, CA, EA, FA, GA, HA, OA, PA, QA, and RA have 40-foot joint spacings. Out of the 612 20-foot long panels, only 28 panels have cracked. In the 40-foot JRC sections, 951 transverse cracks were recorded in the 908 panels. This drastic change in performance is a direct result of the joint spacings and emphasizes the importance of selecting the proper joint spacing in pavement design.

On Project 4, Sections DA, DB, and DC were designed to include hinge-jointed panels. To date, the panels are performing well. Some minor cracking has been noted in Section DB, but this cracking is due to construction problems, and should not be considered when evaluating pavement performance. As part of the evaluation of this design, deflection testing was conducted on these test sections. The LTEs indicate all of the sections are performing well. As shown in Table 28B, the average LTEs at the hinge joints are 90, 83, and 90 for Sections G1, G2, and G3, respectively. The average LTEs at the dowel joints are 92, 89, and 86 for Sections G1, G2, and G3, respectively.

### **Objectives 3 and 4**

Objective 3 was to evaluate the effect of asphalt cement viscosity grades on the performance of full-depth AC pavements. This objective was addressed in detail under Objective 1. Objective 4 was to evaluate the effect of 40-, 20-, and 15-foot joint spacings and 3 hinge joint designs on the performance of PCC pavements with tied shoulders. This objective was addressed in detail under Objective 2.

### **FUTURE MONITORING**

The Maintenance Management Information System (MMIS) is currently being updated to account for maintenance performed on Projects 1, 2, 3, and 4 to date. Maintenance data will continue to be collected, and in conjunction with other performance data, will be available for life cycle cost performance evaluations at the end of the projects' lives. The performance of these projects will be incorporated into the statewide database of pavements designed using mechanistically-based procedures.

### **SUMMARY**

The Illinois Department of Transportation (IDOT) constructed four demonstration projects in 1986 to evaluate proposed mechanistically-based pavement design procedures developed by the University of Illinois (1, 2) and to determine the effects of design variables on pavement performance. Project 1 was a full-depth AC pavement on FA 401 (U.S. 20) in northern Illinois, and Project 2 was a jointed PCC pavement on FA 401. Project 3 was a full-depth AC pavement on FA 409 (U.S. 50) in south central Illinois. Project 4 was also located on FA 409 and contained both jointed PCC and CRC pavements. The test section layouts of these four projects are shown in Figures 2, 4, 6, and 7, respectively. These demonstration projects were proposed in an experimental

features work plan entitled, "Evaluating Pavement Design Features". This report detailed the construction and performance monitoring of these four demonstration projects.

These projects were instrumented during construction and performance monitoring has been conducted since that time. Performance monitoring has included visual distress surveys, maintenance activity monitoring, and full-depth AC pavement coring and analysis. Deflection testing with IDOT's Dynatest 8002 Falling Weight Deflectometer (FWD) has been conducted on all four projects and strain gauge testing performed on the PCC sections to determine structural response. Moisture monitoring, consisting of underdrain outflow, subgrade moisture, and depth of frost penetration measurements, was conducted on Projects 3 and 4. Surface response monitoring consisting of ride quality and friction data, was conducted on all four projects. Based on an analysis of all the construction and performance data collected over the past six years, the following observations can be made:

- o After six years of service, the distress surveys showed that the demonstration projects were in general performing as predicted by the proposed mechanistically-based design procedures (1, 2).
- Projects 1 and 3 showed little signs of thermal cracking, alligator or fatigue cracking, or rutting, key indicators of full-depth AC pavement performance. Sections K, M, and M1, the 9.5-inch full-depth AC sections on Project 3, were the primary exceptions. Full-depth patching has been required in these sections to replace failed pavement. Some alligator cracking was found in Sections O and P on Project 3 as well. A portion of the cracking in Section P occurred at entrance and exit ramps used as access locations for haul trucks. The early-life loadings apparently accelerated the fatigue damage in these areas. The remainder of the alligator cracking in Sections O and P seemed less fatigue-related distress than surface distress showing a pattern similar to alligator cracking.
- Slab cracking, the major mode of failure in PCC pavements, was basically noted only in the 40-foot JRCP sections. Nearly all of the 40-foot JRCP panels cracked at mid-slab. This finding validates the PCC mechanistically-based design procedure, which advocates the use of hinge joints to control mid-panel cracking in longer slabs.
- o Moisture damage ranging from slight to severe was found throughout the full-depth AC pavement sections on Project 3 during a 1989 coring study. These 1989 cores were taken during a period of hot, wet weather. Subsequent cores taken in 1991 during a cooler, drier period showed less signs of moisture damage and had higher tensile strengths. On the basis of these findings, it appeared that the effects of moisture damage may be cyclic in nature, corresponding to the degree of pavement saturation. Additional research is needed to investigate this phenomenon.

- o An analysis of  $E_{AC}$  backcalculated from FWD data taken on Project 3 showed a slight decrease in  $E_{AC}$  with age. Algorithms designed to backcalculate  $E_{AC}$  from FWD data were developed assuming uniform AC thickness and materials of consistent quality. The presence of patching in Sections K, M, and M1 and moisture damage throughout Project 3 made the use of these algorithms questionable. Laboratory  $E_{AC}$  and split tensile testing conducted by the University of Illinois on cores taken shortly after construction (13) and in 1991 (M. R. Thompson, unpublished data) verified that the expected trend of increased AC stiffness and strength as a result of the aging process had occurred.
- o Deflection testing was conducted on the three hinge joint sections on Projects 2 and 4. On Project 2, hinge joint load transfer efficiencies (LTEs) averaged between 91 and 92 percent, while dowel joint LTEs averaged 90 to 91 percent. On Project 4, hinge joint LTEs averaged 83 to 90 percent and dowel joint LTEs averaged 86 to 92 percent. Little apparent difference in joint LTEs between the three designs was noted, with all three designs performing equally well.
- o Pavement/shoulder joint LTEs measured shortly after construction on Project 4 averaged 83 to 93 percent, indicating good load transfer between the pavement and the tied shoulder. The data showed some variability because the #5 tie bars were spaced at 30-inch centers, and individual deflection tests may have been taken directly over a tie bar (high LTE) or in the space between tie bars (low LTE). Additional FWD testing is planned to determine pavement/shoulder joint LTEs over time.

A primary objective of the experimental features projects was to determine the effect of several design variables on pavement performance. For full-depth AC pavements the design variables were AC thickness, underdrains, asphalt cement viscosity grade, and lime-modified subgrade. For PCC pavements the design variables were slab thickness, underdrains, joint seals, and joint spacing.

## **Full-Depth AC Pavement**

### AC Thickness

In general, the 9.5-inch thick sections on Project 3 showed more distress than the 11- or 12.5-inch thick sections. The 9.5-inch thick sections showed more transverse and alligator cracking, and in the case of the AC-20 sections, more rutting. Deflection testing supported the visual distress survey findings. Full-depth patching of failed areas has been required only in the 9.5-inch thick sections. The expected trend of improved pavement performance with increased thickness was apparent, but the trend was obscured by the fact that all of the 11- and 12.5-inch thick sections were constructed on lime-modified subgrades, whereas approximately only 50 percent of the 9.5-inch thick sections were. The effect of a lime-modified subgrade will be discussed shortly. Project 1 did not contain varying AC layer thicknesses.

### Underdrains

Analysis of the effect of underdrains was confined to Project 3. The FWD data and subgrade moisture measurements did not indicate that underdrains were consistently successful in removing water from beneath the pavement or improving  $E_{Ri}$ . The presence of underdrains thus did not appear to have a measureable effect on pavement performance.

### Asphalt Cement Viscosity Grades

After six years of service, little difference in performance between the AC-10 and AC-20 sections on Project 1 was noted. The data suggested little difference in rutting potential between the AC-10 and AC-20 sections on Project 3. Considerably more fatigue cracking was noted in the AC-20 sections on Project 3 than in the AC-10 sections. However, the poorer performance of the AC-20 sections appeared to be less a function of the asphalt cement viscosity grade than a function of moisture damage and soft subgrades. Long-term monitoring will be required to determine the effect of asphalt cement viscosity on the performance of these projects.

### Lime-Modified Subgrade

Use of lime-modified subgrades was limited to Project 3. Sections K and M1 were the only sections constructed on an untreated subgrade, and were among the worst performing sections. Other sections that were lime-modified exhibited rutting and fatigue-related cracking as well. The sections exhibiting rutting and fatigue-related distresses in general had low  $E_{Ri}$  backcalculated from FWD testing. The presence of adequate subgrade support was essential to good pavement performance. Although a lime-modified subgrade does not guarantee good pavement performance, it does provide a stable construction platform to compact a full-depth AC pavement against, and it helps decrease the potential for subgrade deformation.

### **PCC Pavement**

#### Slab Thickness

None of the CRCP sections on Project 4, with various slab thicknesses, are showing signs of distress. In the JRCF sections on Project 4, the 7.5- and 8.5-inch thick test sections contain more low severity transverse cracks than the 9.5-inch thick sections. The 7.5- and 8.5-inch thick sections did have fewer medium severity cracks than the 9.5-inch thick sections. In the JRCF sections on Project 4, the 7.5-inch thick sections have the most distress and the 9.5-inch thick sections have the least with no distress. In general, the expected trend of improved pavement performance with increased slab thickness was apparent. Project 2 did not contain PCC slabs of varying thickness.

### Underdrains

The analysis of the effect of underdrains on pavement performance was confined to Project 4. The subgrade moisture measurements did not indicate that underdrains were consistently successful in removing water from beneath the pavement. The presence of underdrains does not appear to have a measureable effect on pavement performance to date.

### Joint Sealant

The analysis of the effect of using a joint sealant in the pavement/shoulder joint on project performance was confined to Project 4. Both the subgrade moisture and underdrain outflow test results indicate that the proper use of joint sealant does seem to have a positive effect on controlling the moisture content of the subgrade.

### Joint Spacing

Joint spacing does have a significant impact on pavement performance. The fact that all of the 40-foot JRPC panels cracked validates the PCC mechanistically-based hinge joint design. The 40-foot panels were showing significantly more distress than the 15-foot, 20-foot, or hinge-jointed panels.

Monitoring of the four demonstration projects will continue. Distress surveys will be made, deflection testing conducted, and hinge joint measurements monitored periodically. Friction, rutting, and ride quality measurements will be made as well. These performance data, in conjunction with maintenance activity data, will provide valuable information on the performance of pavement and the validity of pavement design procedures in Illinois.



## REFERENCES

1. M. R. Thompson and K. Cation. A Proposed Full-Depth Asphalt Concrete Thickness Design Procedure. Civil Engineering Studies, Transportation Engineering Series No. 45, Illinois Cooperative Highway and Transportation Series No. 213, University of Illinois, Urbana, Illinois, July 1986.
2. D. G. Zollinger and E. J. Barenberg. Proposed Mechanistic Based Design Procedure for Jointed Concrete Pavements. Civil Engineering Studies, Transportation Engineering Series No. 57, Illinois Cooperative Highway Research Program Series No. 225, University of Illinois, Urbana, Illinois, May 1989.
3. Illinois Department of Transportation. Section 7: Pavement Design. In Design Manual, Illinois Department of Transportation, Bureau of Design, Springfield, Illinois, revised January 1983.
4. Illinois Department of Transportation. Supplement to Section 7: Mechanistic Pavement Design. In Design Manual, Illinois Department of Transportation, Bureau of Design, Springfield, Illinois, August 1989; PCC design curves revised August 1992.
5. M. W. Mueller and A. J. Patel. Evaluation of Mechanistic Pavement Design in Illinois Experimental Project 621: Pavement Instrumentation. Report No. 106. Illinois Department of Transportation, Springfield, Illinois, February 1989.
6. Illinois Department of Transportation - District 8. Contract Number 40448 Contract Documents, Illinois Department of Transportation, District 8, Fairview, Illinois, December 1985.
7. Illinois Department of Transportation. Standard Specifications for Road and Bridge Construction. Illinois Department of Transportation, Springfield, Illinois, Adopted October 1, 1983.
8. Illinois Department of Transportation. Pavement Condition Rating Survey Distress Guide. Illinois Department of Transportation, Office of Planning and Programming, Springfield, Illinois, issued May 1988.
9. Illinois Department of Transportation. Illinois Procedure for Determining Stripping and the Effectiveness of Anti-stripping Additives on Asphalt Concrete Paving Mixtures. Illinois Department of Transportation, Bureau of Materials and Physical Research, Springfield, Illinois, issued January 2, 1991.
10. J. B. DuBose. Comparison of the South Dakota Road Profiler with other Rut Measurement Methods. In Transportation Research Record 1311, Transportation Research Board, National Research Council, Washington, D.C., 1991, pp. 1-6.
11. M. R. Thompson. ILLI-PAVE Based NDT Analysis Procedures. In Nondestructive Testing of Pavements and Backcalculation of Moduli. ASTM STP 1026, A. J. Bush III and G. Y. Baladi, Editors, ASTM, Philadelphia, 1989, pp. 487-501.

12. University of Illinois. The ILLI-PAVE Program for Pavement Analysis-Users Manual. Department of Civil Engineering, University of Illinois, Urbana, Illinois, Spring 1979.
13. H. J. Hill and M. R. Thompson. Early Life Study of the FA 409 Full-Depth Asphalt Concrete Pavement Sections. Illinois Cooperative Highway and Transportation Research Program, University of Illinois, Urbana, Illinois, Interim Report, June 1988.
14. A. M. Schutzbach. Case Study of a Full-Depth Asphalt Concrete Inlay. In Transportation Research Record 1337, Transportation Research Board, National Research Council, Washington, D.C., 1992, pp. 42-50.
15. A. M. Tabatabaie and E. J. Barenberg. Finite-Element Analysis of Jointed or Cracked Concrete Pavements. In Transportation Research Record 671, Transportation Research Board, National Research Council, Washington, D.C., 1978, pp. 11-19.
16. A. M. Ioannides. Analysis of Slabs-on-Grade for a Variety of Loading and Support Conditions. Ph.D. Thesis, Department of Civil Engineering, University of Illinois, Urbana, Illinois, 1983.
17. D. B. Zollinger and E. J. Barenberg. Background for Development of Mechanistic Based Design Procedure for Jointed Concrete Pavements. Civil Engineering Studies, Transportation Engineering Series No. 56, Illinois Cooperative Highway Research Program Series No. 224, University of Illinois, Urbana, Illinois, May 1989.
18. M. A. Nasim, S. M. Karamihas, T. D. Gillespe, W. Hansen, and D. Cebon. Behavior of a Rigid Pavement Under Moving Dynamic Loads. In Transportation Research Record 1307, Transportation Research Board, National Research Council, Washington, D.C., 1991, pp. 129-135.
19. J. E. LaCroix, Summary of 1987 Roadometer Tests of New Pavements: Report IHR-504 Ride Quality of New Pavements. Illinois Department of Transportation, Bureau of Materials and Physical Research, Springfield, Illinois, May 1988.
20. J. E. LaCroix. A Summary of the Illinois Skid-Accident Reduction Program: August 1985 to December 1986. Illinois Department of Transportation, Bureau of Materials and Physical Research, Springfield, Illinois, December 1986.

## DISCLAIMER

This paper is based on the results of the experimental feature Evaluating Pavement Design Features. This experimental feature was sponsored by the Illinois Department of Transportation (Division of Highways) and the U. S. Department of Transportation (Federal Highway Administration).

The contents of this paper reflect the views of the authors who are responsible for the facts and accuracy of the data presented herein. The contents do not necessarily reflect the official views or policies of the Illinois Department of Transportation nor the Federal Highway Administration.

Trademark or manufacturer's names appear in this report only because they are considered essential to the object of this document and do not constitute an endorsement of product by the Federal Highway Administration or the Illinois Department of Transportation.

## ACKNOWLEDGEMENTS

The authors gratefully acknowledge the contributions of the following people, without whose help and support this report would not have been possible: Brenda Miller and Becky Hermes for manuscript preparation; Tom Courtney for illustrations; the entire Pavement Technology Unit for data collection; Audrey Lyons, Joe Vespa, Mary Milcic, Paul Jenkins, and LaDonna Blecha for data collection and review; and David Lippert, Eric Harm, Ernest Barenberg, and Marshall Thompson for manuscript review.

TABLE 1A: DESIGN ESALs FOR PROJECTS 1 AND 2

PAVEMENT TYPE	AC LAYER OR SLAB THICKNESS (INCHES)	SECTIONS	BACKCALCULATED DESIGN ESALs
FULL-DEPTH AC			
AC 10	13.0	A	$3.5 \times 10^6$
AC 20	13.0	B	$5.5 \times 10^6$
JOINTED PCC			
20' JPCP	10.0	C, F	$11.7 \times 10^6$
40' JRCP	10.0	D, G4	$11.7 \times 10^6$
15' JPCP	10.0	E, H	$18.0 \times 10^6$
20' HINGE JOINTED	10.0	G1, G2	$11.7 \times 10^6$
13' 4" HINGE JOINTED	10.0	G3	$18.0 \times 10^6$

TABLE 1B: DESIGN ESALS FOR PROJECTS 3 AND 4

PAVEMENT TYPE	AC LAYER OR SLAB THICKNESS (INCHES)	SECTIONS	BACKCALCULATED DESIGN ESALS
FULL-DEPTH AC			
AC-10	9.5	A, B	$0.5 \times 10^6$
AC-10	12.5	C, D	$1.9 \times 10^6$
AC-20	12.5	E, H, I	$2.6 \times 10^6$
AC-20	9.5	J, K, L, M, N1, N, O	$0.7 \times 10^6$
AC 20	11.0	P	$1.4 \times 10^6$
CRC	7.0	W, X, Y, Z	$1.8 \times 10^6$
CRC	8.0	S, T, U, V	$4.3 \times 10^6$
CRC	9.0	R	$9.4 \times 10^6$
JOINTED PCC			
20' JPCP	7.5	MA, NA	$0.64 \times 10^6$
20' JPCP	8.5	IA, JA, KA, LA	$1.5 \times 10^6$
20' JPCP	9.5	AA	$2.6 \times 10^6$
40' JRCP	7.5"	OA, PA, QA, RA	$0.64 \times 10^6$
40' JRCP	8.5"	CA, EA, FA, GA, HA	$1.5 \times 10^6$
40' JRCP	9.5"	BA	$2.6 \times 10^6$
20' HINGE JOINTED	8.5"	DA, DB	$1.5 \times 10^6$
13' 4" HINGE JOINTED	8.5"	DC	$1.9 \times 10^6$

TABLE 2: ASPHALT CONCRETE SURFACE MIXTURE DESIGN DATA FOR PROJECT 1

TEST	SPECIFICATION	SURFACE MIX FORMULA
Gradation, % Passing		
3/4"	100	100
1/2"	90-100	99
3/8"	66-100	89
#4	24-65	53
#8	16-48	33
#16	10-32	26
#30	—a	21
#50	4-15	13
#100	3-10	8
#200	3-9	4.9
Asphalt, % of Total Mix	3-9	5.7
Air Voids, %	3-5	4.0
Voids in the Mineral Aggregate, %	15 Minimum	14.6
Marshall Stability, lbs.	2000 Minimum	2425
Marshall Flow, 1/100 in.	8-16	7.2
Tensile Strength Ratio	—a	

—a Denotes No Specification

TABLE 3: ASPHALT CONCRETE BINDER MIXTURE DESIGN DATA FOR PROJECT 1

TEST	SPECIFICATION	BINDER MIX FORMULA
Gradation, % Passing		
1"	100	100
3/4"	82-100	98
1/2"	50-82	73
3/8"	—a	56
#4	24-50	40
#8	16-36	30
#16	10-25	23
#30	—a	18
#50	4-12	11
#100	3-9	7
#200	2-6	4.0
Asphalt, % of Total Mix	3-9	4.7
Air Voids, %	3-5	5.0
Voids in the Mineral Aggregate, %	14 Minimum	14.0
Marshall Stability, lbs.	2000 Minimum	2630
Marshall Flow, 1/100 in.	8-16	8.2
Tensile Strength Ratio	—a	0.76

—a Denotes No Specification

TABLE 4: ASPHALT CONCRETE SURFACE MIXTURE DESIGN DATA FOR PROJECT 3

TEST	SPECIFICATION	SURFACE MIX FORMULA
Gradation, % Passing		
3/4"	100	100
1/2"	90-100	100
3/8"	66-100	99
#4	24-65	58
#8	16-48	36
#16	10-32	26
#30	—a	18
#50	4-15	11
#100	3-10	7
#200	2-6	5.5
Asphalt, % of Total Mix	3-9	7.1
Air Voids, %	3-5	5.0
Voids in the Mineral Aggregate, %	15 Minimum	16.0
Marshall Stability, lbs.	2000 Minimum	2345
Marshall Flow, 1/100 in.	8-16	8.2
Tensile Strength Ratio	—a	0.50

—a Denotes No Specification



TABLE 5: ASPHALT CONCRETE BINDER MIXTURE DESIGN DATA FOR PROJECT 3

TEST	SPECIFICATION	BINDER MIX FORMULA
Gradation, % Passing		
1"	100	100
3/4"	82-100	92
1/2"	50-82	68
3/8"	—a	56
#4	24-50	38
#8	16-36	30
#16	10-25	23
#30	—a	15
#50	4-12	8
#100	3-9	5
#200	2-6	3.5
Asphalt, % of Total Mix	3-9	5.3
Air Voids, %	3-5	4.8
Voids in the Mineral Aggregate, %	14 Minimum	14.9
Marshall Stability, lbs.	2000 Minimum	2140
Marshall Flow, 1/100 in.	8-16	8.8
Tensile Strength Ratio	—a	0.73

—a Denotes No Specification

TABLE 6: DESIGN VS. AVERAGE PRODUCTION VALUES FOR ASPHALT CONCRETE FOR PROJECT 1

MIXTURE	DESIGN			PRODUCTION		
	ASPHALT, % OF TOTAL MIX	% PASSING #200 SIEVE	AIR VOIDS, %	ASPHALT, % OF TOTAL MIX	% PASSING #200 SIEVE	AIR VOIDS, %
BINDER (AC-10)	4.7	4.0	5.0	4.7	3.9	4.7
BINDER (AC-20)	4.7	4.0	5.0	4.6	4.5	5.0
SURFACE (AC-10)	5.7	4.9	4.0	5.6	4.4	3.4
SURFACE (AC-20)	5.7	4.9	4.0	5.9	5.5	2.3

TABLE 7: DESIGN VS. AVERAGE PRODUCTION VALUES FOR ASPHALT CONCRETE FOR PROJECT 3 (CLINTON COUNTY)

MIXTURE	DESIGN			PRODUCTION		
	ASPHALT, % OF TOTAL MIX	% PASSING #200 SIEVE	AIR VOIDS, %	ASPHALT, % OF TOTAL MIX	% PASSING #200 SIEVE	AIR VOIDS, %
BINDER (AC-10)	—	—	—	—	—	—
BINDER (AC-20)	5.3	3.5	4.8	4.7	3.7	3.6
SURFACE (AC-10)	—	—	—	—	—	—
SURFACE (AC-20)	7.1	5.5	5.0	6.9	4.9	6.7

TABLE 8: DESIGN VS. AVERAGE PRODUCTION VALUES FOR ASPHALT CONCRETE FOR PROJECT 3 (ST. CLAIR COUNTY)

MIXTURE	DESIGN			PRODUCTION		
	ASPHALT, % OF TOTAL MIX	% PASSING #200 SIEVE	AIR VOIDS, %	ASPHALT, % OF TOTAL MIX	% PASSING #200 SIEVE	AIR VOIDS, %
BINDER (AC-10)	5.3	3.5	4.8	4.4	3.4	4.6
BINDER (AC-20)	5.3	3.5	4.8	4.4	3.4	4.1
SURFACE (AC-10)	7.1	5.5	5.0	7.0	5.4	5.4
SURFACE (AC-20)	7.1	5.5	5.0	7.0	5.0	7.3

TABLE 9: PCC MIX DESIGN FOR PROJECT 2

INGREDIENT	QUANTITY, POUNDS
CEMENT	455
FLY ASH	120
CA-07	1967
FA-01	1036
WATER	259
TOTAL	3837

TABLE 10: PCC MIX DESIGN FOR PROJECT 4

INGREDIENT	QUANTITY, POUNDS
CEMENT	575
FLY ASH	—
CA-07	1890
FA-01	1123
WATER	249.9
TOTAL	3837.9

TABLE 11: PCC DAILY MATERIAL PROPERTY TESTS FOR PROJECT 2

DATE	SLUMP (IN)	AIR (%)	FLEXURAL	STRENGTH
			7 DAY	14 DAY
8/12/86	1.5,1.75	6.8,7.3,6.6,8.0,5.8, 7.6,6.8	710	766
8/13/86	1.1,1.0,1.8	7.0,7.8,8.4,6.3,7.0, 5.9,7.0,5.0,7.0	747,770	815,825
8/18/86	2.0,2.0,1.25	5.3,6.8,5.9,7.6,7.3, 5.2,6.4,7.2,6.3,6.6, 5.8,5.6,7.6	742,758	763,788
8/19/86	2.0,2.0	7.3,7.5,5.2,6.9,5.8, 7.8,6.8	636	733
8/21/86	1.25,1.50	6.5,6.1,5.3,6.3,6.2	771	888,866
8/27/86	1.75	7.8,7.6	794	—
8/28/86	2.0,1.5	6.8,6.7,7.9,7.6	—	960,765
8/29/86	2.0,1.25	7.1,7.6,7.3	844	860
9/02/86	1.75,1.50	6.3,6.0,8.0,6.3,7.1	—	854,829
9/03/86	3.0	8.0,7.1	685	724
9/04/86	2.75	7.9,7.3,8.0,7.5,5.2	758	—
9/05/86	3.0,3.0	5.5,6.7,7.0,7.1,5.4,6.1	860	890,905
9/08/86	—	6.8,7.1,6.6,5.8	833	823
9/09/86	2.0	7.8,7.2	820	743
9/12/86	3.0,5.0,5.0	7.3,8.0,7.4	653	738
9/15/86	3.0	9.0,7.6,9.9,9.2,7.3,7.3	725	740,766
9/16/86	3.0	8.0,6.7,7.0	650	1027,869
9/18/86	2.0	5.1,6.9,5.1,5.0	—	823,882

AVG = 2.22 IN  
 STD DEV = 1.00 IN  
 N = 30

AVG = 6.87%  
 STD DEV = 0.98%  
 N = 90

AVG = 750 PSI, 826 PSI  
 STD DEV = 68 PSI, 76 PSI  
 N = 17, 25

SPEC.: 3 IN MAX

SPEC.: 5-8%

SPEC.: 14 DAY - 650 PSI MIN;  
 620 PSI W/ FLY ASH

TABLE 12: CRCP DAILY MATERIAL PROPERTY TESTS FOR PROJECT 4

DATE	SLUMP (IN)	AIR (%)	FLEXURAL STRENGTH	
			7 DAY	14 DAY
4/16/86	3.75	5.6	—	—
4/18/86	3.5, 3.5	6.3, 5.4	835	861
4/24/86	3.0	6.2	797	895
4/25/86	3.25, 3.25	6.7, 6.1, 6.1	754	807, 807
6/26/86	3.0	6.1	727	905
7/03/86	3.0	6.2	689	666
7/08/86	3.0, 2.75, 2.0	5.6, 6.9	666	695
7/15/86	3.25	6.7, 6.5, 6.5	686	799
7/16/86	2.0	5.1, 6.4	—	—
7/18/86	2.5	6.0, 6.4	775	904
7/22/86	2.5, 3.0	8.0, 7.1, 7.7	781	932
7/23/86	3.0, 2.5	5.6, 6.0	—	—
8/18/86	2.0, 2.25	6.8, 7.4	—	—
8/20/87	2.5	7.3	—	—

AVG = 2.83 IN  
 STD DEV = 0.51 IN  
 N = 21

AVG = 6.41%  
 STD DEV = 0.70%  
 N = 26

AVG = 745 PSI      827 PSI  
 STD DEV = 57 PSI    90 PSI  
 N = 9                      10

SPEC.: 3 IN MAX

SPEC.: 5-8%

SPEC.: 14 DAY - 650 PSI MIN;  
 620 PSI W/ FLY ASH

TABLE 13: JOINTED PCC DAILY MATERIAL PROPERTY TESTS FOR PROJECT 4

DATE	SLUMP (IN)	AIR (%)	FLEXURAL STRENGTH	
			7 DAY	14 DAY
4/10/86	3.5,3.5,2.5, 3.0,3.0	5.4,5.6,5.8,5.4,5.4	804	898
4/16/86	3.75	7.7,5.2	813	859
6/30/86	2.0,2.0	5.7,5.2,5.3,5.2	814	921
7/02/86	2.0	5.3,5.0,5.6,6.1,5.0,5.9	742	720
7/28/86	2.75,3.0	6.0	792	788
7/29/86	3.25	6.9	—	—
7/30/86	2.75,3.75,2.0	7.8,7.8,7.4	1043	832
8/04/86	2.25	7.0,7.9	—	—
8/08/86	1.75	6.4,6.6	898	936
8/11/86	2.50	7.1	—	—
8/13/86	2.0,2.0,2.5, 2.25	5.2,6.8,5.2,6.2	714	797
8/14/86	2.0	7.0,6.8,7.2	—	—
8/15/86	2.25	7.2,7.4	785	869
8/18/86	2.0	7.2	—	—
8/19/86	2.25,2.5	6.4,6.4	763	933
8/20/86	2.5	7.8	—	—
8/22/86	3.5,3.0	8.0,6.6,8.0	—	—
8/25/86	2.0,3.0,2.75, 2.5	7.1,7.6,6.8,7.3,6.9,6.8	709	731
8/26/86	3.0,3.0	6.8,7.2	—	—

AVG = 2.62 IN  
 STD DEV = 0.56 IN  
 N = 36

AVG = 6.5%  
 STD DEV = 0.93%  
 N = 51

AVG = 807 PSI, 844 PSI  
 STD DEV = 94 PSI, 77 PSI  
 N = 11, 11

SPEC.: 3 IN MAX

SPEC.: 5-8%

SPEC.: 14 DAY - 650 PSI MIN;  
 620 PSI W/ FLY ASH



TABLE 14A: 1990 DISTRESS SUMMARY FOR PROJECT 1

SECTION	LENGTH (FEET)	DISTRESS	SEVERITY	AMOUNT				UNITS OF MEASURE
				EB		WB		
				PL	DL(a)	PL	DL(a)	
A (EB) 4 lanes	7000 <sup>(b)</sup>	RAVELING & WEATHERING	LOW	2029	574			LANE FT.
A (WB) 4 lanes	7000 <sup>(b)</sup>	RAVELING & WEATHERING	LOW			370	390	LANE FT.
		LONG. CRACKING	LOW			63		LINEAL FT.
		ALLIGATOR CRACKING	LOW			5	23	LANE FT.
		TRANS. CRACKING	LOW			1	1	NUMBER
A 2 lanes	1644	RAVELING & WEATHERING	LOW		160		239	LANE FT.
B	11484	RAVELING & WEATHERING	LOW		586		430	LANE FT.
		TRANS. CRACKING	LOW		2		1	NUMBER
		ASPHALT BLEEDING	LOW				3	LANE FT.
		LONG. CRACKING	LOW		29		6	LINEAL FT.
		CNTRLINE CRACKING	LOW		20			LINEAL FT.

(a) ESALs at the time of the survey were 90,000

(b) Includes a 400 foot taper to two lanes

TABLE 14B: 1992 DISTRESS SUMMARY FOR PROJECT 1

SECTION	LENGTH (FEET)	DISTRESS	SEVERITY	AMOUNT				UNITS OF MEASURE
				EB		WB		
				PL	DL(a)	PL	DL(a)	
A (EB) 4 lanes	7000 <sup>(b)</sup>	RAVELING &						
		WEATHERING	LOW	2565	934			LANE FT.
		CNTRLINE CRACKING	LOW		4760			LINEAL FT.
		BLOCK CRACKING	LOW	7	52			LANE FT.
		CENTER OF LANE	LOW	9	185			LINEAL FT.
		ALLIGATOR CRACKING	LOW		28			LANE FT.
		LONG. CRACKING	LOW		21			LINEAL FT.
A (WB) 4 lanes	7000 <sup>(b)</sup>	RAVELING &						
		WEATHERING	LOW			2044	538	LANE FT.
		LONG. CRACKING	LOW			92		LINEAL FT.
		ALLIGATOR CRACKING	LOW			5	85	LANE FT.
		TRANS. CRACKING	LOW			2	1	NUMBER
		CENTER OF LANE	LOW				77	LINEAL FT.
		BLOCK CRACKING	LOW			9		LANE FT.
		CNTRLINE CRACKING	LOW				3133	LINEAL FT.
A 2 lanes	1644	RAVELING &						
		WEATHERING	LOW		206		242	LANE FT.
		CNTRLINE CRACKING	LOW		1644			LINEAL FT.
B	11484 <sup>(c)</sup>	RAVELING &						
		WEATHERING	LOW		230		195	LANE FT.
		TRANS. CRACKING	LOW		2		1	NUMBER
		ASPHALT BLEEDING	LOW		49		334	LANE FT.
		LONG. CRACKING	LOW		43		52	LINEAL FT.
		CNTR OF LANE	LOW		50			LINEAL FT.
		BLOCK CRACKING	LOW		92		342	LANE FT.
		CNTRLINE CRACKING	LOW		5156			LINEAL FT.
		ALLIGATOR CRACKING	LOW		18		334	LANE FT.

(a) ESALs at the time of the survey were 200,000

(b) Includes a 400 foot taper to two lanes

(c) 4,900 feet not summarized due to SHRP test sections

TABLE 15A: 1990 DISTRESS SUMMARY FOR PROJECT 3

SECTION	LENGTH (FEET)	DISTRESS	SEVERITY	AMOUNT				UNITS OF MEASURE
				EB		WB		
				PL	DL(a)	PL	DL(b)	
A	2850	ASPHALT BLEEDING CNTRLINE CRACKING	LOW LOW		65 167		100	LANE FT. LINEAL FT.
B	1000	ASPHALT BLEEDING	LOW		43		50	LANE FT.
C	1019	ASPHALT BLEEDING	LOW		48		16	LANE FT.
D	1164	ASPHALT BLEEDING	LOW		18		48	LANE FT.
E	6000	ASPHALT BLEEDING	LOW		63		61	LANE FT.
H	900	ASPHALT BLEEDING	LOW		14			LANE FT.
I	2000	ASPHALT BLEEDING	LOW		33		1	LANE FT.
J	300	ASPHALT BLEEDING	LOW		15			LANE FT.
K	2423	ASPHALT BLEEDING ALLIGATOR CRACKING ALLIGATOR CRACKING PERM PATCH DETER.	LOW LOW MEDIUM LOW		2 712 8 1086		18	LANE FT. LANE FT. LANE FT. SQUARE FT.
L	677	ASPHALT BLEEDING	LOW		3		1	LANE FT.
M (EB) 4 lanes	300	ASPHALT BLEEDING LONG. CRACKING PERM PATCH DETER.	LOW LOW LOW	100	2 100 420			LANE FT. LINEAL FT. SQUARE FT.
M (WB) 4 lanes	300	LONG. CRACKING	LOW				87	LINEAL FT.
M 2 lanes	1100	ASPHALT BLEEDING ALLIGATOR CRACKING PERM PATCH DETER. LONG. CRACKING	LOW LOW LOW LOW		4 156 204 65		4 62	LANE FT. LANE FT. SQUARE FT. LINEAL FT.
M1 (EB)	2400	ALLIGATOR CRACKING ASPHALT BLEEDING LONG. CRACKING PERM PATCH DETER. TRANS. CRACKING	LOW LOW LOW MEDIUM LOW		28 3 20 270 1			LANE FT. LANE FT. LINEAL FT. SQUARE FT. NUMBER
M1 (WB)	2400	ALLIGATOR CRACKING ASPHALT BLEEDING LONG. CRACKING TRANS. CRACKING	LOW LOW LOW				134 19 26 2	LANE FT. LANE FT. LINEAL FT. NUMBER
N (EB)	1400	ASPHALT BLEEDING	LOW	1	7			LANE FT.
N (WB)	1400	ASPHALT BLEEDING	LOW				1	LANE FT.

TABLE 15A: 1990 DISTRESS SUMMARY FOR PROJECT 3 (CONT.)

SECTION	LENGTH (FEET)	DISTRESS	SEVERITY	AMOUNT				UNITS OF MEASURE
				EB		WB		
				PL	DL(a)	PL	DL(b)	
O (EB)	1000	ASPHALT BLEEDING	LOW		5			LANE FT.
O (WB)	1000	ASPHALT BLEEDING TRANS. CRACKING	LOW LOW			1 1	1	LANE FT. NUMBER
P (EB) 4 lanes	2500	ASPHALT BLEEDING ALLIGATOR CRACKING LONG. CRACKING TRANS. CRACKING	LOW LOW LOW LOW	19  15	15 123  1			LANE FT. LANE FT. LINEAL FT. NUMBER
P (WB) 4 lanes	2500	ASPHALT BLEEDING LONG. CRACKING	LOW LOW				2 85	LANE FT. LINEAL FT.
P 2 lanes	12431	ASPHALT BLEEDING ALLIGATOR CRACKING LOCAL DISTRESS	LOW LOW LOW		62 51 1		65	LANE FT. LANE FT. NUMBER

(a) ESALs at the time of the survey were 180,000

(b) ESALs at the time of the survey were 130,000

TABLE 15B: 1992 DISTRESS SUMMARY FOR PROJECT 3

SECTION	LENGTH (FEET)	DISTRESS	SEVERITY	AMOUNT		UNITS OF MEASURE	
				EB PL	DL(a)		WB PL
A	2850	ASPHALT BLEEDING	LOW		88	103	LANE FT.
		CENTER OF LANE	LOW		78		LINEAL FT.
		CNTRLINE CRACKING	LOW		970		LINEAL FT.
		TRANS. CRACKING	LOW		1		NUMBER
B	1000	ASPHALT BLEEDING	LOW		57	60	LANE FT.
		CNTRLINE CRACKING	LOW		1000		LINEAL FT.
C	1019	ASPHALT BLEEDING	LOW		71	31	LANE FT.
		CNTRLINE CRACKING	LOW		1019		LINEAL FT.
D	1164	ASPHALT BLEEDING	LOW		48	82	LANE FT.
		CNTRLINE CRACKING	LOW		400		LINEAL FT.
		LOCAL DISTRESS	LOW		1		NUMBER
E	6000	ASPHALT BLEEDING	LOW		78	66	LANE FT.
		CNTRLINE CRACKING	LOW		6000		LINEAL FT.
H	900	ASPHALT BLEEDING	LOW		14		LANE FT.
		CNTRLINE CRACKING	LOW		500		LINEAL FT.
I	2000	ASPHALT BLEEDING	LOW		36	1	LANE FT.
		CNTRLINE CRACKING	LOW		2000		LINEAL FT.
J	300	ASPHALT BLEEDING	LOW		15		LANE FT.
		CNTRLINE CRACKING	LOW		300		LINEAL FT.
K	2423	ASPHALT BLEEDING	LOW		2		LANE FT.
		ALLIGATOR CRACKING	LOW		692		LANE FT.
		ALLIGATOR CRACKING	MEDIUM		8		LANE FT.
		PERM. PATCH DETER.	LOW		1284		SQUARE FT.
		CNTRLINE CRACKING	LOW		2219		LINEAL FT.
L	677	ASPHALT BLEEDING	LOW		3	2	LANE FT.
		CNTRLINE CRACKING	LOW		177		LINEAL FT.
M (EB) 4 lanes	300	ASPHALT BLEEDING	LOW		1		LANE FT.
		ALLIGATOR CRACKING	LOW		90		LANE FT.
		PERM. PATCH DETER.	LOW		420		SQUARE FT.
M (WB) 4 lanes	300	CNTRLINE CRACKING	LOW			200	LINEAL FT.
		LONG. CRACKING					87
M 2 lanes	1100	ASPHALT BLEEDING	LOW		4	4	LANE FT.
		ALLIGATOR CRACKING	LOW		130		LANE FT.
		CNTRLINE CRACKING	LOW		145		LINEAL FT.
		PERM. PATCH DETER.	MEDIUM		816		SQUARE FT.
		LONG. CRACKING	LOW				67

TABLE 15B: 1992 DISTRESS SUMMARY FOR PROJECT 3 (CONT.)

SECTION	LENGTH (FEET)	DISTRESS	SEVERITY	AMOUNT				UNITS OF MEASURE
				EB		WB		
				PL	DL(a)	PL	DL(b)	
M1 (EB)	2400	ALLIGATOR CRACKING	LOW		28			LANE FT.
		ASPHALT BLEEDING	LOW	3	132			LANE FT.
		LONG. CRACKING	LOW	20				LINEAL FT.
		CNTRLINE CRACKING	LOW		2400			LINEAL FT.
		PERM PATCH DETER.	LOW		180			SQUARE FT.
		PERM PATCH DETER.	MEDIUM		270			SQUARE FT.
		TRANS. CRACKING	LOW	3	1			NUMBER
		CORRUGATION	LOW	21				LANE FT.
		LOCAL DISTRESS	LOW		1			NUMBER
M1 (WB)	2400	ALLIGATOR CRACKING	LOW			94	166	LANE FT.
		ASPHALT BLEEDING	LOW				24	LANE FT.
		CNTRLINE CRACKING	LOW				1000	LINEAL FT.
		LONG. CRACKING	LOW		26	47		LINEAL FT.
		TRANS. CRACKING	LOW		2	1		NUMBER
N (EB)	1400	ASPHALT BLEEDING	LOW	1	8			LANE FT.
		ALLIGATOR CRACKING	LOW	6				LANE FT.
N (WB)	1400	ASPHALT BLEEDING	LOW				1	LANE FT.
		CNTRLINE CRACKING	LOW				1400	LINEAL FT.
		LONG. CRACKING	LOW				10	LINEAL FT.
		TRANS. CRACKING	LOW			1	1	NUMBER
O (EB)	1000	ASPHALT BLEEDING	LOW		168			LANE FT.
		ALLIGATOR CRACKING	LOW	68	100			LANE FT.
O (WB)	1000	ASPHALT BLEEDING	LOW			1	1	LANE FT.
		TRANS. CRACKING	LOW			1		NUMBER
		ALLIGATOR CRACKING	LOW			75		LANE FT.
		CENTER OF LANE	LOW			11		LINEAL FT.
		CNTRLINE CRACKING	LOW				1000	LINEAL FT.
		BLOCK CRACKING	LOW			21		LANE FT.
P (EB) 4 lanes	2500	ASPHALT BLEEDING	LOW	20	11			LANE FT.
		ALLIGATOR CRACKING	LOW	123	124			LANE FT.
		LONG. CRACKING	LOW	15				LINEAL FT.
		TRANS. CRACKING	LOW	1	1			NUMBER
		BLOCK CRACKING	LOW	121				LANE FT.
P (WB) 4 lanes	2500	ALLIGATOR CRACKING	LOW			62	394	LANE FT.
		CNTRLINE CRACKING	LOW				2405	LINEAL FT.
		LOCAL DISTRESS	LOW				1	NUMBER
P	12431 <sup>(c)</sup>	ASPHALT BLEEDING	LOW		68		60	LANE FT.
		CENTER OF LANE	LOW		8			LINEAL FT.
		CNTRLINE CRACKING	LOW		5651			LINEAL FT.
		ALLIGATOR CRACKING	LOW		22		354	LANE FT.

(a) ESALs at the time of the survey were 280,000

(b) ESALs at the time of the survey were 230,000

(c) 3349 feet not summarized due to SHRP test sections

TABLE 16A: 1990 DISTRESS SUMMARY FOR PROJECT 2

SECTION	LENGTH (FEET)	DISTRESS	SEVERITY	AMOUNT				UNITS OF MEASURE
				EB		WB		
				PL	DL(a)	PL	DL(a)	
C	1662	TRANS. CRACKING TRANS. CRACKING	LOW MEDIUM		1		1	NUMBER NUMBER
D	3215	TRANS. CRACKING	LOW		76		76	NUMBER
E	965							
F	1043							
G1	400							
G2	400							
G3	400							
G4 (EB) 4 lanes	2138 <sup>(b)</sup>	TRANS. CRACKING	LOW	51	58			NUMBER
G4 (WB) 4 lanes	2138 <sup>(c)</sup>	TRANS. CRACKING	LOW			25	36	NUMBER
G4 2 lanes	2897	TRANS. CRACKING	LOW		74		75	NUMBER
H (EB)	1441							
H (WB)	1441							

(a) ESALs at the time of the survey were 140,000

(b) Includes a 219-foot taper to four lanes

(c) Includes a 788-foot taper to two lanes

TABLE 16B: 1992 DISTRESS SUMMARY FOR PROJECT 2

SECTION	LENGTH (FEET)	DISTRESS	SEVERITY	AMOUNT				UNITS OF MEASURE
				EB PL	DL(a)	WB PL	DL(a)	
C	1662	TRANS. CRACKING TRANS. CRACKING	MEDIUM HIGH		1		1	NUMBER NUMBER
D	3215	TRANS. CRACKING TRANS. CRACKING	LOW MEDIUM		73 1		76 1	NUMBER NUMBER
E	965							
F	1043							
G1	400							
G2	400							
G3	400							
G4 (EB) 4 lanes	2138 <sup>(b)</sup>	TRANS. CRACKING	LOW	51	58			NUMBER
G4 (WB) 4 lanes	2138 <sup>(c)</sup>	TRANS. CRACKING	LOW			32	52	NUMBER
G4 2 lanes	2897	TRANS. CRACKING	LOW		74		78	NUMBER
H (EB)	1441							
H (WB)	1441							

(a) ESALs at the time of the survey were 370,000

(b) Includes a 219-foot taper to four lanes

(c) Includes a 788-foot taper to two lanes



TABLE 17A: 1990 DISTRESS SUMMARY FOR PROJECT 4

SECTION	LENGTH (FEET)	DISTRESS	SEVERITY	AMOUNT				UNITS OF MEASURE
				EB		WB		
				PL	DL(a)	PL	DL(b)	
R	2521	CONST. JT. DETER.	LOW		1		1	NUMBER
S (EB) 4 lanes	7356	CONST. JT. DETER.	LOW	3	3			NUMBER
S (WB) 4 lanes	7356	CONST. JT. DETER.	LOW	3	3			NUMBER
S 2 lanes	3544	CONST. JT. DETER.	LOW				1	NUMBER
		CONST. JT. DETER.	MEDIUM		1			NUMBER
		TRANS. CRACKING	LOW		1			NUMBER
T	1000							
U	1000							
V	1000							
W	1100							
X	1000	CONST. JT. DETER.	LOW		1		1	NUMBER
Y	1000							
Z	1500	CONST. JT. DETER.	LOW		1		1	NUMBER
AA	1000							
BA	2120	CONST. JT. DETER.	LOW		1		1	NUMBER
		TRANS. CRACKING	LOW		40		42	NUMBER
		TRANS. CRACKING	MEDIUM		14		12	NUMBER
CA	1960	LOCAL DISTRESS	MEDIUM		1			NUMBER
		TRANS. CRACKING	LOW		39		37	NUMBER
		TRANS. CRACKING	MEDIUM		11		13	NUMBER
DA	440	LONG. CRACKING	LOW				2(c)	LINEAL FT.
DB	400	TRANS. CRACKING	LOW		1(c)	1(d)	3(c)	NUMBER
		LONG. CRACKING	LOW				2(c)	LINEAL FT.
DC	360							
EA	3920	LONG. CRACKING	LOW		147			LINEAL FT.
		LONG. CRACKING	MEDIUM		7			LINEAL FT.
		LOCAL DISTRESS	HIGH				1	NUMBER
		TRANS. CRACKING	LOW		71		68	NUMBER
		TRANS. CRACKING	MEDIUM		35		34	NUMBER
FA	1640	TRANS. CRACKING	LOW		39		36	NUMBER
		TRANS. CRACKING	MEDIUM		6		9	NUMBER

TABLE 17A: 1990 DISTRESS SUMMARY FOR PROJECT 4 (CONT.)

SECTION	LENGTH (FEET)	DISTRESS	SEVERITY	AMOUNT		UNITS OF MEASURE
				EB PL DL(a)	WB PL DL(b)	
GA	2000	SPALLING	MEDIUM	1		NUMBER
		TRANS. CRACKING	LOW	56	53	NUMBER
		TRANS. CRACKING	MEDIUM	1	2	NUMBER
HA	2000	LOCAL DISTRESS	MEDIUM	1		NUMBER
		TRANS. CRACKING	LOW	54	50	NUMBER
IA	1020	PERM. PATCH DETER.	LOW	96		SQUARE FT.
		SPALLING	LOW	1		NUMBER
		TRANS. CRACKING	LOW	1	1	NUMBER
		TRANS. CRACKING	MEDIUM	1	1	NUMBER
		CONST. JT. DETER.	LOW	1	1	NUMBER
JA	1000	SPALLING	MEDIUM		1	NUMBER
		TRANS. CRACKING	MEDIUM	2	2	NUMBER
KA	1000	TRANS. CRACKING	LOW		1	NUMBER
LA	1100	TRANS. CRACKING	LOW	6	1	NUMBER
MA	1100	CONST. JT. DETER.	LOW	1	1	NUMBER
NA	1000	FAULTING		0.04	0.19	INCHES
		TRANS. CRACKING	LOW	2	1	NUMBER
		TRANS. CRACKING	HIGH	1	2	NUMBER
OA	2000	PERM. PATCH DETER.	LOW	72	576	SQUARE FT.
		SPALLING	LOW	9	1	NUMBER
		TRANS. CRACKING	LOW	61	56	NUMBER
		TRANS. CRACKING	MEDIUM	1		NUMBER
PA	2000	TRANS. CRACKING	LOW	46	49	NUMBER
		TRANS. CRACKING	MEDIUM	5		NUMBER
QA	2000	TRANS. CRACKING	LOW	61	61	NUMBER
RA	2520	TRANS. CRACKING	LOW	42	57	NUMBER
		TRANS. CRACKING	MEDIUM	16		NUMBER

(a) ESALs at the time of the survey were 260,000

(b) ESALs at the time of the survey were 210,000

(c) Recorded by PASCO in 1989

(d) Distress is located in a left turn lane

TABLE 17B: 1992 DISTRESS SUMMARY FOR PROJECT 4

SECTION	LENGTH (FEET)	DISTRESS	SEVERITY	AMOUNT				UNITS OF MEASURE
				EB PL	DL(a)	WB PL	DL(b)	
R	2521	CONST. JT. DETER.	LOW		1		1	NUMBER
S (EB) 4 lanes	7356	CONST. JT. DETER.	LOW	3	3			NUMBER
S (WB) 4 lanes	7356	CONST. JT. DETER.	LOW			3	3	NUMBER
S 2 lanes	3544	CONST. JT. DETER.	LOW				1	NUMBER
		CONST. JT. DETER.	MEDIUM		1			NUMBER
		TRANS. CRACKING	LOW		1			NUMBER
T	1000							
U	1000							
V	1000							
W	1100							
X	1000	CONST. JT. DETER.	LOW		1		1	NUMBER
Y	1000							
Z	1500	CONST. JT. DETER.	LOW		1		1	NUMBER
AA	1000							
BA	2120	CONST. JT. DETER.	LOW		1		1	NUMBER
		TRANS. CRACKING	LOW		33		27	NUMBER
		TRANS. CRACKING	MEDIUM		21		27	NUMBER
		TRANS. CRACKING	HIGH		1			NUMBER
CA	1960	LOCAL DISTRESS	MEDIUM		1			NUMBER
		TRANS. CRACKING	LOW		21		15	NUMBER
		TRANS. CRACKING	MEDIUM		20		27	NUMBER
DA	440	LONG. CRACKING	LOW				2(c)	LINEAL FT.
DB	400	TRANS. CRACKING	LOW		1(d)	1(e)	5(d)	NUMBER
		LONG. CRACKING					2(c)	LINEAL FT.
DC	360							
EA	3920	LONG. CRACKING	LOW		186			LINEAL FT.
		LOCAL DISTRESS	HIGH				1	NUMBER
		LOCAL DISTRESS	LOW		1			NUMBER
		TRANS. CRACKING	LOW		44		52	NUMBER
		TRANS. CRACKING	MEDIUM		64		53	NUMBER
		SPALLING	LOW		2			NUMBER
		LONG. CRACKING	MEDIUM		10			LINEAL FT.

TABLE 17B: 1992 DISTRESS SUMMARY FOR PROJECT 4 (CONT.)

SECTION	LENGTH (FEET)	DISTRESS	SEVERITY	AMOUNT		UNITS OF MEASURE
				PL <sup>EB</sup> DL <sup>(a)</sup>	PL <sup>WB</sup> DL <sup>(b)</sup>	
FA	1640	TRANS. CRACKING	LOW	34	33	NUMBER
		TRANS. CRACKING	MEDIUM	13	12	NUMBER
		CONST. JT. DETER.	LOW	1	1	NUMBER
GA	2000	SPALLING	MEDIUM	1		NUMBER
		TRANS. CRACKING	LOW	52	42	NUMBER
		TRANS. CRACKING	MEDIUM	5	3	NUMBER
HA	2000	LOCAL DISTRESS	MEDIUM	1		NUMBER
		TRANS. CRACKING	LOW	45	53	NUMBER
		TRANS. CRACKING	MEDIUM	9	1	NUMBER
IA	1020	PERM. PATCH DETER.	LOW	96		SQUARE FT.
		SPALLING	LOW	1		NUMBER
		TRANS. CRACKING	LOW	1	1	NUMBER
		TRANS. CRACKING	MEDIUM	1	1	NUMBER
		CONST. JT. DETER.	LOW	1	1	NUMBER
JA	1000	SPALLING	MEDIUM		1	NUMBER
		TRANS. CRACKING	MEDIUM	3	3	NUMBER
KA	1000	TRANS. CRACKING	LOW		1	NUMBER
LA	1100	TRANS. CRACKING	LOW	6	1	NUMBER
MA	1100	TRANS. CRACKING	LOW	1	1	NUMBER
NA	1000	TRANS. CRACKING	LOW	3	3	NUMBER
		TRANS. CRACKING	MEDIUM	1		NUMBER
		TRANS. CRACKING	HIGH	1	2	NUMBER
OA	2000	PERM. PATCH DETER.	LOW	120	792	SQUARE FT.
		SPALLING	LOW	9	4	NUMBER
		TRANS. CRACKING	LOW	47	46	NUMBER
		TRANS. CRACKING	MEDIUM	17	11	NUMBER
PA	2000	LOCAL DISTRESS	MEDIUM		1	NUMBER
		TRANS. CRACKING	LOW	28	45	NUMBER
		TRANS. CRACKING	MEDIUM	24	6	NUMBER
QA	2000	TRANS. CRACKING	LOW	32	38	NUMBER
		TRANS. CRACKING	LOW	30	23	NUMBER
		SPALLING	LOW		1	NUMBER
		CONST. JT. DETER.	LOW	1	1	NUMBER
RA	2520	TRANS. CRACKING	LOW	27	39	NUMBER
		TRANS. CRACKING	MEDIUM	33	22	NUMBER
		SPALLING	LOW		3	NUMBER

(a) ESALs at the time of the survey were 430,000

(b) ESALs at the time of the survey were 390,000

(c) Recorded by PASCO in 1989

(d) Recorded by the June 1992 field review

(e) Distress located in a left turn lane

TABLE 18: SUMMARY OF FULL-DEPTH REPAIRED AREAS ON PROJECT 3

SECTION	SECTION INFORMATION	PATCH LOCATION	DESCRIPTION	DATE PATCHED
K	9.5" AC-20 UNDERDRAINS UNTREATED SUBGRADE	STA 602+50	EASTBOUND LANE INNER WHEELPATH PATCH DIMENSIONS: 6' X 60' = 40 SQ. YDS. * NOTE: THIS LOCATION WAS "SKIN" PATCHED IN AUGUST 1988. **NOTE: REPAIR CONSISTED OF 3-4" OF CRUSHED STONE AND 5-6" OF ASPHALT CONCRETE.	7/26/89
		STA 609+00	EASTBOUND LANE INNER WHEELPATH PATCH DIMENSIONS: 6' X 70' = 47 SQ. YDS. * NOTE: THIS LOCATION WAS "SKIN" PATCHED IN AUGUST 1988.	8/1/89
		STA 609+75	EASTBOUND LANE INNER WHEELPATH PATCH DIMENSIONS: 6' X 38' = 25 SQ. YDS. * NOTE: THIS LOCATION WAS "SKIN" PATCHED IN AUGUST 1988.	8/2/89
		STA 602+45 TO STA 602+86	EASTBOUND LANE INNER WHEELPATH PATCH DIMENSIONS: 9' X 41' = 41 SQ. YDS. * NOTE: STA 602+45 TO 602+86 WAS REPLACEMENT OF 1989 PATCH.	7/25/90
		STA 609+93 TO STA 610+28	EASTBOUND LANE INNER WHEELPATH PATCH DIMENSIONS: 6' X 35' = 23.3 SQ. YDS.	6/5/91

TABLE 18: SUMMARY OF FULL-DEPTH REPAIRED AREAS ON PROJECT 3 (CONT.)

SECTION	SECTION INFORMATION	PATCH LOCATION	DESCRIPTION	DATE PATCHED
M	9.5" AC-20 NO UNDERDRAINS LIME-MODIFIED SUBGRADE	STA 2568+25	EASTBOUND LANE OUTER WHEELPATH PLUS 2' SHOULDER PATCH DIMENSIONS: 8.5' X 61' = 58 SQ. YDS. * NOTE: THIS LOCATION WAS "SKIN" PATCHED IN AUGUST 1988. **NOTE: THIS STATION IS WITHIN 100' OF SECTION M1, WHICH HAS NO LIME-MODIFIED SUBGRADE.	8/7/89
		STA 2563+77	EASTBOUND LANE OUTER WHEELPATH PLUS 1' SHOULDER ESTIMATED PATCH DIMENSIONS: 7' X 34' = 26 SQ. YDS.	8/8/89
		STA 2562+57 TO STA 2562+91	EASTBOUND LANE INNER WHEELPATH PATCH DIMENSIONS: 6' X 34' = 22.7 SQ. YDS.	6/5/91
		STA 2562+91 TO STA 2563+57	EASTBOUND LANE OUTER WHEELPATH PATCH DIMENSIONS: 6' X 66' = 44 SQ. YDS.	6/5/91

TABLE 18: SUMMARY OF FULL-DEPTH REPAIRED AREAS ON PROJECT 3 (CONT.)

SECTION	SECTION INFORMATION	PATCH LOCATION	DESCRIPTION	DATE PATCHED
M1	9.5" AC-20 NO UNDERDRAINS UNTREATED SUBGRADE	STA 2578+00	EASTBOUND LANE OUTER WHEELPATH PLUS 2' SHOULDER PATCH DIMENSIONS: 9' X 45' = 45 SQ. YDS.	7/28/89
		STA 2578+09 TO STA 2578+43	EASTBOUND LANE OUTER WHEELPATH PLUS 1' SHOULDER PATCH DIMENSIONS: 8' X 34' = 30.2 SQ. YDS.	6/5/91

TABLE 19: 1989 CORE DATA SUMMARY FOR PROJECTS 1 AND 3

PROJECT 1						
UNCONDITIONED TENSILE STRENGTHS, PSI						
	RANGE	AVERAGE	STD. DEV.	C.O.V., %	NO. OF LIFTS	STRIPPING
AC-10	77.8 - 213.5	156.05	39.44	25.27	20	SLIGHT TO NONE
AC-20	132.3 - 269.5	183.09	43.44	23.67	18	SLIGHT TO NONE
PROJECT 3						
UNCONDITIONED TENSILE STRENGTHS, PSI						
	RANGE	AVERAGE	STD. DEV.	C.O.V., %	NO. OF LIFTS	STRIPPING
AC-10	0 - 182.2 *	78.01	59.31	76.03	28	SLIGHT TO SEVERE
AC-20	0 - 276.9 *	103.38	48.89	47.29	51	SLIGHT TO SEVERE

\* 0 DENOTES LIFT NOT RECOVERABLE



TABLE 20: HAND-MEASURED RUT DEPTH DATA HISTORY FOR PROJECT 1

AVERAGE RUT DEPTHS, INCHES			
YEAR	SECTION	EASTBOUND DRIVING LANE	WESTBOUND DRIVING LANE
1988 <sup>(a)</sup>	A	0.08 (n=83)	0.10 (n=83)
	B	0.08 (n=114)	0.08 (n=114)
1990 <sup>(b)</sup>	A	0.11 (n=6)	0.11 (n=5)
	B	0.09 (n=6)	0.09 (n=6)
1992 <sup>(c)</sup>	A	0.10 (n=5)	0.14 (n=5)
	B	0.06 (n=6)	0.07 (n=6)

(a) ESALs at the time of the survey were 60,000

(b) ESALs at the time of the survey were 90,000

(c) ESALs at the time of the survey were 200,000

TABLE 21A: 1988 HAND-MEASURED RUT DEPTH DATA FOR PROJECT 3

AVERAGE RUT DEPTHS, INCHES

SECTION	EASTBOUND DRIVING LANE <sup>(a)</sup>	WESTBOUND DRIVING LANE <sup>(b)</sup>
A	0.09 (n=28)	0.04 (n=30)
B	0.23 (n=10)	0.07 (n=10)
C	0.13 (n=9)	0.06 (n=10)
D	0.14 (n=12)	0.08 (n=12)
E	0.10 (n=60)	0.02 (n=60)
H	0.10 (n=10)	0.03 (n=10)
I	0.08 (n=21)	0.02 (n=21)
J	0.12 (n=4)	0.06 (n=4)
K	0.28 (n=25)	0.06 (n=24)
L	0.12 (n=7)	0.04 (n=7)
M	0.20 (n=16)	0.08 (n=16)
M1	0.07 (n=23)	0.07 (n=24)
N	0.06 (n=15)	0.02 (n=15)
O	0.08 (n=11)	0.06 (n=11)
P	0.08 (n=148)	0.06 (n=148)

(a) ESALs at the time of the survey were 80,000

(b) ESALs at the time of the survey were 60,000

TABLE 21B: 1989 HAND-MEASURED RUT DEPTH DATA FOR PROJECT 3

AVERAGE RUT DEPTHS, INCHES

SECTION	EASTBOUND DRIVING LANE <sup>(a)</sup>	WESTBOUND DRIVING LANE <sup>(b)</sup>
A	0.10 (n=25)	0.04 (n=29)
B	0.28 (n=11)	0.10 (n=11)
C	0.16 (n=10)	0.06 (n=11)
D	0.16 (n=12)	0.10 (n=12)
E	0.10 (n=60)	0.02 (n=60)
H	0.14 (n=10)	0.04 (n=10)
I	0.08 (n=21)	0.02 (n=21)
J	0.14 (n=4)	0.14 (n=4)
K	0.33 (n=25)	0.14 (n=25)
L	0.11 (n=7)	0.08 (n=7)
M	0.24 (n=15)	0.10 (n=15)
M1	0.10 (n=23)	0.10 (n=25)
N	0.07 (n=15)	0.00 (n=15)
O	0.12 (n=11)	0.08 (n=11)
P	0.10 (n=148)	0.09 (n=148)

(a) ESALs at the time of the survey were 150,000

(b) ESALs at the time of the survey were 110,000

TABLE 21C: 1990 HAND-MEASURED RUT DEPTH DATA FOR PROJECT 3

AVERAGE RUT DEPTHS, INCHES

SECTION	EASTBOUND DRIVING LANE <sup>(a)</sup>	WESTBOUND DRIVING LANE <sup>(b)</sup>
A	0.05 (n=1)	0.05 (n=1)
B	0.28 (n=1)	0.08 (n=1)
C	N/A	N/A
D	0.10 (n=1)	0.12 (n=1)
E	0.10 (n=4)	0.00 (n=4)
H	N/A	N/A
I	0.12 (n=1)	0.00 (n=1)
J	N/A	N/A
K	0.37 (n=3)	0.15 (n=3)
L	N/A	N/A
M	N/A	0.20 (n=1)
M1	0.03 (n=2)	0.00 (n=1)
N	N/A	0.02 (n=1)
O	0.10 (n=1)	N/A
P	0.10 (n=10)	0.08 (n=11)

N/A = Not available

(a) ESALs at the time of the survey were 180,000

(b) ESALs at the time of the survey were 130,000

TABLE 21D: 1992 HAND-MEASURED RUT DEPTH DATA SUMMARY FOR PROJECT 3

AVERAGE RUT DEPTHS, INCHES

SECTION	EASTBOUND DRIVING LANE <sup>(a)</sup>	WESTBOUND DRIVING LANE <sup>(b)</sup>
A	0.08 (n=2)	0.04 (n=2)
B	0.46 (n=2)	0.12 (n=2)
C	N/A	N/A
D	0.15 (n=1)	0.12 (n=1)
E	0.13 (n=4)	0.00 (n=4)
H	0.45 (n=1)	0.05 (n=1)
I	0.10 (n=1)	0.02 (n=1)
J	0.45 (n=1)	0.38 (n=1)
K	0.64 (n=10)	0.42 (n=10)
L	N/A	N/A
M	0.05 (n=1)	0.18 (n=1)
M1	0.05 (n=1)	0.00 (n=1)
N	N/A	0.05 (n=1)
O	0.10 (n=1)	0.05 (n=1)
P	0.10 (n=9)	0.12 (n=2)

N/A = Not available

(a) ESALs at the time of the survey were 280,000

(b) ESALs at the time of the survey were 230,000

TABLE 22A: SUMMARY OF ROAD PROFILER RUT DEPTHS FOR PROJECT 1

AVERAGE RUT DEPTHS, INCHES						
SECTION	1990 <sup>(a)</sup>		1991 <sup>(b)</sup>		1992 <sup>(c)</sup>	
	EAST	WEST	EAST	WEST	EAST	WEST
A (AC-10)	0.08	0.10	0.04	0.04	0.08	0.08
B (AC-20)	0.08	0.11	0.04		0.06	0.08

(a) ESALS at the time of the survey were 100,000

(b) ESALS at the time of the survey were 160,000

(c) ESALS at the time of the survey were 190,000

TABLE 22B: SUMMARY OF ROAD PROFILER RUT DEPTHS FOR PROJECT 3

AVERAGE RUT DEPTHS, INCHES

SECTION	1990		1991		1992	
	EAST(a)	WEST(b)	EAST(c)	WEST(d)	EAST(e)	WEST(f)
A	0.24	0.18	0.18	0.14	0.30	0.22
B	0.38	0.21	0.33	0.18	0.24	0.20
C	0.25	0.18	0.25	0.14	0.28	0.22
D	0.23	0.22	0.18	0.21	0.22	0.19
E	0.19	0.17	0.16	0.14	0.22	0.18
H	0.30	0.23	0.23	0.21	0.23	0.23
I	0.19	0.22	0.17	0.20	0.41	0.34
J	0.36	0.26	0.27	0.21	0.44	0.43
K	0.36	0.35	0.37	0.34	0.36	0.28
L	0.31	0.24	0.25	0.17	N/A	N/A
M	0.55	0.26	0.16	0.20	0.44	0.34
M1	0.27	0.16	0.30	0.22	0.37	0.16
N	0.26	0.24	0.23	0.21	0.30	0.23
O	0.23	0.22	0.22	0.20	0.27	0.22
P	0.20	0.19	0.16	0.16	0.22	0.20

N/A = Not available

- (a) ESALs at the time of the survey were 200,000
- (b) ESALs at the time of the survey were 150,000
- (c) Esals at the time of the survey were 240,000
- (d) Esals at the time of the survey were 190,000
- (e) ESALs at the time of the survey were 280,000
- (f) ESALs at the time of the survey were 230,000

TABLE 23: FWD STATISTICS FOR DEFLECTIONS FOR PROJECT 1

AC-10																		
DATE	DIR	TEMP <sup>a</sup>	# OF TESTS	D0 <sup>b</sup> (MILS)			D1 <sup>b</sup> (MILS)			D2 <sup>b</sup> (MILS)			D3 <sup>b</sup> (MILS)			AREAC (INCHES)		
*	*	*	*	AVG.	S.D.	CV(%)	AVG.	S.D.	CV(%)	AVG.	S.D.	CV(%)	AVG.	S.D.	CV(%)	AVG.	S.D.	CV(%)
11/17/87	E	50	17	3.43	0.33	9.75	2.72	0.32	11.76	2.20	0.30	13.63	1.71	0.26	15.38	26.19	0.93	3.53
	W	46	16	3.41	0.74	21.84	2.75	0.67	24.52	2.22	0.55	24.72	1.71	0.41	23.77	26.40	1.25	4.74
5/31/88	E	99	9	11.51	1.73	15.00	6.44	0.96	14.97	3.80	0.45	11.83	2.01	0.26	13.14	17.78	0.81	4.54
	E	109	8	10.96	3.41	31.08	6.11	2.49	40.81	4.04	1.38	34.22	2.38	0.71	29.74	18.33	1.60	8.72
5/01/88	W	97	12	8.07	1.81	22.37	5.16	1.27	24.57	3.32	0.79	23.75	1.97	0.44	22.34	20.10	1.15	5.70
	W	90	4	7.43	3.02	40.57	5.16	2.71	52.56	3.68	1.99	54.06	2.46	1.33	54.05	21.65	2.26	10.45
5/08/89	E	68	17	4.60	0.78	16.97	3.51	0.59	16.90	2.74	0.48	17.53	2.05	0.37	18.15	24.98	0.77	3.07
	W	68	16	4.53	0.91	20.14	3.45	0.79	22.79	2.70	0.61	22.56	2.01	0.46	22.73	24.90	1.13	4.53
7/09/90	E	89	17	8.14	1.80	22.14	5.21	1.27	24.45	3.38	0.80	23.68	2.12	0.47	22.34	20.27	1.23	6.06
	W	89	14	9.61	2.28	23.77	5.86	1.76	30.09	3.58	1.17	32.60	2.15	0.74	34.56	19.05	1.62	8.50
3/20/91	E	69	17	4.70	0.72	15.30	3.57	0.59	16.48	2.61	0.48	18.21	1.84	0.37	20.05	24.13	0.99	4.09
	W	69	16	5.18	1.23	23.72	3.82	0.99	25.93	2.73	0.74	26.96	1.85	0.51	27.65	23.31	1.54	6.59

AC-20																		
DATE	DIR	TEMP <sup>a</sup>	# OF TESTS	D0 <sup>b</sup> (MILS)			D1 <sup>b</sup> (MILS)			D2 <sup>b</sup> (MILS)			D3 <sup>b</sup> (MILS)			AREAC (INCHES)		
*	*	*	*	AVG.	S.D.	CV(%)	AVG.	S.D.	CV(%)	AVG.	S.D.	CV(%)	AVG.	S.D.	CV(%)	AVG.	S.D.	CV(%)
11/17/87	E	49	23	3.31	0.57	17.20	2.71	0.52	18.98	2.27	0.46	20.18	1.82	0.39	21.58	27.25	1.12	4.11
	W	47	23	3.37	0.49	14.63	2.75	0.46	16.72	2.28	0.40	17.71	1.81	0.34	18.71	27.08	1.23	4.56
5/31/88	E	109	21	9.78	1.85	18.94	5.87	1.39	23.63	4.10	1.06	25.86	2.58	0.80	31.05	19.75	1.88	9.51
	E	126	2	15.15	4.26	28.15	9.75	2.16	22.19	6.09	0.67	11.04	3.28	0.06	1.72	20.09	1.74	8.66
5/01/88	W	90	9	7.54	0.59	7.76	5.58	0.46	8.18	4.10	0.41	9.88	2.84	0.34	11.96	23.67	1.07	4.52
	W	86	14	6.27	1.26	20.12	4.39	1.12	25.48	3.19	0.93	29.01	2.17	0.72	33.29	22.50	1.89	8.41
5/08/89	E	68	23	4.34	0.80	18.50	3.42	0.69	20.13	2.79	0.55	19.54	2.16	0.46	21.38	26.14	1.57	6.01
	W	68	24	4.45	0.60	13.52	3.51	0.55	15.77	2.81	0.50	17.89	2.16	0.44	20.48	25.88	1.36	5.25
7/09/90	E	89	22	7.56	1.26	16.68	5.09	1.22	23.86	3.65	1.00	27.32	2.47	0.79	31.82	21.66	2.18	10.07
	W	89	21	8.25	1.65	19.94	5.48	1.46	26.60	3.78	1.08	28.64	2.49	0.79	31.88	21.09	1.69	8.03
3/20/91	E	69	22	4.32	0.77	17.75	3.38	0.66	19.62	2.64	0.58	22.16	1.95	0.50	25.36	25.32	1.41	5.58
	W	69	22	4.70	0.75	16.01	3.64	0.68	18.64	2.78	0.59	21.24	2.03	0.50	24.54	24.89	1.39	5.60



TABLE 24A: FWD STATISTICS FOR DEFLECTIONS FOR 5/87 (EASTBOUND) FOR PROJECT 3

SECTION *	TEMP <sup>d</sup> *	# OF TESTS *	D0 <sup>b</sup> (MILS)			D1 <sup>b</sup> (MILS)			D2 <sup>b</sup> (MILS)			D3 <sup>b</sup> (MILS)		
			AVG.	S.D.	CV(%)	AVG.	S.D.	CV(%)	AVG.	S.D.	CV(%)	AVG.	S.D.	CV(%)
A	92.5	7	18.12	6.52	35.96	11.87	5.01	42.18	7.68	3.00	39.13	4.70	1.59	33.77
B	92.8	5	24.70	4.40	17.83	17.64	3.98	22.55	11.88	3.42	28.78	7.55	2.41	31.88
C	91.2	5	16.85	3.30	19.60	11.21	3.41	30.45	8.56	2.96	34.55	6.14	2.32	37.82
D	91.6	7	19.88	3.91	19.67	14.39	3.80	26.38	10.55	3.00	28.42	7.12	2.07	29.08
E	92.1	33	14.07	3.49	24.78	10.40	3.00	28.84	7.84	2.28	29.13	5.53	1.58	28.55
H	92.7	6	20.62	6.96	33.76	15.44	6.30	40.81	11.36	5.06	44.57	7.85	3.76	47.98
I	92.9	11	20.94	3.00	14.35	15.28	2.56	16.74	10.74	1.98	18.45	7.10	1.44	20.22
K	95.6	13	31.05	8.10	26.10	22.14	6.65	30.06	14.49	4.85	33.48	9.11	3.29	36.06
L	95.9	5	20.12	3.06	15.19	14.36	2.40	16.70	9.94	1.67	16.78	6.82	1.02	14.94
M	95.8	6	21.01	4.17	19.87	14.54	3.37	23.19	9.47	2.10	22.19	5.83	1.14	19.62
M1	95.4	4	17.71	8.41	47.50	11.23	5.52	49.15	7.52	2.61	34.67	4.87	1.02	20.92
N	95.4	8	13.08	4.18	31.98	8.28	2.74	33.14	5.90	1.59	26.91	4.07	1.01	24.78
O	95.3	6	16.56	3.32	20.08	11.06	2.67	24.19	7.62	1.91	25.12	4.88	1.24	25.50
P	94.0	77	16.06	4.54	28.29	10.23	3.23	31.57	6.68	1.90	28.39	4.26	1.09	25.64

SECTION *	TEMP <sup>d</sup> *	# OF TESTS *	EAC <sup>e</sup> (KSI)			ERI <sup>f</sup> (KSI)			AREAC (INCHES)		
			AVG.	S.D.	CV(%)	AVG.	S.D.	CV(%)	AVG.	S.D.	CV(%)
A	92.5	7	136.74	9.56	6.99	6.79	3.27	48.13	20.40	0.92	4.52
B	92.8	5	143.25	16.98	11.85	2.96	2.13	71.82	21.99	1.51	6.86
C	91.2	5	109.71	15.96	14.55	4.51	4.00	88.86	21.89	2.41	11.03
D	91.6	7	145.85	25.83	17.71	3.03	3.00	98.81	22.95	1.66	7.22
E	92.1	33	218.26	50.24	23.02	5.01	3.23	64.38	23.74	1.27	5.35
H	92.7	6	173.71	26.92	15.50	5.00	4.14	82.92	23.48	1.60	6.81
I	92.9	11	169.15	32.78	19.38	2.50	1.45	58.21	22.88	0.73	3.18
K	95.6	13	126.83	26.84	21.16	4.23	3.57	84.30	21.75	1.60	7.36
L	95.9	5	166.69	15.08	9.05	2.48	1.00	40.31	22.56	1.21	5.36
M	95.8	6	152.00	18.14	11.93	4.04	2.51	62.12	21.30	0.92	4.34
M1	95.4	4	118.76	18.14	15.27	5.95	2.41	40.60	20.68	1.15	5.58
N	95.4	8	157.14	72.50	46.14	8.11	2.84	35.00	21.04	1.18	5.63
O	95.3	6	140.93	17.74	12.59	6.09	3.22	52.84	21.19	1.40	6.60
P	94.0	77	142.27	22.09	15.53	7.64	2.82	36.85	20.21	1.00	4.93

TABLE 24A: FWD STATISTICS FOR DEFLECTIONS FOR 5/87 (WESTBOUND) FOR PROJECT 3 (CONT.)

SECTION *	TEMP <sup>d</sup> *	# OF TESTS *	D0 <sup>b</sup> (MILS)			D1 <sup>b</sup> (MILS)			D2 <sup>b</sup> (MILS)			D3 <sup>b</sup> (MILS)		
			AVG.	S.D.	CV(%)	AVG.	S.D.	CV(%)	AVG.	S.D.	CV(%)	AVG.	S.D.	CV(%)
A	88.9	7	13.39	3.58	26.73	9.13	2.81	30.76	6.15	1.91	31.05	3.96	1.16	29.29
B	88.9	6	18.29	3.50	19.13	12.57	3.16	25.12	8.70	2.47	28.37	5.73	1.67	29.20
C	87.6	5	12.26	2.68	21.82	8.37	2.26	26.99	6.00	1.78	29.74	4.07	1.35	33.30
D	87.6	6	16.17	3.35	20.72	12.39	3.01	24.31	9.36	2.42	25.89	6.59	1.77	26.90
E	87.6	33	11.43	2.39	20.90	8.72	2.14	24.49	6.77	1.71	25.29	4.95	1.27	25.64
H	87.4	5	13.05	2.20	16.82	9.82	2.09	21.25	7.55	1.88	24.88	5.48	1.49	27.26
I	87.2	11	13.82	2.64	19.13	10.75	2.23	20.76	8.27	1.83	22.16	6.01	1.39	23.18
K	87.9	15	22.96	4.50	19.60	17.44	3.68	21.08	12.18	2.78	22.82	8.11	2.04	25.11
L	87.6	4	17.02	5.03	29.53	12.69	4.41	34.77	9.33	3.05	32.66	6.72	1.82	27.08
M	87.3	8	17.45	3.31	18.97	12.94	2.51	19.39	8.94	1.85	20.73	5.85	1.36	23.31
M1	86.9	13	13.64	2.85	20.93	9.47	2.68	28.31	6.35	2.06	32.48	4.15	1.44	34.59
N	86.6	8	12.21	2.93	23.96	8.73	2.24	25.64	6.45	1.41	21.85	4.61	0.94	20.44
O	86.3	6	12.48	3.01	24.14	9.22	2.76	29.95	6.70	2.10	31.31	4.57	1.57	34.39
P	84.7	80	11.54	2.54	22.01	8.18	2.05	25.03	5.82	1.37	23.63	4.01	0.87	21.77

SECTION *	TEMP <sup>d</sup> *	# OF TESTS *	EAC <sup>e</sup> (KSI)			ERI <sup>f</sup> (KSI)			AREAC <sup>c</sup> (INCHES)		
			AVG.	S.D.	CV(%)	AVG.	S.D.	CV(%)	AVG.	S.D.	CV(%)
A	88.9	7	205.75	25.07	12.18	8.49	3.28	38.64	21.36	0.85	3.99
B	88.9	6	157.49	46.05	29.24	4.60	2.78	60.43	21.69	1.61	7.41
C	87.6	5	206.33	72.95	35.36	8.28	3.50	42.33	21.93	1.65	7.51
D	87.6	6	227.94	11.84	5.20	3.32	2.48	74.54	24.44	1.17	4.79
E	87.6	33	293.55	63.01	21.46	6.00	2.97	49.44	24.72	1.19	4.81
H	87.4	5	238.06	29.24	12.28	4.92	3.24	65.81	24.30	1.37	5.62
I	87.2	11	296.03	64.63	21.83	3.93	2.09	53.14	25.06	0.77	3.07
K	87.9	15	223.84	57.66	25.76	2.41	1.82	75.51	23.55	1.24	5.26
L	87.6	4	229.23	70.56	30.78	3.12	1.45	46.61	23.85	1.55	6.50
M	87.3	8	253.65	75.69	29.84	4.17	2.30	55.15	23.04	1.14	4.93
M1	86.9	13	235.21	44.68	19.00	8.17	3.32	40.70	21.54	1.56	7.25
N	86.6	8	225.84	21.04	9.31	6.59	2.45	37.23	23.23	1.21	5.22
O	86.3	6	274.04	45.39	16.56	7.10	3.99	56.17	23.27	1.67	7.20
P	84.7	80	257.23	42.37	16.47	8.23	2.52	30.65	22.58	1.00	4.44

TABLE 24B: FWD STATISTICS FOR DEFLECTIONS FOR 9/87 (EASTBOUND) FOR PROJECT 3

SECTION *	TEMP <sup>d</sup> *	# OF TESTS *	D0 <sup>b</sup> (MILS)			D1 <sup>b</sup> (MILS)			D2 <sup>b</sup> (MILS)			D3 <sup>b</sup> (MILS)		
			AVG.	S.D.	CV(%)	AVG.	S.D.	CV(%)	AVG.	S.D.	CV(%)	AVG.	S.D.	CV(%)
A	73.0	7	10.12	2.34	23.12	7.53	1.89	25.14	5.38	1.22	22.65	3.75	0.73	19.34
B	73.1	5	12.00	1.62	13.47	9.64	1.61	16.67	7.38	1.40	18.96	5.38	1.15	21.38
C	74.1	5	8.17	1.50	18.31	6.51	1.45	22.27	5.26	1.32	25.00	4.12	1.17	28.40
D	74.3	6	9.38	1.93	20.63	7.55	1.90	25.20	6.03	1.66	27.56	4.59	1.35	29.32
E	74.9	30	7.55	1.43	18.96	6.12	1.28	20.86	4.93	1.04	21.10	3.79	0.81	21.24
H	75.6	5	9.01	1.06	11.80	7.25	0.99	13.71	5.68	0.84	14.72	4.28	0.67	15.58
I	75.9	10	10.09	1.31	12.94	8.20	1.09	13.25	6.37	0.89	14.02	4.71	0.73	15.55
K	76.1	19	13.20	2.43	18.42	10.14	1.73	17.07	7.34	1.23	16.72	5.31	0.91	17.16
L	77.1	5	10.68	1.74	16.33	8.48	1.45	17.05	6.48	0.96	14.83	4.89	0.62	12.72
M	77.0	7	12.37	3.62	29.24	9.60	2.69	28.00	6.96	1.64	23.52	4.88	0.89	18.29
M1	77.5	11	10.40	3.41	32.74	7.95	2.55	32.05	5.69	1.57	27.59	3.93	0.98	24.92
N	77.8	7	10.21	3.66	35.85	7.93	2.61	32.99	5.85	1.87	31.89	4.16	1.48	35.48
O	78.1	5	11.65	3.46	29.72	8.77	2.85	32.51	6.23	2.02	32.41	4.16	1.35	32.56
P	79.1	74	10.21	2.65	25.96	7.61	2.02	26.55	5.50	1.32	23.98	3.84	0.82	21.46

SECTION *	TEMP <sup>d</sup> *	# OF TESTS *	EAC <sup>e</sup> (KSI)			ERIF <sup>f</sup> (KSI)			AREAC <sup>c</sup> (INCHES)		
			AVG.	S.D.	CV(%)	AVG.	S.D.	CV(%)	AVG.	S.D.	CV(%)
A	73.0	7	391.36	57.36	14.66	8.91	2.06	23.16	23.58	0.88	3.74
B	73.1	5	465.20	56.43	12.13	4.89	2.01	41.16	25.64	1.00	3.92
C	74.1	5	505.42	103.08	20.40	8.01	3.36	41.92	26.15	1.44	5.49
D	74.3	6	486.94	75.65	15.54	6.70	3.76	56.19	26.10	1.47	5.62
E	74.9	30	648.02	163.18	25.18	8.80	2.44	27.73	26.53	1.07	4.02
H	75.6	5	571.09	115.44	20.21	7.34	1.72	23.46	26.01	0.62	2.39
I	75.9	10	588.96	112.15	19.04	6.25	1.73	27.63	26.11	0.52	2.00
K	76.1	19	403.94	120.00	29.71	4.95	1.98	39.94	24.40	1.29	5.30
L	77.1	5	495.62	98.52	19.88	5.76	1.63	28.21	25.58	0.97	3.81
M	77.0	7	435.52	115.79	26.59	5.89	1.98	33.62	24.59	0.81	3.31
M1	77.5	11	501.70	218.57	43.57	8.50	2.69	31.70	24.37	1.93	7.93
N	77.8	7	551.69	228.12	41.35	8.13	3.88	47.69	24.98	2.84	11.36
O	78.1	5	375.79	114.50	30.47	8.01	3.81	47.49	23.49	1.42	6.05
P	79.1	74	395.26	109.87	27.80	8.70	2.38	27.39	23.74	1.23	5.16

TABLE 24B: FWD STATISTICS FOR DEFLECTIONS FOR 9/87 (WESTBOUND) FOR PROJECT 3 (CONT.)

SECTION *	TEMP <sup>d</sup> *	# OF TESTS *	D0 <sup>b</sup> (MILS)			D1 <sup>b</sup> (MILS)			D2 <sup>b</sup> (MILS)			D3 <sup>b</sup> (MILS)		
			AVG.	S.D.	CV(%)	AVG.	S.D.	CV(%)	AVG.	S.D.	CV(%)	AVG.	S.D.	CV(%)
A	89.3	6	10.71	3.10	28.94	7.39	2.31	31.18	5.02	1.35	26.94	3.27	0.76	23.22
B	89.2	5	14.86	3.66	24.67	10.82	3.16	29.16	7.72	2.42	31.36	5.22	1.61	30.88
C	87.3	4	10.60	2.42	22.86	7.61	1.95	25.56	5.62	1.59	28.21	3.97	1.28	32.27
D	87.2	7	11.88	2.08	17.51	8.83	1.78	20.21	6.71	1.45	21.59	4.75	1.08	22.67
E	87.1	29	9.04	1.67	18.44	6.87	1.54	22.47	5.43	1.26	23.24	4.04	0.94	23.31
H	86.9	5	10.24	1.44	14.09	7.38	1.15	15.61	5.61	0.83	14.79	4.09	0.64	15.59
I	86.8	10	11.85	2.17	18.31	9.06	2.09	23.05	6.98	1.70	24.39	5.06	1.28	25.25
K	88.5	20	19.42	3.48	17.90	13.84	2.92	21.10	9.38	2.30	24.48	6.22	1.68	27.04
L	88.3	4	14.40	3.73	25.92	10.87	3.26	29.95	7.99	2.07	25.86	5.75	1.04	18.14
M	88.2	7	15.33	3.65	23.77	11.28	2.65	23.49	7.80	1.72	21.99	5.14	1.05	20.34
M1	88.0	11	11.25	2.09	18.62	7.68	1.37	17.85	5.29	0.84	15.94	3.62	0.55	15.16
N	87.9	7	9.73	2.44	25.11	7.25	1.81	24.94	5.56	1.30	23.39	4.00	1.06	26.40
O	87.8	5	11.05	3.13	28.31	7.94	2.63	33.11	5.73	1.82	31.86	3.91	1.25	31.98
P	85.5	74	10.61	2.51	23.66	7.76	1.98	25.53	5.73	1.34	23.35	3.98	0.81	20.46

SECTION *	TEMP <sup>d</sup> *	# OF TESTS *	EAC <sup>e</sup> (KSI)			ERIF <sup>f</sup> (KSI)			AREAC <sup>c</sup> (INCHES)		
			AVG.	S.D.	CV(%)	AVG.	S.D.	CV(%)	AVG.	S.D.	CV(%)
A	89.3	6	273.15	56.15	20.56	10.49	2.47	23.58	21.77	0.92	4.22
B	89.2	5	225.50	25.64	11.37	5.55	2.59	46.68	22.97	1.15	5.02
C	87.3	4	275.63	83.14	30.16	8.50	3.55	41.77	23.17	1.55	6.70
D	87.2	7	266.01	86.97	32.69	6.30	2.87	45.50	24.02	1.71	7.12
E	87.1	29	341.27	86.88	25.46	8.18	2.65	32.43	24.88	1.28	5.15
H	86.9	5	252.67	36.84	14.58	7.33	2.00	27.25	23.61	0.61	2.60
I	86.8	10	293.47	62.22	21.20	5.69	2.66	46.79	24.68	1.33	5.38
K	88.5	20	187.17	40.69	21.74	3.88	2.40	61.77	22.16	1.23	5.54
L	88.3	4	332.65	169.92	51.08	4.10	2.03	49.45	24.12	1.61	6.69
M	88.2	7	264.73	58.19	21.98	5.37	2.29	42.58	23.01	1.00	4.35
M1	88.0	11	252.24	53.40	21.17	9.27	1.72	18.57	21.91	1.62	7.38
N	87.9	7	303.94	54.99	18.09	8.33	3.42	41.10	24.35	1.97	8.10
O	87.8	5	268.61	48.38	18.01	8.67	3.83	44.20	22.79	1.77	7.75
P	85.5	74	292.41	61.80	21.13	8.29	2.31	27.91	23.51	1.01	4.31

TABLE 24C: FWD STATISTICS FOR DEFLECTIONS FOR 5/88 (EASTBOUND) FOR PROJECT 3

SECTION *	TEMP <sup>d</sup> *	# OF TESTS *	D0 <sup>b</sup> (MILS)			D1 <sup>b</sup> (MILS)			D2 <sup>b</sup> (MILS)			D3 <sup>b</sup> (MILS)		
			AVG.	S.D.	CV(%)	AVG.	S.D.	CV(%)	AVG.	S.D.	CV(%)	AVG.	S.D.	CV(%)
A	81.0	7	13.73	2.35	17.08	10.29	1.92	18.65	7.23	1.37	18.92	4.69	0.86	18.35
B	80.0	5	15.78	3.43	21.71	12.54	2.89	23.06	9.35	2.32	24.82	6.41	1.71	26.73
C	81.1	5	9.88	2.27	23.01	7.75	1.96	25.35	6.26	1.73	27.61	4.72	1.41	29.84
D	81.1	6	11.39	1.78	15.63	8.95	1.55	17.32	6.98	1.34	19.16	5.09	1.07	21.10
E	81.1	30	8.97	1.76	19.59	7.24	1.53	21.12	5.77	1.24	21.55	4.33	0.94	21.70
H	81.1	5	13.70	3.78	27.59	10.91	3.41	31.28	8.47	2.80	33.00	6.27	2.20	35.01
I	80.7	10	12.90	1.81	14.04	10.50	1.65	15.73	8.09	1.38	17.11	5.82	1.09	18.80
K	79.0	85	29.22	14.87	50.89	20.49	8.02	39.13	13.03	3.44	26.40	8.16	1.71	21.00
L	79.0	3	15.52	1.76	11.31	12.22	1.16	9.52	8.98	0.87	9.66	6.33	0.68	10.80
M	79.0	7	20.72	9.69	46.76	15.21	6.04	39.71	10.26	2.94	28.63	6.49	1.18	18.13
M1	79.0	12	16.59	7.30	44.04	12.36	5.29	42.81	8.58	3.34	38.88	5.52	1.82	32.95
N	79.0	7	11.80	4.61	39.01	8.71	2.94	33.79	6.23	1.90	30.58	4.29	1.45	33.83
O	79.0	5	14.71	3.83	26.01	10.42	2.62	25.11	7.05	1.50	21.31	4.45	0.83	18.57
P	79.4	74	12.59	3.48	27.62	9.10	2.56	28.07	6.45	1.67	25.86	4.32	1.02	23.69

SECTION *	TEMP <sup>d</sup> *	# OF TESTS *	EAC <sup>e</sup> (KSI)			ERIF <sup>f</sup> (KSI)			AREA <sup>c</sup> (INCHES)		
			AVG.	S.D.	CV(%)	AVG.	S.D.	CV(%)	AVG.	S.D.	CV(%)
A	81.0	7	310.97	64.84	20.85	6.35	2.19	34.44	23.36	1.21	5.20
B	80.0	5	355.72	107.63	30.26	3.49	2.15	61.64	25.02	0.62	2.48
C	81.1	5	342.02	71.40	20.87	6.56	3.25	49.55	25.74	0.82	3.19
D	81.1	6	354.15	57.31	16.18	5.49	2.45	44.63	25.39	1.08	4.25
E	81.1	30	536.96	135.35	25.21	7.34	2.59	35.30	26.23	1.08	4.14
H	81.1	5	353.78	67.40	19.05	4.09	2.57	62.79	25.55	0.94	3.69
I	80.7	10	471.29	94.35	20.02	4.05	1.93	47.77	25.94	0.76	2.93
K	79.0	85	203.41	133.21	65.49	1.88	1.64	87.49	22.44	2.55	11.37
L	79.0	3	383.13	135.25	35.30	2.97	0.94	31.71	24.93	1.83	7.33
M	79.0	7	236.86	75.42	31.84	3.02	1.31	43.41	23.18	1.53	6.61
M1	79.0	12	325.77	204.89	62.89	5.22	3.75	71.77	23.81	2.34	9.82
N	79.0	7	416.13	218.84	52.59	7.77	3.58	46.04	24.03	3.34	13.91
O	79.0	5	229.15	55.95	24.42	6.94	2.19	31.63	22.21	1.43	6.43
P	79.4	74	275.66	79.79	28.94	7.44	2.65	35.58	22.96	1.14	4.96

TABLE 24C: FWD STATISTICS FOR DEFLECTIONS FOR 5/88 (WESTBOUND) FOR PROJECT 3 (CONT.)

SECTION *	TEMP <sup>d</sup> *	# OF TESTS *	D0 <sup>b</sup> (MILS)			D1 <sup>b</sup> (MILS)			D2 <sup>b</sup> (MILS)			D3 <sup>b</sup> (MILS)		
			AVG.	S.D.	CV(%)	AVG.	S.D.	CV(%)	AVG.	S.D.	CV(%)	AVG.	S.D.	CV(%)
A	88.9	7	13.53	3.86	28.51	9.76	2.97	30.42	6.60	1.80	27.34	4.11	0.98	23.92
B	88.8	5	19.65	4.93	25.10	14.23	4.14	29.10	9.73	2.91	29.91	6.16	1.81	29.43
C	85.8	5	11.46	3.27	28.58	8.02	2.23	27.86	5.92	1.56	26.32	4.09	1.03	25.21
D	85.2	6	12.95	1.04	8.04	9.93	0.97	9.73	7.58	0.81	10.67	5.28	0.59	11.20
E	85.2	30	10.19	1.88	18.45	7.79	1.61	20.74	6.06	1.23	20.24	4.34	0.87	19.98
H	85.2	5	13.73	2.04	14.84	9.98	1.49	14.92	7.63	1.18	15.52	5.33	0.95	17.89
I	84.2	9	13.77	3.16	22.98	10.58	2.47	23.30	8.01	1.87	23.30	5.64	1.31	23.16
K	86.9	13	24.39	5.02	20.59	17.23	3.43	19.93	11.09	2.18	19.65	6.74	1.38	20.44
L	86.9	3	21.46	7.96	37.07	15.72	5.71	36.33	10.67	3.41	31.97	7.04	1.58	22.42
M	85.9	7	23.39	6.54	27.97	16.48	3.88	23.52	10.57	1.88	17.83	6.24	1.05	16.84
M1	85.9	11	14.53	2.56	17.64	10.02	1.96	19.59	6.59	1.29	19.63	4.06	0.86	21.15
N	84.9	7	9.96	3.43	34.45	7.45	2.44	32.72	5.60	1.49	26.60	3.88	0.97	24.95
O	84.9	5	12.30	3.76	30.58	8.65	2.98	34.42	6.08	1.99	32.69	3.96	1.28	32.26
P	84.9	73	12.15	3.07	25.30	8.95	2.39	26.74	6.54	1.55	23.62	4.37	0.89	20.29

SECTION *	TEMP <sup>d</sup> *	# OF TESTS *	EAC <sup>e</sup> (KSI)			ERIF <sup>f</sup> (KSI)			AREAC <sup>c</sup> (INCHES)		
			AVG.	S.D.	CV(%)	AVG.	S.D.	CV(%)	AVG.	S.D.	CV(%)
A	88.9	7	267.55	51.79	19.36	7.97	2.74	34.43	22.36	0.62	2.76
B	88.8	5	184.77	35.85	19.40	4.67	2.25	48.18	22.39	0.72	3.23
C	85.8	5	226.21	97.50	43.10	8.04	2.81	34.97	22.84	0.97	4.23
D	85.2	6	273.40	57.57	21.06	4.87	1.33	27.32	24.67	1.07	4.34
E	85.2	30	329.70	110.05	33.38	7.29	2.36	32.35	24.81	1.10	4.42
H	85.2	5	181.25	30.43	16.79	4.90	2.14	43.67	23.73	1.04	4.40
I	84.2	9	333.64	226.97	68.03	4.51	2.32	51.48	24.67	1.33	5.37
K	86.9	13	168.25	70.42	41.85	2.86	2.11	73.96	21.72	1.61	7.43
L	86.9	3	211.19	76.52	36.23	2.49	1.96	78.63	22.93	0.86	3.74
M	85.9	7	175.80	67.35	38.31	3.30	1.77	53.77	21.75	1.42	6.54
M1	85.9	11	224.75	66.24	29.47	8.07	2.19	27.15	21.47	1.55	7.24
N	84.9	7	329.50	102.36	31.07	8.63	3.23	37.43	24.32	2.01	8.26
O	84.9	5	247.37	89.34	36.12	8.54	3.93	46.01	22.18	2.04	9.19
P	84.9	73	267.38	72.72	27.20	7.22	2.36	32.69	23.50	0.97	4.14

TABLE 24D: FWD STATISTICS FOR DEFLECTIONS FOR 5/89 (EASTBOUND) FOR PROJECT 3

SECTION *	TEMP <sup>d</sup> *	# OF TESTS *	DO <sup>b</sup> (MILS)			D1 <sup>b</sup> (MILS)			D2 <sup>b</sup> (MILS)			D3 <sup>b</sup> (MILS)		
			AVG.	S.D.	CV(%)	AVG.	S.D.	CV(%)	AVG.	S.D.	CV(%)	AVG.	S.D.	CV(%)
A	67	13	10.60	2.61	24.57	8.10	1.85	22.86	5.70	1.05	18.34	3.80	0.51	13.51
B	67	10	13.12	1.94	14.81	10.75	1.56	14.50	8.22	1.21	14.66	5.87	0.91	15.51
C	67	10	7.89	1.24	15.71	6.31	1.03	16.31	5.02	0.83	16.48	3.77	0.64	16.95
D	67	11	9.94	1.99	20.07	7.80	1.44	18.44	6.06	1.02	16.78	4.44	0.70	15.87
E	70	60	7.67	1.50	19.55	6.21	1.31	21.06	4.96	1.04	20.94	3.78	0.78	20.58
H	71	9	11.27	2.82	25.00	8.99	2.38	26.50	6.93	1.85	26.71	5.07	1.40	27.62
I	73	20	11.51	1.81	15.75	9.29	1.38	14.81	7.15	0.98	13.71	5.23	0.69	13.25
K	76	52	17.51	4.69	26.79	12.87	2.85	22.18	8.63	1.36	15.80	5.50	0.75	13.58
L	78	4	13.40	0.82	6.14	10.99	0.37	3.35	8.51	0.15	1.78	6.30	0.15	2.34
L	81	5	16.14	1.77	10.97	12.65	1.03	8.16	9.18	0.56	6.05	6.46	0.51	7.85

SECTION *	TEMP <sup>d</sup> *	# OF TESTS *	EAC <sup>e</sup> (KSI)			ERI <sup>f</sup> (KSI)			AREAC <sup>c</sup> (INCHES)		
			AVG.	S.D.	CV(%)	AVG.	S.D.	CV(%)	AVG.	S.D.	CV(%)
A	67	13	500.19	140.15	28.02	8.69	1.64	18.87	24.02	1.36	5.66
B	67	10	548.46	166.60	30.38	3.86	1.67	43.32	26.06	1.05	4.04
C	67	10	550.59	108.66	19.73	8.83	1.91	21.69	26.11	0.96	3.69
D	67	11	450.24	154.75	34.37	6.92	1.89	27.28	25.54	1.24	4.85
E	70	60	673.77	189.28	28.09	8.87	2.34	26.37	26.40	1.09	4.14
H	71	9	470.49	154.19	32.77	5.78	2.57	44.51	25.63	1.14	4.44
I	73	20	538.71	182.06	33.80	5.02	1.55	30.93	25.93	0.87	3.36
K	76	52	341.79	159.48	46.66	4.48	1.50	33.54	22.96	1.87	8.17
L	78	4	538.09	187.98	34.93	2.93	0.22	7.44	26.33	0.78	2.96
L	81	5	360.97	76.72	21.25	2.75	0.71	25.67	24.73	1.25	5.04

TABLE 24D: FWD STATISTICS FOR DEFLECTIONS FOR 5/89 (EASTBOUND) FOR PROJECT 3 (CONT.)

SECTION *	TEMP <sup>d</sup> *	# OF TESTS *	D0 <sup>b</sup> (MILS)			D1 <sup>b</sup> (MILS)			D2 <sup>b</sup> (MILS)			D3 <sup>b</sup> (MILS)		
			AVG.	S.D.	CV(%)	AVG.	S.D.	CV(%)	AVG.	S.D.	CV(%)	AVG.	S.D.	CV(%)
M	82	20	28.52	19.81	69.48	17.40	7.12	40.96	9.36	2.58	27.60	5.50	1.47	26.64
M1	83	26	19.22	18.73	97.43	12.11	7.75	64.04	6.94	2.10	30.32	4.24	1.25	29.51
N	83	14	10.92	6.06	55.48	7.87	3.76	47.76	5.70	2.23	39.20	3.96	1.49	37.62
O	83	10	15.66	4.82	30.76	10.23	3.37	32.90	6.42	1.84	28.67	3.75	0.86	23.04
P	81	11	9.78	1.78	18.24	6.75	1.46	21.56	4.73	1.09	22.98	3.21	0.75	23.34
P	77	21	14.49	2.38	16.43	10.47	1.94	18.52	7.35	1.34	18.19	4.91	0.88	17.95

SECTION *	TEMP <sup>d</sup> *	# OF TESTS *	EAC <sup>e</sup> (KSI)			ERI <sup>f</sup> (KSI)			AREA <sup>c</sup> (INCHES)		
			AVG.	S.D.	CV(%)	AVG.	S.D.	CV(%)	AVG.	S.D.	CV(%)
M	82	20	174.14	90.06	51.72	4.95	3.14	63.44	20.46	3.47	16.94
M1	83	26	224.90	124.87	55.52	7.79	4.05	52.00	21.78	3.26	14.95
N	83	14	381.87	183.43	48.03	8.76	4.24	48.37	24.22	3.82	15.76
O	83	10	174.59	55.01	31.51	8.99	2.62	29.15	20.27	1.04	5.13
P	81	11	283.27	60.03	21.19	10.69	2.41	22.54	21.98	0.96	4.35
P	77	21	235.11	42.11	17.91	5.85	2.05	35.14	22.77	0.97	4.26



TABLE 24D: FWD STATISTICS FOR DEFLECTIONS FOR 5/89 (WESTBOUND) FOR PROJECT '3 (CONT.)

SECTION *	TEMP <sup>d</sup> *	# OF TESTS *	D0 <sup>b</sup> (MILS)			D1 <sup>b</sup> (MILS)			D2 <sup>b</sup> (MILS)			D3 <sup>b</sup> (MILS)		
			AVG.	S.D.	CV(%)	AVG.	S.D.	CV(%)	AVG.	S.D.	CV(%)	AVG.	S.D.	CV(%)
A	69.9	13	8.31	1.57	18.88	6.52	1.22	18.64	4.80	0.82	17.12	3.37	0.52	15.41
B	68.9	10	13.13	3.61	27.47	10.15	2.86	28.21	7.46	2.07	27.81	5.27	1.42	27.02
C	67.0	4	7.05	1.26	17.90	5.68	0.99	17.52	4.53	0.80	17.72	3.44	0.61	17.70
D	67.0	6	8.12	0.67	8.19	6.62	0.63	9.51	5.34	0.55	10.22	4.07	0.47	11.54
E	65.3	30	6.55	1.12	17.12	5.40	0.93	17.30	4.41	0.75	17.06	3.46	0.59	16.97
H	64.7	4	7.69	1.54	20.07	6.03	0.99	16.49	4.80	0.65	13.45	3.72	0.49	13.07
I	64.0	11	9.19	2.33	25.39	7.52	1.90	25.25	5.97	1.35	22.68	4.55	0.90	19.82
K	63.0	47	17.31	3.94	22.77	12.44	2.20	17.70	8.03	1.04	12.97	5.10	0.61	11.88
L	62.0	2	13.96	0.92	6.58	11.22	0.33	2.96	8.45	0.15	1.76	6.13	0.06	1.04
M	62.0	7	13.69	2.03	14.81	10.70	1.64	15.35	7.78	1.24	15.89	5.45	0.92	16.89
M1	61.1	12	10.63	3.44	32.40	7.86	2.04	25.90	5.54	1.00	17.99	3.82	0.50	12.98
N	61.0	7	6.38	1.59	24.97	5.18	1.25	24.05	4.21	0.78	18.54	3.30	0.47	14.25
O	60.6	6	8.15	1.26	15.44	6.31	0.99	15.70	4.73	0.76	16.08	3.37	0.57	17.03
P	60.6	5	6.80	0.56	8.20	5.34	0.50	9.44	4.15	0.43	10.31	3.14	0.30	9.58
P	78.5	34	12.79	2.25	17.57	9.43	1.69	17.91	6.88	1.15	16.77	4.69	0.75	16.08

SECTION *	TEMP <sup>d</sup> *	# OF TESTS *	EAC <sup>e</sup> (KSI)			ERIF <sup>f</sup> (KSI)			AREAC <sup>c</sup> (INCHES)		
			AVG.	S.D.	CV(%)	AVG.	S.D.	CV(%)	AVG.	S.D.	CV(%)
A	69.9	13	669.40	167.52	25.02	10.07	1.74	17.32	24.86	1.03	4.13
B	68.9	10	384.58	111.72	29.05	5.36	3.09	57.71	24.51	0.68	2.78
C	67.0	4	703.83	256.54	36.45	9.85	2.02	20.54	26.33	0.74	2.82
D	67.0	6	599.54	129.09	21.53	7.87	1.33	16.94	26.68	0.96	3.60
E	65.3	30	894.44	404.05	45.17	9.79	1.86	18.97	27.18	1.15	4.23
H	64.7	4	527.33	154.17	29.24	8.93	1.51	16.97	26.01	1.54	5.90
I	64.0	11	670.56	263.50	39.30	6.72	2.37	35.19	26.71	1.20	4.50
K	63.0	47	322.15	216.94	67.34	5.28	1.43	27.03	22.29	1.84	8.26
L	62.0	2	466.57	180.22	38.63	3.20	0.10	3.09	25.56	0.85	3.32
M	62.0	7	404.56	91.40	22.59	4.65	1.90	40.83	24.57	0.54	2.20
M1	61.1	12	459.42	190.20	41.40	8.63	1.46	16.88	23.81	1.96	8.21
N	61.0	7	718.50	162.48	22.61	10.28	1.51	14.68	27.04	1.74	6.44
O	60.6	6	555.81	145.78	26.23	10.06	1.96	19.45	24.78	1.54	6.20
P	60.6	5	636.31	101.96	16.02	10.81	1.05	9.70	25.50	0.95	3.74
P	78.5	34	267.87	76.01	28.37	6.31	1.89	29.99	23.55	1.02	4.35

TABLE 24E: FWD STATISTICS FOR DEFLECTIONS FOR 10/89 (EASTBOUND) FOR PROJECT 3

SECTION *	TEMP <sup>d</sup> *	# OF TESTS *	D0 <sup>b</sup> (MILS)			D1 <sup>b</sup> (MILS)			D2 <sup>b</sup> (MILS)			D3 <sup>b</sup> (MILS)		
			AVG.	S.D.	CV(%)	AVG.	S.D.	CV(%)	AVG.	S.D.	CV(%)	AVG.	S.D.	CV(%)
A	59.9	7	8.23	1.39	16.90	6.51	1.15	17.62	4.79	0.70	14.54	3.42	0.39	11.34
B	60.1	5	8.83	1.60	18.15	7.32	1.39	19.02	5.77	1.25	21.71	4.31	0.97	22.49
C	61.3	5	6.10	0.74	12.16	4.85	0.71	14.60	3.99	0.61	15.36	3.12	0.53	17.04
D	61.5	6	6.98	1.06	15.18	5.59	0.88	15.78	4.52	0.71	15.66	3.51	0.54	15.41
E	61.9	30	5.71	0.87	15.23	4.64	0.72	15.62	3.78	0.58	15.49	2.98	0.46	15.43
H	62.5	4	8.37	1.45	17.32	6.49	1.08	16.71	4.95	0.68	13.73	3.68	0.42	11.51
I	62.7	10	8.05	1.24	15.36	6.57	0.91	13.93	5.20	0.65	12.50	3.95	0.43	10.89
K	63.1	20	12.56	5.53	44.05	9.23	3.10	33.55	6.37	1.31	20.56	4.47	0.58	12.90
L	63.7	5	10.87	1.44	13.22	8.77	0.87	9.90	6.65	0.46	6.84	4.90	0.47	9.69
M	64.1	12	17.42	7.18	41.20	13.13	5.19	39.56	8.11	2.15	26.46	5.23	1.13	21.51
M1	65.0	15	7.85	2.33	29.69	6.00	1.55	25.78	4.42	0.83	18.86	3.17	0.43	13.70
N	65.8	7	7.65	4.21	55.05	5.87	2.97	50.63	4.45	1.94	43.58	3.27	1.28	39.19
O	66.2	5	11.96	1.60	13.41	9.08	1.21	13.35	6.05	0.67	11.14	3.77	0.40	10.51
P	67.9	75	10.11	2.93	29.01	7.66	2.25	29.36	5.64	1.46	25.89	3.98	0.89	22.39

SECTION *	TEMP <sup>d</sup> *	# OF TESTS *	EAC <sup>e</sup> (KSI)			ERI <sup>f</sup> (KSI)			AREA <sup>c</sup> (INCHES)		
			AVG.	S.D.	CV(%)	AVG.	S.D.	CV(%)	AVG.	S.D.	CV(%)
A	59.9	7	711.99	172.58	24.24	9.87	1.27	12.83	25.00	0.90	3.60
B	60.1	5	836.50	351.41	42.01	7.39	2.43	32.89	26.65	0.59	2.20
C	61.3	5	595.80	138.06	23.17	10.93	1.82	16.62	26.42	1.04	3.95
D	61.5	6	608.26	175.29	28.82	9.62	1.73	18.02	26.39	0.73	2.77
E	61.9	30	829.54	189.81	22.88	11.40	1.62	14.25	26.82	0.79	2.94
H	62.5	4	502.43	60.73	12.09	9.03	1.30	14.44	25.10	0.54	2.16
I	62.7	10	712.67	176.27	24.73	8.23	1.27	15.47	26.56	0.94	3.53
K	63.1	20	483.24	256.11	53.00	6.82	1.48	21.73	23.94	2.37	9.90
L	63.7	5	626.69	194.47	31.03	5.69	1.18	20.72	25.91	2.00	7.71
M	64.1	12	346.34	184.66	53.32	5.24	2.45	46.83	23.07	2.19	9.48
M1	65.0	15	610.34	225.54	36.95	10.71	1.51	14.06	24.89	2.11	8.47
N	65.8	7	712.19	379.87	53.34	10.75	4.13	38.46	25.66	3.80	14.80
O	66.2	5	467.37	41.25	8.83	8.75	1.18	13.46	23.11	0.51	2.22
P	67.9	75	414.13	127.83	30.87	8.33	2.49	29.91	24.25	0.98	4.06

TABLE 24E: FWD STATISTICS FOR DEFLECTIONS FOR 10/89 (WESTBOUND) FOR PROJECT 3 (CONT.)

SECTION *	# OF TEMP <sup>d</sup> *	# OF TESTS *	D0 <sup>b</sup> (MILS)			D1 <sup>b</sup> (MILS)			D2 <sup>b</sup> (MILS)			D3 <sup>b</sup> (MILS)		
			AVG.	S.D.	CV(%)	AVG.	S.D.	CV(%)	AVG.	S.D.	CV(%)	AVG.	S.D.	CV(%)
A	80.8	5	9.91	2.09	21.05	7.07	1.46	20.67	4.88	0.91	18.63	3.32	0.50	15.13
B	80.7	5	14.39	2.58	17.96	10.60	1.95	18.41	7.53	1.57	20.83	5.12	1.15	22.54
C	77.7	5	8.81	2.62	29.69	6.48	2.00	30.79	4.94	1.44	29.16	3.63	1.08	29.80
D	77.5	6	8.52	0.83	9.76	6.52	0.53	8.15	5.10	0.28	5.44	3.78	0.11	2.84
E	77.1	30	7.44	1.22	16.36	5.66	0.99	17.57	4.52	0.78	17.24	3.45	0.59	17.05
H	76.6	5	9.03	1.53	16.89	6.61	0.86	12.95	5.01	0.50	9.93	3.68	0.35	9.50
I	76.3	10	10.59	2.72	25.70	7.92	1.92	24.29	6.04	1.28	21.25	4.39	0.85	19.34
K	78.8	12	17.31	4.02	23.20	11.73	2.39	20.41	7.32	1.41	19.28	4.65	0.81	17.45
L	78.2	4	13.89	1.14	8.18	10.98	0.69	6.31	8.09	0.48	5.95	5.73	0.22	3.91
M	78.0	7	16.77	4.79	28.56	12.18	2.70	22.14	7.95	1.14	14.32	5.07	0.65	12.80
M1	77.6	12	10.16	2.27	22.31	7.31	1.59	21.71	5.17	0.84	16.31	3.63	0.47	13.05
N	77.1	7	9.47	3.47	36.70	7.28	2.74	37.62	5.51	1.80	32.76	4.01	1.17	29.13
O	76.9	5	9.69	1.90	19.58	7.13	1.40	19.63	5.16	1.21	23.49	3.59	1.01	28.11
P	73.8	74	9.73	2.51	25.77	7.27	1.91	26.22	5.46	1.30	23.73	3.91	0.81	20.77

SECTION *	TEMP <sup>d</sup> *	# OF TESTS *	EAC <sup>e</sup> (KSI)			ER1 <sup>f</sup> (KSI)			AREA <sup>c</sup> (INCHES)		
			AVG.	S.D.	CV(%)	AVG.	S.D.	CV(%)	AVG.	S.D.	CV(%)
A	80.8	5	344.31	63.11	18.33	10.21	1.65	16.18	22.56	0.64	2.85
B	80.7	5	271.87	81.60	30.01	5.47	2.69	49.15	23.23	0.69	2.98
C	77.7	5	349.47	124.37	35.59	9.45	3.27	34.65	24.03	0.79	3.27
D	77.5	6	388.66	62.97	16.20	8.69	0.33	3.78	25.09	0.84	3.36
E	77.1	30	422.83	114.69	27.12	9.84	1.91	19.41	25.21	1.29	5.11
H	76.6	5	331.19	69.65	21.03	9.02	1.06	11.79	24.03	1.34	5.59
I	76.3	10	308.93	79.94	25.88	7.14	2.31	32.34	24.50	1.50	6.13
K	78.8	12	213.16	62.77	29.45	6.45	1.99	30.95	20.96	1.44	6.85
L	78.2	4	423.68	103.37	24.40	3.90	0.42	10.76	24.98	0.44	1.78
M	78.0	7	298.31	92.77	31.10	5.36	1.59	29.72	22.57	1.77	7.86
M1	77.6	12	327.71	57.53	17.55	9.22	1.48	16.07	23.15	1.75	7.57
N	77.1	7	411.84	59.05	14.34	8.35	3.02	36.18	25.01	1.90	7.59
O	76.9	5	405.01	179.00	44.20	9.52	2.97	31.18	23.54	2.28	9.67
P	73.9	74	361.64	95.19	26.32	8.47	2.43	28.67	24.19	1.09	4.51

TABLE 24F: FWD STATISTICS FOR DEFLECTIONS FOR 8/90 (EASTBOUND) FOR PROJECT 3

SECTION *	TEMP <sup>d</sup> *	# OF TESTS *	D0 <sup>b</sup> (MILS)			D1 <sup>b</sup> (MILS)			D2 <sup>b</sup> (MILS)			D3 <sup>b</sup> (MILS)		
			AVG.	S.D.	CV(%)	AVG.	S.D.	CV(%)	AVG.	S.D.	CV(%)	AVG.	S.D.	CV(%)
A	83.0	7	14.64	3.94	26.93	10.47	2.40	22.91	6.67	0.97	14.55	4.17	0.36	8.62
B	83.2	5	16.23	4.55	28.05	12.39	3.66	29.54	8.76	2.82	32.23	5.94	2.04	34.32
C	83.5	5	10.73	1.46	13.59	8.07	1.24	15.35	6.03	1.03	17.07	4.29	0.79	18.38
D	83.6	6	12.09	2.82	23.28	9.33	2.13	22.85	6.88	1.42	20.66	4.81	0.92	19.07
E	84.4	30	9.42	1.75	18.58	7.45	1.39	18.65	5.62	1.01	18.03	4.07	0.70	17.25
H	85.3	4	14.10	2.45	17.39	10.28	1.89	18.41	6.96	1.19	17.15	4.70	0.79	16.71
I	85.7	10	13.37	1.70	12.69	10.51	1.43	13.65	7.69	1.05	13.58	5.37	0.73	13.62
K	86.8	12	19.39	2.96	15.25	14.06	2.07	14.71	9.22	1.48	16.07	6.08	1.09	17.85
L	86.9	2	16.17	0.50	3.06	13.00	0.42	3.27	9.39	0.11	1.17	6.50	0.04	0.69
M	86.9	7	28.29	8.01	28.32	18.96	4.32	22.78	11.10	1.93	17.38	6.36	0.95	14.86
M1	87.2	12	14.03	6.49	46.27	9.99	4.08	40.80	6.44	1.91	29.57	4.07	0.88	21.55
N	87.5	7	11.28	6.31	56.00	8.23	4.21	51.12	5.69	2.28	40.08	3.83	1.31	34.11
O	87.9	5	20.50	3.23	15.76	13.83	2.13	15.43	8.00	1.08	13.49	4.30	0.55	12.80
P	88.7	75	15.80	5.10	32.27	11.13	3.57	32.04	7.24	1.98	27.38	4.56	1.03	22.47

SECTION *	TEMP <sup>d</sup> *	# OF TESTS *	EAC <sup>e</sup> (KSI)			ER1 <sup>f</sup> (KSI)			AREA <sup>c</sup> (INCHES)		
			AVG.	S.D.	CV(%)	AVG.	S.D.	CV(%)	AVG.	S.D.	CV(%)
A	83.0	7	320.41	105.69	32.99	7.58	1.06	13.95	22.05	1.33	6.02
B	83.2	5	317.77	79.29	24.95	4.74	2.51	52.93	23.70	0.75	3.17
C	83.5	5	341.10	91.77	26.90	7.39	2.22	30.07	24.12	1.07	4.43
D	83.6	6	429.73	184.25	42.87	6.12	2.29	37.34	24.55	1.38	5.61
E	84.4	30	584.31	187.99	32.17	7.96	1.92	24.13	25.29	0.90	3.55
H	85.3	4	294.84	29.89	10.14	6.31	1.82	28.86	22.66	0.15	0.65
I	85.7	10	414.97	60.36	14.55	4.75	1.49	31.43	24.75	0.76	3.05
K	86.8	12	241.75	68.57	28.36	3.63	1.80	49.63	22.32	1.22	5.47
L	86.9	2	456.56	42.82	9.38	2.64	0.06	2.27	25.04	0.20	0.82
M	86.9	7	149.30	60.12	40.27	3.11	1.23	39.54	20.51	1.75	8.55
M1	87.2	12	340.88	142.96	41.94	8.06	2.52	31.20	22.79	2.35	10.31
N	87.5	7	416.72	167.36	40.16	9.06	3.87	42.69	23.99	3.31	13.79
O	87.9	5	178.48	30.66	17.18	7.28	1.56	21.39	20.09	0.49	2.42
P	88.7	75	248.25	73.92	29.78	6.80	2.54	37.35	21.83	1.07	4.89

TABLE 24F: FWD STATISTICS FOR DEFLECTIONS FOR 8/90 (WESTBOUND) FOR PROJECT 3 (CONT.)

SECTION *	TEMP <sup>d</sup> *	# OF TESTS *	D0 <sup>b</sup> (MILS)			D1 <sup>b</sup> (MILS)			D2 <sup>b</sup> (MILS)			D3 <sup>b</sup> (MILS)		
			AVG.	S.D.	CV(%)	AVG.	S.D.	CV(%)	AVG.	S.D.	CV(%)	AVG.	S.D.	CV(%)
A	78.1	6	10.11	1.89	18.66	7.52	1.30	17.30	5.27	0.87	16.53	3.57	0.49	13.81
B	78.2	5	15.50	3.00	19.38	11.54	2.12	18.35	8.02	1.62	20.18	5.45	1.13	20.81
C	78.8	5	9.25	2.01	21.73	7.36	1.76	23.94	5.59	1.38	24.62	4.08	0.98	24.06
D	78.9	6	9.66	0.76	7.89	7.56	0.45	6.01	5.76	0.24	4.19	4.21	0.18	4.18
E	78.9	30	8.36	1.45	17.33	6.63	1.23	18.50	5.16	0.93	18.10	3.86	0.70	18.13
H	78.9	5	10.69	1.83	17.11	7.89	1.05	13.35	5.78	0.57	9.87	4.15	0.33	7.94
I	79.0	10	11.82	3.16	26.77	9.21	2.46	26.67	6.84	1.59	23.25	4.92	1.05	21.46
K	78.4	12	21.10	5.21	24.70	14.88	3.31	22.25	9.36	2.10	22.45	5.90	1.37	23.31
L	78.4	4	16.30	1.89	11.58	12.52	1.15	9.20	8.92	0.62	6.97	6.13	0.29	4.67
M	78.4	7	20.35	5.09	24.98	14.81	2.78	18.75	9.49	1.30	13.69	5.86	0.77	13.07
M1	88.8	12	16.21	4.58	28.25	11.28	3.17	28.14	7.11	1.62	22.73	4.48	0.79	17.60
N	88.9	7	12.98	5.37	41.38	9.79	3.81	38.92	6.96	2.27	32.60	4.83	1.34	27.69
O	89.0	5	14.73	2.87	19.51	10.80	2.14	19.85	7.40	1.65	22.24	4.93	1.26	25.50
P	89.5	74	14.56	4.23	29.08	9.84	3.00	30.49	6.58	1.75	26.55	4.34	0.98	22.50

SECTION *	TEMP <sup>d</sup> *	# OF TESTS *	EAC <sup>e</sup> (KSI)			ERIF <sup>f</sup> (KSI)			AREAC <sup>c</sup> (INCHES)		
			AVG.	S.D.	CV(%)	AVG.	S.D.	CV(%)	AVG.	S.D.	CV(%)
A	78.1	6	466.10	188.88	40.52	9.40	1.54	16.40	23.44	1.15	4.92
B	78.2	5	336.71	160.32	47.61	4.82	2.29	47.51	23.32	1.10	4.71
C	78.8	5	580.94	113.46	19.53	8.09	2.76	34.14	25.36	0.79	3.12
D	78.9	6	467.93	87.26	18.65	7.43	0.49	6.55	25.23	0.79	3.13
E	78.9	30	567.39	123.72	21.81	8.59	2.09	24.31	25.70	0.97	3.79
H	78.9	5	342.38	84.30	24.62	7.61	0.93	12.17	23.85	1.17	4.93
I	79.0	10	413.28	94.30	22.82	5.94	2.52	42.39	24.95	1.39	5.58
K	78.4	12	218.14	67.28	30.84	4.16	1.99	47.81	21.59	1.31	6.08
L	78.4	4	324.87	74.87	23.05	3.21	0.46	14.23	24.12	0.73	3.02
M	78.4	7	319.04	212.64	66.65	3.83	1.47	38.30	22.44	1.85	8.26
M1	88.8	12	231.51	42.19	18.22	6.86	2.07	30.17	21.59	1.66	7.68
N	88.9	7	393.22	167.52	42.60	6.35	2.74	43.16	24.34	2.22	9.10
O	89.0	5	342.15	198.41	57.99	6.05	2.53	41.73	22.94	1.95	8.50
P	89.5	74	203.60	59.10	29.03	7.35	2.61	35.54	21.38	1.24	5.79

TABLE 24G: FWD STATISTICS FOR DEFLECTIONS FOR 8/91 (EASTBOUND) FOR PROJECT 3

SECTION *	TEMP <sup>d</sup> *	# OF TESTS *	D0 <sup>b</sup> (MILS)			D1 <sup>b</sup> (MILS)			D2 <sup>b</sup> (MILS)			D3 <sup>b</sup> (MILS)		
			AVG.	S.D.	CV(%)	AVG.	S.D.	CV(%)	AVG.	S.D.	CV(%)	AVG.	S.D.	CV(%)
A	80	7	14.44	2.05	14.17	10.02	1.62	16.15	6.51	0.80	12.27	4.08	0.40	9.75
B	80	5	15.99	3.71	23.21	11.94	3.04	25.49	8.28	2.43	29.40	5.65	1.84	32.54
C	80	5	10.94	1.65	15.04	8.03	1.52	18.93	5.97	1.25	20.96	4.30	1.01	23.44
D	80	6	11.40	1.88	16.52	8.68	1.52	17.55	6.47	1.13	17.45	4.58	0.80	17.42
E	80	30	9.32	1.57	16.84	7.15	1.35	18.87	5.40	1.04	19.25	3.93	0.74	18.90
H	80	4	14.05	2.62	18.68	10.24	2.14	20.87	6.98	1.47	21.10	4.65	0.98	21.12
I	80	10	13.09	1.88	14.33	10.04	1.40	13.94	7.29	1.02	14.02	5.06	0.72	14.31
J	80	2	19.08	4.04	21.17	14.16	2.36	16.64	9.38	1.08	11.47	6.03	0.42	6.97
K	80	12	17.52	3.45	19.69	12.97	2.57	19.85	8.86	1.78	20.14	6.04	1.34	22.16
L	80	2	16.93	0.68	3.99	12.65	0.03	0.28	8.84	0.17	1.98	5.99	0.20	3.34
M	80	5	24.53	3.13	12.75	17.28	2.00	11.57	10.59	1.10	10.36	6.28	0.74	11.71
M1	80	11	14.05	5.02	35.72	10.32	3.45	33.43	6.95	1.95	28.00	4.56	1.12	24.60
N	80	7	9.91	4.55	45.91	7.26	3.01	41.47	5.16	1.76	34.16	3.62	1.16	32.11
O	80	5	17.26	2.50	14.51	11.97	1.94	16.18	7.39	1.09	14.71	4.31	0.58	13.47
P	80	39	13.23	3.35	25.34	9.65	2.57	26.64	6.57	1.61	24.41	4.36	0.95	21.81

SECTION *	TEMP <sup>d</sup> *	# OF TESTS *	EAC <sup>e</sup> (KSI)			ER1 <sup>f</sup> (KSI)			AREAC (INCHES)		
			AVG.	S.D.	CV(%)	AVG.	S.D.	CV(%)	AVG.	S.D.	CV(%)
A	80	7	235.75	51.45	21.83	7.84	1.12	14.34	21.47	0.90	4.17
B	80	5	291.15	55.20	18.96	5.08	2.56	50.41	23.20	1.30	5.58
C	80	5	291.28	58.63	20.13	7.49	2.75	36.68	23.58	1.13	4.80
D	80	6	342.87	68.89	20.09	6.63	2.04	30.81	24.34	0.73	2.98
E	80	30	454.30	112.62	24.79	8.41	2.19	26.04	24.65	0.98	3.96
H	80	4	278.76	16.34	5.86	6.53	2.17	33.17	22.63	0.34	1.50
I	80	10	368.22	94.57	25.68	5.42	1.64	30.34	24.25	1.09	4.48
J	80	2	303.92	120.97	39.80	3.41	0.70	20.70	22.98	1.30	5.68
K	80	12	268.13	59.07	22.03	3.89	2.25	57.83	23.02	0.99	4.30
L	80	2	269.58	62.62	23.23	3.43	0.34	9.91	23.39	0.87	3.72
M	80	5	174.63	28.88	16.54	3.12	0.94	30.18	21.24	0.85	3.99
M1	80	11	341.52	133.96	39.22	6.87	2.84	41.32	23.26	1.75	7.53
N	80	7	437.34	173.22	39.61	9.60	3.74	38.99	23.94	2.79	11.65
O	80	5	214.79	30.79	14.33	7.25	1.66	22.95	20.95	0.40	1.93
P	80	39	310.03	73.05	23.56	7.30	2.61	35.77	22.73	1.00	4.42

TABLE 24G: FWD STATISTICS FOR DEFLECTIONS FOR 8/91 (WESTBOUND) FOR PROJECT 3 (CONT.)

SECTION *	TEMP <sup>d</sup> *	# OF TESTS *	D0 <sup>b</sup> (MILS)			D1 <sup>b</sup> (MILS)			D2 <sup>b</sup> (MILS)			D3 <sup>b</sup> (MILS)		
			AVG.	S.D.	CV(%)	AVG.	S.D.	CV(%)	AVG.	S.D.	CV(%)	AVG.	S.D.	CV(%)
A	82	6	13.03	2.91	22.35	9.43	1.98	20.96	6.20	1.16	18.70	3.89	0.60	15.41
B	82	4	22.86	3.08	13.49	16.17	2.79	17.22	10.46	2.20	20.99	6.59	1.46	22.13
C	82	6	13.89	3.91	28.15	10.22	2.98	29.17	7.13	2.09	29.38	4.77	1.50	31.49
D	82	5	12.60	1.11	8.82	9.41	0.52	5.48	6.79	0.26	3.82	4.61	0.37	7.94
E	82	29	10.15	1.89	18.61	7.84	1.60	20.38	5.87	1.17	19.94	4.15	0.81	19.48
H	82	5	14.08	1.28	9.10	9.72	0.88	9.01	6.64	0.67	10.08	4.48	0.52	11.59
I	82	10	15.09	3.69	24.48	11.37	2.90	25.51	7.92	1.96	24.77	5.33	1.26	23.59
K	82	11	25.60	4.64	18.11	17.51	2.73	15.59	10.31	1.64	15.87	6.10	1.10	18.10
L	82	4	20.60	1.87	9.10	15.30	1.24	8.10	10.23	0.78	7.64	6.70	0.39	5.81
M	82	6	26.94	5.63	20.92	18.85	3.19	16.91	11.29	1.60	14.20	6.49	1.00	15.34
M1	82	12	16.41	4.41	26.89	12.06	3.16	26.21	7.92	1.87	23.60	5.08	1.08	21.28
N	82	7	12.41	5.32	42.89	9.54	3.99	41.82	6.79	2.34	34.46	4.73	1.32	27.95
O	82	5	14.33	2.79	19.47	10.76	2.20	20.43	7.44	1.63	21.96	4.99	1.28	25.65
P	82	37	13.81	3.67	26.58	9.73	2.78	28.56	6.59	1.72	26.06	4.32	1.01	23.28

SECTION *	TEMP <sup>d</sup> *	# OF TESTS *	EAC <sup>e</sup> (KSI)			ERIF <sup>f</sup> (KSI)			AREAC <sup>c</sup> (INCHES)		
			AVG.	S.D.	CV(%)	AVG.	S.D.	CV(%)	AVG.	S.D.	CV(%)
A	82	6	343.12	117.71	34.30	8.47	1.73	20.44	22.33	1.01	4.54
B	82	4	167.13	19.24	11.51	3.17	1.93	60.95	21.60	1.00	4.63
C	82	6	303.48	102.45	33.76	6.65	3.20	48.12	23.07	1.48	6.43
D	82	5	312.40	82.52	26.41	6.38	0.94	14.69	23.72	1.25	5.26
E	82	29	434.12	120.41	27.74	7.79	2.25	28.93	24.65	1.07	4.34
H	82	5	215.58	44.39	20.59	6.76	1.36	20.15	21.88	1.01	4.63
I	82	10	326.62	86.74	26.56	5.15	2.70	52.32	23.52	1.53	6.50
K	82	11	169.71	46.82	27.59	3.61	1.76	48.58	20.60	1.38	6.69
L	82	4	242.40	48.50	20.01	2.42	0.45	18.48	22.86	0.47	2.07
M	82	6	182.42	73.49	40.28	2.95	1.49	50.62	21.12	1.59	7.51
M1	82	12	322.87	177.75	55.05	5.58	2.50	44.74	22.68	1.39	6.15
N	82	7	449.92	197.50	43.90	6.60	2.91	44.18	24.66	2.05	8.31
O	82	5	370.78	167.74	45.24	5.94	2.48	41.75	23.38	1.64	7.02
P	82	37	254.16	92.80	36.51	7.43	2.75	36.95	22.06	1.18	5.35

TABLE 25: FWD NOTE SUMMARY

---

- a Pavement temperature at nominal 4-inch depth
- b D0, D1, D2, and D3 are surface deflections at 0, 12, 24, and 36-inch offsets (respectively) from the center of the loading plate.
- c  $\text{Area (inch)} = 6 \left( 1 + 2 \frac{D1}{D0} + 2 \frac{D2}{D0} + \frac{D3}{D0} \right)$  (Reference 15)
- d Effective temperature corresponds to the temperature at a depth of  $0.35 \times$  (asphalt concrete pavement thickness).
- e  $\text{LOG } E_{AC} \text{ (ksi)} = 1.846 - (4.902 \times \log (D0-D1)) + (5.189 \times \log (D0-D2)) - (1.282 \times \log (D1-D3))$   
 $R^2 = 0.998$  SEE = 0.018 (M. R. Thompson, unpublished data)
- f  $E_{Ri} \text{ (ksi)} = 24.7 - (5.41 \times D3) + (0.31 \times D3^2)$  (Reference 15)  
 $R^2 = 0.98$  SEE = 0.64
-



TABLE 26: COMPARISON OF CORE SPLIT TENSILE STRENGTHS FROM PROJECT 3

CORE DATA FROM CONSTRUCTION - 1986  
(TESTED BY THE UNIVERSITY OF ILLINOIS)

	UNCONDITIONED TENSILE STRENGTHS, PSI (77° F)				MOISTURE DAMAGE
	AVERAGE	STD. DEV.	C.O.V., %	NO. OF LIFTS	
AC-10 BINDER	98	18	18.29	39	NOT MEASURED
AC-20 BINDER	125	24	19.38	89	NOT MEASURED

CORE DATA FROM AUGUST 1989  
(TESTED BY IDOT)

	UNCONDITIONED TENSILE STRENGTHS, PSI (77° F)				MOISTURE DAMAGE
	AVERAGE	STD. DEV.	C.O.V., %	NO. OF LIFTS	
AC-10 BINDER	78	59	76.03	28	SLIGHT TO SEVERE
AC-20 BINDER	103	49	47.29	51	SLIGHT TO SEVERE

CORE DATA FROM SEPTEMBER 1991  
(SPLIT TENSILES TESTED BY UNIVERSITY OF ILLINOIS,  
 STRIPPING MEASURED BY IDOT)

	UNCONDITIONED TENSILE STRENGTHS, PSI (77° F)				MOISTURE DAMAGE
	AVERAGE	STD. DEV.	C.O.V., %	NO. OF LIFTS	
AC-10 BINDER	142	28	19.72	26	SLIGHT TO SEVERE
AC-20 BINDER	160	24	15.00	52	SLIGHT TO SEVERE

TABLE 27A: FWD STATISTICS FOR HINGE AND DOWEL JOINT DEFLECTIONS AND AREAS FOR PROJECT 2

AVERAGE JOINT DEFLECTIONS <sup>a</sup> (HINGE AND DOWEL COMBINED)								
DATE	DIR	TEMP	# OF TESTS <sup>b</sup>	DO. (MILS)	D1. (MILS)	D2. (MILS)	D3. (MILS)	AREA <sup>c</sup> (INCH)
10/17/89	W	46	71	4.2	3.2	2.5	1.9	25.3
10/17/89	E	46	71	4.1	3.2	2.5	1.9	25.6
07/10/90	W	80	71	3.1	2.6	2.2	1.8	28.0
07/10/90	E	78	75	2.9	2.5	2.1	1.7	28.4
08/19/91	W	76	72	2.9	2.5	2.0	1.7	27.9
08/19/91	E	78	71	2.8	2.3	1.9	1.6	27.8

a Tests taken in outer wheelpath

b Data represents average of 8000 lb. drops normalized to 9000 lb. load

c Area (inch) =  $6 \left( 1 + 2 \frac{D1}{DO} + 2 \frac{D2}{DO} + \frac{D3}{DO} \right)$

TABLE 27B: FWD STATISTICS FOR HINGE AND DOWEL JOINT LOAD TRANSFER EFFICIENCY (LTE) FOR PROJECT 2

DATE	DIR	TEMP	SECTION G1 <sup>a</sup>				SECTION G2 <sup>a</sup>				SECTION G3 <sup>a</sup>			
			HINGE JOINTS		DOWEL JOINTS		HINGE JOINTS		DOWEL JOINTS		HINGE JOINTS		DOWEL JOINTS	
			# OF TESTS <sup>b</sup>	LTE <sup>c</sup> (%)	# OF TESTS <sup>b</sup>	LTE <sup>c</sup> (%)	# OF TESTS <sup>b</sup>	LTE <sup>c</sup> (%)	# OF TESTS <sup>b</sup>	LTE <sup>c</sup> (%)	# OF TESTS <sup>b</sup>	LTE <sup>c</sup> (%)	# OF TESTS <sup>b</sup>	LTE <sup>c</sup> (%)
10/17/89	W	46	30	89.8	33	89.2	30	90.4	30	84.4	60	86.2	30	83.8
10/17/89	E	46	30	87.9	33	88.1	30	86.6	30	84.8	63	88.2	27	84.2
07/10/90	W	80	30	95.5	33	93.0	27	94.7	33	95.5	60	93.2	30	92.2
07/10/90	E	78	30	94.5	33	95.7	30	96.8	30	95.9	60	94.2	30	93.7
08/19/91	W	76	30	92.5	33	91.7	33	95.4	30	93.8	60	92.0	30	90.9
08/19/91	E	78	30	89.9	33	89.8	30	91.0	30	91.2	60	91.6	30	92.1
			AVG.	91.7	AVG.	91.3	AVG.	92.5	AVG.	90.9	AVG.	90.9	AVG.	89.5

a Tests taken in outer wheelpath

b Data represents average of 4000, 8000 and 12,000 lb. drops per location, each normalized to 9000 lb. load

c Load transfer efficiency calculated by dividing the deflection 12 inches from the load, on the unloaded side of the joint, by the deflection directly beneath the loaded plate

TABLE 28A: FWD STATISTICS FOR HINGE AND DOWEL JOINT DEFLECTIONS AND AREAS FOR PROJECT 4

		JOINT DEFLECTIONS (AVG.) <sup>a</sup> (HINGE AND DOWEL COMBINED)						
DATE	DIR	TEMP	# OF TESTS <sup>b</sup>	DO. (MILS)	D1. (MILS)	D2. (MILS)	D3. (MILS)	AREA <sup>d</sup> (INCH)
10/12/89	W	68	71	7.3	5.6	4.3	3.2	24.9
10/12/89	E	63	70	8.3	6.4	4.9	3.6	25.1
08/16/90	W	73	71	7.3	5.7	4.4	3.3	25.7
08/16/90	E	73	26 <sup>c</sup>	6.2	4.9	3.8	3.0	25.8
08/06/91	W	83	71	6.4	5.0	3.9	3.0	25.9
08/06/91	E	83	71	6.0	4.9	3.9	3.0	26.7

a Tests taken in outer wheelpath

b Data represents average of 8000 lb. drops normalized to 9000 lb. load

c Testing not completed due to rain, all locations not tested

d Area (inch) =  $6 \left( 1 + 2 \frac{D1}{DO} + 2 \frac{D2}{DO} + \frac{D3}{DO} \right)$

TABLE 28B: FWD STATISTICS FOR HINGE AND DOWEL JOINT LOAD TRANSFER EFFICIENCY (LTE) FOR PROJECT 4

DATE	DIR	TEMP	SECTION DA <sup>a</sup>				SECTION DB <sup>a</sup>				SECTION DC <sup>a</sup>			
			HINGE JOINTS		DOWEL JOINTS		HINGE JOINTS		DOWEL JOINTS		HINGE JOINTS		DOWEL JOINTS	
			# OF TESTS <sup>b</sup>	LTE <sup>d</sup> (%)	# OF TESTS <sup>b</sup>	LTE <sup>d</sup> (%)	# OF TESTS <sup>b</sup>	LTE <sup>d</sup> (%)	# OF TESTS <sup>b</sup>	LTE <sup>d</sup> (%)	# OF TESTS <sup>b</sup>	LTE <sup>d</sup> (%)	# OF TESTS <sup>b</sup>	LTE <sup>d</sup> (%)
10/12/89	W	68	33	89.9	33	87.5	30	85.8	30	90.6	54	89.4	33	87.3
10/12/89	E	63	33	87.6	30	96.2	30	79.5	33	94.5	54	89.1	33	88.3
08/16/90	W	73	33	89.3	33	92.1	30	80.5	30	86.4	57	88.6	30	83.0
08/16/90	E	73	c	c	c	c	c	c	c	c	48	89.1	30	84.8
08/06/91	W	83	33	89.4	33	90.9	33	83.1	27	85.4	54	90.5	33	85.1
08/06/91	E	83	33	93.5	33	92.0	30	86.3	30	87.7	54	92.0	33	86.0
			AVG.	89.9	AVG.	91.7	AVG.	83.0	AVG.	88.9	AVG.	89.8	AVG.	85.8

a Tests taken in outer wheelpath

b Data represents average of 4000, 8000 and 12,000 lb. drops per location, each normalized to 9000 lb. load

c Testing not completed due to rain, no data available

d Load transfer efficiency calculated by dividing the deflection 12 inches from the load, on the unloaded side of the joint, by the deflection directly beneath the loaded plate

TABLE 28C: FWD STATISTICS FOR PAVEMENT/SHOULDER JOINT LOAD  
TRANSFER EFFICIENCY (LTE) FOR PROJECT 4

FA 409				AIR	PAVT				AVG
SEC	STA	DATE	TIME	TEMP	SURF	TEST	LOAD	SHLD	SHLD
				(F)	TEMP(F)	LOC.	(LBS.)	LTE	LTE
								(%)	(%)
R	2993.20	09/02/86	10:30 AM	80-81	86-103	Ap Sh	8928	93	
W	3156.36	09/02/86	10:30 AM	80-81	86-103	Ap Sh	9288	93	
W	3161.87	09/02/86	10:30 AM	80-81	86-103	Ap Sh	8976	91	
X	3168.02	09/02/86	10:30 AM	80-81	86-103	Ap Sh	9304	94	
Z	3185.49	09/02/86	10:30 AM	80-81	86-103	Ap Sh	9784	88	92
R	2993.20	09/02/86	10:30 AM	80-81	86-103	Lv Sh	8712	97	
W	3156.36	09/02/86	10:30 AM	80-81	86-103	Lv Sh	8592	84	
W	3161.87	09/02/86	10:30 AM	80-81	86-103	Lv Sh	8624	89	
W	3168.02	09/02/86	10:30 AM	80-81	86-103	Lv Sh	8440	100	
Z	3185.49	09/02/86	10:30 AM	80-81	86-103	Lv Sh	7936	100	94
								AVG LTE	93

				AIR	PAVT				AVG
SEC	STA	DATE	TIME	TEMP	SURF	TEST	LOAD	SHLD	SHLD
				(F)	TEMP(F)	LOC.	(LBS.)	LTE	LTE
								(%)	(%)
X	3168.02	09/03/86	11:00 AM	80-83	93-98	Ap Sh	10576	77	
W	3156.36	09/03/86	11:00 AM	80-83	93-98	Ap Sh	9952	91	
W	3161.60	09/03/86	11:00 AM	80-83	93-98	Ap Sh	9880	84	
Z	3185.49	09/03/86	11:00 AM	80-83	93-98	Ap Sh	10144	93	
AA	3216.10	09/03/86	11:00 AM	80-83	93-98	Ap Sh	9352	95	
BA	3226.38	09/03/86	11:00 AM	80-83	93-98	Ap Sh	9664	92	
NA	3432.10	09/03/86	11:00 AM	80-83	93-98	Ap Sh	9984	90	
QA	3485.70	09/03/86	11:00 AM	80-83	93-98	Ap Sh	10016	100	90
X	3168.02	09/03/86	11:00 AM	80-83	93-98	Lv Sh	9016	82	
W	3156.36	09/03/86	11:00 AM	80-83	93-98	Lv Sh	8872	84	
W	3161.60	09/03/86	11:00 AM	80-83	93-98	Lv Sh	9096	84	
Z	3185.49	09/03/86	11:00 AM	80-83	93-98	Lv Sh	9232	96	
AA	3216.10	09/03/86	11:00 AM	80-83	93-98	Lv Sh	8920	92	
BA	3226.38	09/03/86	11:00 AM	80-83	93-98	Lv Sh	8992	96	
NA	3432.10	09/03/86	11:00 AM	80-83	93-98	Lv Sh	9240	96	
QA	3485.70	09/03/86	11:00 AM	80-83	93-98	Lv Sh	10896	95	91
								AVG LTE	90

TABLE 28C: FWD STATISTICS FOR PAVEMENT/SHOULDER JOINT LOAD TRANSFER EFFICIENCY (LTE) FOR PROJECT 4 (CONT.)

FA 409		DATE	TIME	TEMP (F)	SURF TEMP(F)	TEST LOC.	LOAD (LBS.)	SHLD LTE (%)	AVG	
SEC	STA								LTE (%)	
R	2993.20	09/04/86	06:30 AM	66-74	73-80	Ap Sh	10016	91		
W	3156.87	09/04/86	06:30 AM	66-74	73-80	Ap Sh	9160	90		
W	3161.87	09/04/86	06:30 AM	66-74	73-80	Ap Sh	9560	77		
X	3168.02	09/04/86	06:30 AM	66-74	73-80	Ap Sh	8624	57		
Z	3185.49	09/04/86	06:30 AM	66-74	73-80	Ap Sh	10160	86	80	
R	2993.20	09/04/86	06:30 AM	66-74	73-80	Lv Sh	8712	98		
W	3156.87	09/04/86	06:30 AM	66-74	73-80	Lv Sh	9928	87		
W	3161.87	09/04/86	06:30 AM	66-74	73-80	Lv Sh	8856	91		
X	3168.14	09/04/86	06:30 AM	66-74	73-80	Lv Sh	8848	100		
Z	3185.49	09/04/86	06:30 AM	66-74	73-80	Lv Sh	8872	100	95	
								AVG LTE	88	

FA 409		DATE	TIME	AIR TEMP (F)	PAVT SURF TEMP(F)	TEST LOC.	LOAD (LBS.)	SHLD LTE (%)	AVG	
SEC	STA								LTE (%)	
AA	3216.10	09/04/86	08:45 AM	79-82	80-87	Ap Sh	9728	90		
BA	3226.38	09/04/86	08:45 AM	79-82	80-87	Ap Sh	9792	88		
NA	3432.10	09/04/86	08:45 AM	79-82	80-87	Ap Sh	10256	89		
QA	3485.70	09/04/86	08:45 AM	79-82	80-87	Ap Sh	10224	93	90	
AA	3216.10	09/04/86	08:45 AM	79-82	80-87	Lv Sh	8792	95		
BA	3226.38	09/04/86	08:45 AM	79-82	80-87	Lv Sh	9888	93		
NA	3432.10	09/04/86	08:45 AM	79-82	80-87	Lv Sh	9720	94		
QA	3485.70	09/04/86	08:45 AM	79-82	80-87	Lv Sh	9448	93	94	
								AVG LTE	92	

FA 409		DATE	TIME	AIR TEMP (F)	PAVT SURF TEMP(F)	TEST LOC.	LOAD (LBS.)	SHLD LTE (%)	AVG	
SEC	STA								LTE (%)	
AA	3216.10	09/04/86	01:15 PM	86-88	100-105	Ap Sh	9600	89		
BA	3226.38	09/04/86	01:15 PM	86-88	100-105	Ap Sh	10120	84		
NA	3432.10	09/04/86	01:15 PM	86-88	100-105	Ap Sh	9920	91		
QA	3485.70	09/04/86	01:15 PM	86-88	100-105	Ap Sh	10128	92	89	
AA	3216.10	09/04/86	01:15 PM	86-88	100-105	Lv Sh	9096	91		
BA	3226.38	09/04/86	01:15 PM	86-88	100-105	Lv Sh	8792	97		
NA	3432.10	09/04/86	01:15 PM	86-88	100-105	Lv Sh	9384	94		
QA	3485.70	09/04/86	01:15 PM	86-88	100-105	Lv Sh	10592	94	94	
								AVG LTE	92	

TABLE 28C: FWD STATISTICS FOR PAVEMENT/SHOULDER JOINT LOAD  
TRANSFER EFFICIENCY (LTE) FOR PROJECT 4 (CONT.)

FA 409				AIR	PAVT			SHLD	AVG
SEC	STA	DATE	TIME	TEMP	SURF	TEST	LOAD	LTE	SHLD
				(F)	TEMP(F)	LOC.	(LBS.)	(%)	LTE
									(%)
R	2993.20	09/04/86	03:25 PM	82-88	89-105	Ap Sh	9080	89	
W	3156.23	09/04/86	03:25 PM	82-88	89-105	Ap Sh	9280	88	
W	3161.87	09/04/86	03:25 PM	82-88	89-105	Ap Sh	9432	80	
X	3168.02	09/04/86	03:25 PM	82-88	89-105	Ap Sh	9128	76	
Z	3185.49	09/04/86	03:25 PM	82-88	89-105	Ap Sh	9848	93	85
R	2993.20	09/04/86	03:25 PM	82-88	89-105	Lv Sh	8600	93	
W	3156.23	09/04/86	03:25 PM	82-88	89-105	Lv Sh	9272	92	
W	3161.87	09/04/86	03:25 PM	82-88	89-105	Lv Sh	9104	76	
X	3168.02	09/04/86	03:25 PM	82-88	89-105	Lv Sh	8960	84	
Z	3185.49	09/04/86	03:25 PM	82-88	89-105	Lv Sh	9176	94	88
								AVG LTE	86

FA 409				AIR	PAVT			SHLD	SHLD
SEC	STA	DATE	TIME	TEMP	SURF	TEST	LOAD	LTE	LTE
				(F)	TEMP(F)	LOC.	(LBS.)	(%)	(%)
R	2993.20	09/04/86	06:25 PM	76-82	83-89	Ap Sh	10008	93	
W	3156.23	09/04/86	06:25 PM	76-82	83-89	Ap Sh	9432	95	
W	3161.87	09/04/86	06:25 PM	76-82	83-89	Ap Sh	9872	85	
X	3168.02	09/04/86	06:25 PM	76-82	83-89	Ap Sh	9000	77	88
R	2993.20	09/04/86	06:25 PM	76-82	83-89	Lv Sh	8760	93	
W	3156.23	09/04/86	06:25 PM	76-82	83-89	Lv Sh	8728	82	
W	3161.87	09/04/86	06:25 PM	76-82	83-89	Lv Sh	9456	67	
X	3168.02	09/04/86	06:25 PM	76-82	83-89	Lv Sh	8880	74	79
								AVG LTE	83



TABLE 29: UNDERDRAIN OUTFLOW DATA FOR PROJECTS 3 AND 4

PAVEMENT TYPE	MAX. OUTFLOW		MAX. RAINFALL (inches)	LAG TIME (hours)	RECOVERY TIME (days)
	DATE	GAL./HR.			
20' JOINTED - SEALED	7/20/88	430	N/A	N/A	1.5 - 2.5
20' JOINTED - NOT SEALED	7/20/88	478	N/A	N/A	1.5 - 2.5
40' JOINTED - SEALED	6/5/89	86	0.7	1	1.0 - 2.0
40' JOINTED - NOT SEALED	6/5/89	178	0.7	1	2.0 - 3.0
CRCP - SEALED	9/14/89	70	1.95	1	0.5 - 1.0
CRCP - NOT SEALED	9/14/89	81	1.95	1	1.0 - 1.5
9.5 INCH AC- UNTREATED	6/18/87 <sup>a</sup>	131	N/A	1-5+	VARIABLE
12.5 INCH AC- LIME-MODIFIED	4/13/87	142	N/A	1-5+	VARIABLE

<sup>a</sup>Equipment in this section was not operating on 4/13/87

TABLE 30: MOISTURE GAUGE LOCATIONS FOR PROJECTS 3 AND 4

STATION	PAVEMENT TYPE	GAUGE LOCATIONS	CUT/FILL
571+00	12.5" AC-20, NO UNDERDRAINS, LIME MOD. SUBGRADE	IWP, OWP, SHOULDER	1' FILL
593+80	12.5" AC-20, UNDERDRAINS, LIME MOD. SUBGRADE	OWP	@ GRADE
594+00	12.5" AC-20, UNDERDRAINS, LIME MOD. SUBGRADE	IWP, OWP, SHOULDER	@ GRADE
609+50	9.5" AC-20, UNDERDRAINS, UNTREATED SUBGRADE	OWP	4' FILL
2551+00	9.5" AC-20, UNDERDRAINS, LIME MOD. SUBGRADE	OWP	2.5' FILL
2560+00	9.5" AC-20, NO UNDERDRAINS, LIME MOD. SUBGRADE	OWP	3' FILL
2610+00	9.5" AC-20, NO UNDERDRAINS, LIME MOD. SUBGRADE	OWP	14' CUT
3384+60	8.5" JOINTED PCC, NO UNDERDRAINS, NOT SEALED	CL, OWP, EDGE, SHOULDER	@ GRADE
3393+60	8.5" JOINTED PCC, NO UNDERDRAINS, SEALED	EDGE	3.5' FILL
3404+00	8.5" JOINTED PCC, UNDERDRAINS, SEALED	EDGE	1.5' FILL
3416+00	8.5" JOINTED PCC, UNDERDRAINS, NOT SEALED	CL, OWP, EDGE, SHOULDER	1.5' CUT
3420+00	7.5" JOINTED PCC, UNDERDRAINS, SEALED	OWP	1' CUT

TABLE 31: FROST MEASUREMENTS FROM WINTER MONTHS 1988 - 1990 FOR PROJECT 3

DATE READ	STATION NUMBER	AC LAYER THICKNESS	LIME	UNDERDRAINS	FROST DEPTH (IN)
11-JAN-88	570+50	12.5"	Y	N	N/A
11-JAN-88	593+50	12.5"	Y	Y	15.9
11-JAN-88	609+00	9.5"	N	Y	17.6
11-JAN-88	2551+50	9.5"	Y	Y	15.5
28-JAN-88	570+50	12.5"	Y	N	13.5
28-JAN-88	593+50	12.5"	Y	Y	12.0
28-JAN-88	609+00	9.5"	N	Y	10.8
28-JAN-88	2551+50	9.5"	Y	Y	10.8
10-FEB-88	570+50	12.5"	Y	N	N/A
10-FEB-88	593+50	12.5"	Y	Y	11.2
10-FEB-88	609+00	9.5"	N	Y	13.0
10-FEB-88	2551+50	9.5"	Y	Y	10.9
AVERAGE					13.1
17-FEB-89	570+50	12.5"	Y	N	N/A
17-FEB-89	593+50	12.5"	Y	Y	12.0
17-FEB-89	609+00	9.5"	N	Y	12.5
17-FEB-89	2551+50	9.5"	Y	Y	11.0
24-FEB-89	570+50	12.5"	Y	N	8.0
24-FEB-89	593+50	12.5"	Y	Y	9.0
24-FEB-89	609+00	9.5"	N	Y	8.0
24-FEB-89	2551+50	9.5"	Y	Y	9.0
18-DEC-89	570+50	12.5"	Y	N	16.5
18-DEC-89	593+50	12.5"	Y	Y	16.1
18-DEC-89	609+00	9.5"	N	Y	18.2
18-DEC-89	2551+50	9.5"	Y	Y	15.5
AVERAGE					12.4
11-JAN-90	570+50	12.5"	Y	N	22.0
11-JAN-90	593+50	12.5"	Y	Y	22.0
11-JAN-90	609+00	9.5"	N	Y	24.0
11-JAN-90	2551+50	9.5"	Y	Y	22.0
AVERAGE					22.5

TABLE 32: RIDE QUALITY DATA (ROADOMETER) FOR PROJECTS 1, 2, 3, AND 4

PROJECT	PAVEMENT TYPE	TEST DATE	LANE 1 EAST/NORTH	LANE 2 WEST/SOUTH
1	FULL-DEPTH AC	11-18-87	54	56
		06-05-90	66	67
2	JOINTED PCC	06-05-90	109	98
3	FULL-DEPTH AC (ST CLAIR COUNTY)	03-29-88	61	58
		05-24-90	87	91
3	FULL-DEPTH AC (CLINTON COUNTY)	06-03-87	75	58
		05-24-90	87	81
4	JOINTED PCC	06-03-87	— <sup>a</sup>	77
		05-24-90	93	103
4	CRCP	02-25-87	80	75
		05-24-90	129	117

ADJECTIVE RATING SCALE

PCC PAVEMENT (IN./MILE)	BITUMINOUS PAVEMENT (IN./MILE)	ADJECTIVE RATING
75 OR LESS	60 OR LESS	VERY SMOOTH
76- 90	60- 75	SMOOTH
91-125	76-105	SLIGHTLY ROUGH
126-170	106-145	ROUGH
171-220	146-190	VERY ROUGH
221-375	191-330	UNSATISFACTORY

<sup>a</sup> No data collected on this project

TABLE 33A: RIDE QUALITY DATA (ROAD PROFILER) FOR PROJECT 1

SECTION	1990		1991		1992	
	EAST	WEST	EAST	WEST	EAST	WEST
A	115	104	129	151	112	103
B	89	94	141	N/A	89	90

N/A = Not available

TABLE 33B: RIDE QUALITY DATA (ROAD PROFILER) FOR PROJECT 2

SECTION	1990		1991		1992	
	NORTH	SOUTH	NORTH	SOUTH	NORTH	SOUTH
C	154	150	182	N/A	152	146
D	140	131	179	N/A	151	129
E	132	133	164	N/A	150	136
F	118	124	146	N/A	144	98
G1	113	141	157	N/A	159	121
G2	139	149	176	N/A	190	153
G3	N/A	N/A	N/A	N/A	N/A	N/A
G4	137	150	182	N/A	159	146
H	148	125	201	N/A	166	142

N/A = Not available

TABLE 33C: RIDE QUALITY DATA (ROAD PROFILER) FOR PROJECT 3

SECTION	1990		1991		1992	
	EAST	WEST	EAST	WEST	EAST	WEST
A	108	96	119	104	118	102
B	111	87	134	89	165	146
C	146	136	159	150	103	93
D	106	92	116	94	98	80
E	95	82	103	89	99	88
H	114	100	120	112	92	93
I	88	78	98	84	150	124
J	138	138	128	124	257	119
K	157	122	187	136	112	98
L	99	79	105	89	N/A	N/A
M	128	86	122	88	149	90
M1	114	94	120	101	124	100
N	88	78	96	87	92	83
O	87	70	88	71	84	78
P	83	77	89	81	82	85

TABLE 33D: RIDE QUALITY DATA (ROAD PROFILER) FOR PROJECT 4

SECTION	1990		1991		1992	
	EAST	WEST	EAST	WEST	EAST	WEST
R	77	101	100	104	83	132
S	109	105	146	122	136	150
T	68	83	113	87	92	102
U	62	75	130	86	81	106
V	66	84	102	84	82	103
W	84	84	120	96	92	114
X	71	80	98	78	81	99
Y	81	98	98	92	76	97
Z	86	100	94	118	95	113
AA	106	111	124	123	110	120
BA	108	108	119	110	118	134
CA	84	86	88	89	92	96
DA	153	135	129	111	165	112
EA	89	96	102	100	100	111
FA	90	96	124	128	93	93
GA	108	100	104	98	117	114
HA	78	83	89	99	84	96
IA	86	90	103	92	73	95
JA	87	97	91	82	82	99
KA	75	82	90	77	76	82
LA	80	84	80	82	82	87
MA	79	82	91	72	80	84
NA	78	89	92	82	90	100
OA	83	101	86	100	89	102
PA	73	80	84	83	81	88
QA	84	84	90	84	88	86
RA	79	88	86	100	92	100



TABLE 34: SUMMARY OF TREADED TIRE FRICTION DATA

PROJECT NO.	PAVEMENT TYPE	AGE (YEARS)	FRICTION NUMBERS		AVG.
			EAST	WEST	
1	FULL-DEPTH AC	5.4	55	54	55
		4.5	51	49	50
		3.4	50	51	51
		2.8	50	48	49
		1.6	55	54	55
		0.9	49	50	50
2	JOINTED PCC	5.4	63	64	64
		4.5	64	63	64
		3.4	60	61	61
3	FULL-DEPTH AC (St. Clair Co.)	5.5	50	52	51
		4.8	48	49	49
		3.4	51	54	52
		2.0	43	50	46
3	FULL-DEPTH AC (Clinton Co.)	5.5	52	51	52
		4.7	50	48	49
		3.4	54	52	53
		2.0	49	49	49
		1.0	51	51	51
4	JOINTED PCC	5.1	65	64	65
		4.3	62	61	62
		3.0	66	65	65
4	CRCP	5.1	65	63	64
		4.4	64	63	64
		3.0	67	64	65

TABLE 35: SUMMARY OF SMOOTH TIRE FRICTION DATA

PROJECT NO.	PAVEMENT TYPE	AGE (YEARS)	FRICTION NUMBERS		AVG.
			EAST	WEST	
1	FULL-DEPTH AC	5.4	36	39	38
		4.5	37	40	39
		3.4	37	42	40
		2.8	39	39	39
		1.6	42	45	43
		0.9	39	44	41
2	JOINTED PCC	5.4	61	59	60
		4.5	66	62	64
		3.4	62	60	61
3	FULL-DEPTH AC (St. Clair Co.)	5.5	29	31	30
		4.8	27	31	29
		3.4	31	36	33
		2.0	29	37	33
3	FULL-DEPTH AC (Clinton Co.)	5.5	29	31	34
		4.7	35	34	35
		3.4	38	38	38
		2.0	36	36	36
		1.0	38	38	38
4	JOINTED PCC	5.1	57	49	53
		4.3	55	51	53
		3.0	63	57	60
4	CRCP	5.1	64	60	62
		4.3	60	60	60
		3.0	66	66	66

TABLE 36: FINAL CONSTRUCTION COSTS

---

PROJECT NO.	COMPLETION COST
1	\$3,029,204
2	\$2,489,121
3	\$7,455,551
4	\$9,137,568

---

TABLE 37: EFFECT OF UNDERDRAINS ON  $E_{Ri}$

SEASON	UNDERDRAINS			NO UNDERDRAINS		
	$E_{Ri}$ , (KSI)			$E_{Ri}$ , (KSI)		
	AVG.	STD. DEV.	N	AVG.	STD. DEV.	N
SPRING <sup>a</sup>	6.35	2.26	1061	6.27	2.76	280
FALL <sup>b</sup>	7.59	2.27	1145	6.99	2.17	310

a Includes 5/87, 5/88, and 5/89 FWD test dates

b Includes 9/87, 10/89, 8/90, and 8/91 FWD test dates

TABLE 38: PROJECT 3 RUT DEPTH COMPARISON BY AC TYPE  
(ROAD PROFILER MEASUREMENTS)

ASPHALT TYPE	RUT DEPTHS, INCHES								
	1990			1991			1992		
	EAST	WEST	ALL	EAST	WEST	ALL	EAST	WEST	ALL
AC-10	0.26	0.19	0.23	0.22	0.16	0.19	0.27	0.21	0.24
AC-20	0.23	0.20	0.22	0.19	0.18	0.19	0.26	0.22	0.24

TABLE 39: JRCP CRACK SURVEY SUMMARY FOR PROJECT 4

SECTION	SLAB THICKNESS (INCHES)	NUMBER OF PANELS	LOW SEVERITY CRACKS	MEDIUM SEVERITY CRACKS	HIGH SEVERITY CRACKS
BA	9.5	106	60	48	1
CA, EA, FA, GA & HA	8.5	576	391	207	-
OA, PA, QA & RA	7.5	426	285	166	-

TABLE 40: JPCP CRACK SURVEY SUMMARY FOR PROJECT 4

SECTION	SLAB THICKNESS (INCHES)	NUMBER OF PANELS	LOW SEVERITY CRACKS	MEDIUM SEVERITY CRACKS	HIGH SEVERITY CRACKS
AA	9.5	50	-	-	-
IA, JA, KA & LA	8.5	412	9	8	-
MA & NA	7.5	210	8	1	3

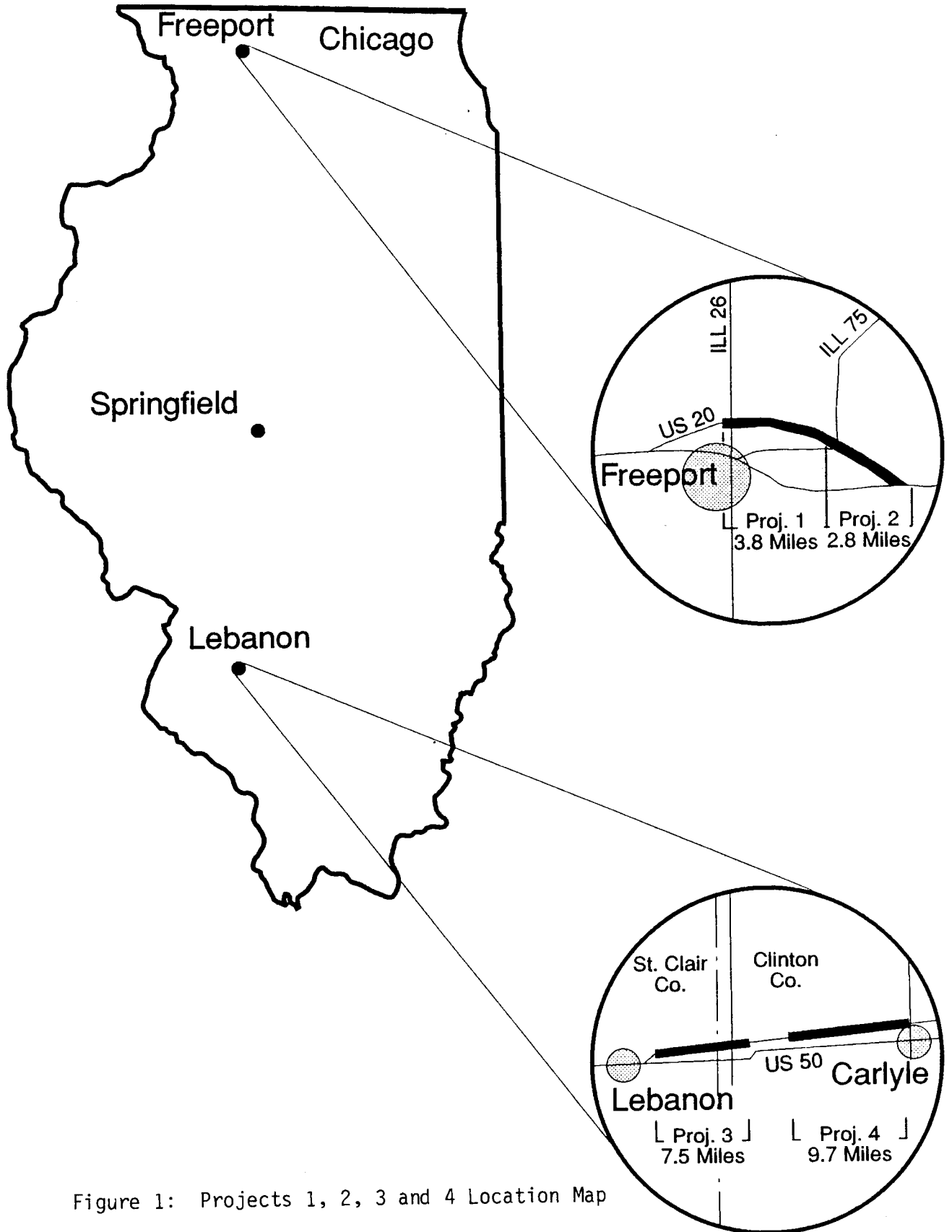


Figure 1: Projects 1, 2, 3 and 4 Location Map



# FA 401 FLEXIBLE PAVEMENT EXPERIMENTAL LAYOUT

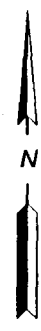
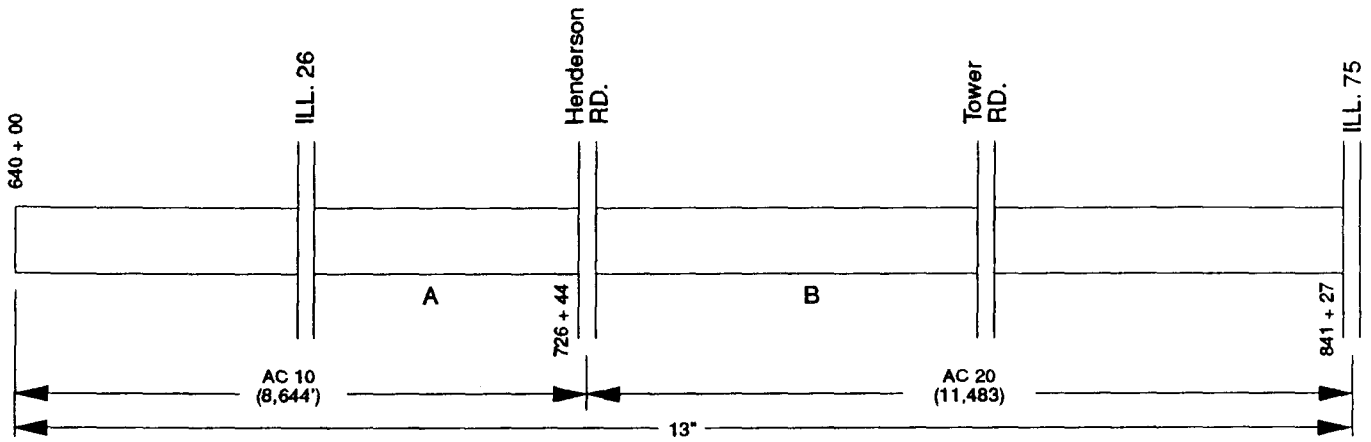
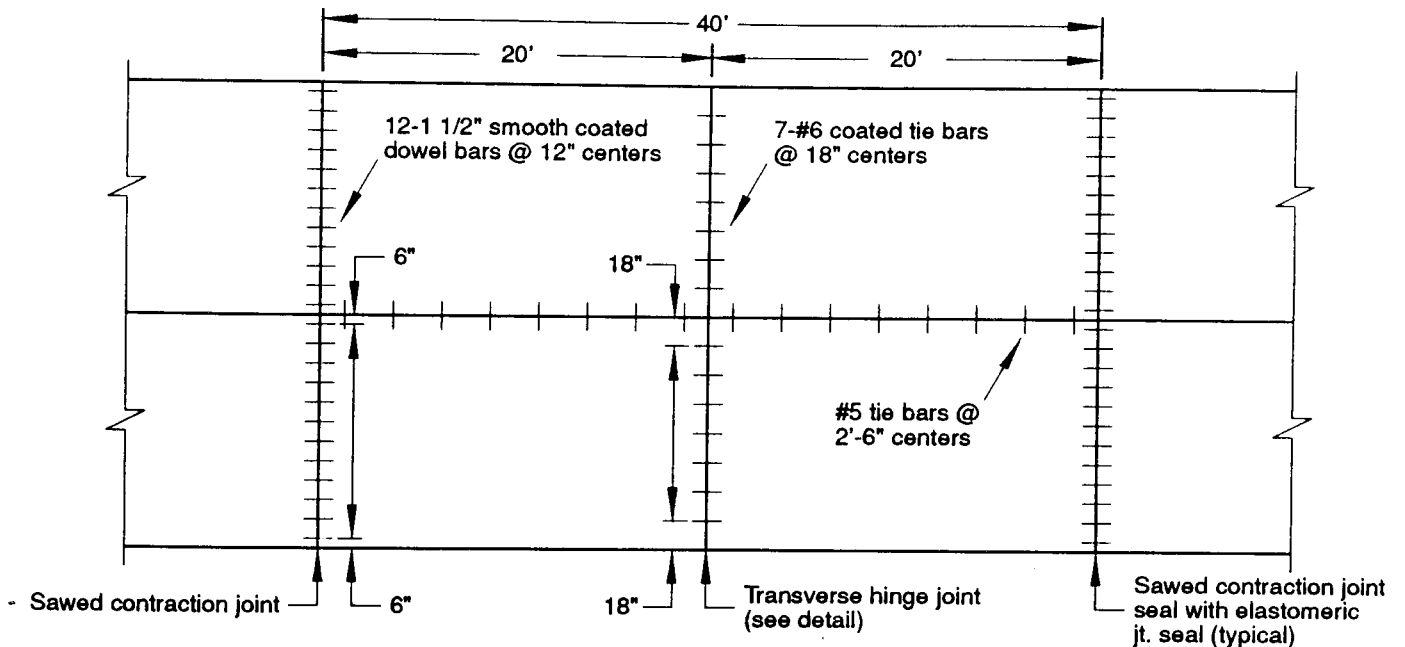


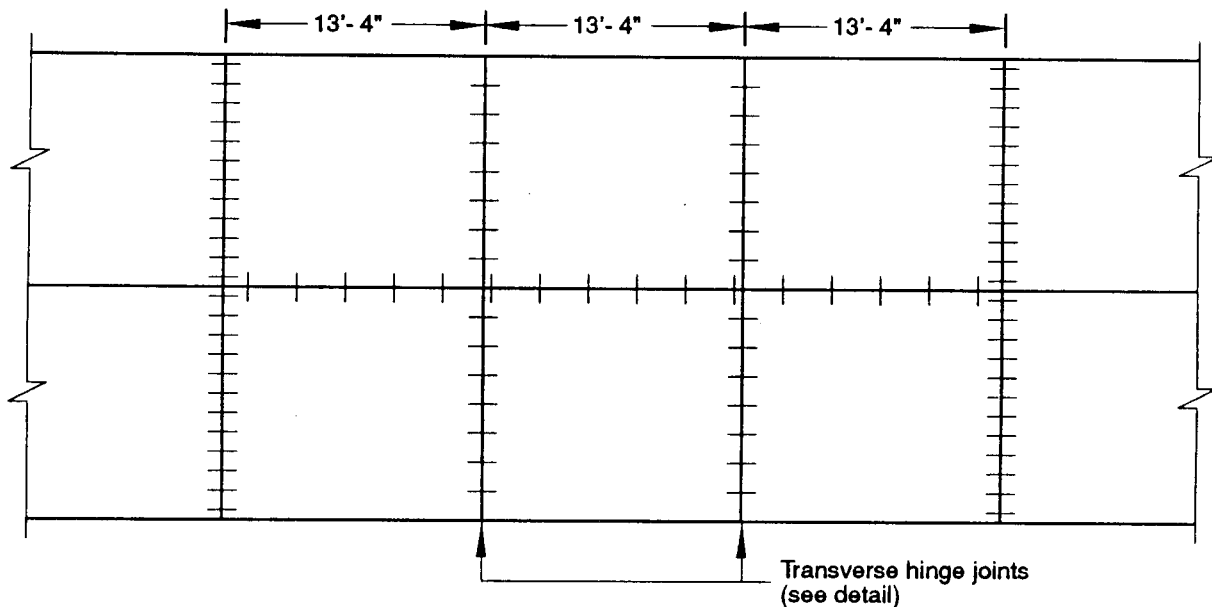
Figure 2: Project 1 Test Section Layout

# Hinge Joints For 40' Panels

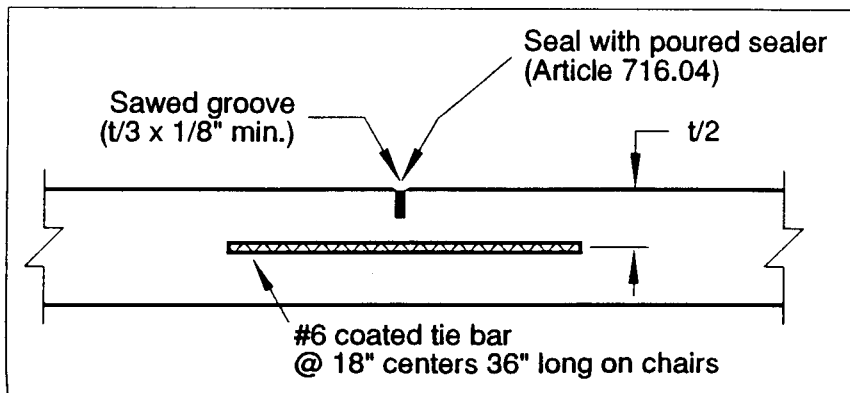
## Design A1, A2



## Design B



### Detail of Transverse Hinge Joint



Notes: Design A1 as shown (non-reinforced)

Design A2 same as A1 except with 7' long full-width pavement fabric, meeting requirements of standard 2347, centered between the hinge and contraction joints

Design B is non-reinforced

Figure 3: Hinge Joint Panel Design

# FA 401 PCC PAVEMENT STRAIN GAUGE TEST SITES

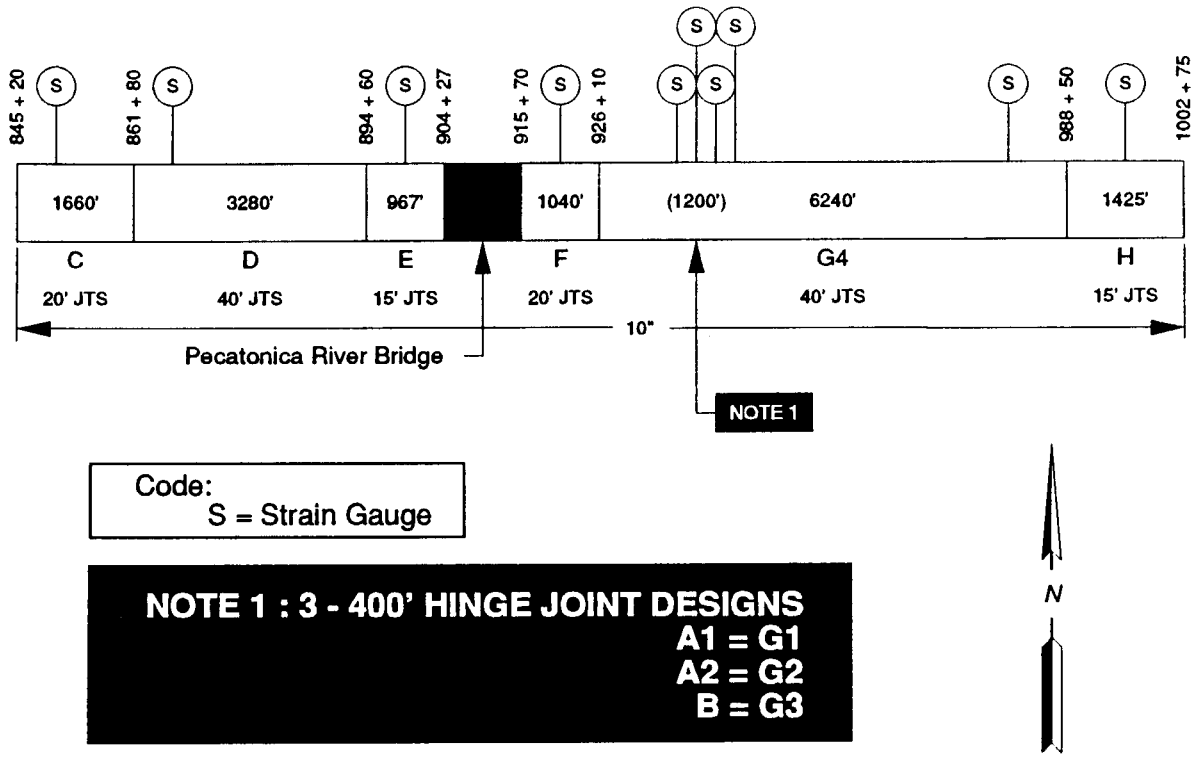


Figure 4: Project 2 Test Section Layout

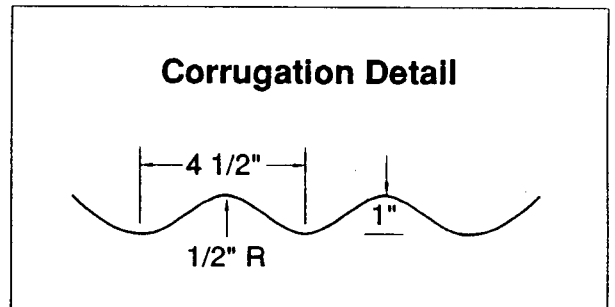
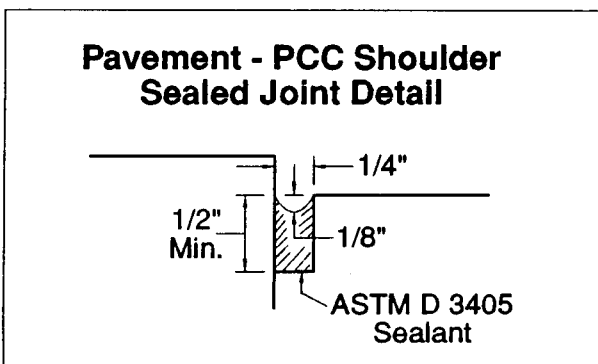
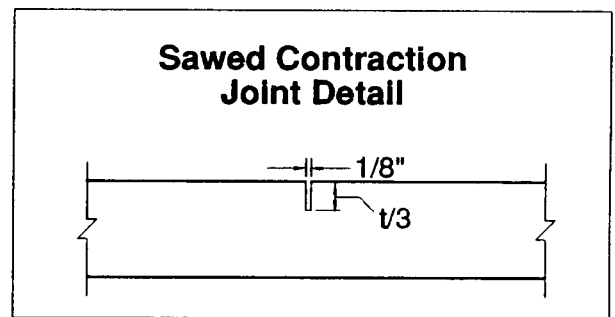
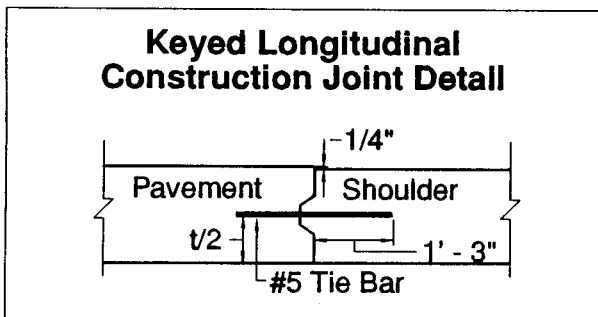
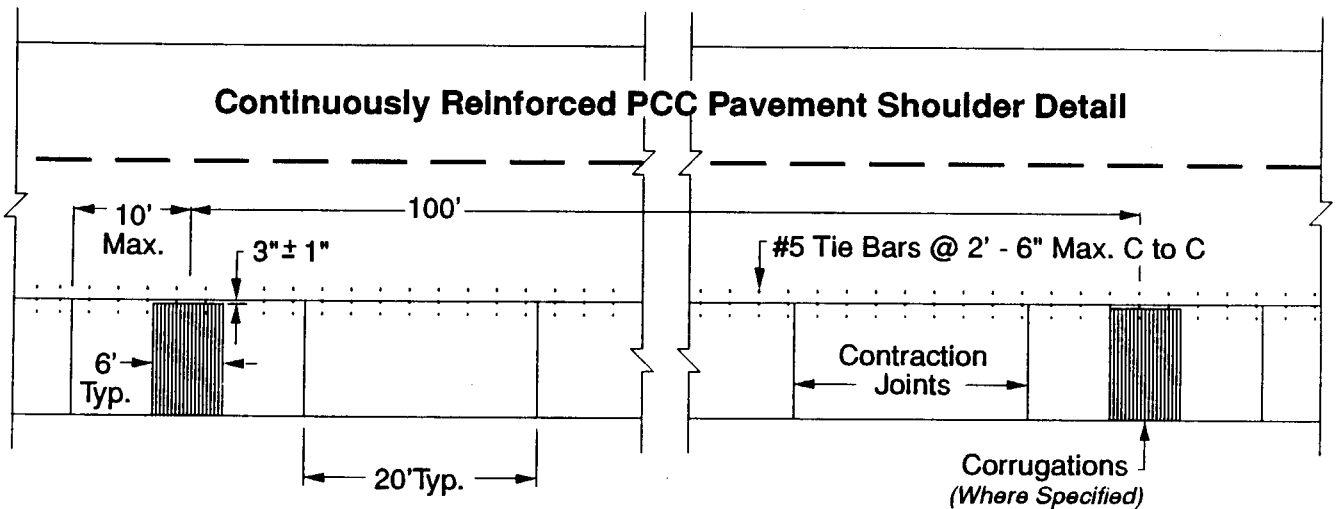
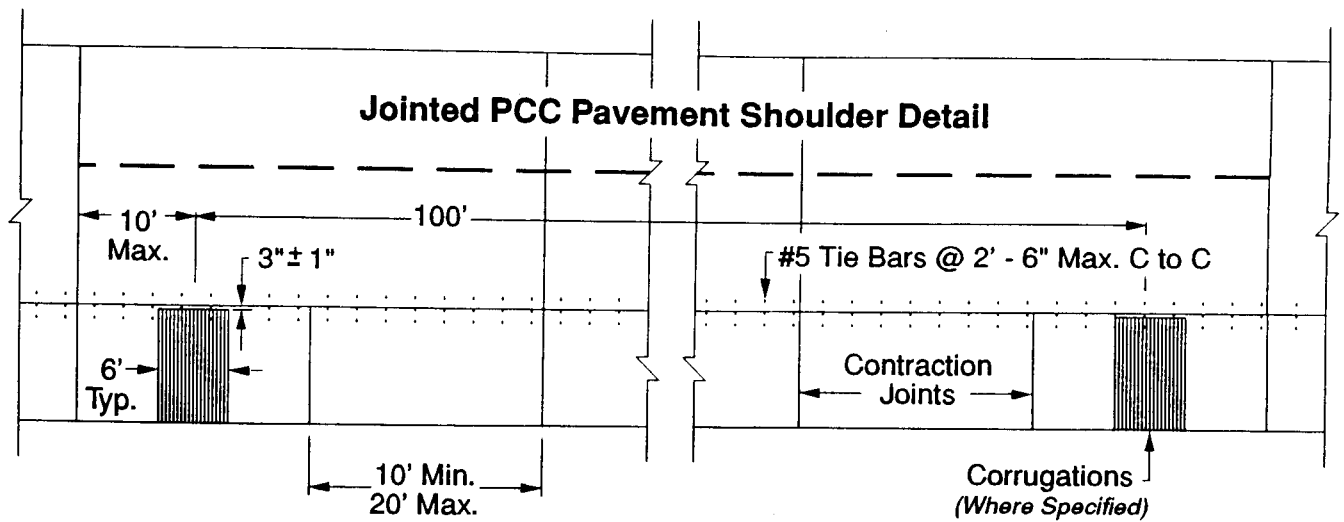
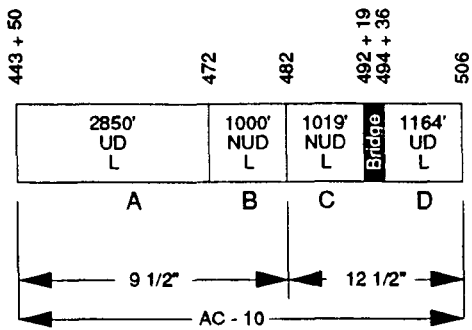
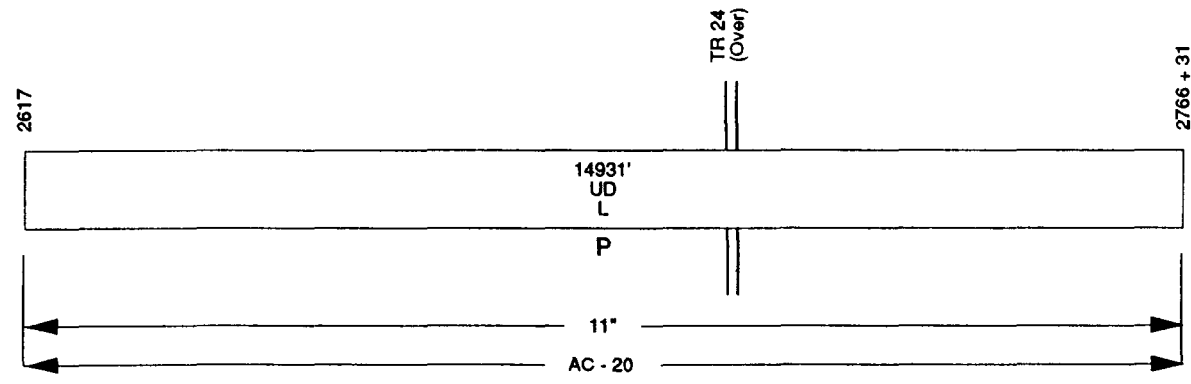
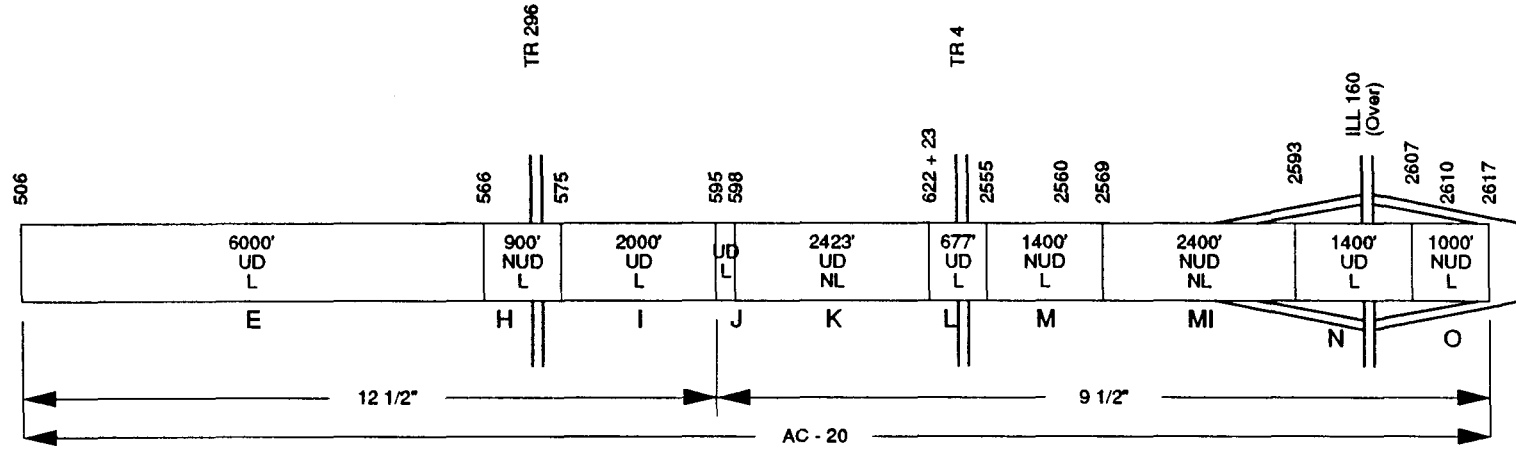


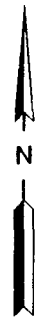
Figure 5: Tied PCC Shoulder Design Detail



# FA 409 AC PAVEMENT



**CODE:**  
 UD = Underdrains  
 NUD = No Underdrains  
 L = Lime Modification  
 NL = No Lime Modification



As - Built  
6/92

Figure 6: Project 3 Test Section Layout

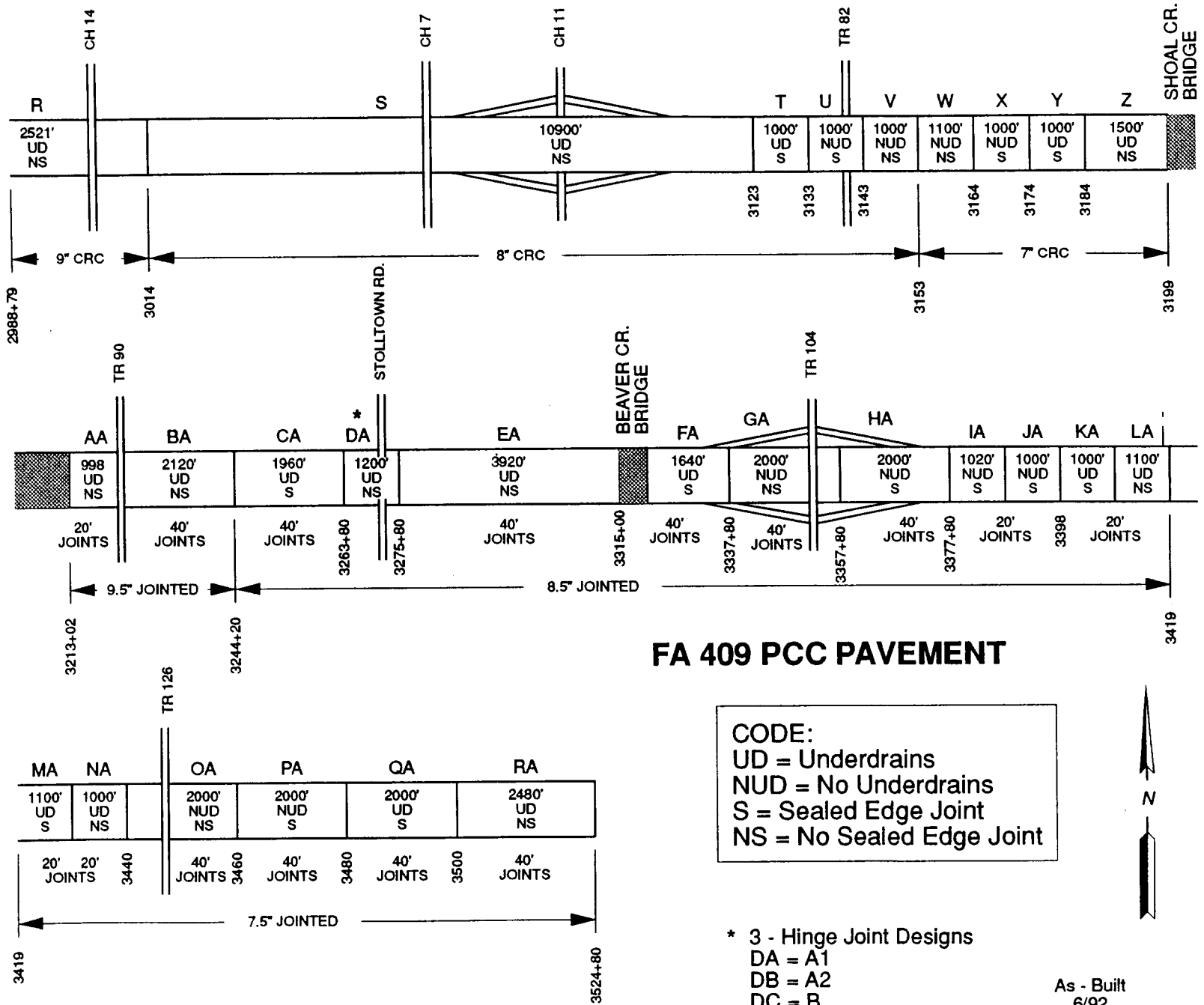


Figure 7: Project 4 Test Section Layout

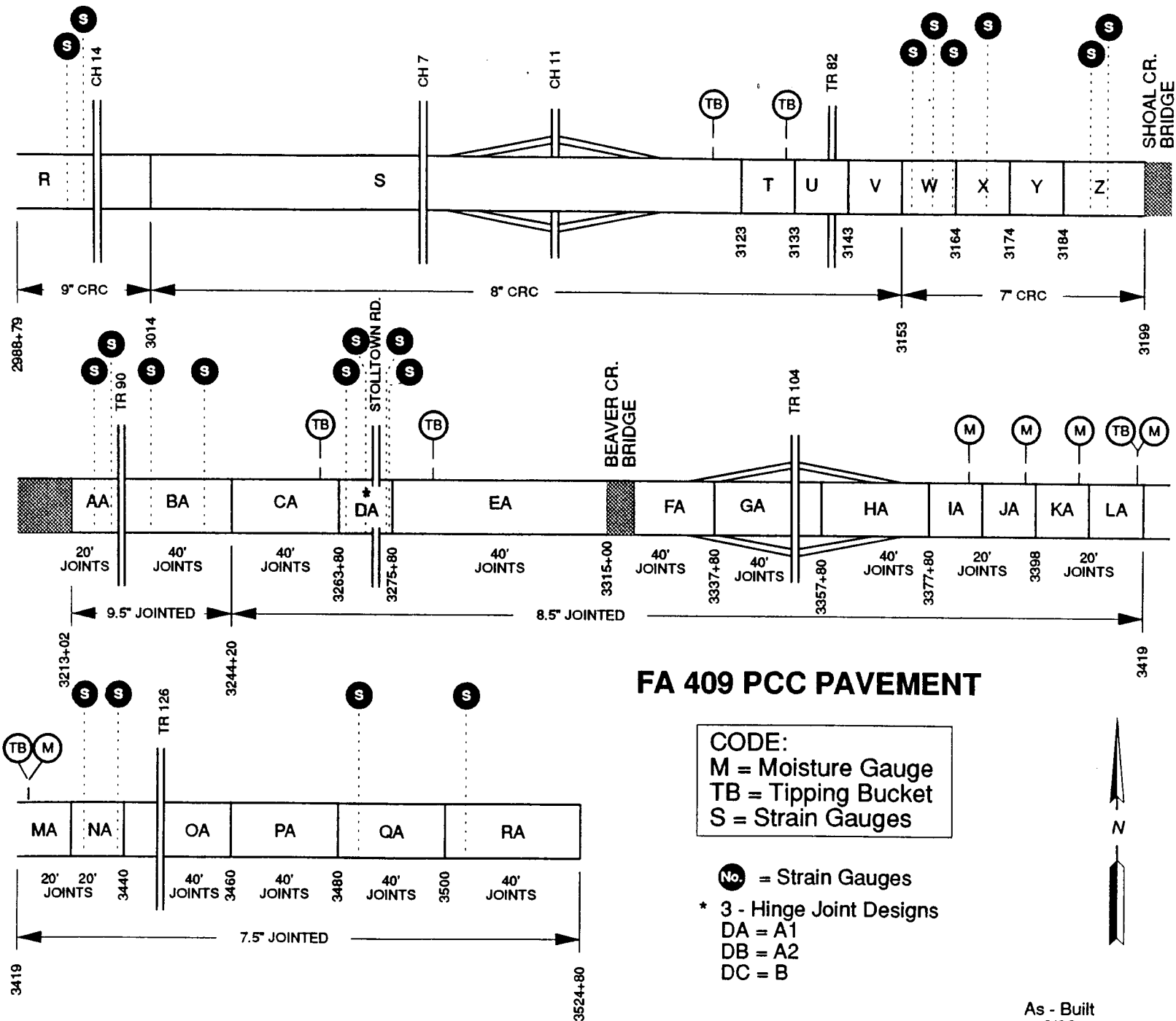
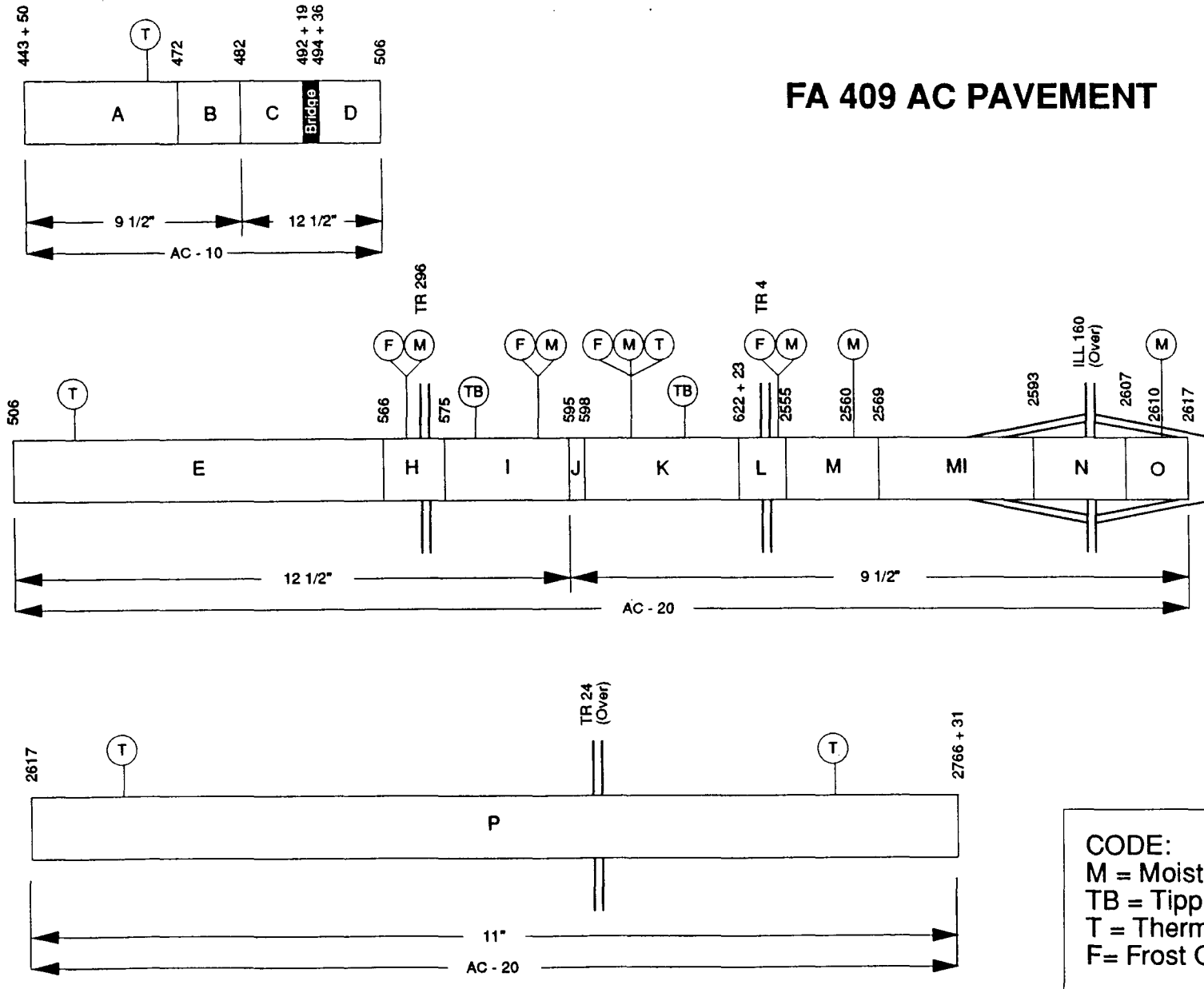


Figure 8: Project 4 Instrumentation Site Locations

# FA 409 AC PAVEMENT



As - Built  
6/92

Figure 9: Project 3 Instrumentation Site Locations



# Intersection Detail of FA Route 409 And County Highway 13

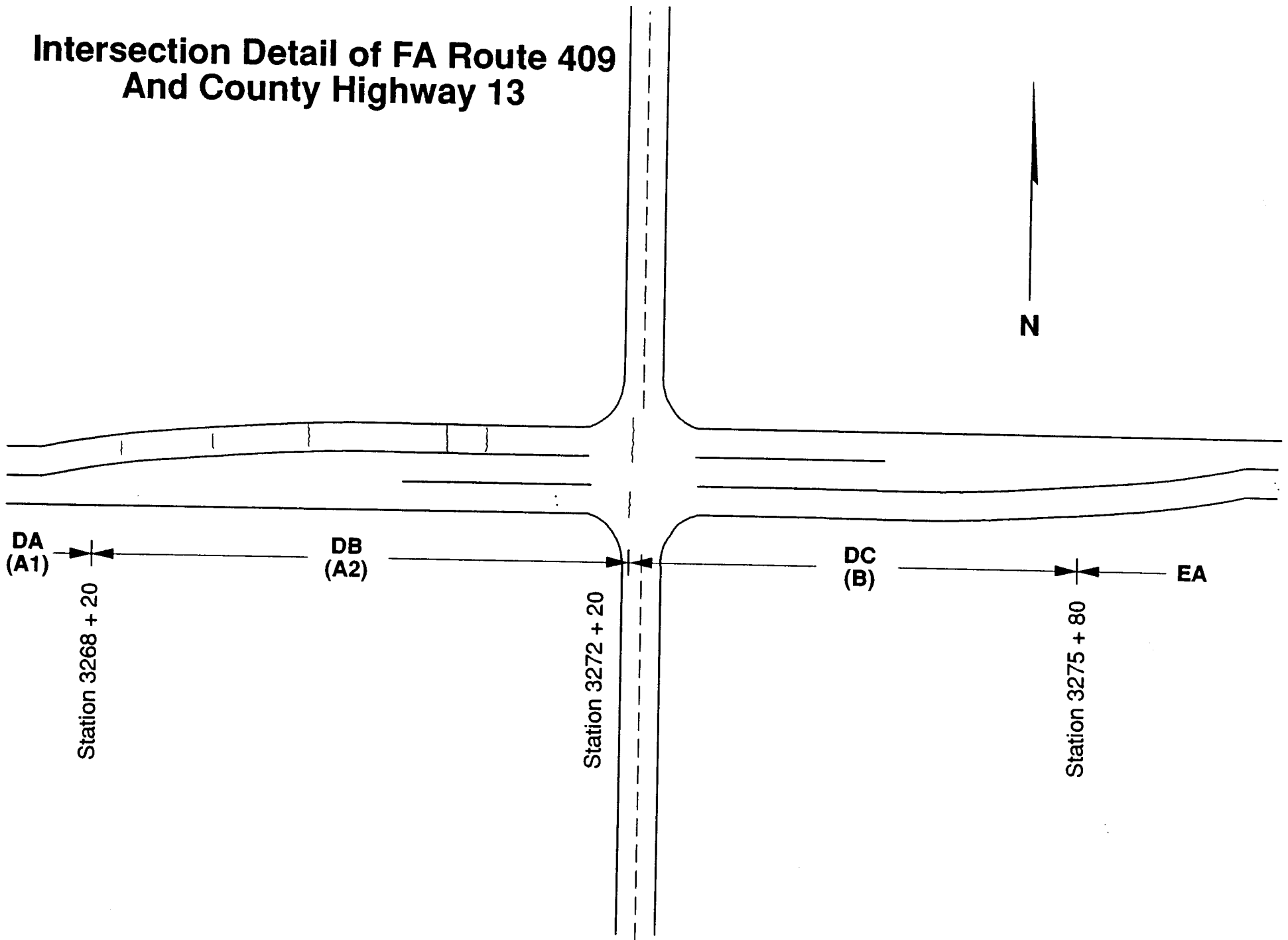
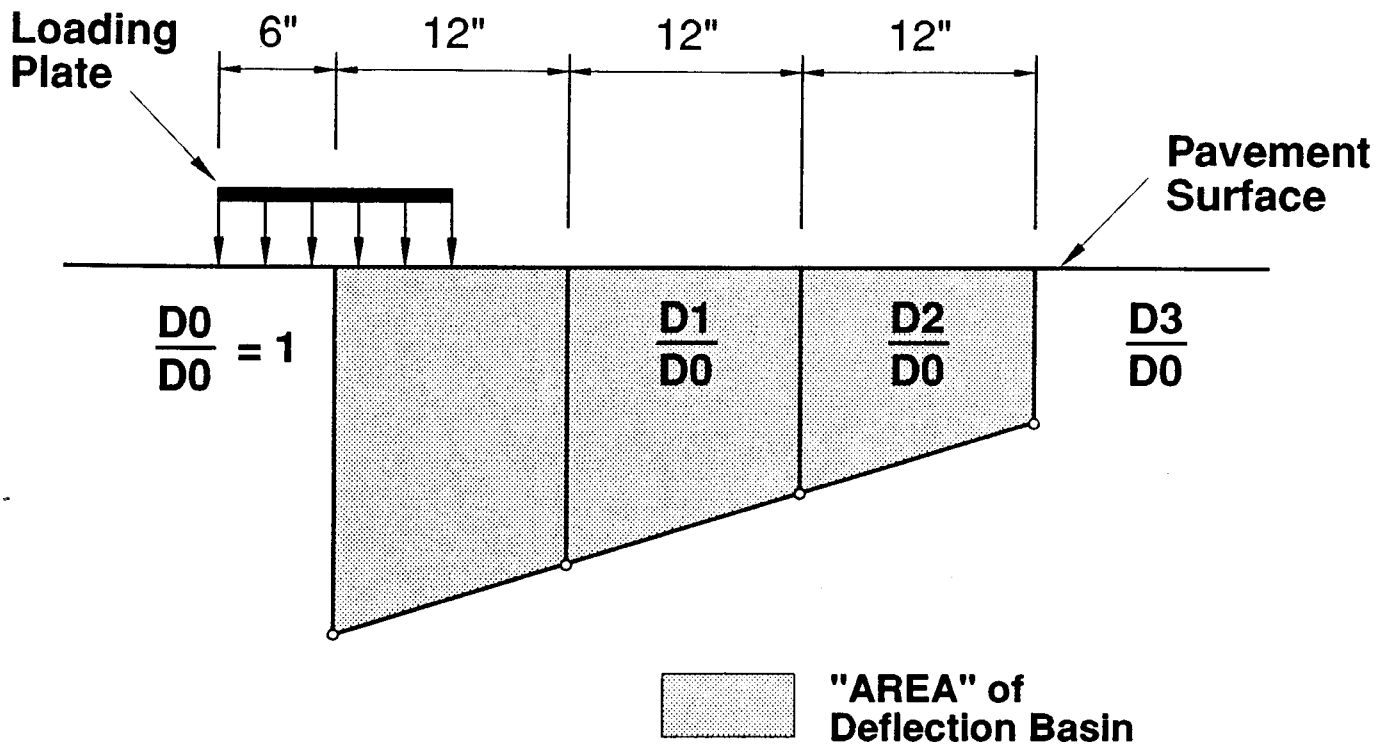


Figure 10: Hinge Jointed Panel Crack Locations on Project 4



$$\text{AREA (inch)} = 6 \left( 1 + 2 \frac{D1}{D0} + 2 \frac{D2}{D0} + \frac{D3}{D0} \right)$$

Figure 11: Deflection Basin Area

# Pavement Temp. Profile

Carlyle FA-409 10/11/89

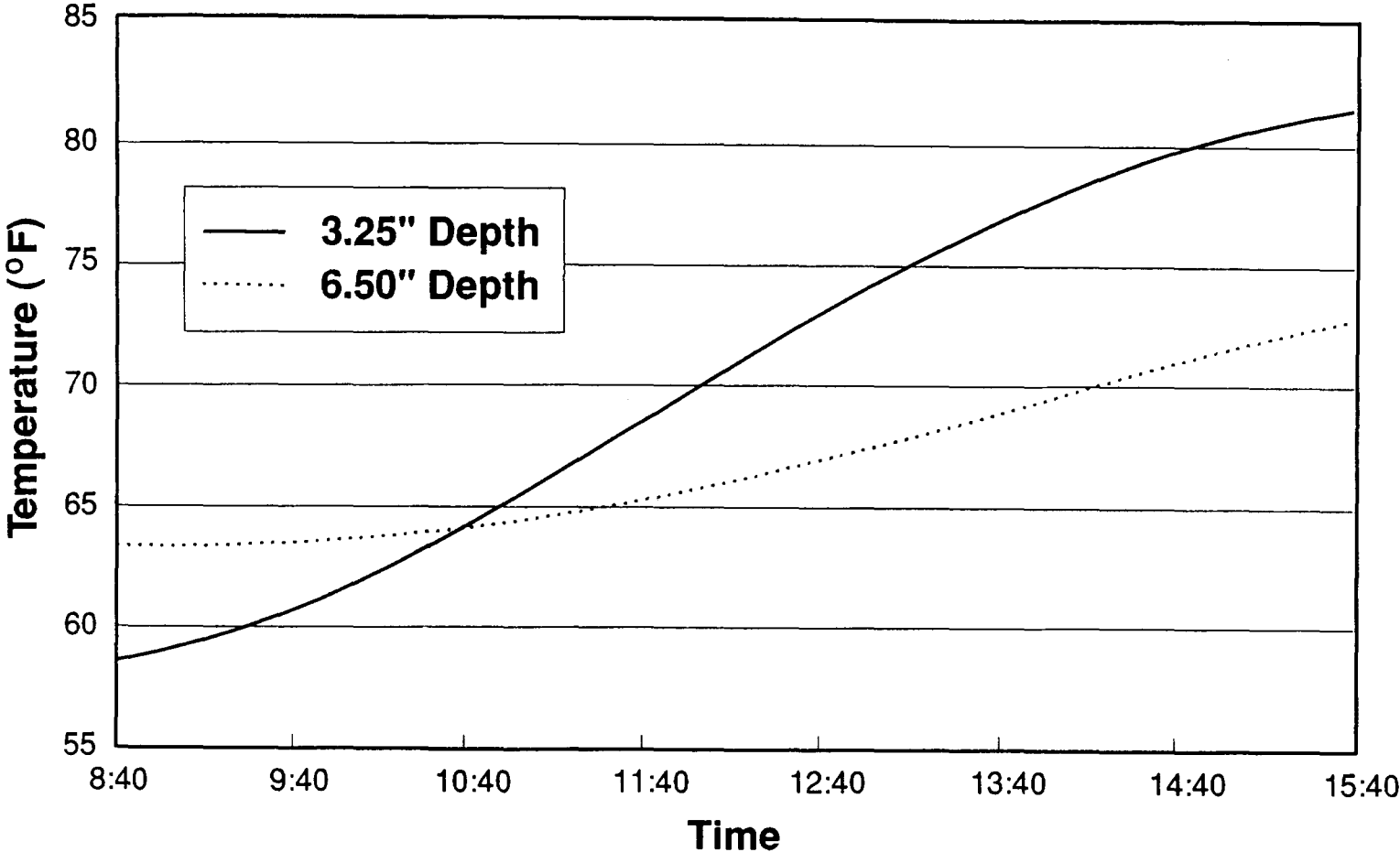


Figure 12: Project 3 Pavement Temperature Profile

# FA 409 5/87 Backcalculated $E_{AC}$ Versus Temperature

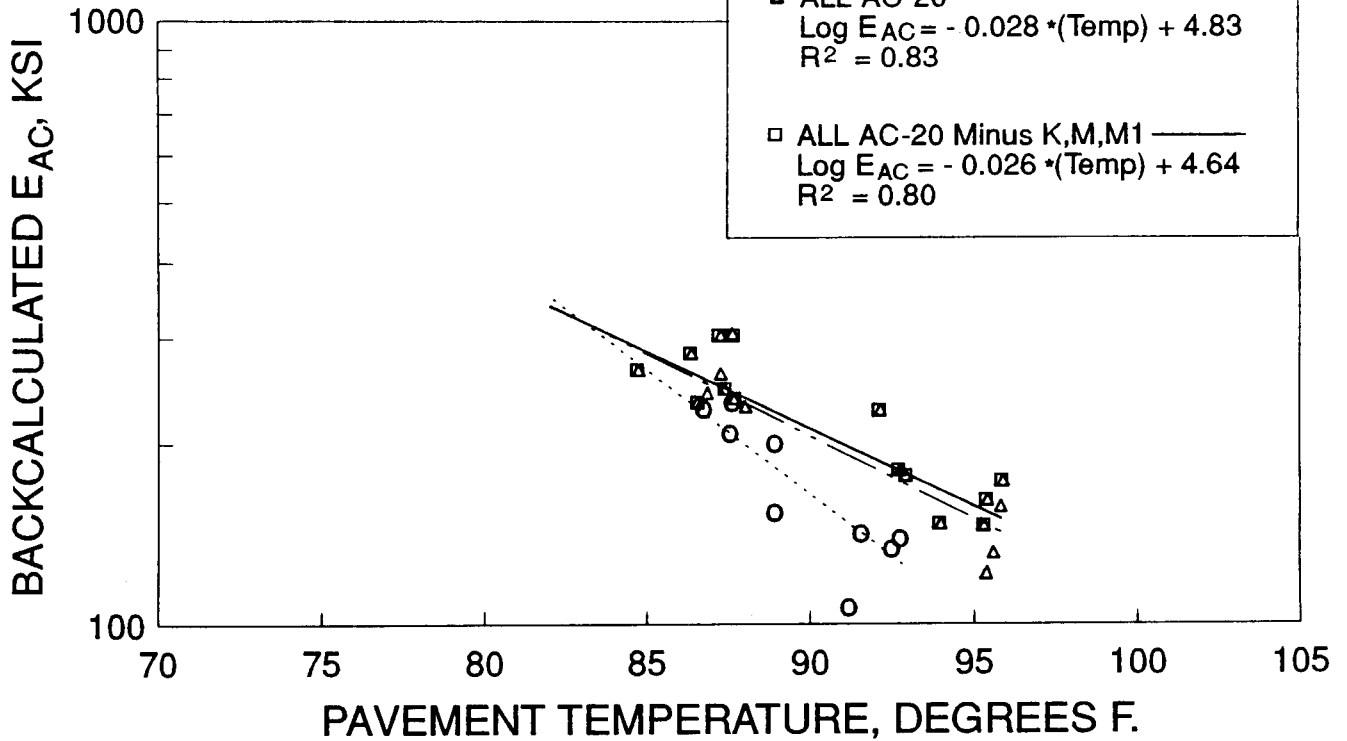


Figure 13: Project 3 FWD Data from May 1987

**FA 409 9/87**  
**Backcalculated E<sub>AC</sub>**  
**Versus Temperature**

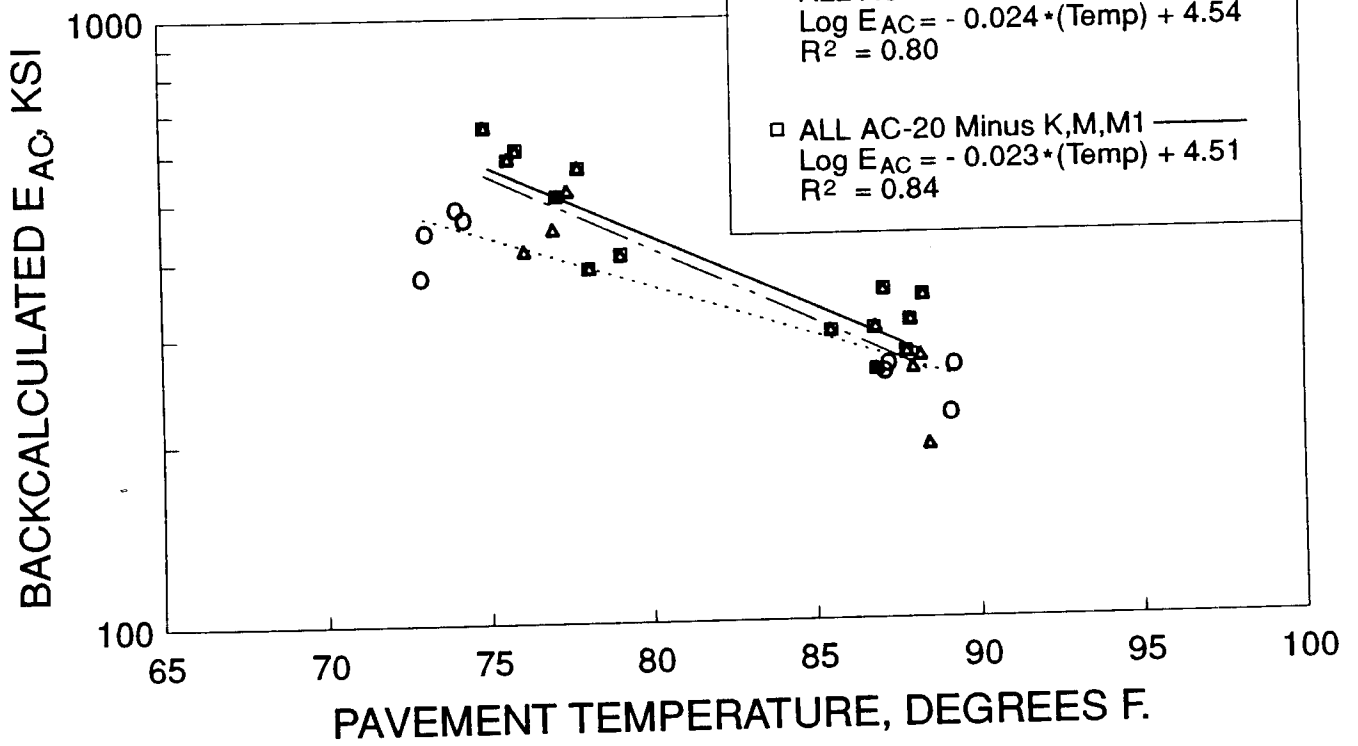


Figure 14: Project 3 FWD Data from September 1987

**FA 409 5/88**  
**Backcalculated E<sub>AC</sub>**  
**Versus Temperature**

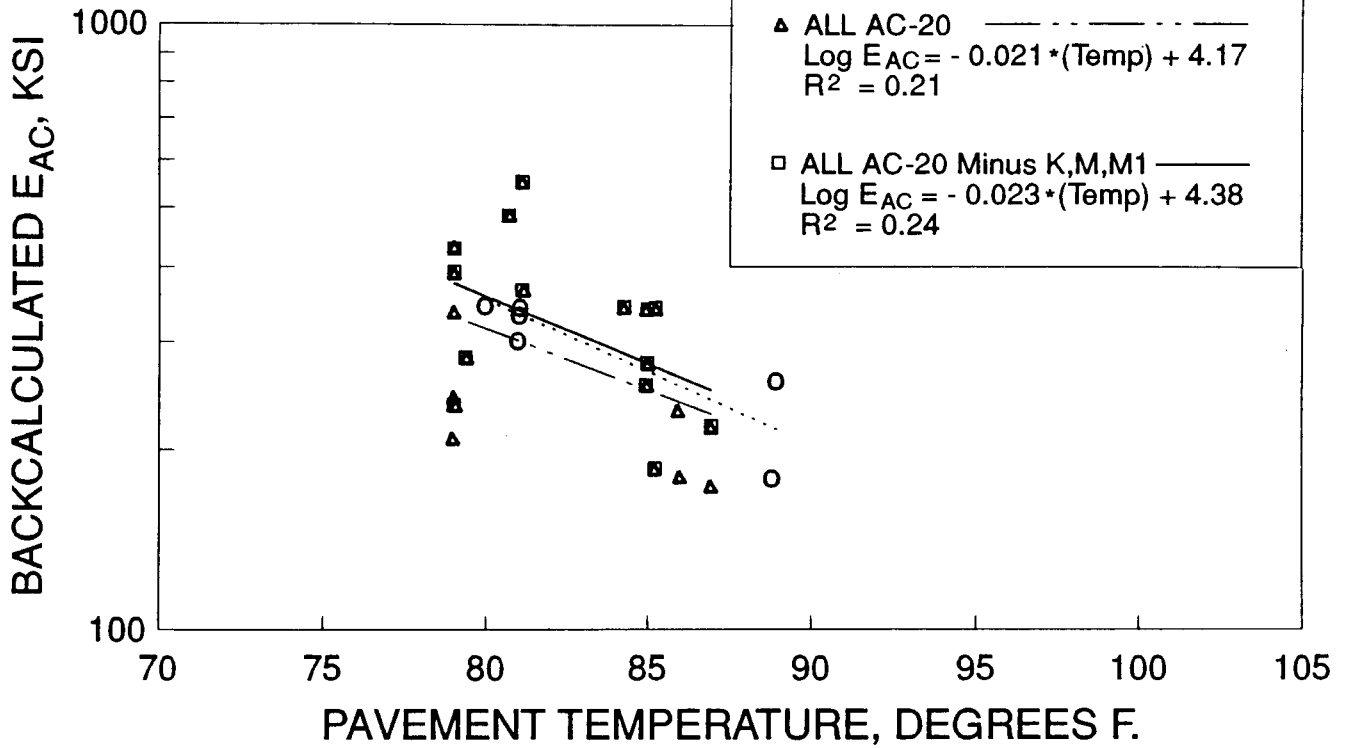


Figure 15: Project 3 FWD Data from May 1988

**FA 409 5/89**  
**Backcalculated E<sub>AC</sub>**  
**Versus Temperature**

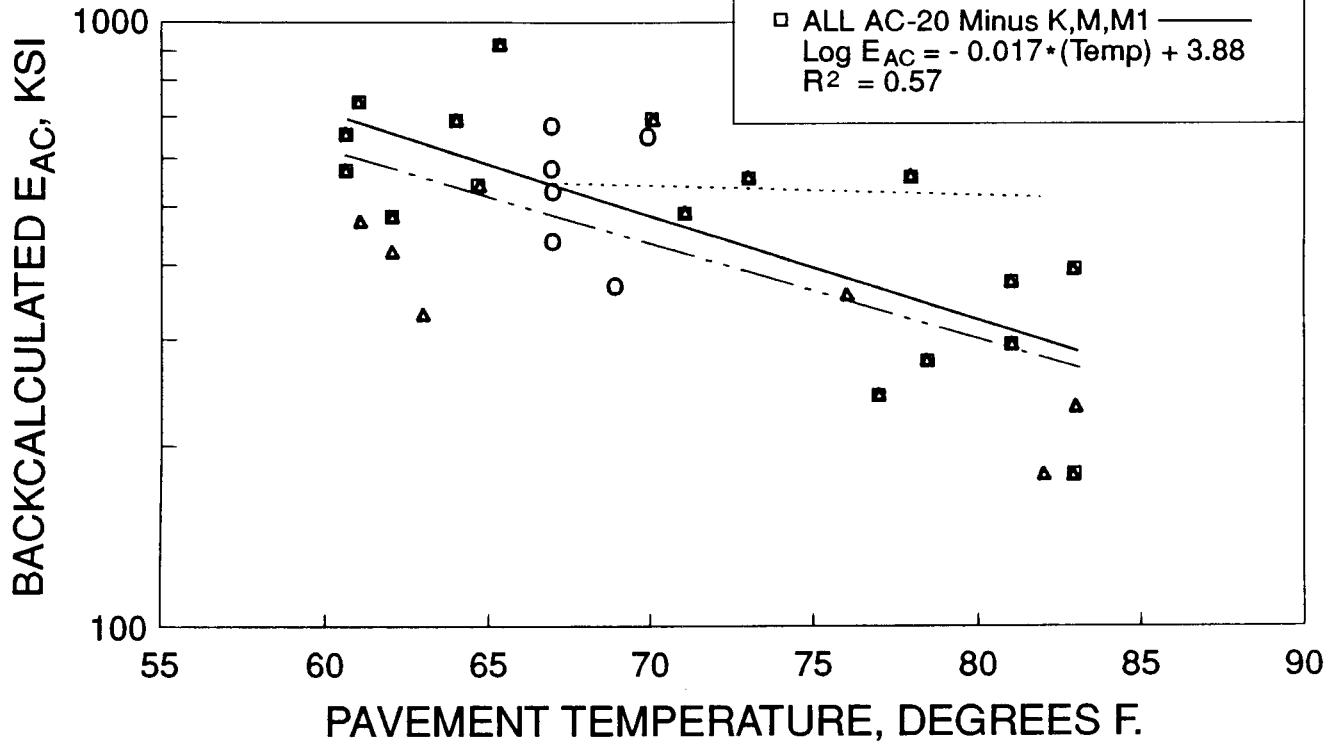


Figure 16: Project 3 FWD Data from May 1989

# FA 409 10/89 Backcalculated E<sub>AC</sub> Versus Temperature

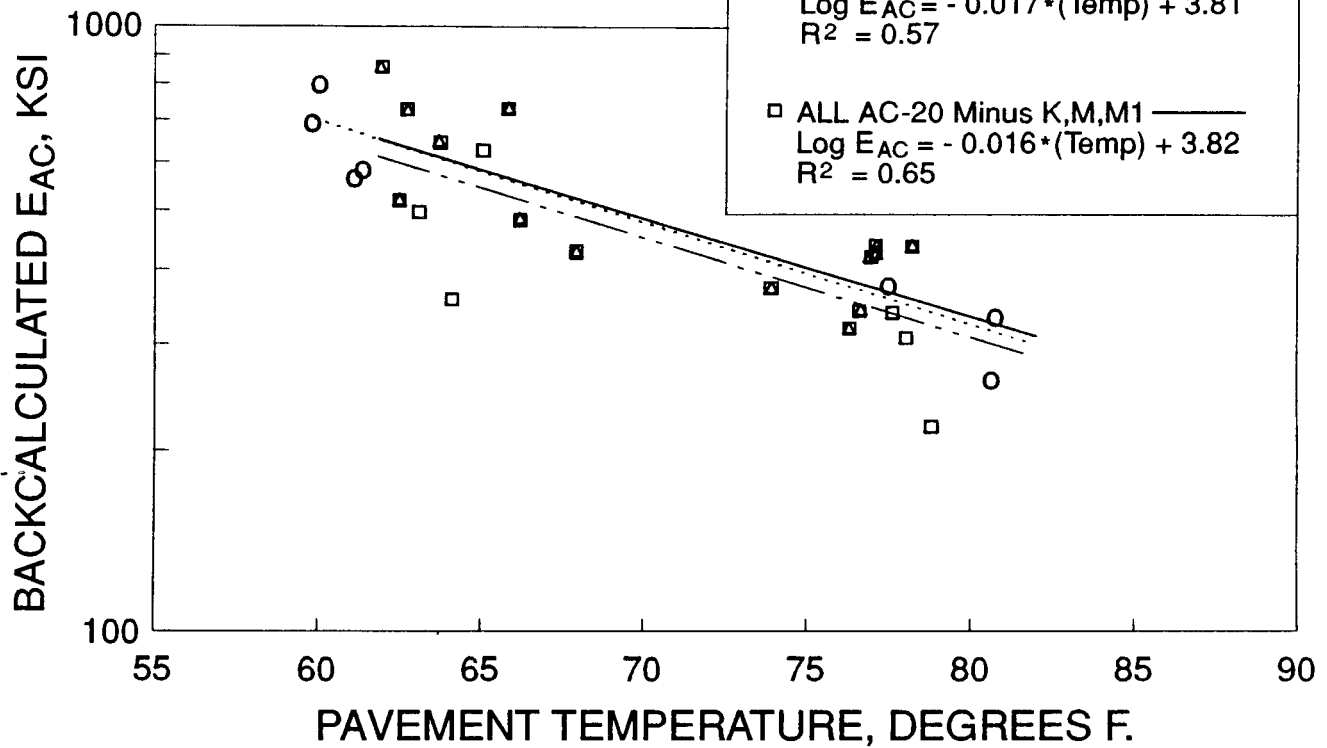


Figure 17: Project 3 FWD Data from October 1989



# FA 409 8/90 Backcalculated $E_{AC}$ Versus Temperature

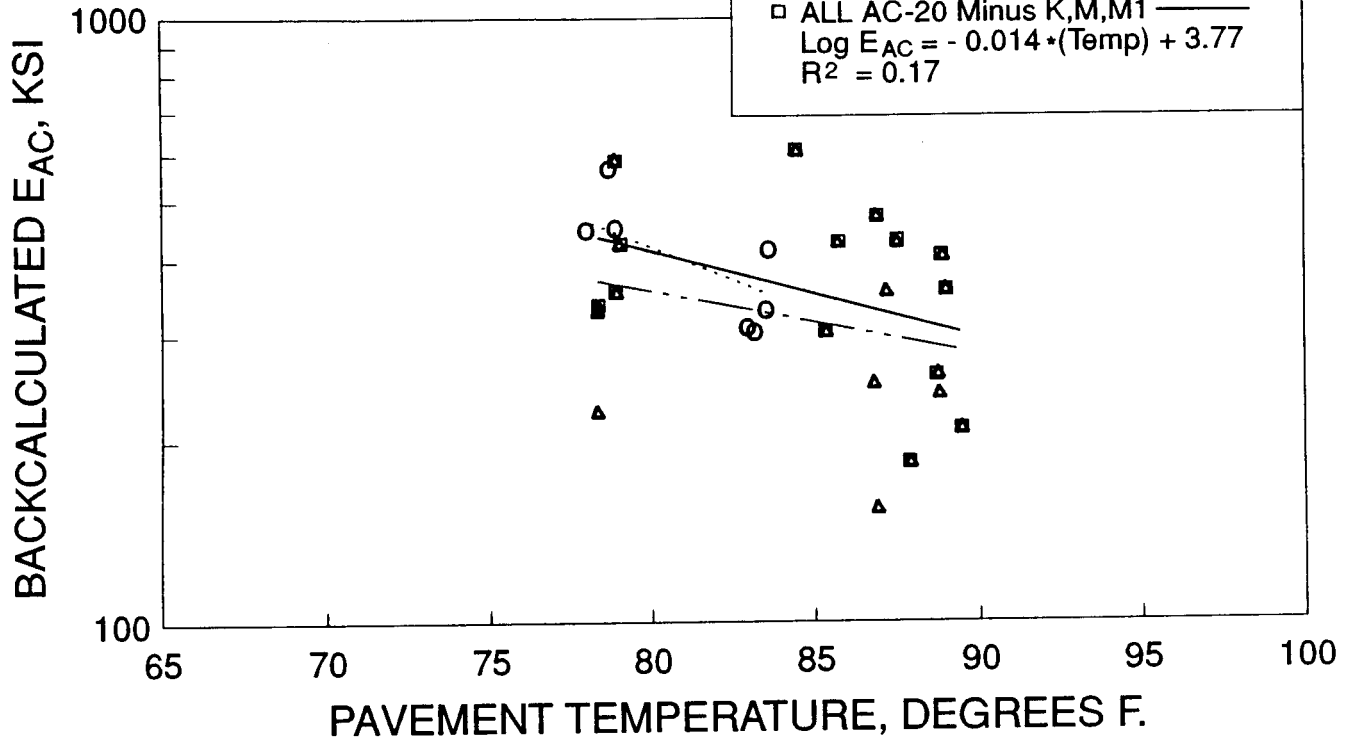


Figure 18: Project 3 FWD Data from August 1990

# FA 409 8/91 Backcalculated E<sub>AC</sub> Versus Temperature

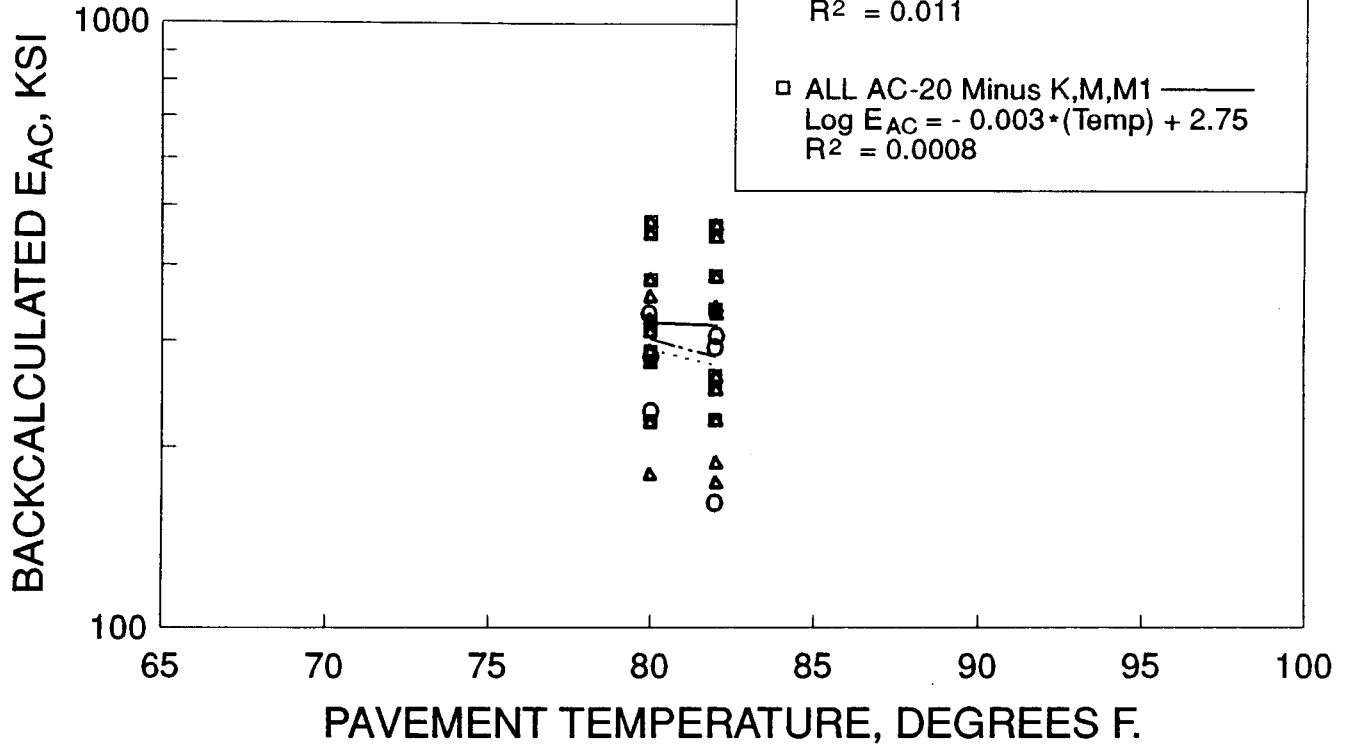


Figure 19: Project 3 FWD Data from August 1991

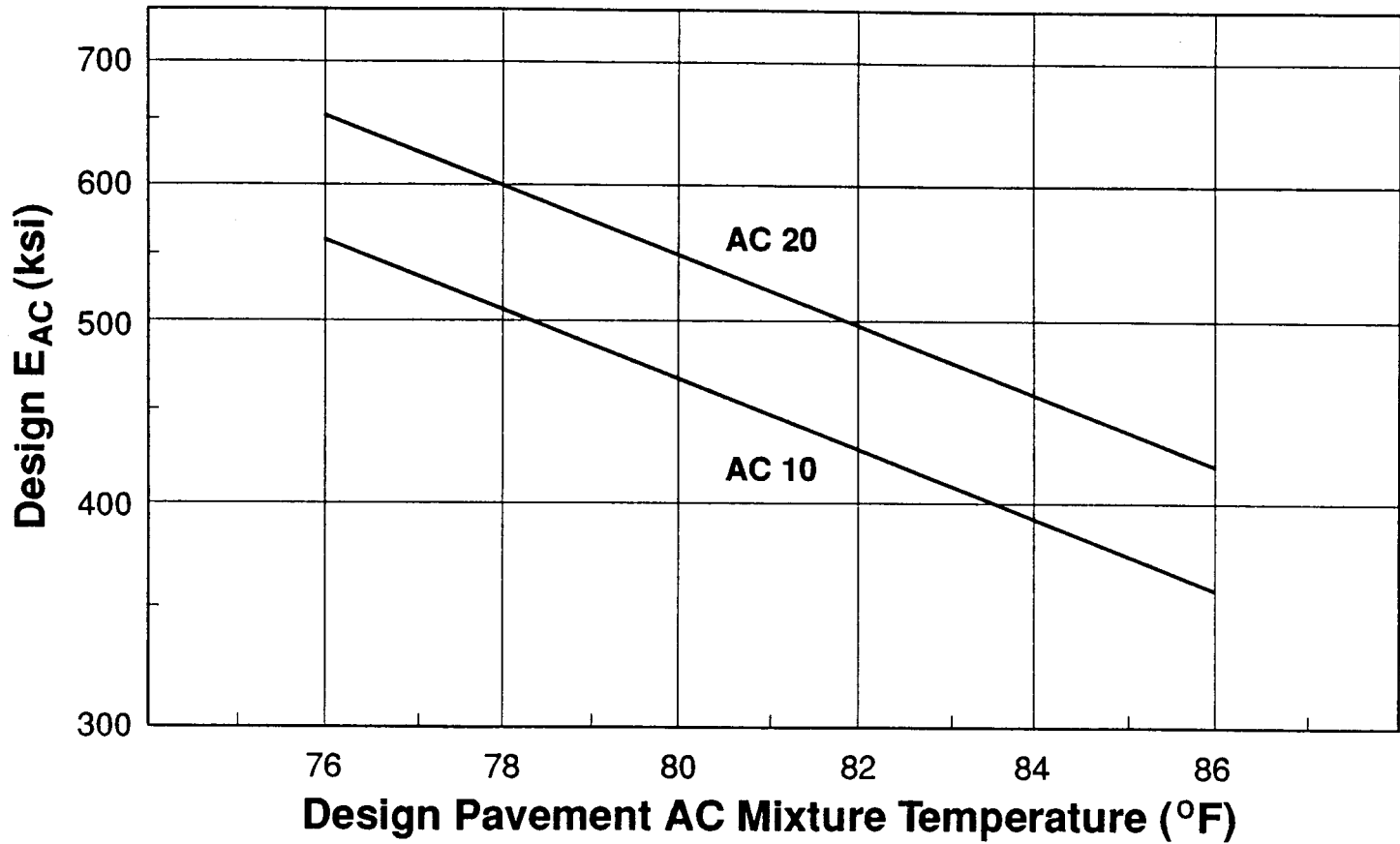


Figure 20: Design  $E_{ac}$  versus Design Pavement Temperature

**FA 409  
Backcalculated  $E_{AC}$   
Versus Age  
82 Degree F. Data**

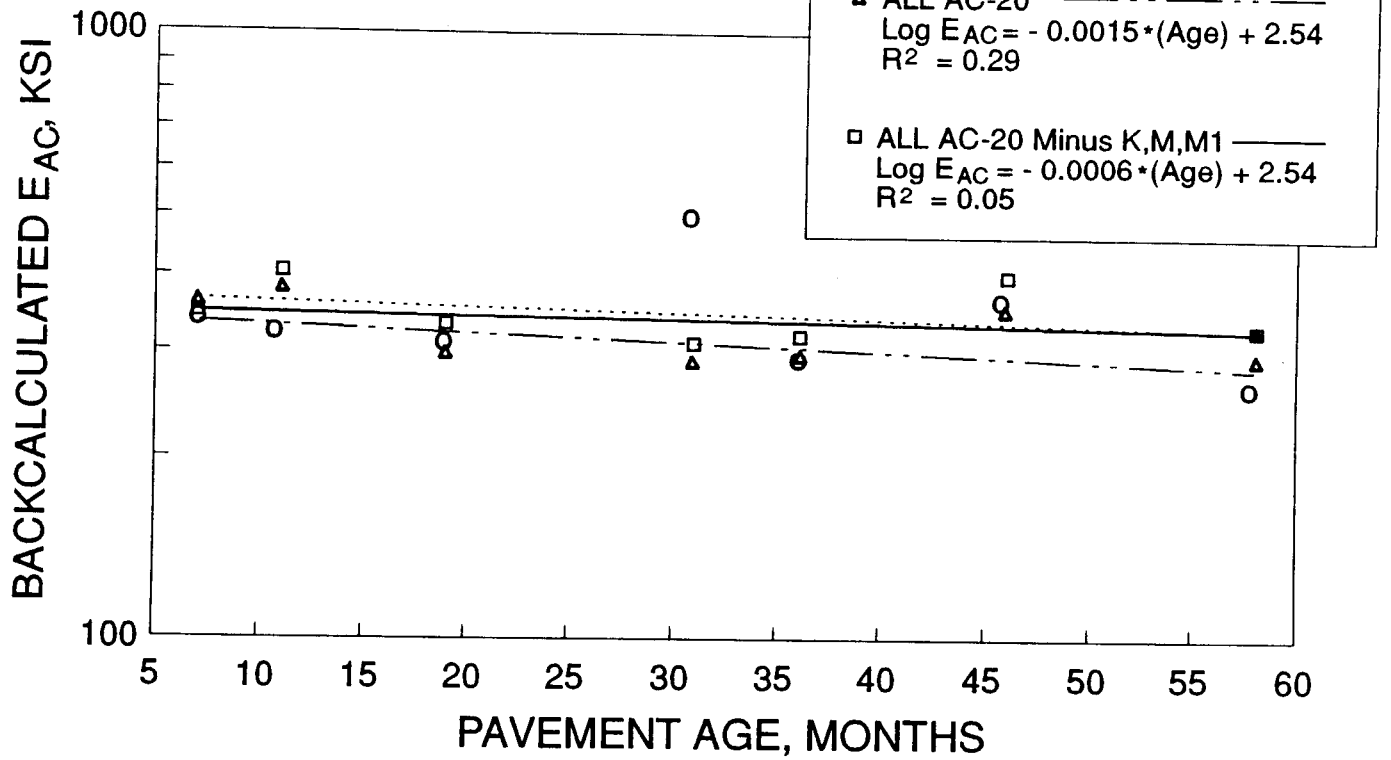
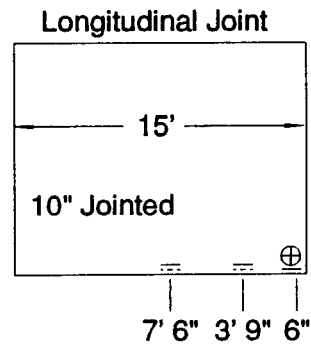
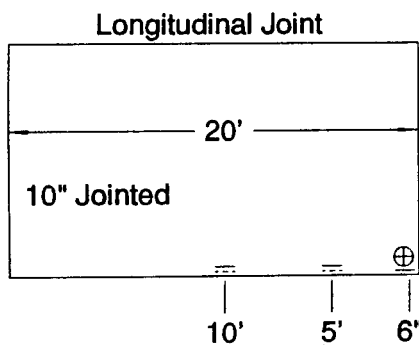
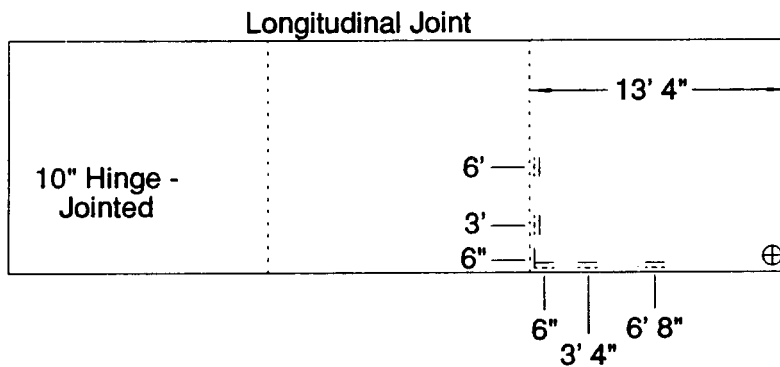
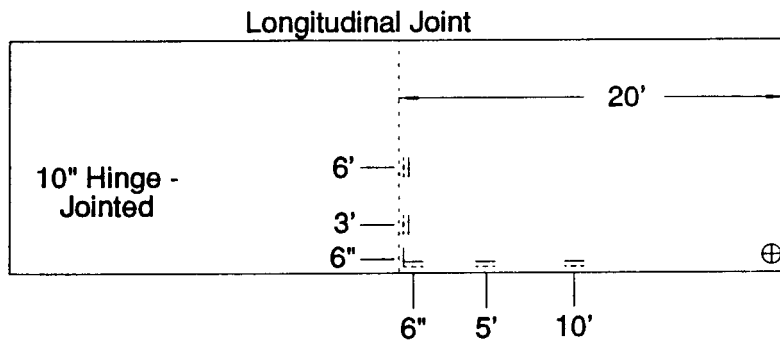
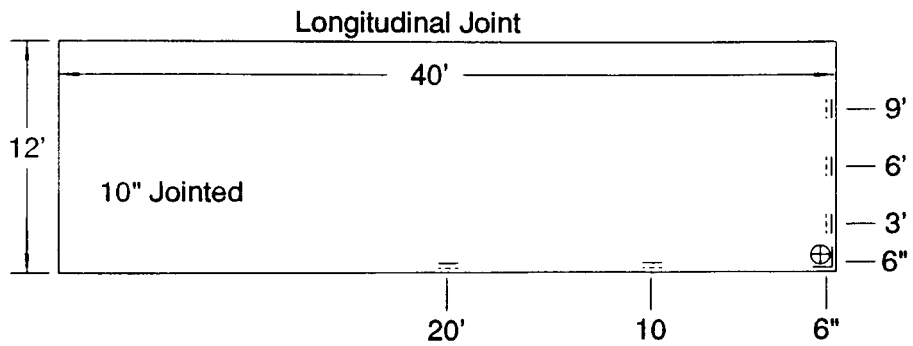


Figure 21: Backcalculated  $E_{AC}$  at 82 Degree F. vs. Pavement Age

# Summary of Gauge Positions

## FA 401



- Strain gauges 1" from top of the pavement
  - Strain gauges 1" from the bottom of the pavement
  - ⊕ Thermocouple
- NOTE : All distances are from the joint or edge of pavement

Figure 22: Project 2 Strain Gauge Location Diagrams

# Summary of Gauge Positions FA 409

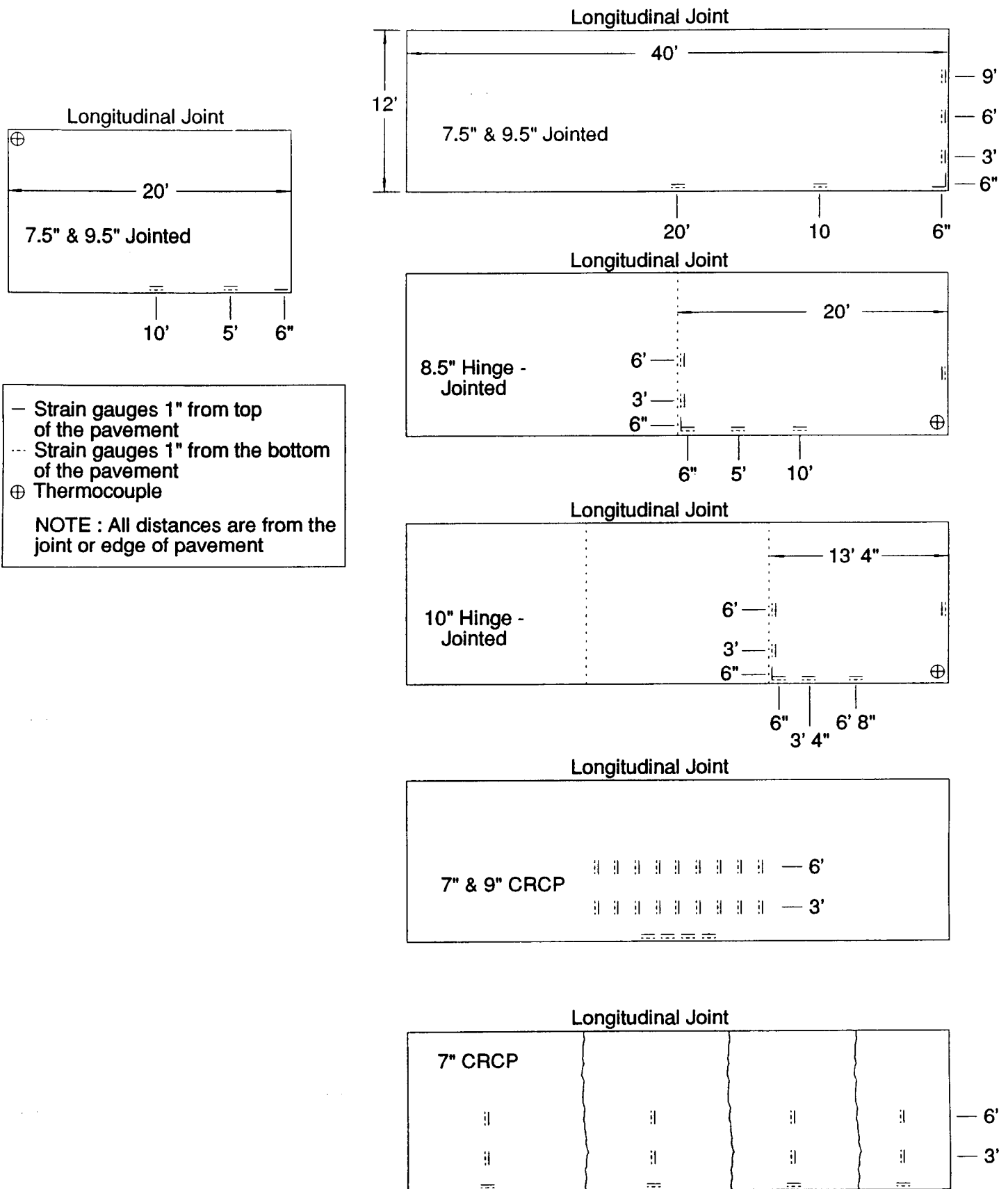


Figure 23: Project 4 Strain Gauge Location Diagrams

## Static Strain Gauge Data

### Mid-slab Longitudinal Edge Gauges

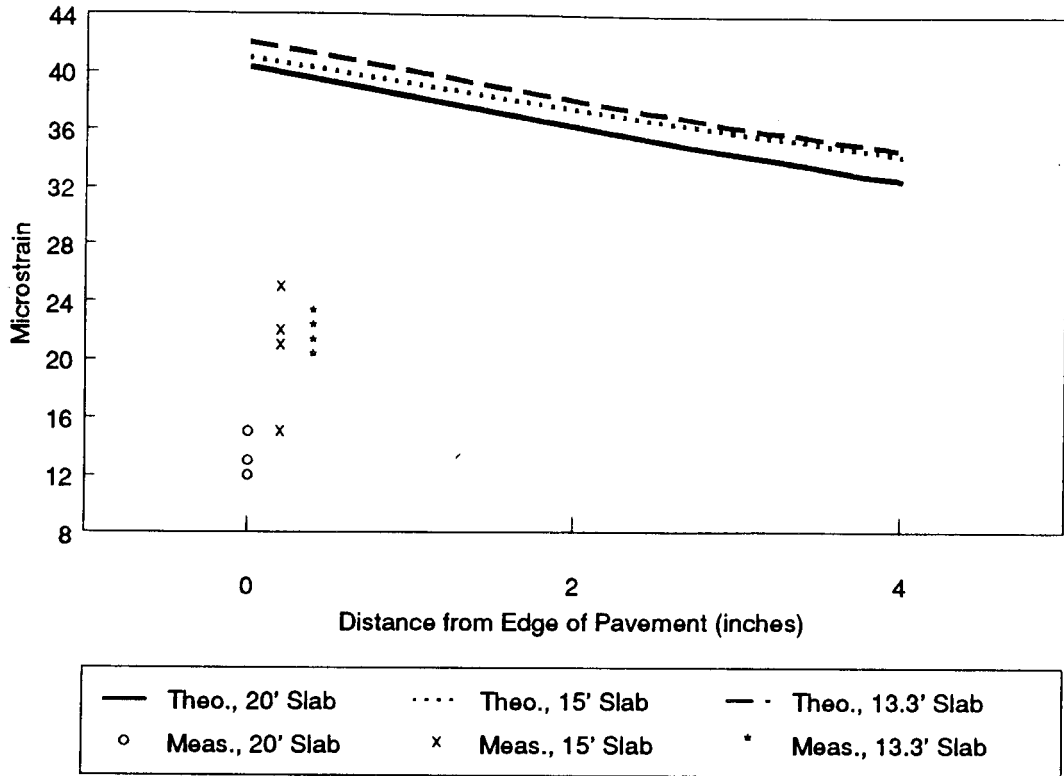


Figure 24A: Sample Static Strain Gauge Data for Longitudinal Edge Gauges

## Static Strain Gauge Data

### Transverse Gauges (36" from EOP)

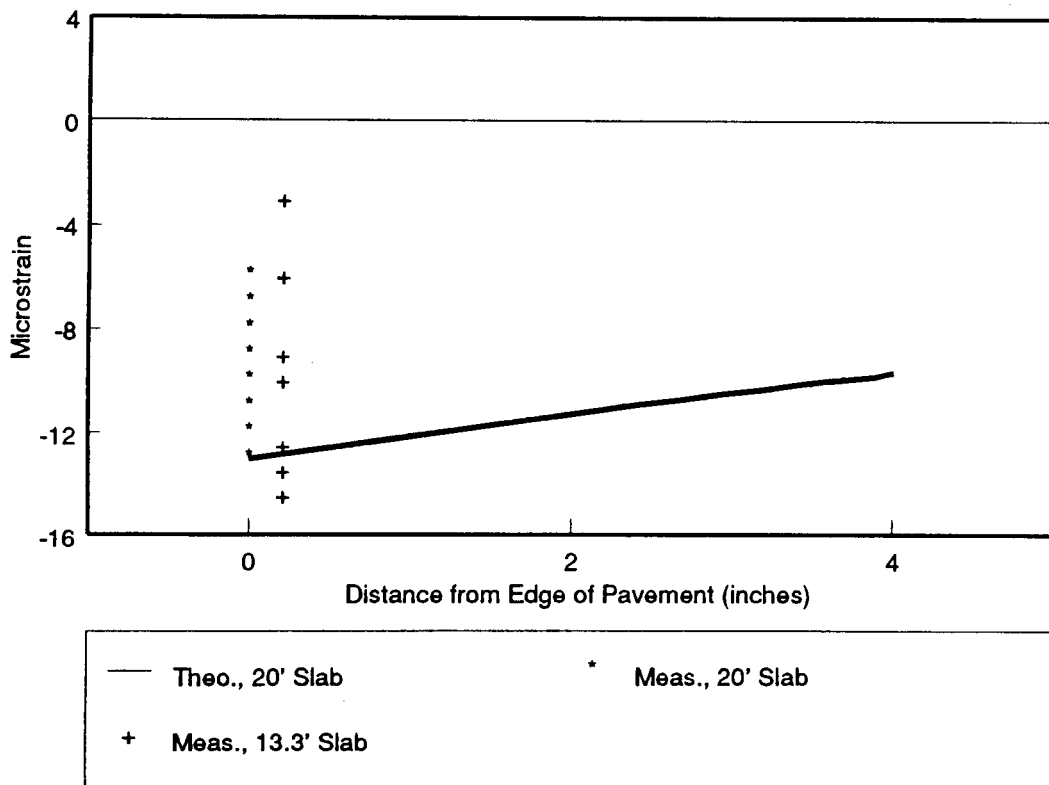


Figure 24B: Sample Static Strain Gauge Data for Transverse Edge Gauges

## Dynamic Data Comparison (3 vs 40 mph)

### Mid-slab Longitudinal Edge Gauges

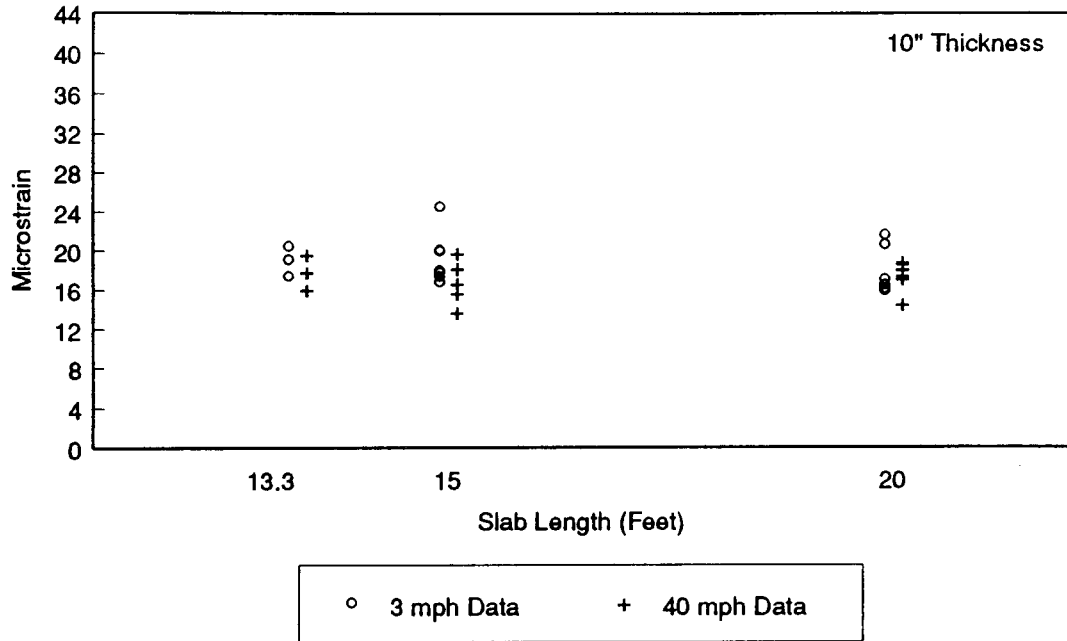


Figure 25A: Dynamic Strain Gauge Data Test Speed Comparison - Mid-Slab Longitudinal Gauges

## Dynamic Data Comparison (3 vs 40 mph)

### Transverse Gauges (36" from EOP)

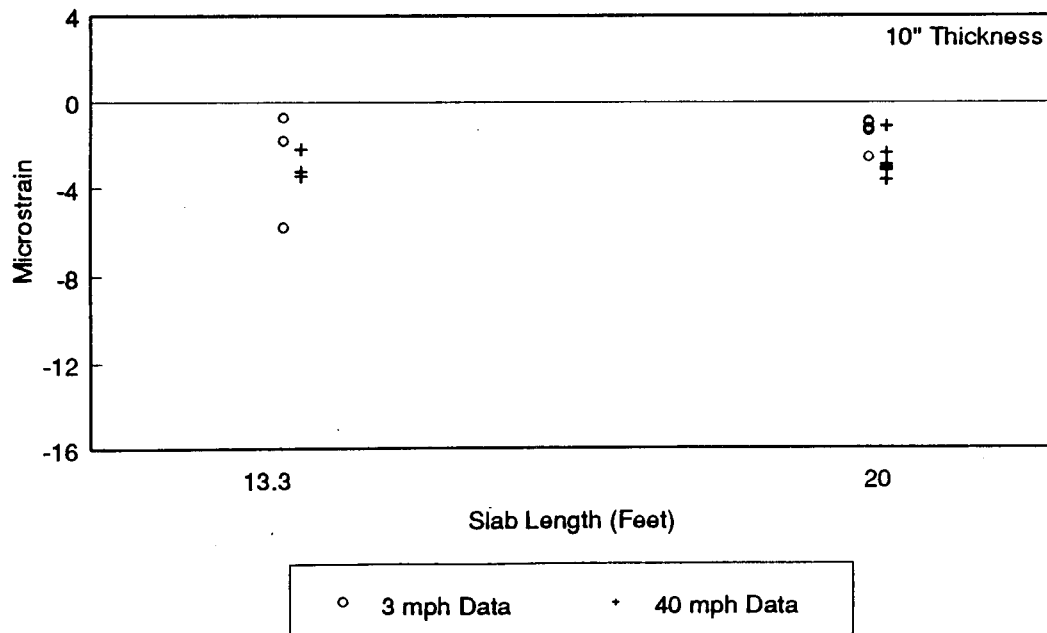


Figure 25B: Dynamic Strain Gauge Data Test Speed Comparison - Transverse Gauges



**STA. 3432 1986 Morning Test @ 40 MPH  
Midslab Gauge in 7.5" JRCP W/20' JTS.**

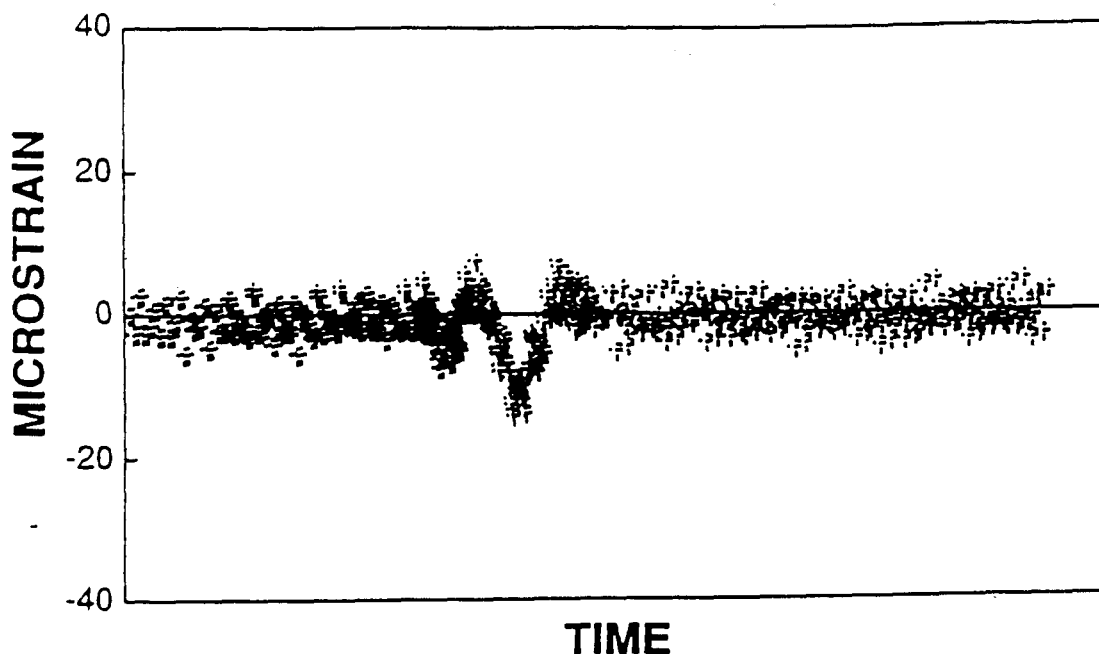


Figure 26A: Typical 1986 Strain Gauge Dynamic Test Data

**STA. 3432 1989 Morning Test @ 40 MPH  
Midslab Gauge in 7.5" JRCP W/20' JTS.**

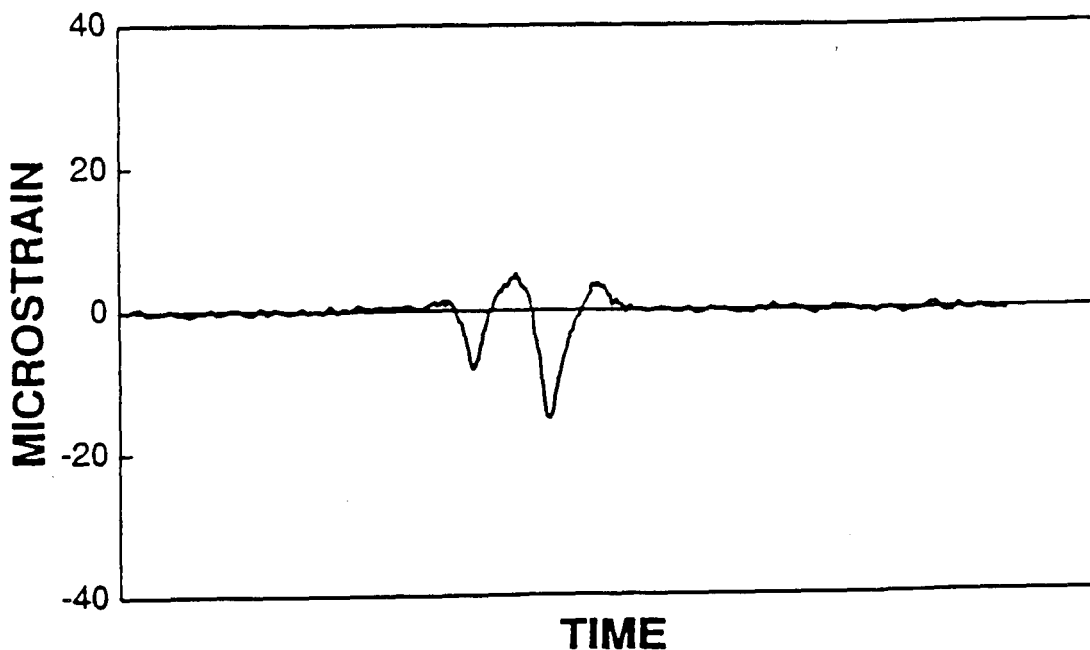


Figure 26B: Typical 1989 Strain Gauge Dynamic Test Data

# Static vs. Dynamic Data Comparison

## Mid-slab Longitudinal Edge Gauges

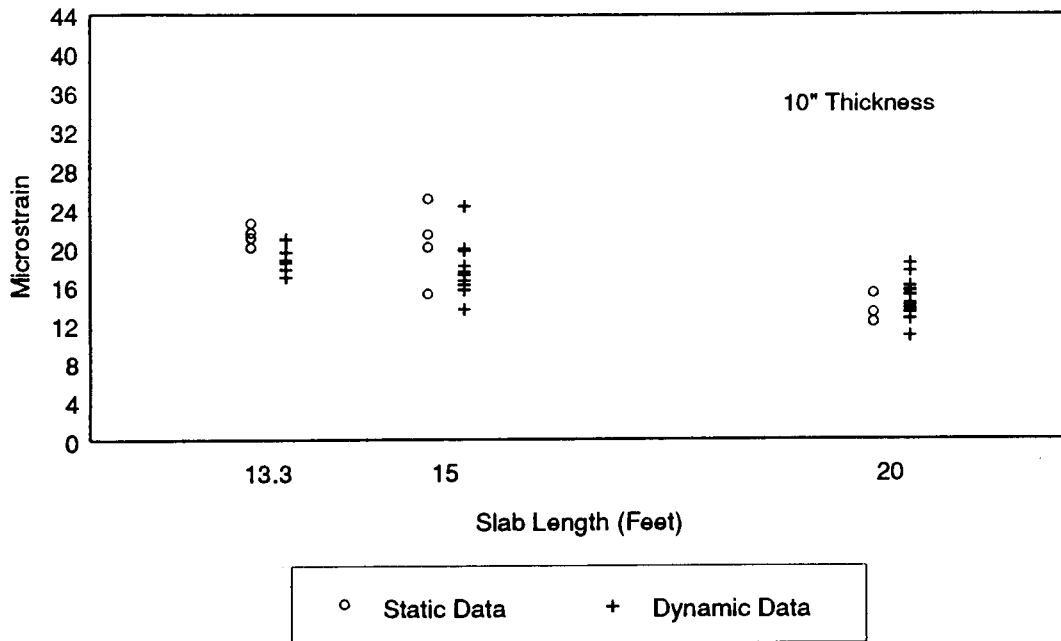


Figure 27A: Static vs. Dynamic Data Comparison for Longitudinal Gauges

# Static vs. Dynamic Data Comparison

## Transverse Gauges (36" from EOP)

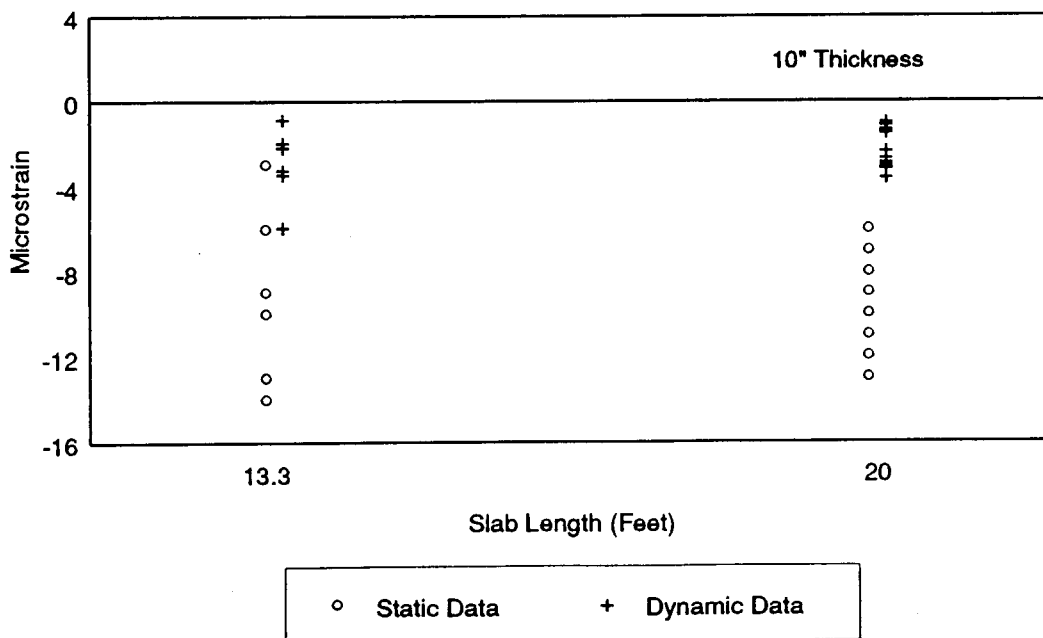


Figure 27B: Static vs. Dynamic Data Comparison for Transverse Gauges

## Gauge Depth Effects

On Theoretical Strain Values  
Longitudinal Gauge - 20' Slab

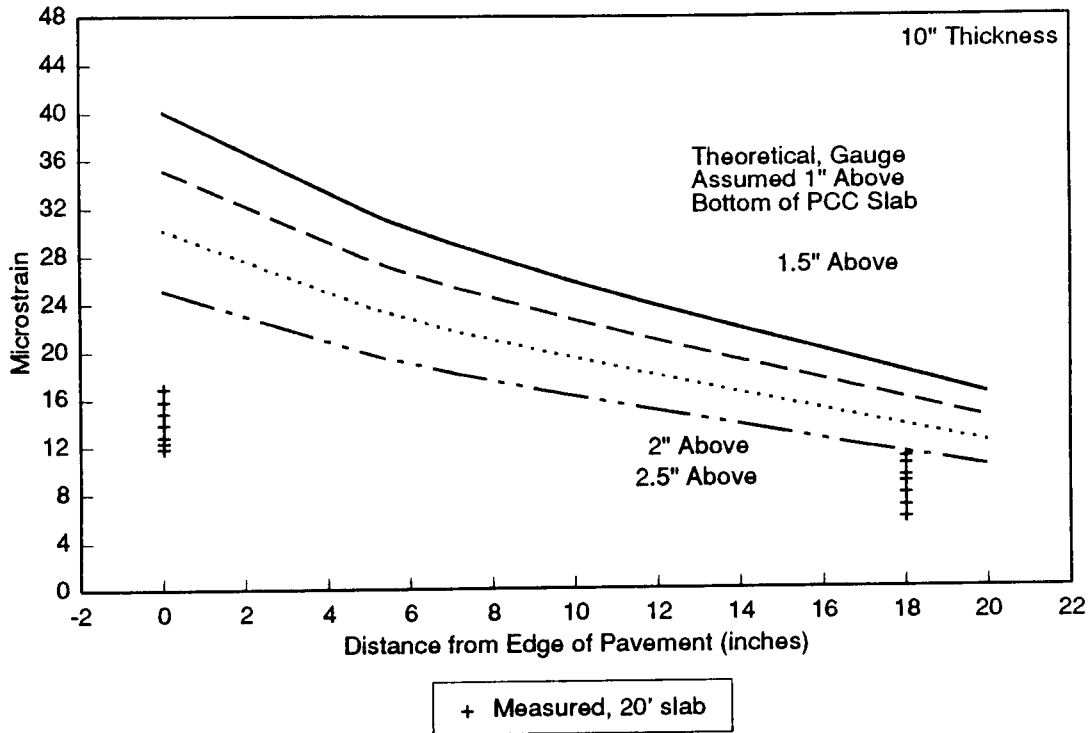


Figure 28: Gauge Depth Effects on Theoretical Strain Values

## Increased E & k Effects

On Theoretical Strain Values  
Longitudinal Gauge - 20' slab

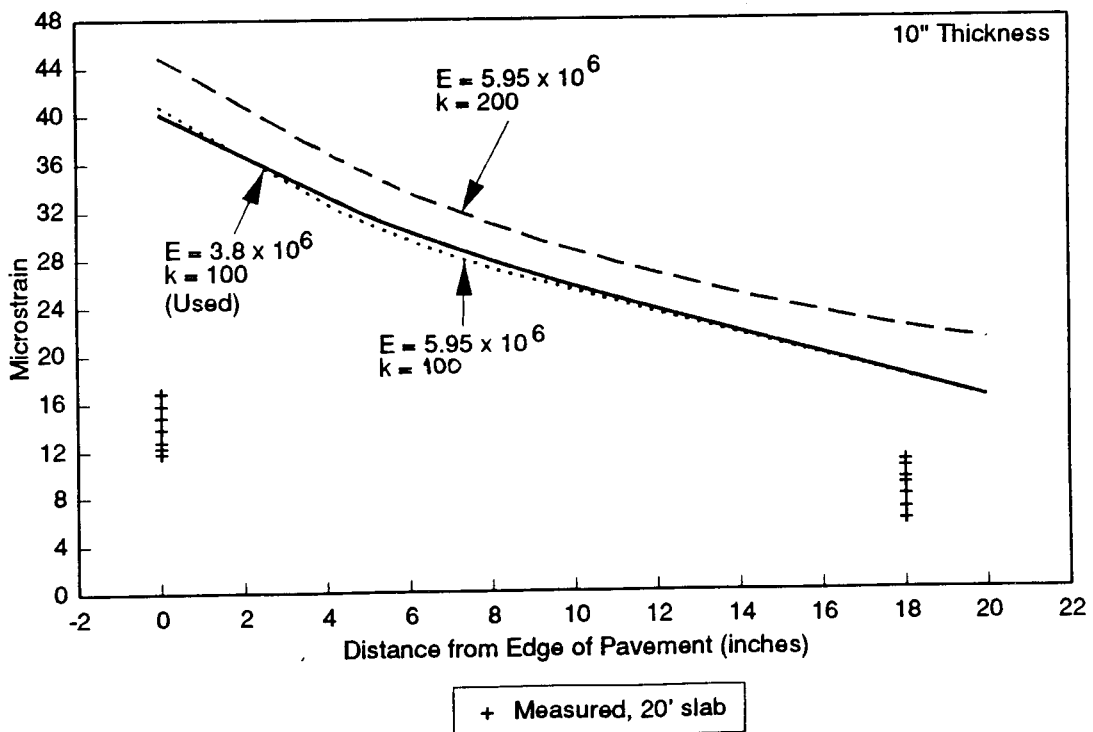


Figure 29: Increased  $E_{pcc}$  and  $k$  Effects on Theoretical Strain Values

# Shoulder Load Transfer Effects

On Theoretical Strain Values  
Longitudinal, 20' slab

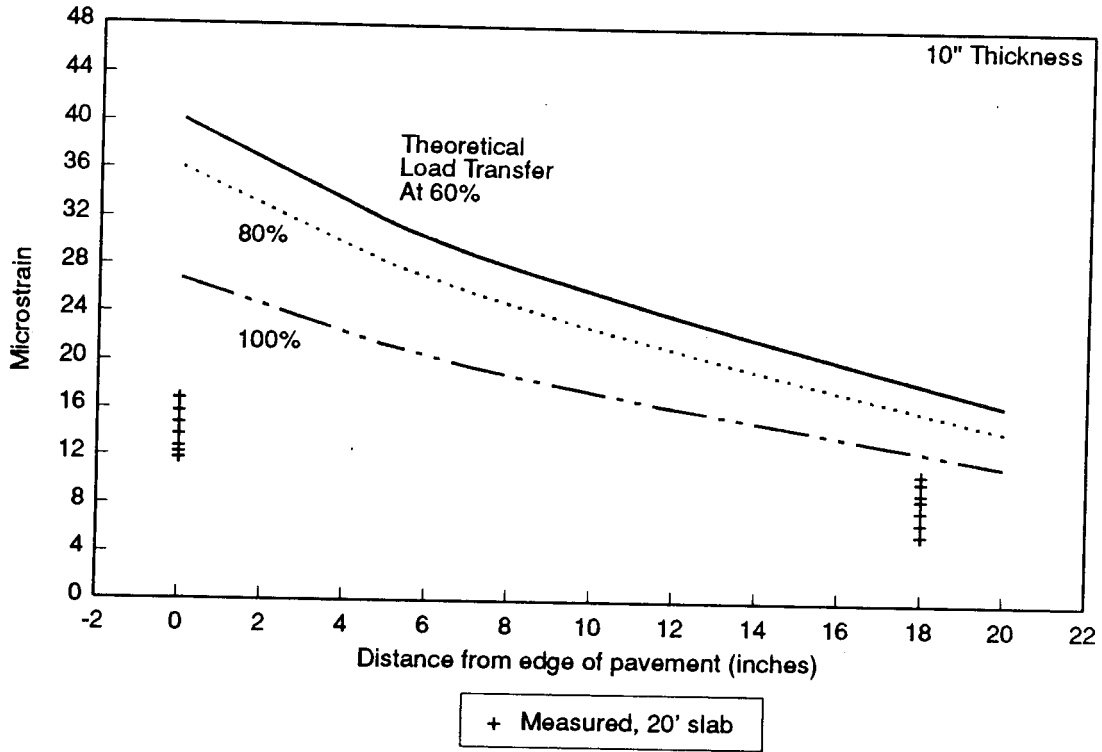


Figure 30: Load Transfer Effects on Theoretical Strain Values

# Unbonded vs. Bonded Effects

On Theoretical Strain Values  
Longitudinal, 20' slab

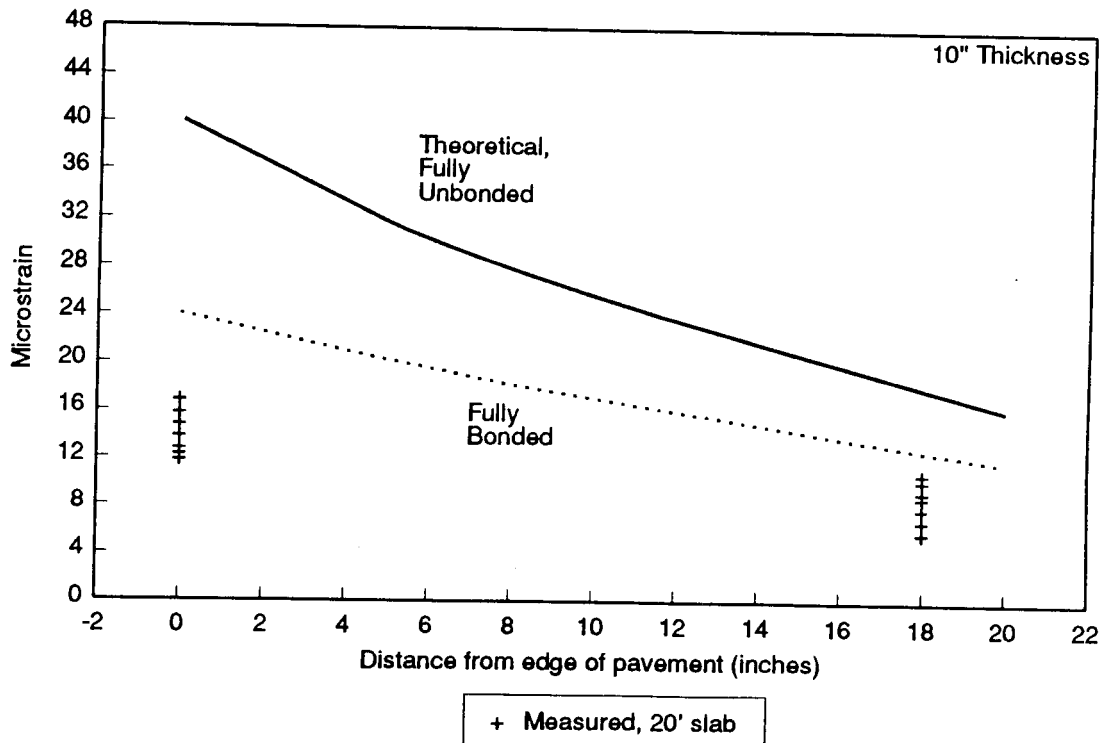


Figure 31: Bonding Effects on Theoretical Strain Values

## Strain Comparison 1

Mid-Slab Longitudinal Edge Gauges

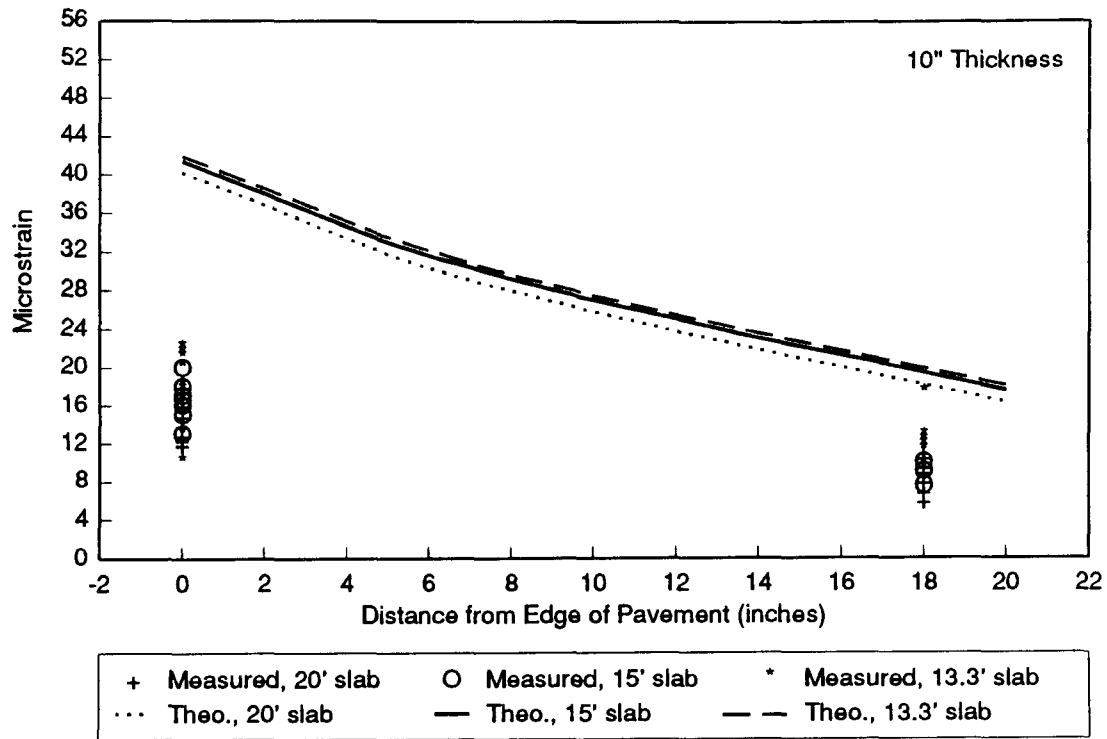


Figure 32A: Strain Data for Mid-slab Gauges in 10-inch Jointed PCC

## Strain Comparison 2

Mid-Slab Longitudinal Edge Gauges

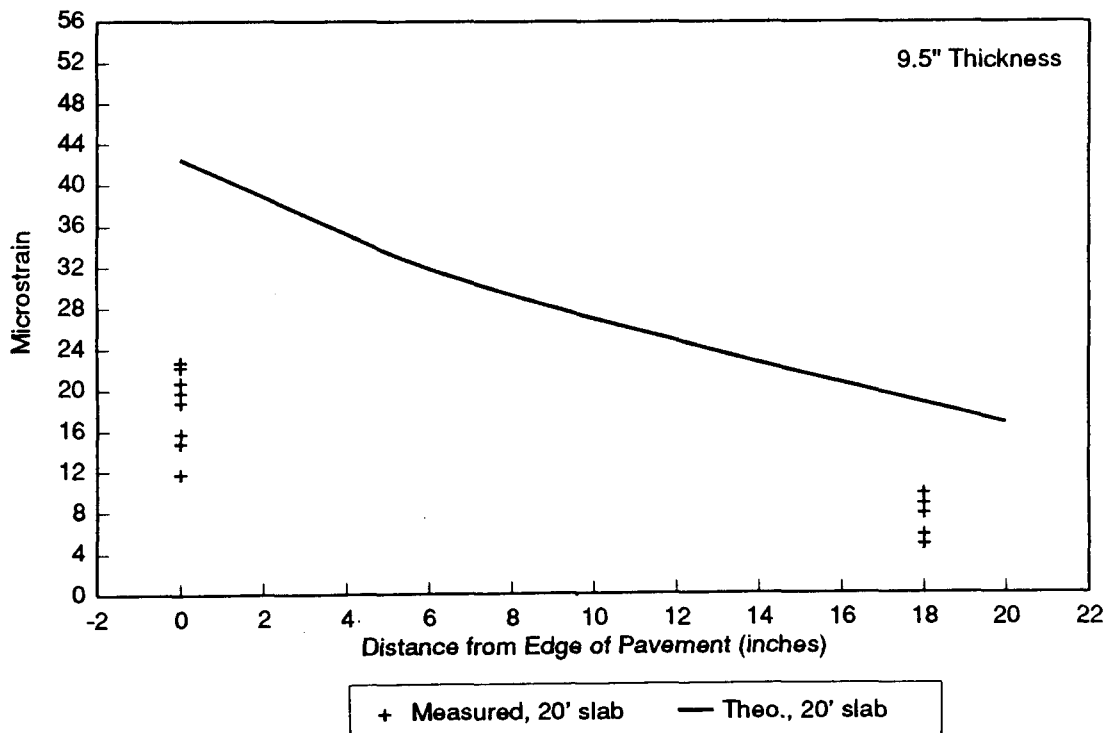


Figure 32B: Strain Data for Mid-slab Gauges in 9.5-inch Jointed PCC

### Strain Comparison 3

Mid-Slab Longitudinal Edge Gauges

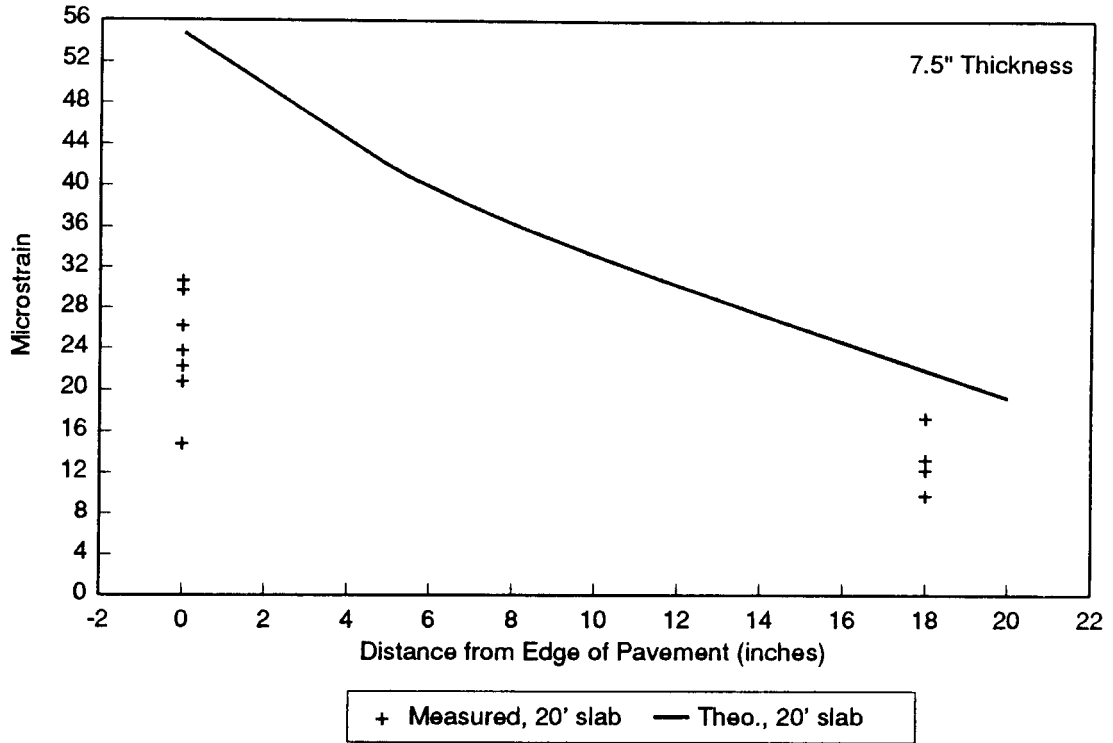


Figure 32C: Strain Data for Mid-slab Gauges in 7.5-inch Jointed PCC

### Strain Comparison 4

Quarter-Slab Longitudinal Edge Gauges

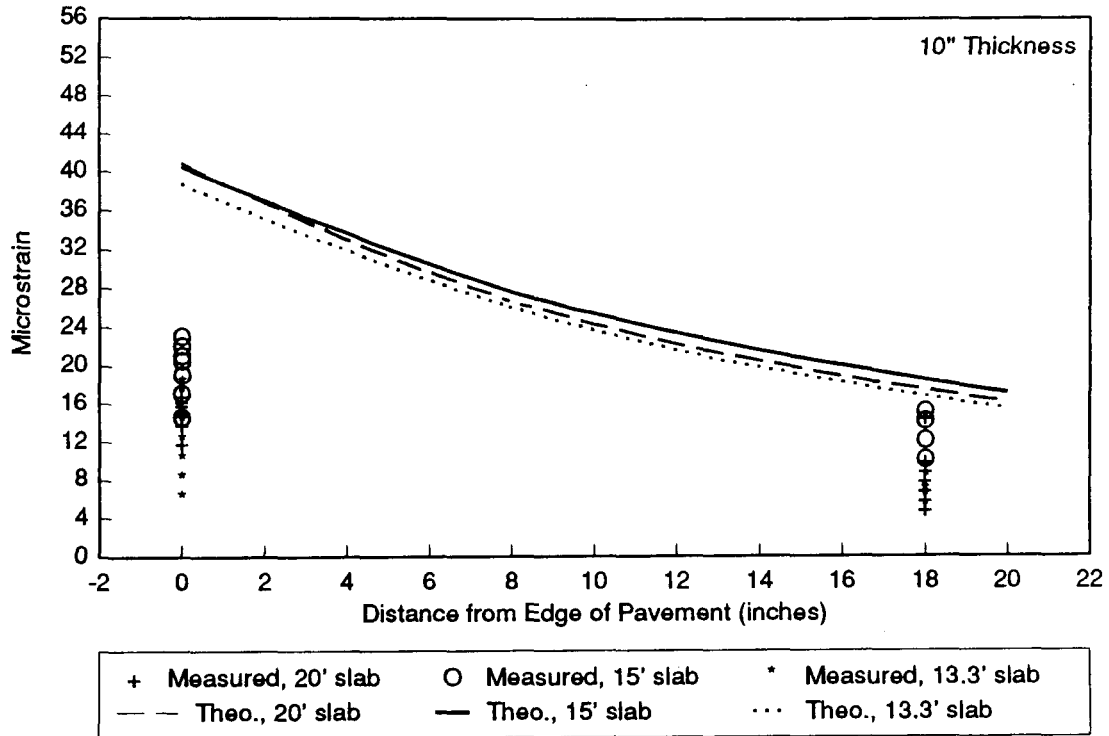


Figure 33A: Strain Data for Quarter-slab Gauges in 10-inch Jointed PCC

### Strain Comparison 5

Quarter-Slab Longitudinal Edge Gauges

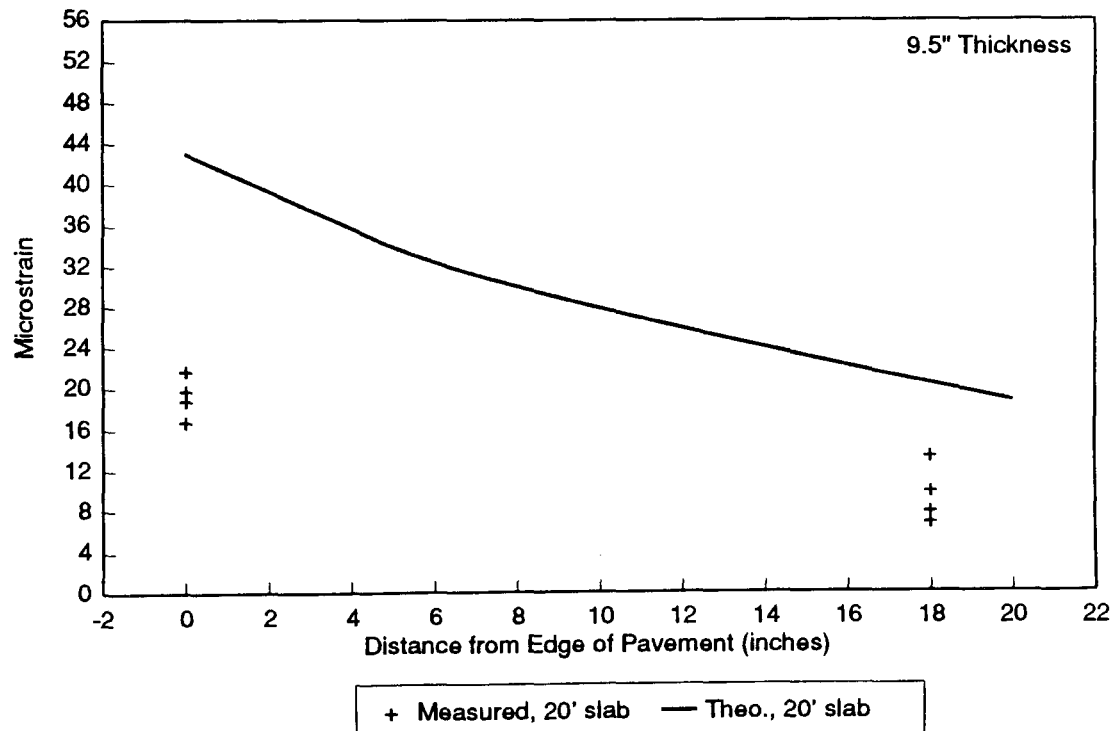


Figure 33B: Strain Data for Quarter-slab Gauges in 9.5-inch Jointed PCC

# Strain Comparison 6

Quarter-Slab Longitudinal Edge Gauges

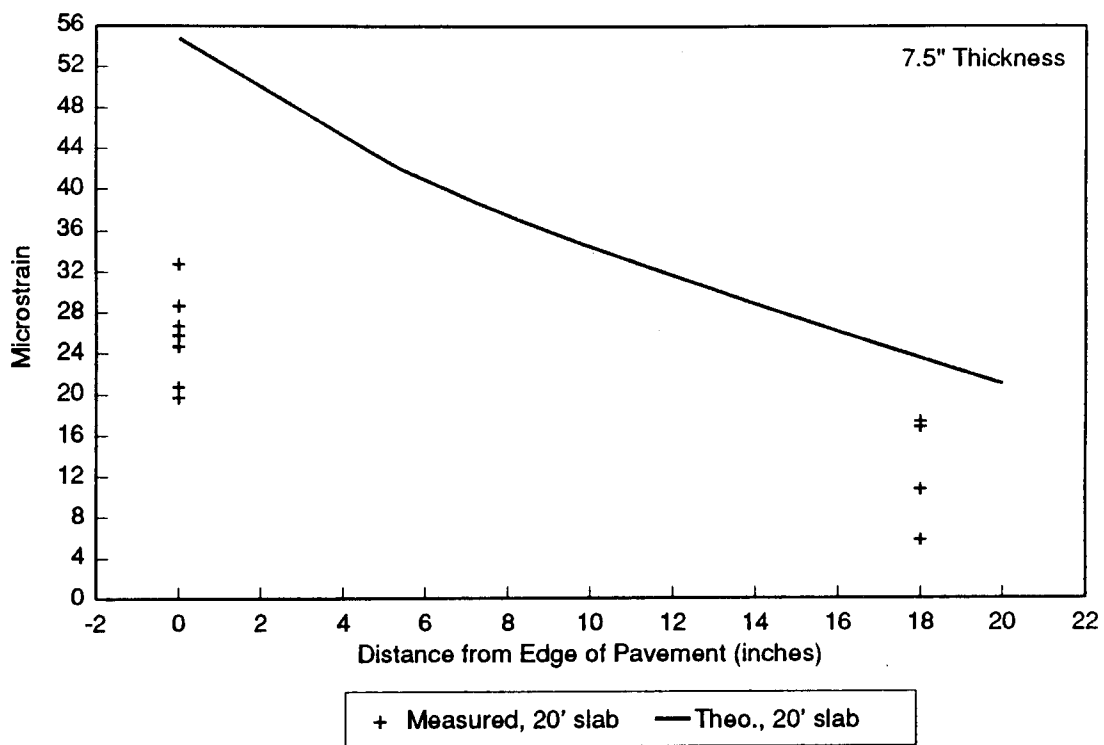


Figure 33C: Strain Data for Quarter-slab Gauges in 7.5-inch Jointed PCC



### Strain Comparison 7 Slab Corner Gauges

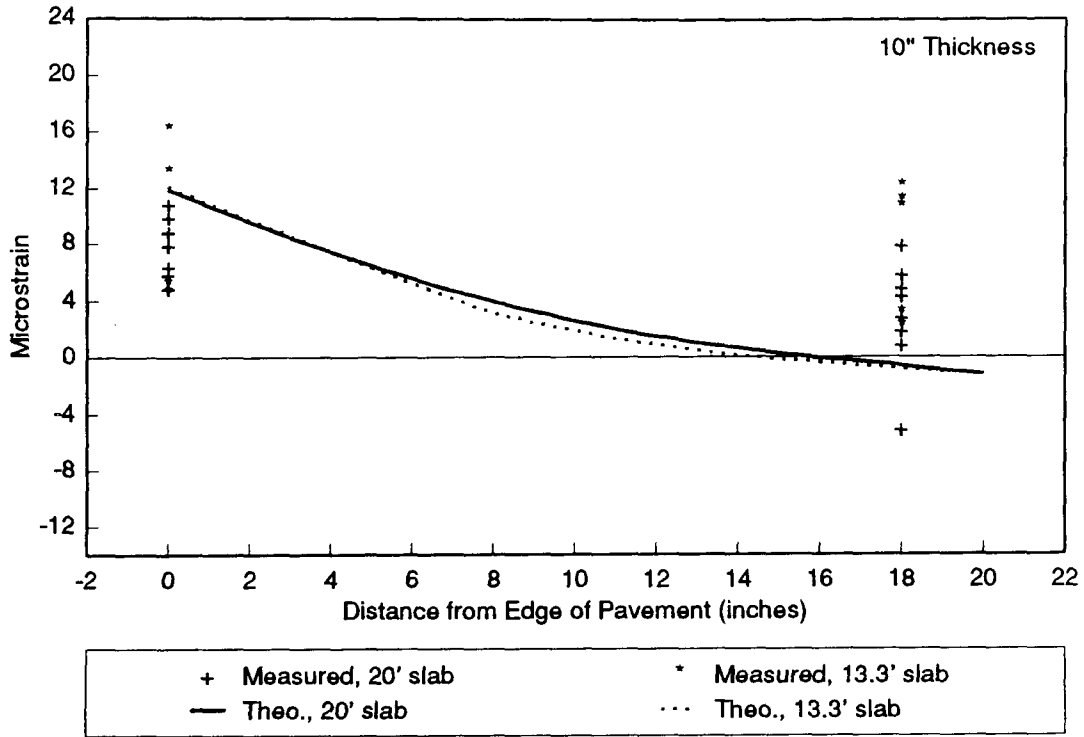


Figure 34A: Strain Data for Corner Gauges in 10-inch Jointed PCC

### Strain Comparison 8 Slab Corner Gauges

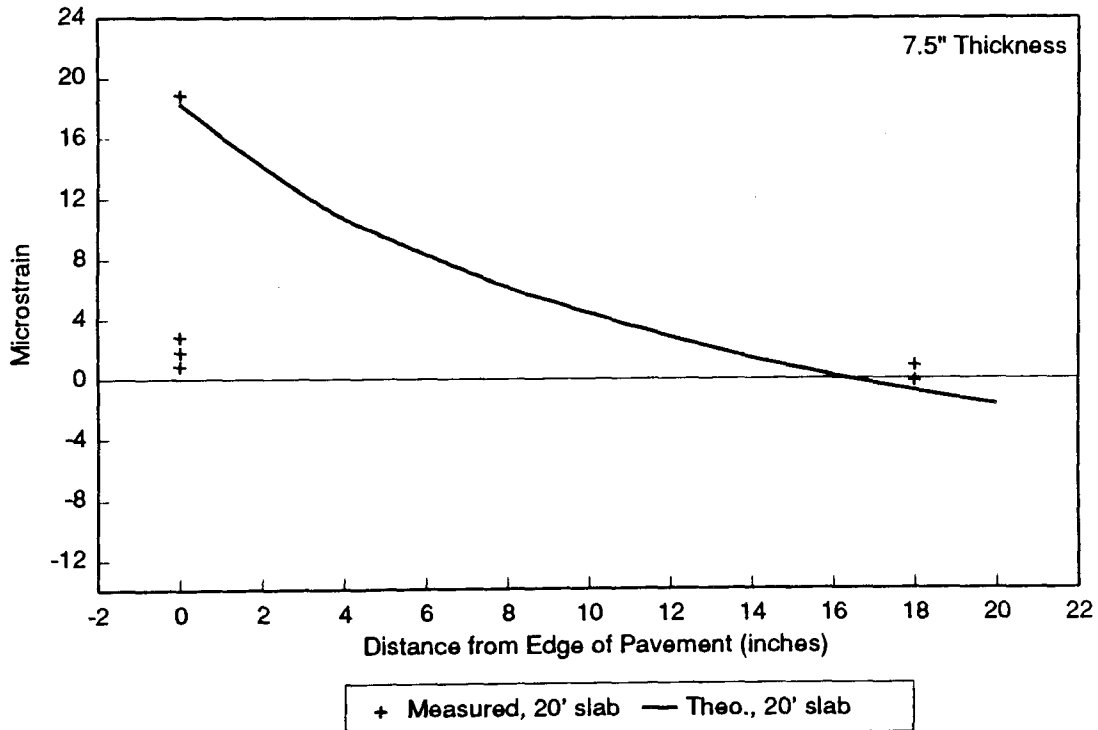


Figure 34B: Strain Data for Corner Gauges in 7.5-inch Jointed PCC

### Strain Comparison 9

Transverse Edge Gauges (6" from EOP)

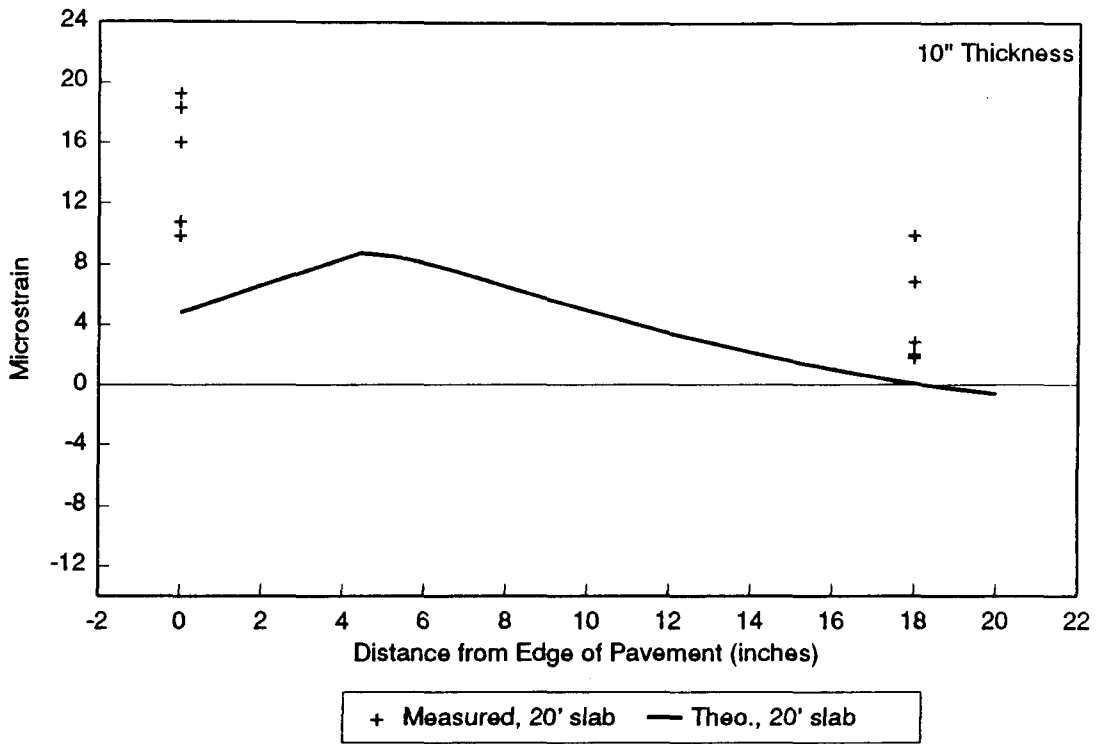


Figure 34C: Strain Data for Transverse Edge Gauges in 10-inch Jointed PCC

### Strain Comparison 10

Transverse Edge Gauges (36" from EOP)

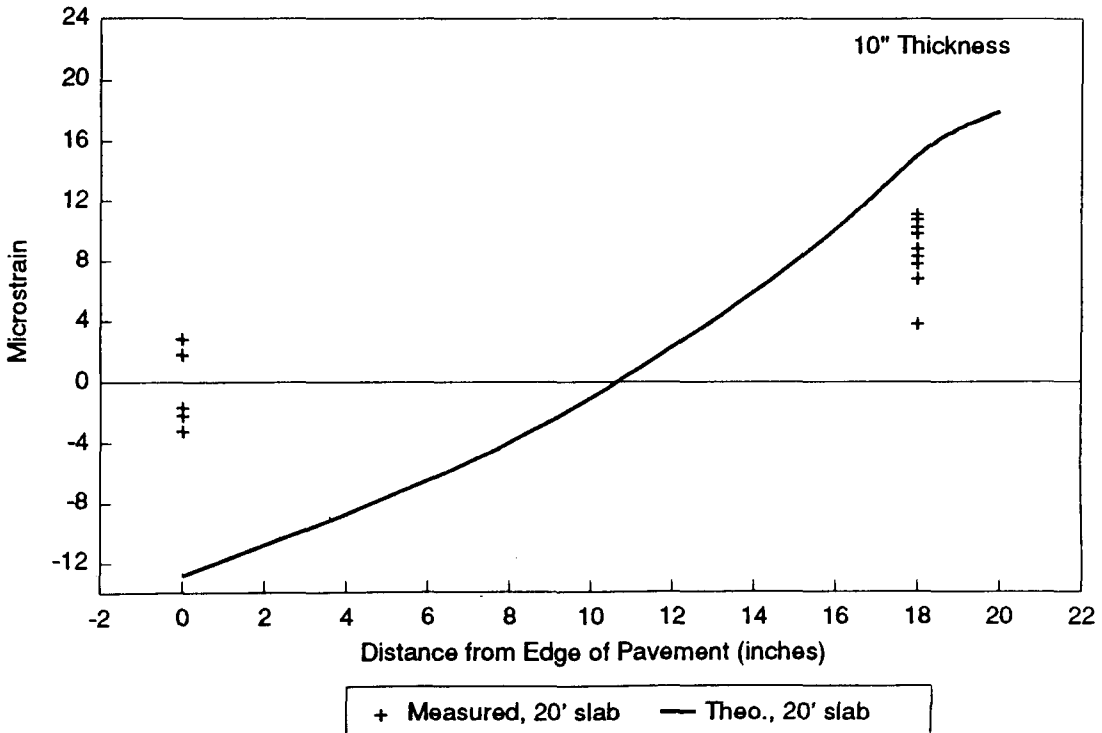


Figure 34D: Strain Data for Transverse Edge Gauges in 10-inch Jointed PCC

### Crack Spacing Effects, CRCP

On Theoretical Strain Values  
Longitudinal Edge Gauges  
Positioned Midslab, Between Joints

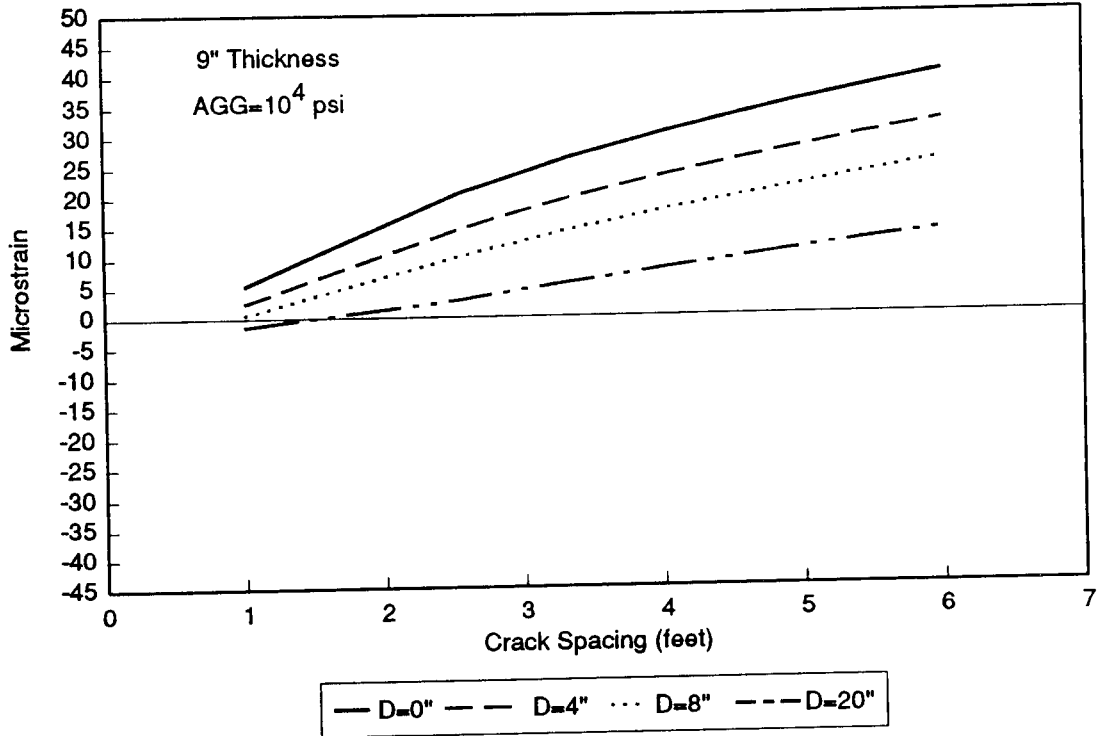


Figure 35: Effect of CRCP Crack Spacing on Longitudinal Strain Gauges

### Crack Spacing Effects, CRCP

On Theoretical Strain Values  
Transverse Edge Gauges  
Positioned 36" From EOP

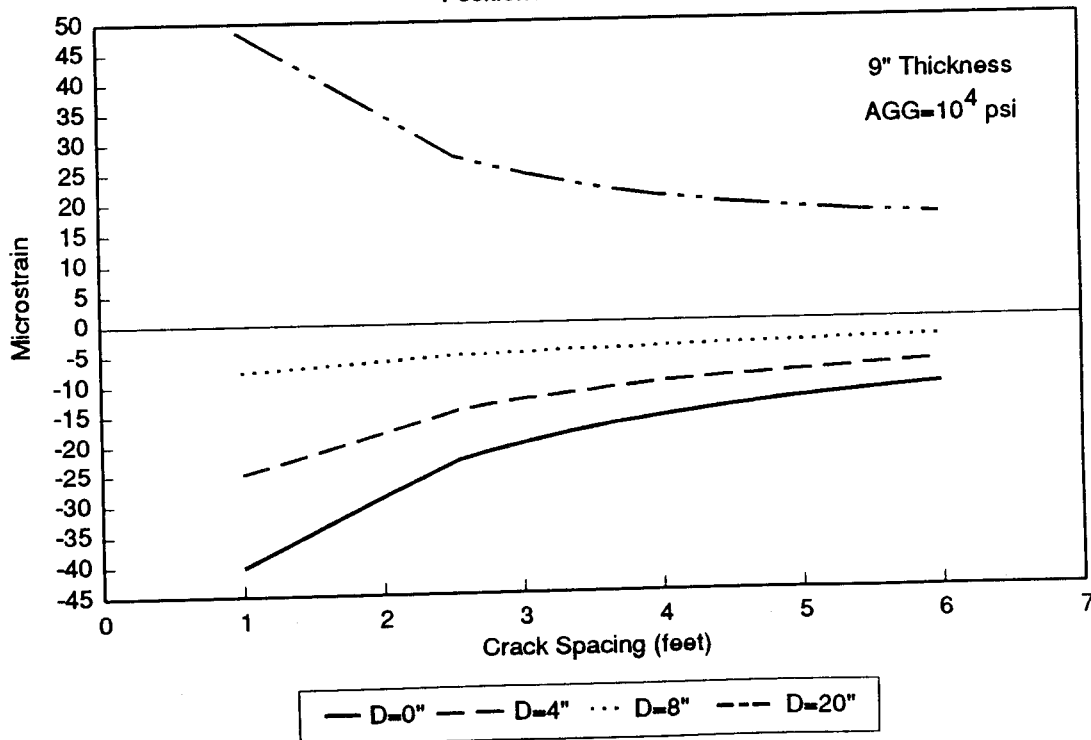


Figure 36: Effect of CRCP Crack Spacing on Transverse Strain Gauges

## Strain Comparison 11, CRCP

Longitudinal Edge Gauges (between cracks)

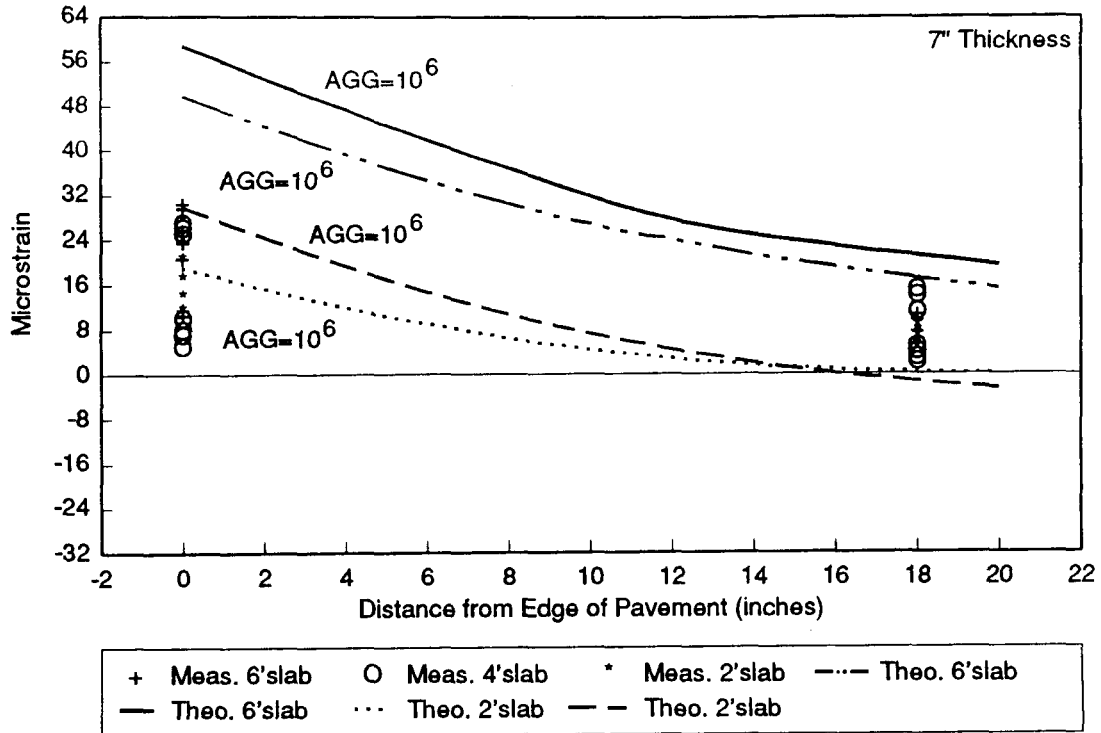


Figure 37A: Strain Data for Longitudinal Edge Gauges in 7-inch CRCP

## Strain Comparison 12, CRCP

Longitudinal Edge Gauges (cracking unknown)

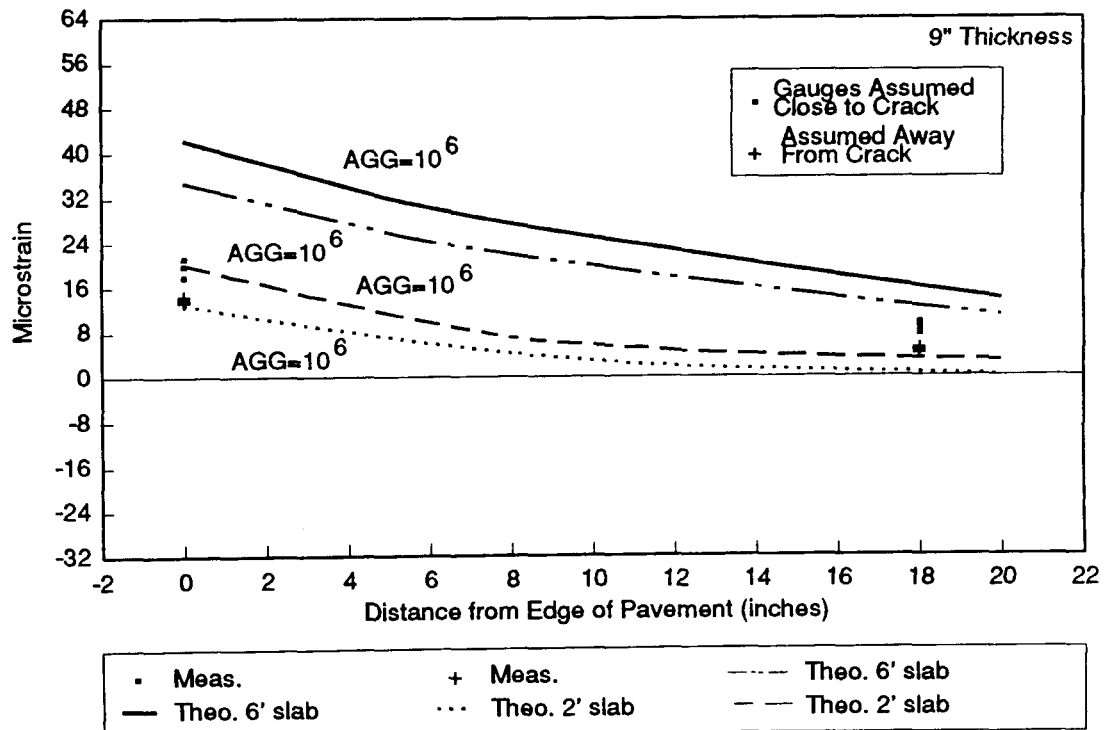
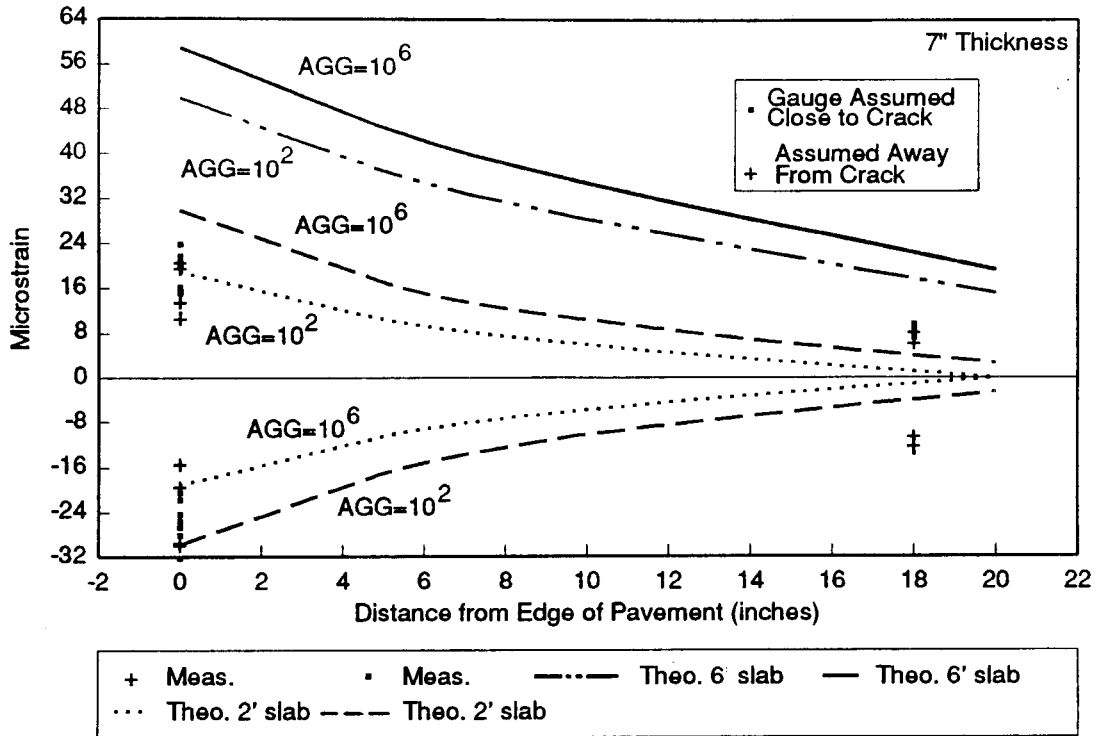


Figure 37B: Strain Data for Longitudinal Edge Gauges in 9-inch CRCP

# Strain Comparison 13, CRCP

Longitudinal Edge Gauges (cracking unknown)



Note: Top gauge strains are greater, thus closer to the theoretical values

Figure 37C: Strain Data for Longitudinal Edge Gauges in 7-inch CRCP

## Strain Comparison 14, CRCP

Transverse Gauges (36" from EOP)  
Positioned Between Cracks

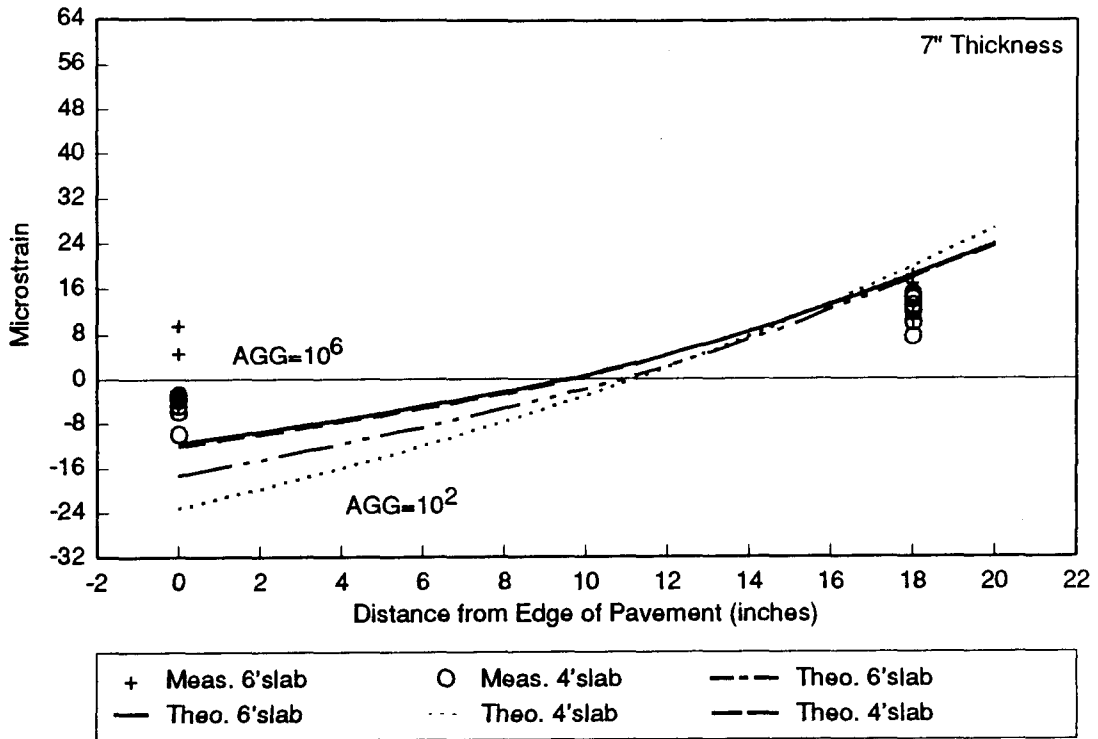


Figure 38A: Strain Data for Transverse Gauges in 7-inch CRCP

## Strain Comparison 15, CRCP

Transverse Edge Gauges (36" from EOP)  
Position of Crack Unknown

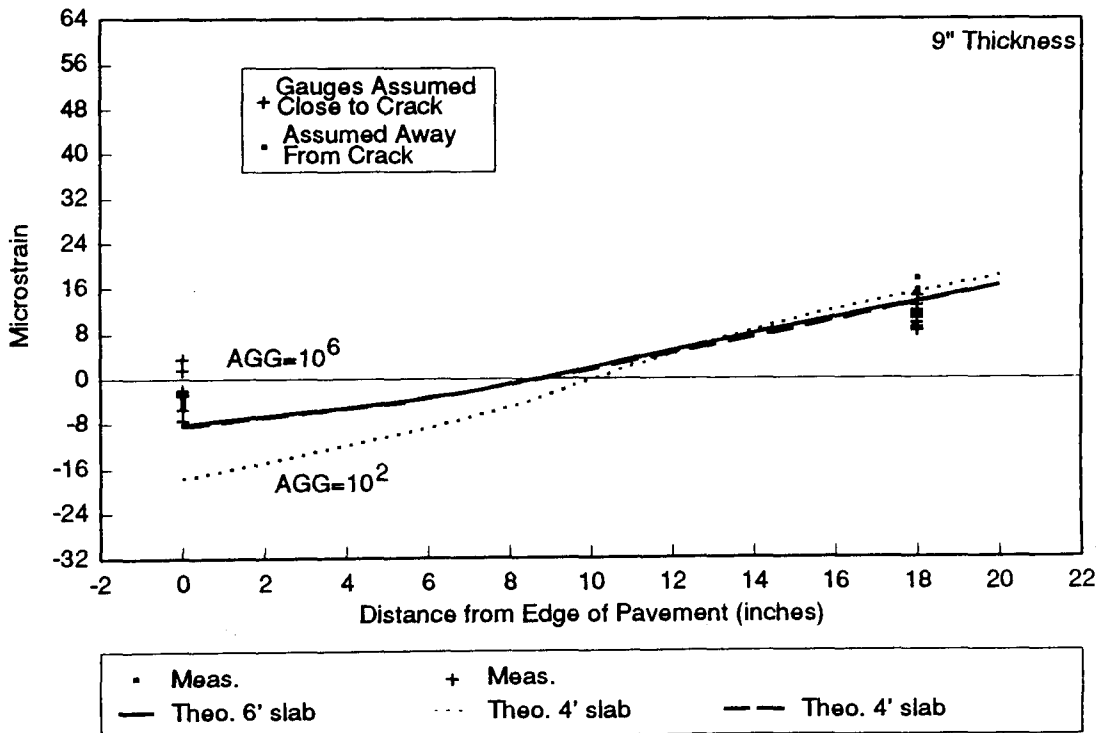


Figure 38B: Strain Data for Transverse Gauges in 9-inch CRCP

# Strain Comparison 16, CRCP

Transverse Edge Gauges (36" from EOP)  
Position of Crack Unknown

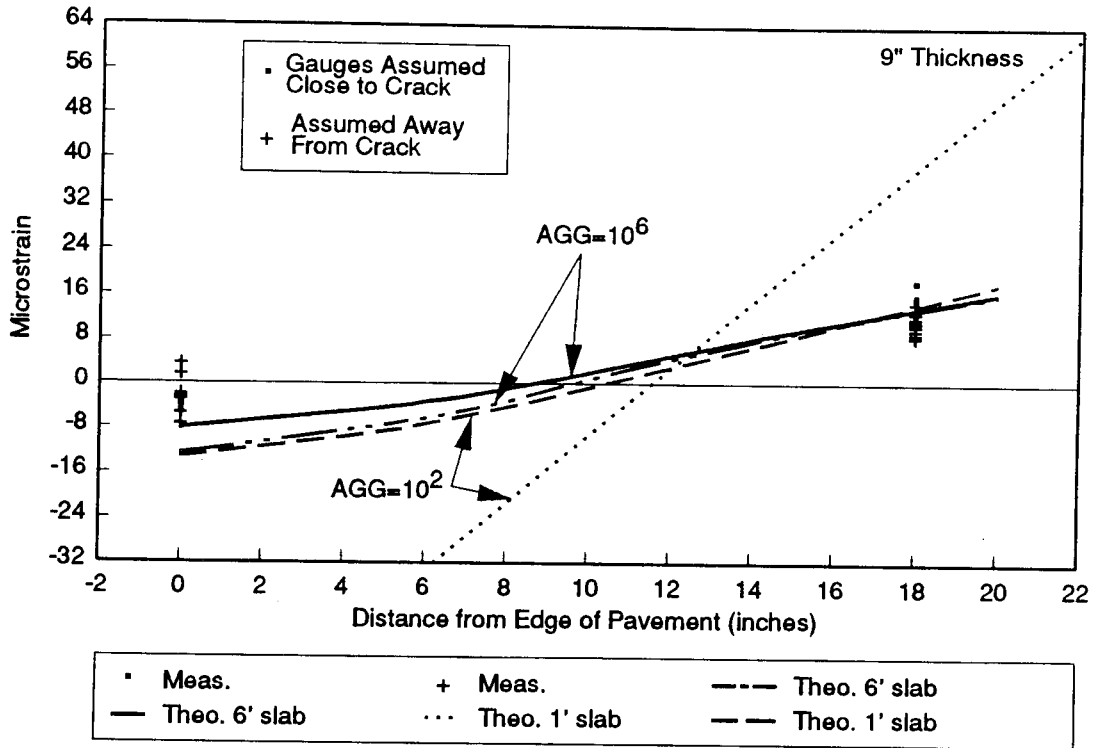


Figure 38C: Strain Data for Transverse Gauges in 9-inch CRCP

## DOWEL JOINT VS. TEMPERATURE

1989 MEASURED MOVEMENT

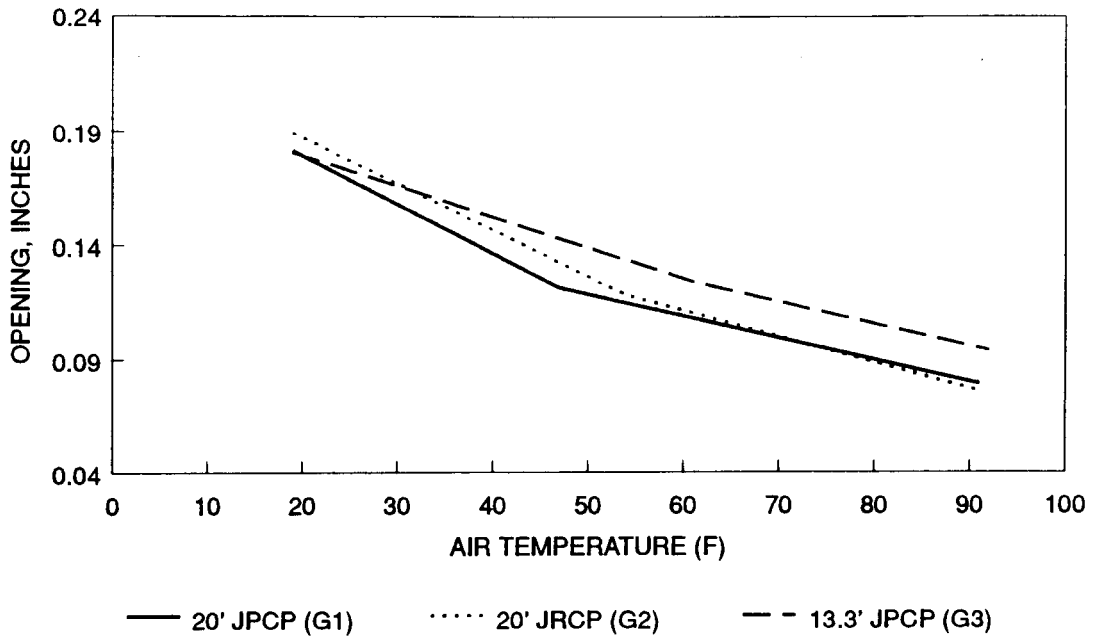


Figure 39A: Dowel Joint Opening vs. Air Temperature

## HINGE JOINT VS. TEMPERATURE

1989 MEASURED MOVEMENT

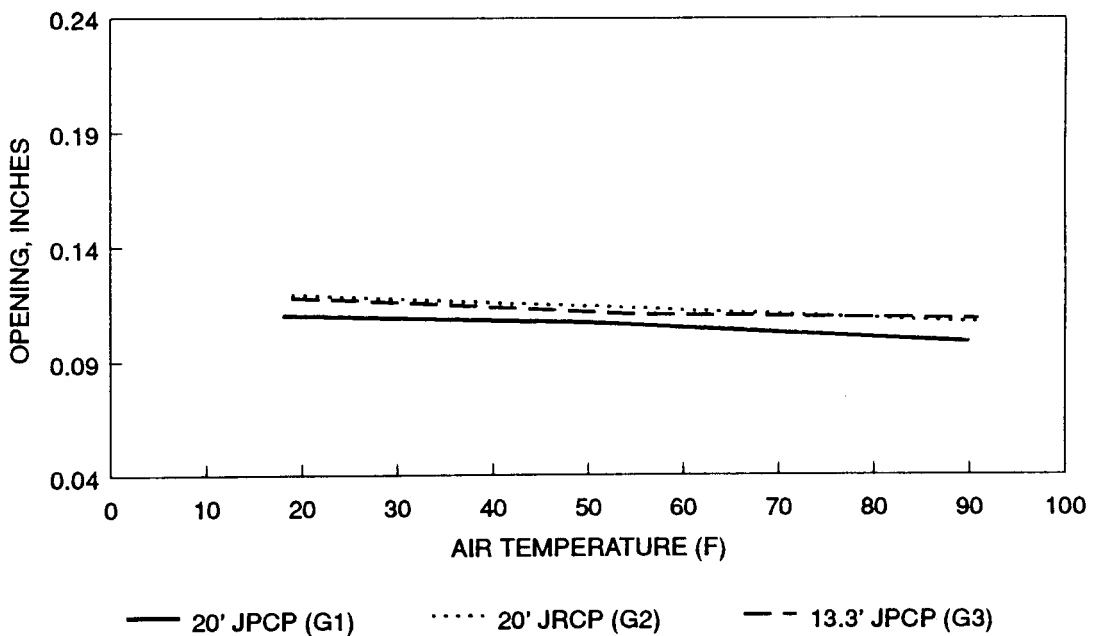


Figure 39B: Hinge Joint Opening vs. Air Temperature



## DOWEL JOINT VS. TEMPERATURE

1989 MEASURED MOVEMENT

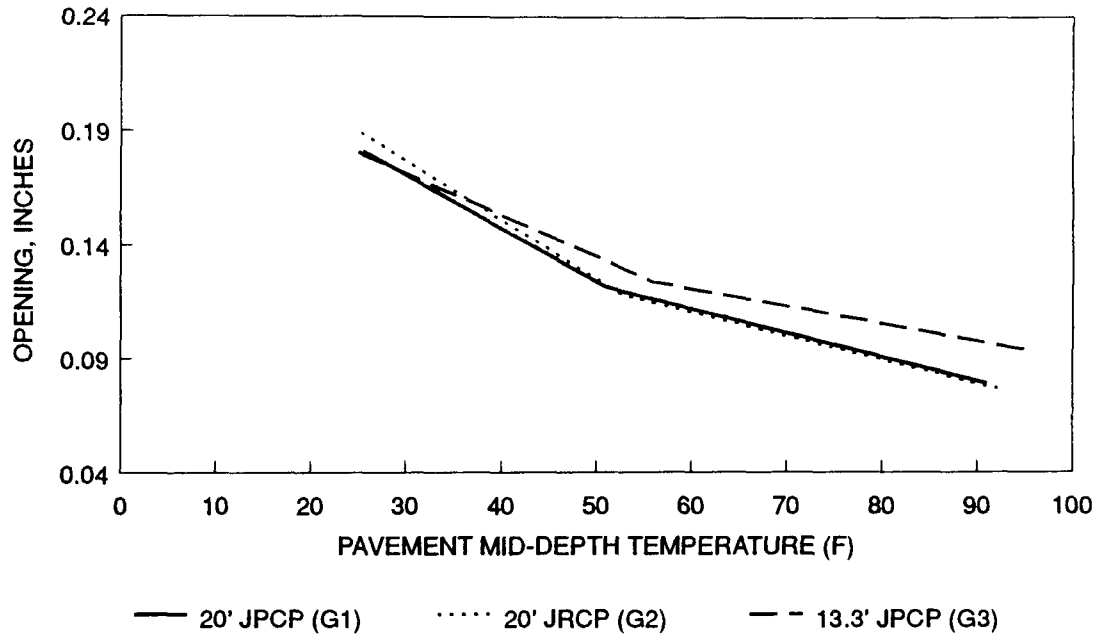


Figure 40A: Dowel Joint Opening vs. Pavement Mid-Depth Temperature

## HINGE JOINT VS. TEMPERATURE

1989 MEASURED MOVEMENT

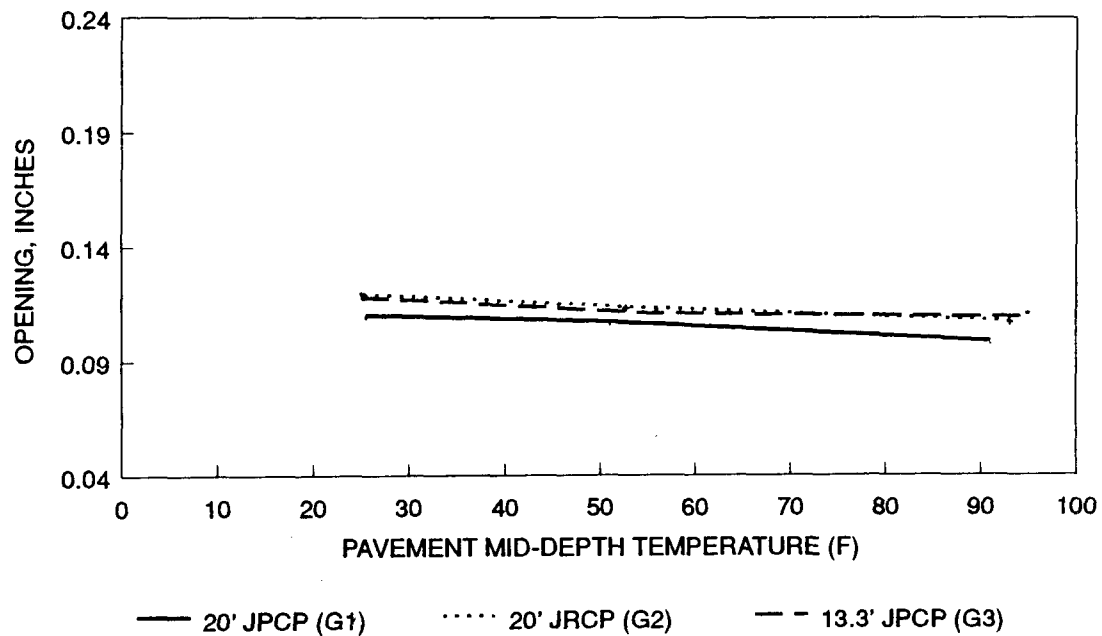
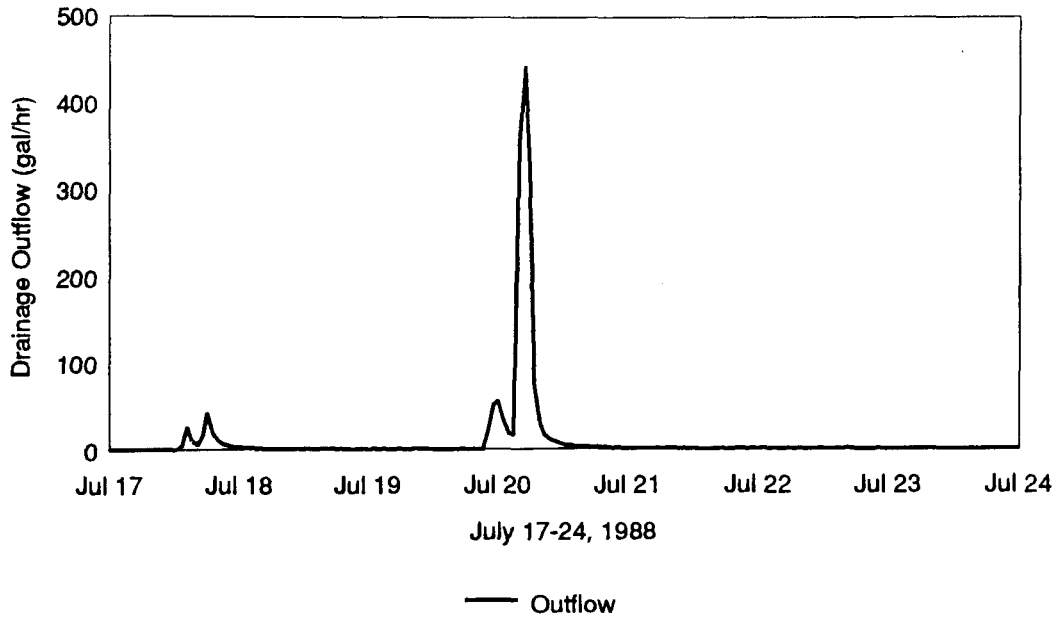


Figure 40B: Hinge Joint Opening vs. Pavement Mid-Depth Temperature

## Subdrainage Outflow and Precipitation

for 7.5" - 20' jt., with edge sealant



## Subdrainage Outflow and Precipitation

for 8.5" - 20' jt., no edge sealant

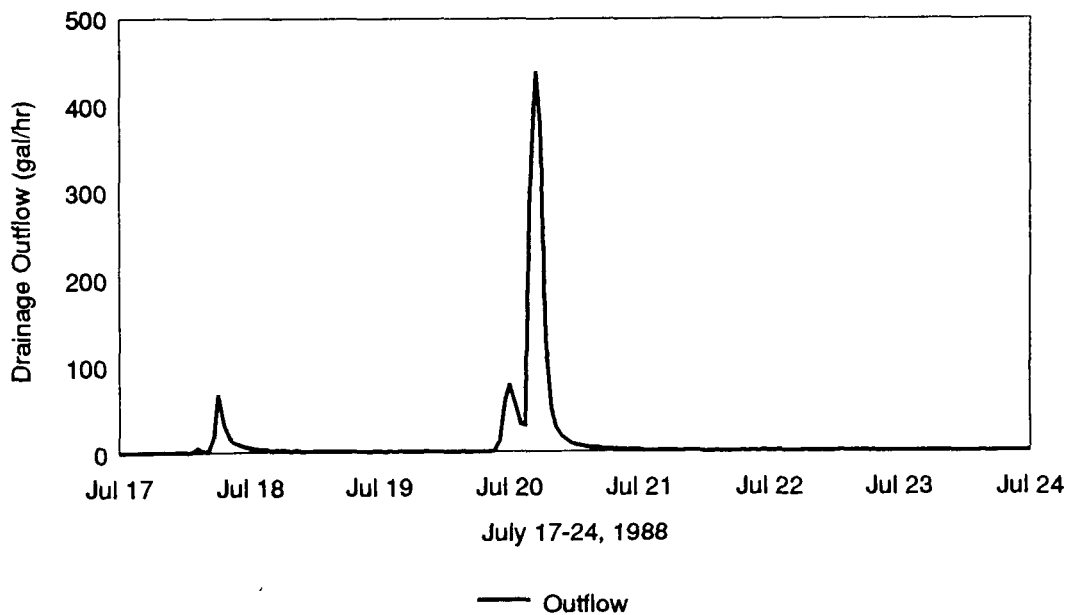
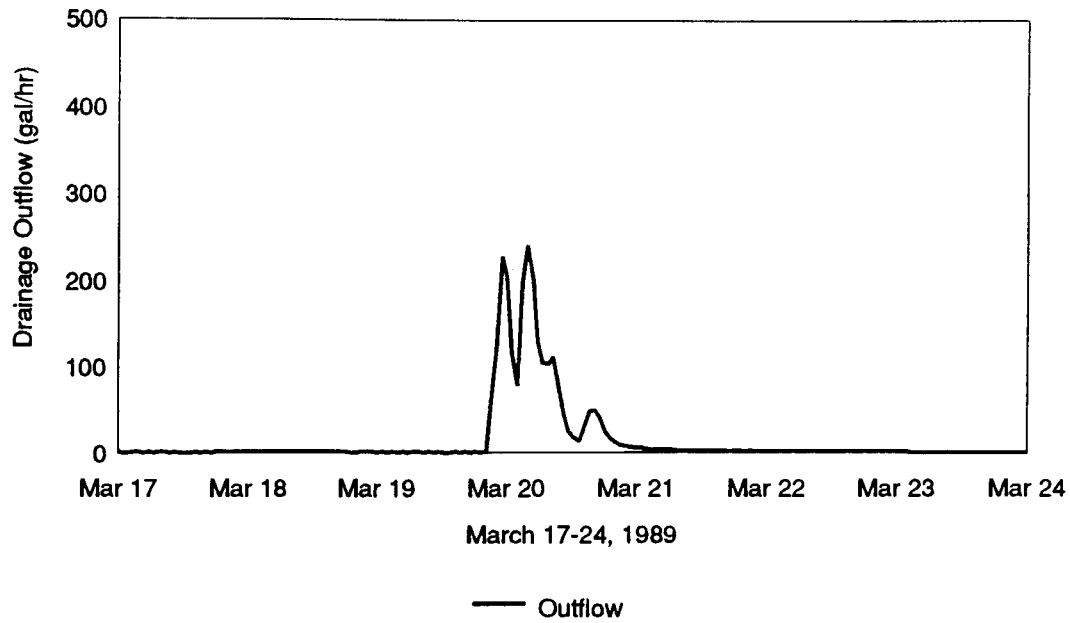


Figure 41: Graphs of Subdrainage Outflow for 20-foot Jointed PCC Test Sections July 1988

## Subdrainage Outflow and Precipitation

for 7.5" - 20' jt., with edge sealant



## Subdrainage Outflow and Precipitation

for 8.5" - 20' jt., no edge sealant

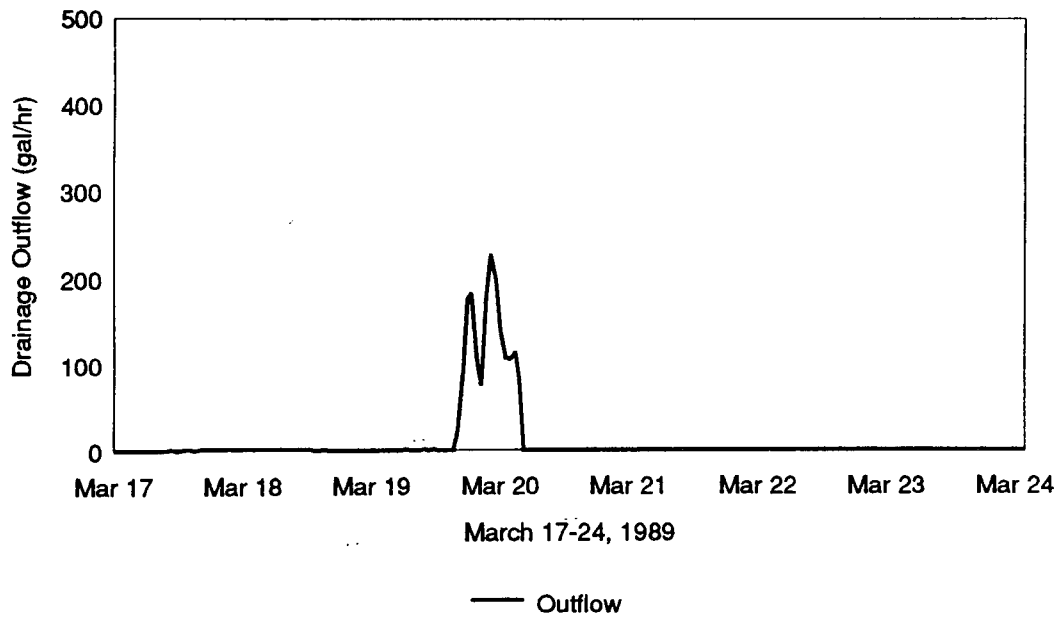
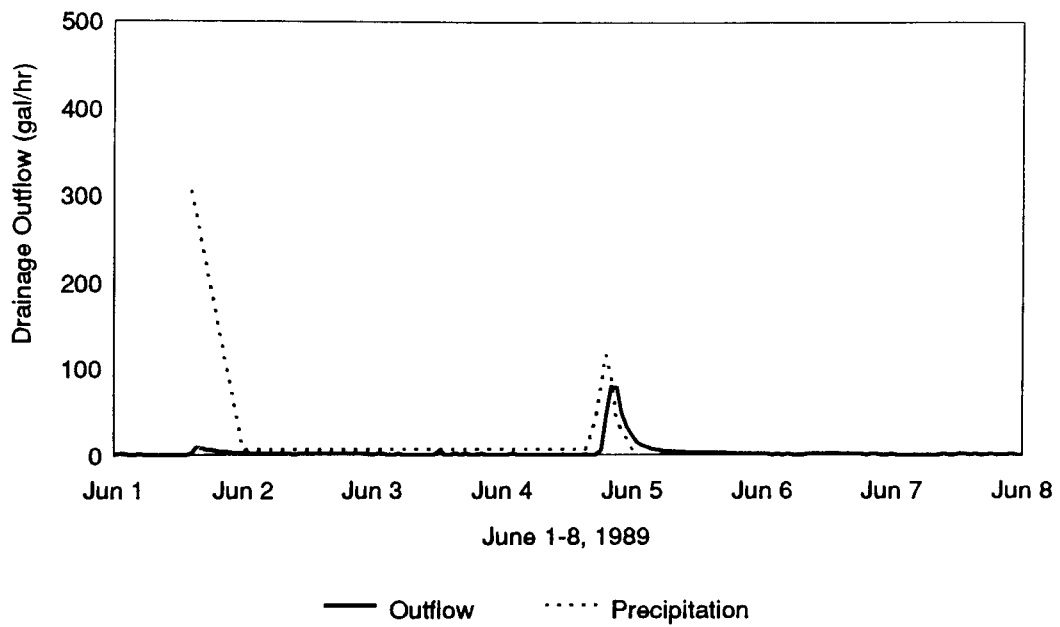


Figure 42: Graphs of Subdrainage Outflow for 20-foot Jointed PCC Test Sections - March 1989

## Subdrainage Outflow and Precipitation

for 8.5" - 40' jt., with edge sealant



## Subdrainage Outflow and Precipitation

for 8.5" - 40' jt., no edge sealant

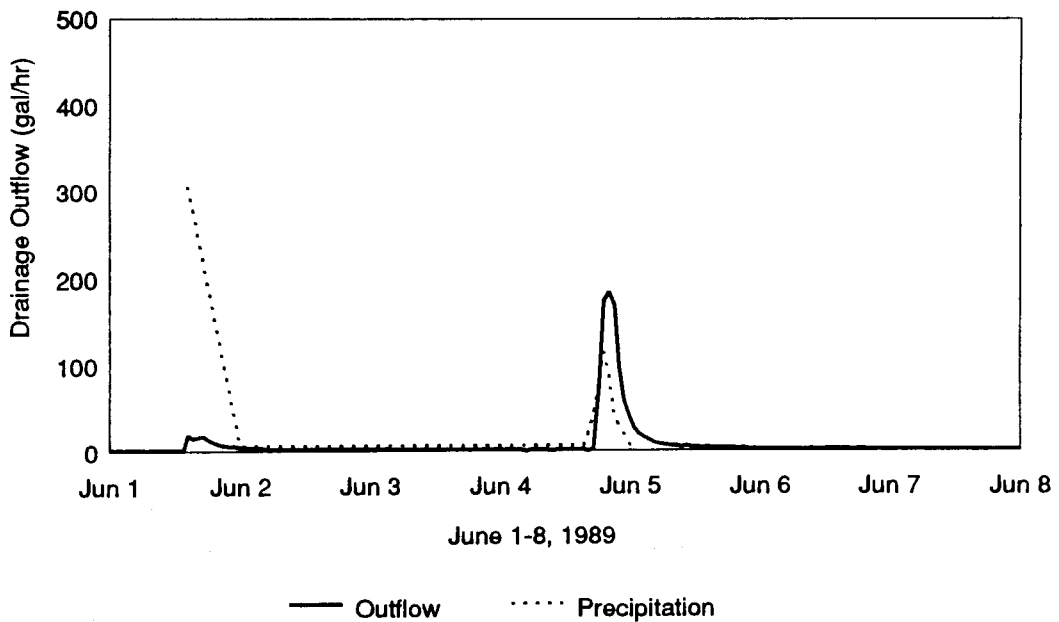
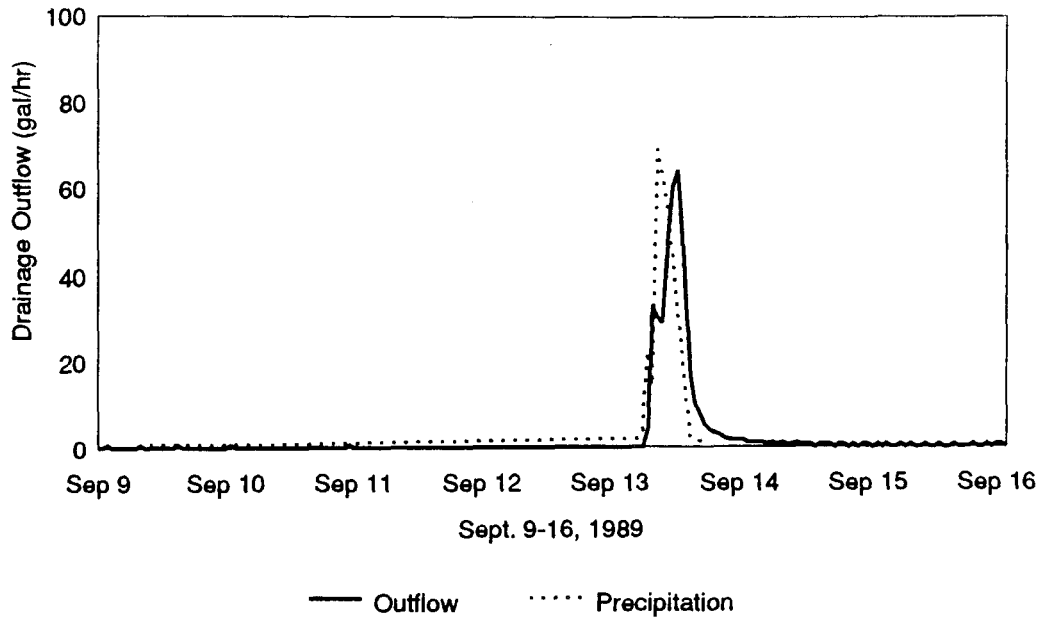


Figure 43: Graphs of Subdrainage Outflow for 40-foot Jointed PCC Test Sections

## Subdrainage Outflow and Precipitation

for 8" CRCP, with edge sealant



## Subdrainage Outflow and Precipitation

for 8" CRCP, no edge sealant

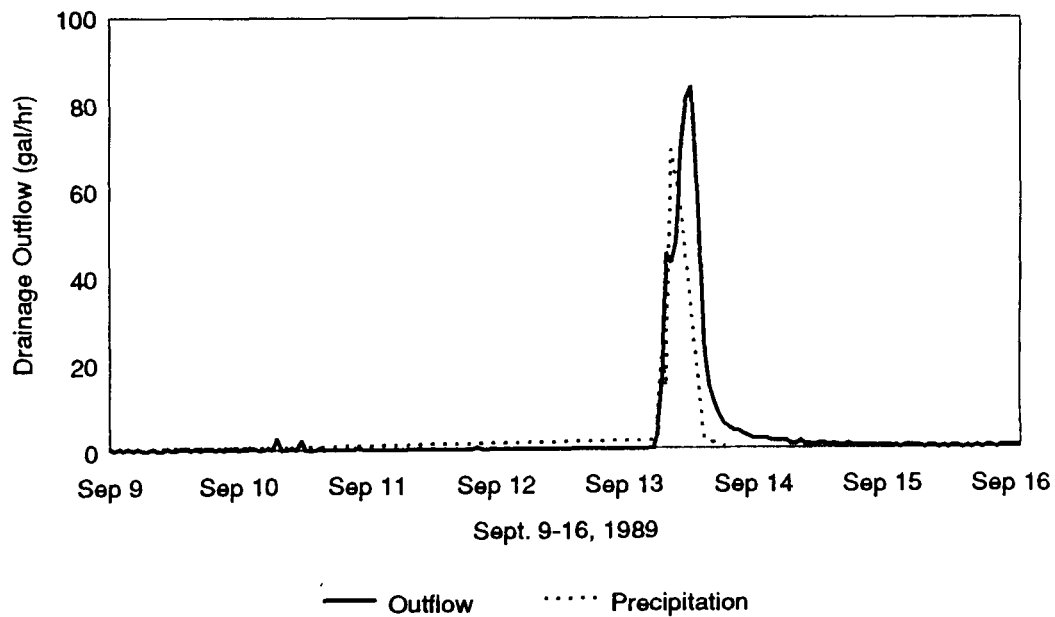
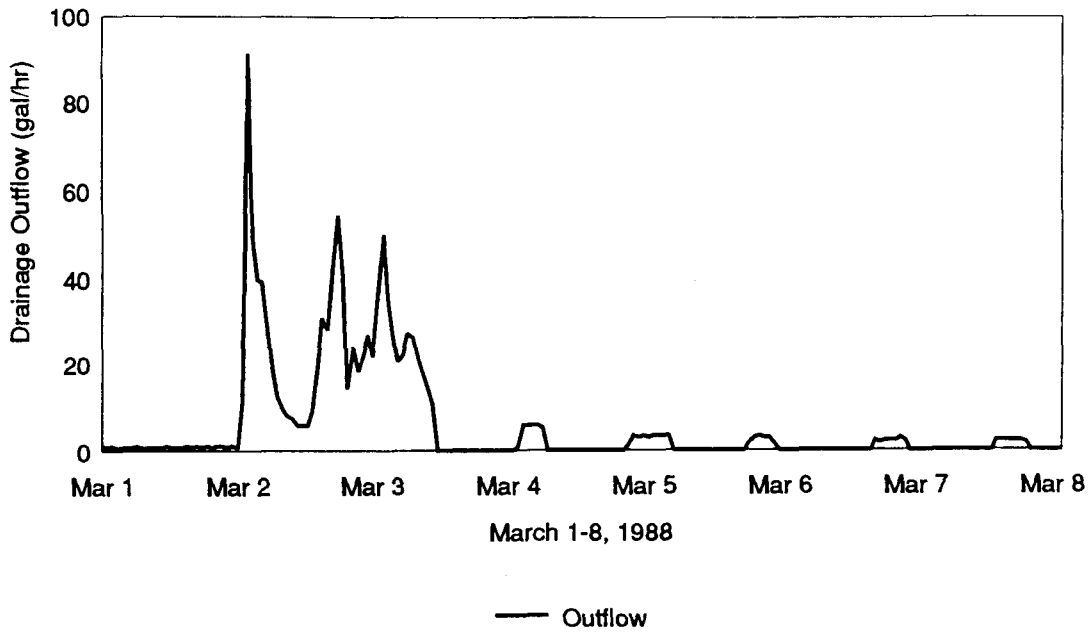


Figure 44: Graphs of Subdrainage Outflow for 8-inch CRCP Test Sections

## Subdrainage Outflow and Precipitation

12.5" Full-Depth AC, (With Lime)



## Subdrainage Outflow and Precipitation

9.5" Full-Depth AC, (Without Lime)

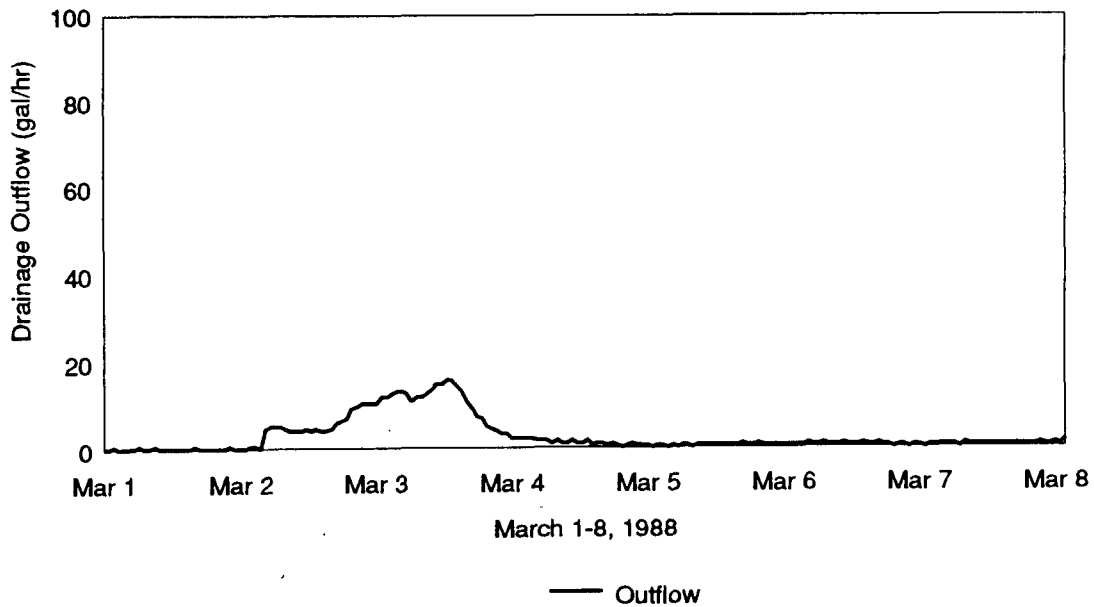


Figure 45: Graphs of Subdrainage Outflow for Full-Depth AC Test Sections

# Moisture Access Tube Installation

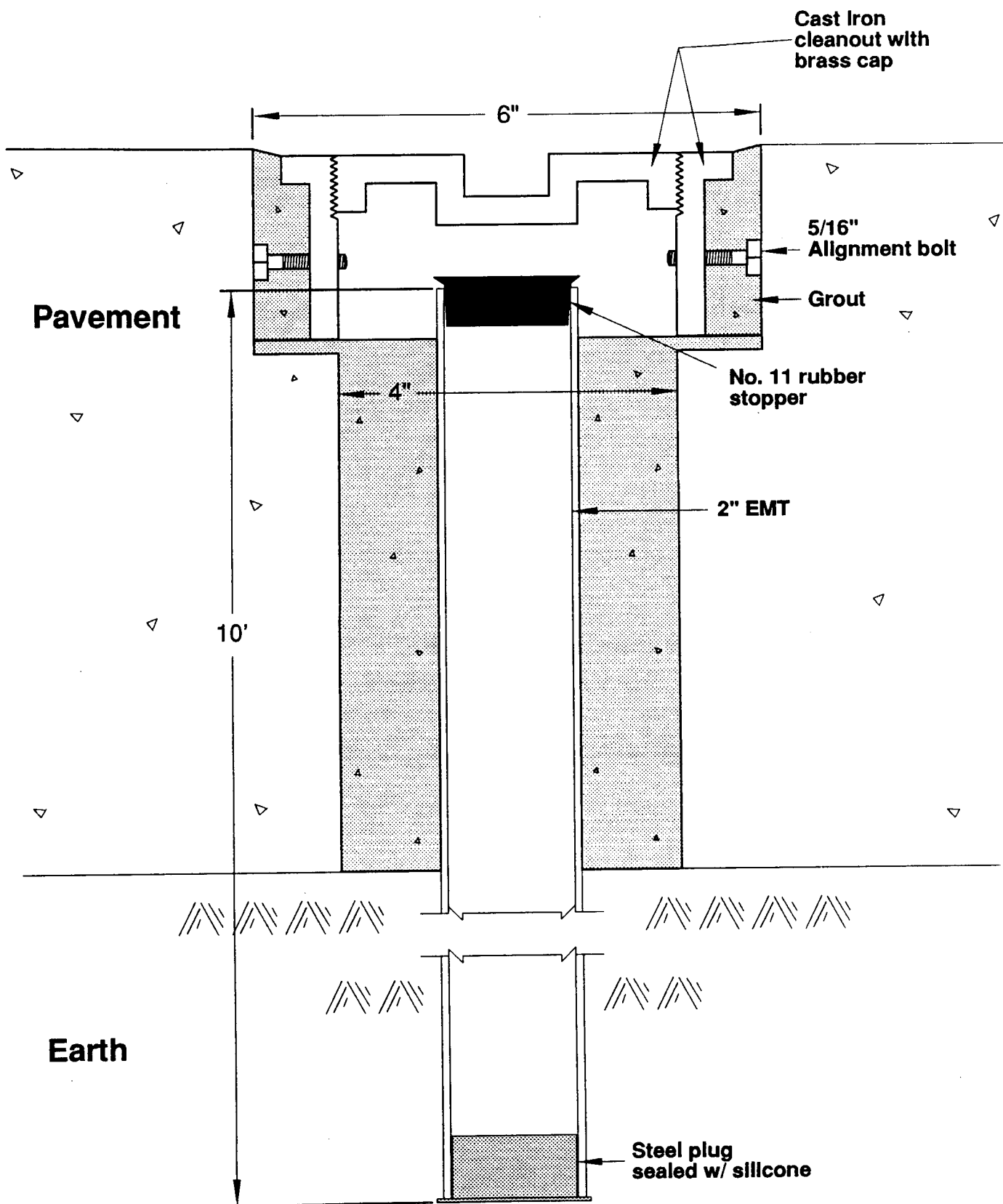


Figure 46: Moisture Access Tube Installation Diagram

### STATION 3416+00 CENTERLINE

8.5" JOINTED (UNDERDRAINS, NOT SEALED)

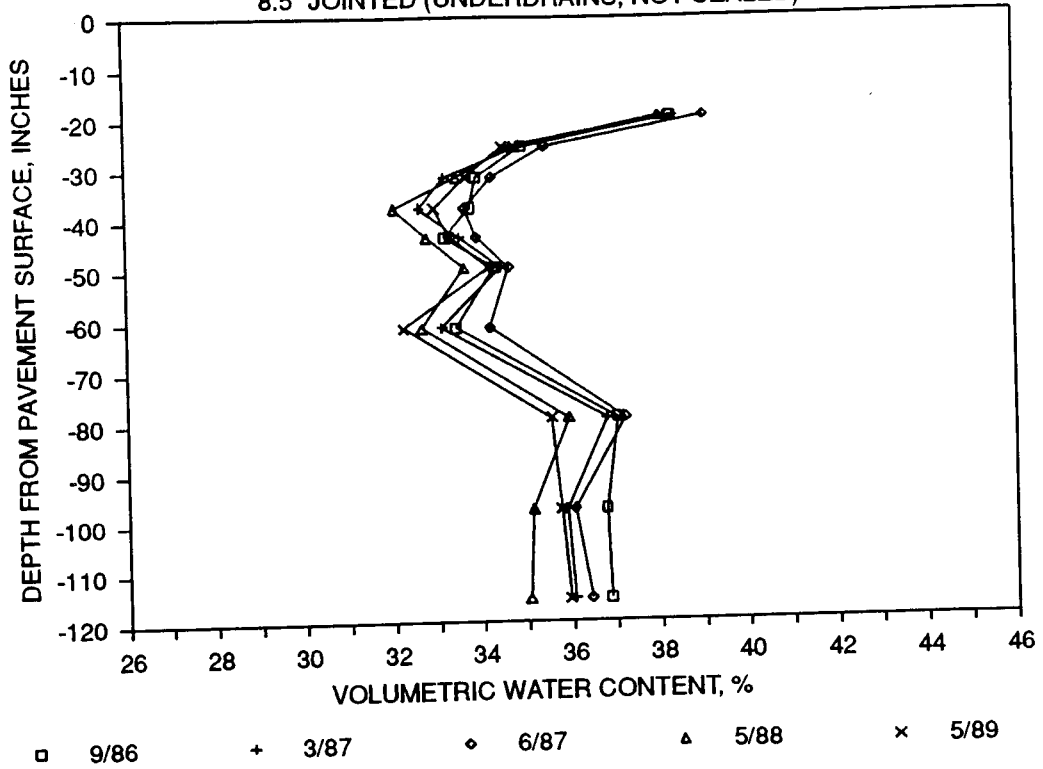


Figure 47A: Centerline Subgrade Moisture Data for Jointed PCC with Underdrains

### STATION 3416+00 OWP

8.5" JOINTED (UNDERDRAINS, NOT SEALED)

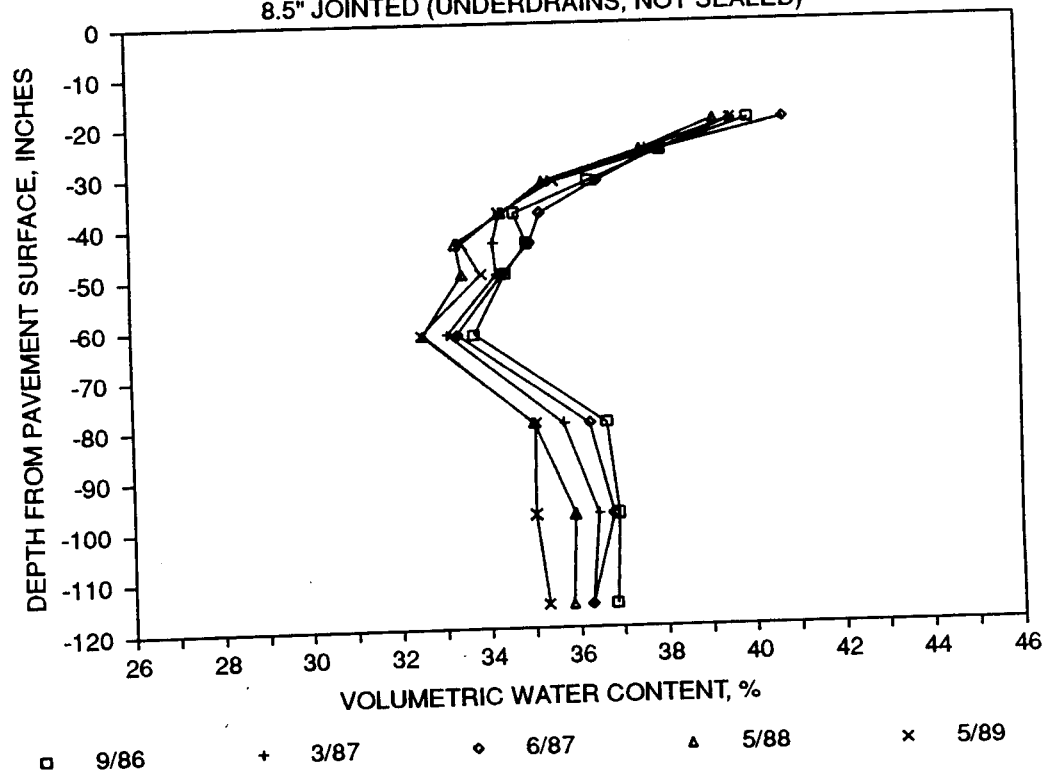


Figure 47B: Outer Wheelpath Subgrade Moisture Data for Jointed PCC with Underdrains



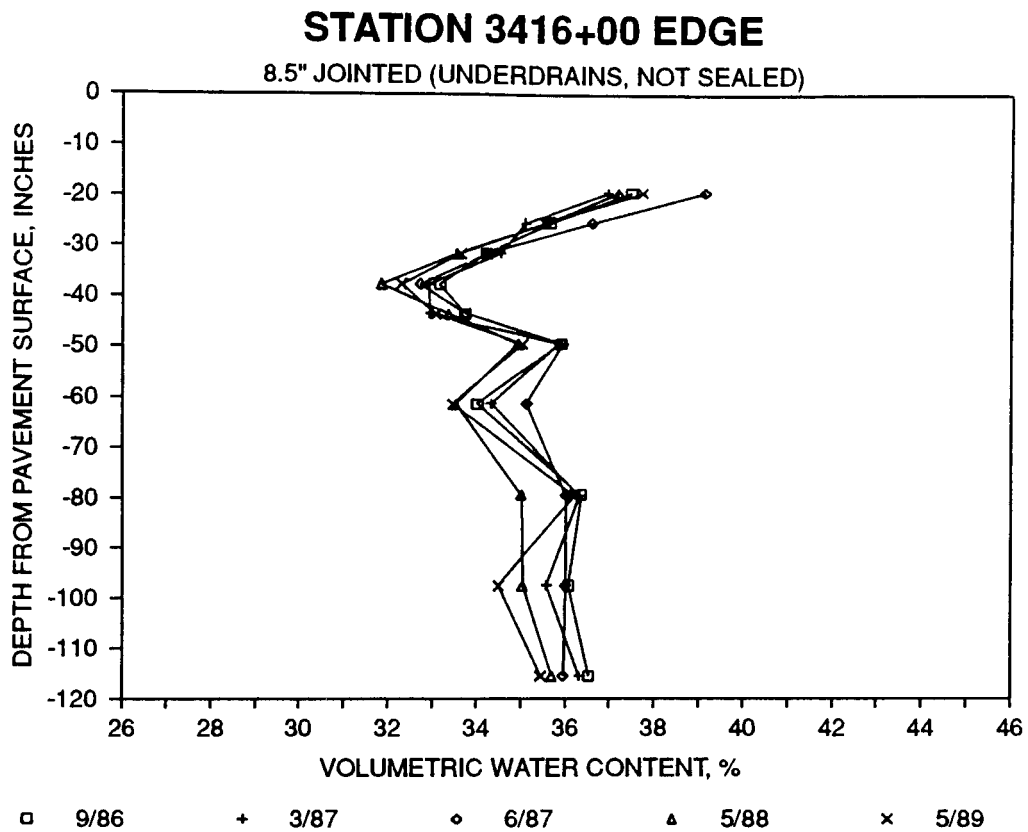


Figure 47C: Edge Subgrade Moisture Data for Jointed PCC with Underdrains

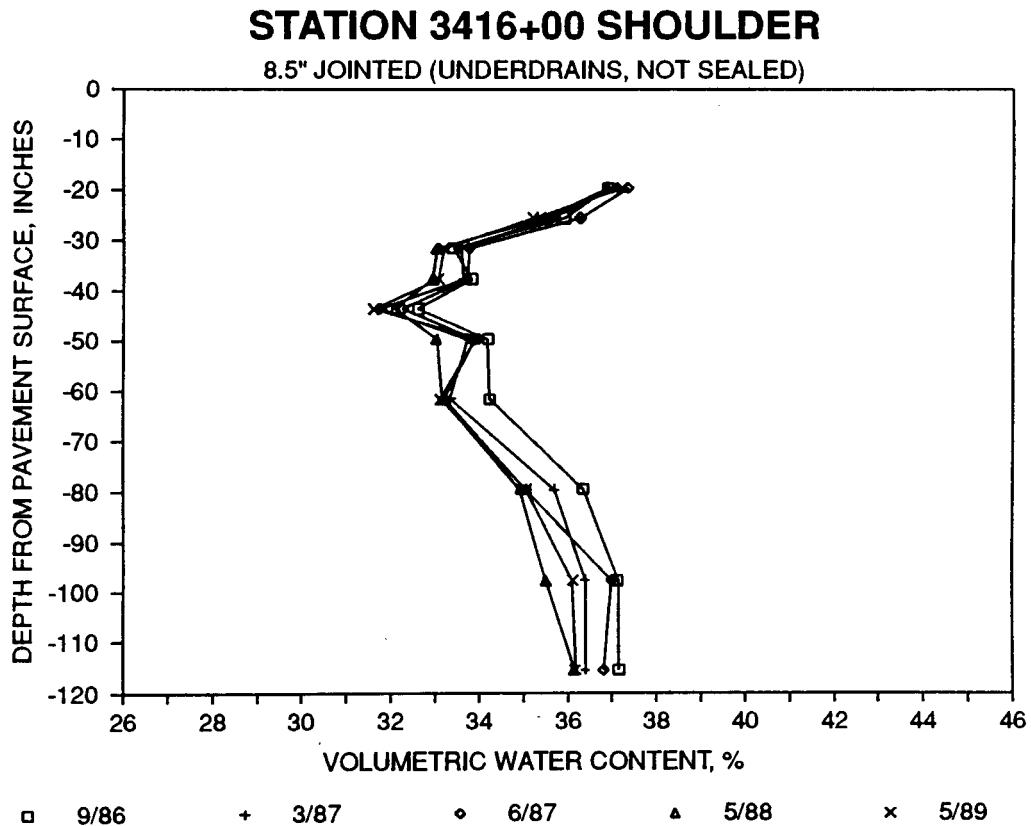


Figure 47D: Shoulder Subgrade Moisture Data for Jointed PCC with Underdrains

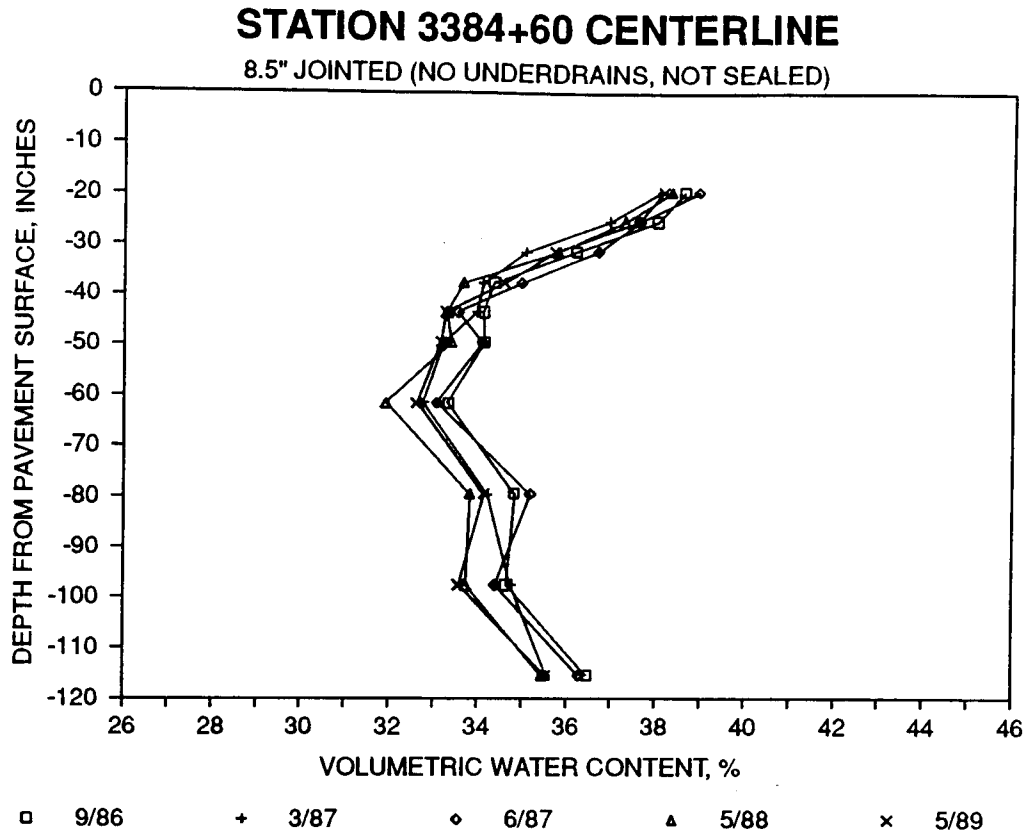


Figure 48A: Centerline Subgrade Moisture Data for Jointed PCC without Underdrains

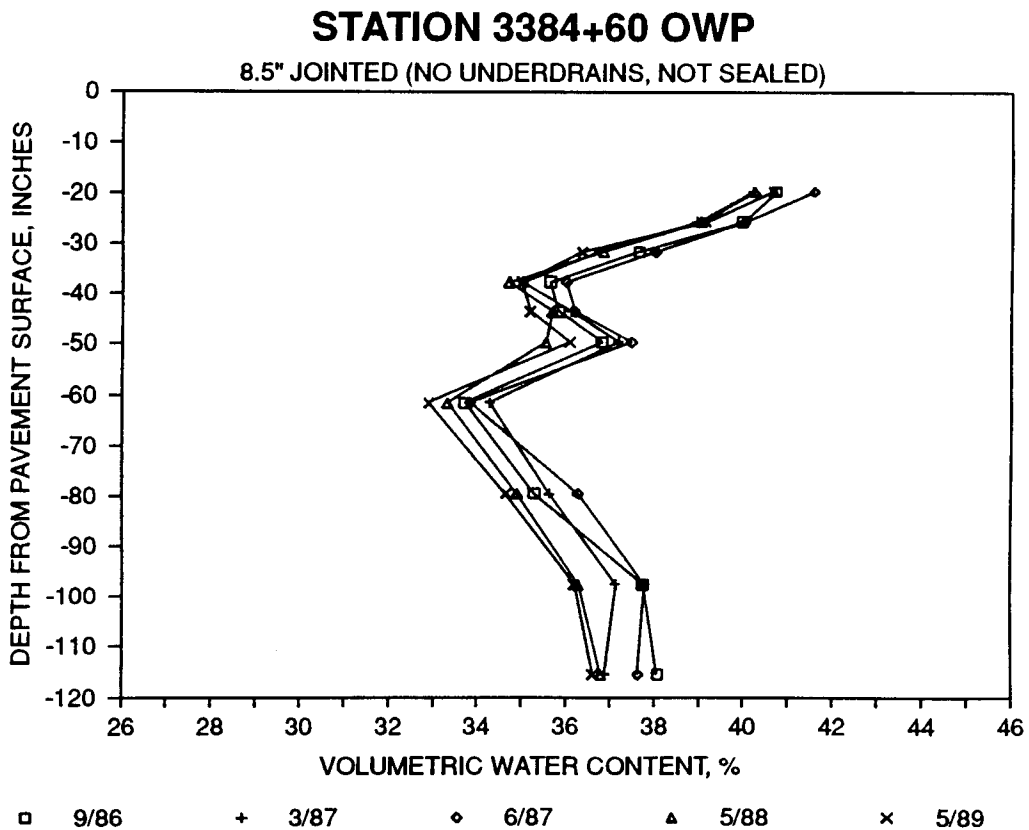


Figure 48B: Outer Wheelpath Subgrade Moisture Data for Jointed PCC without Underdrains

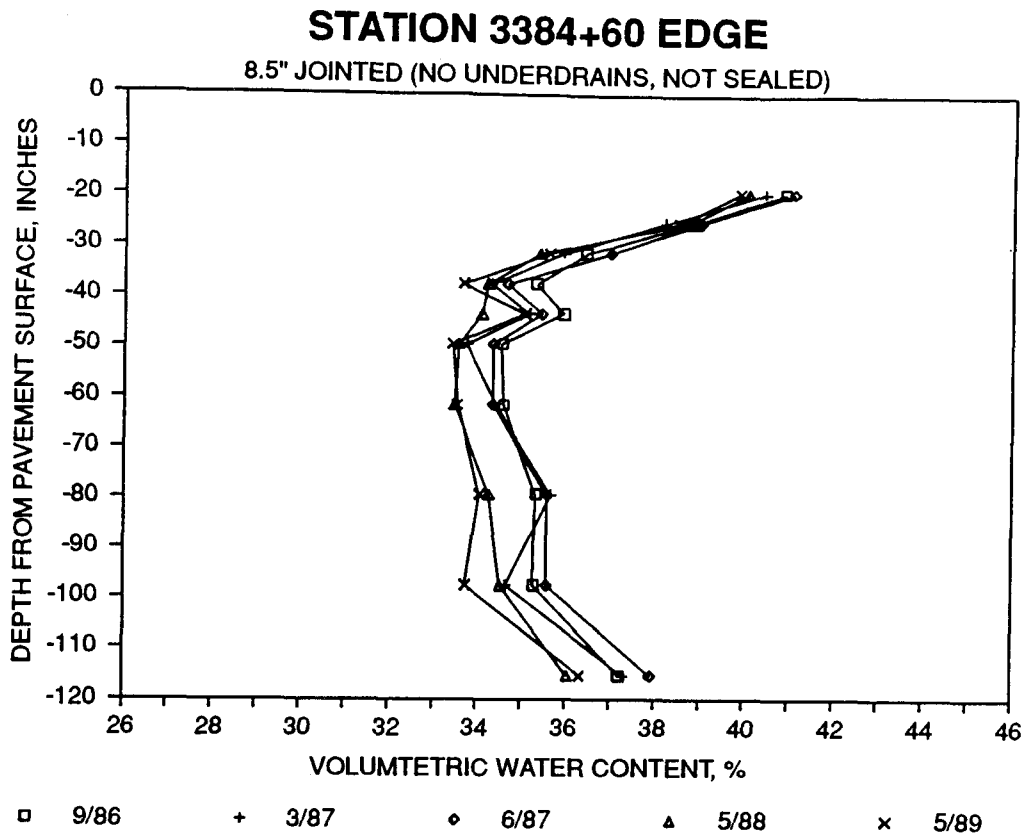


Figure 48C: Edge Subgrade Moisture Data for Jointed PCC without Underdrains

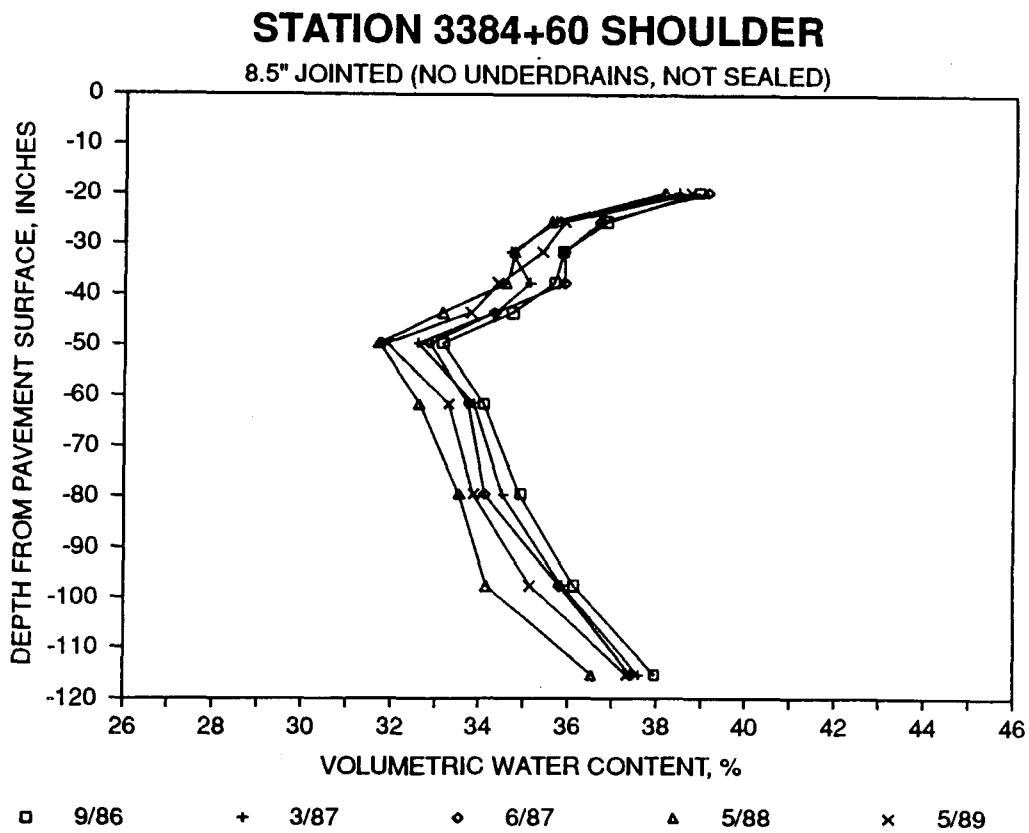
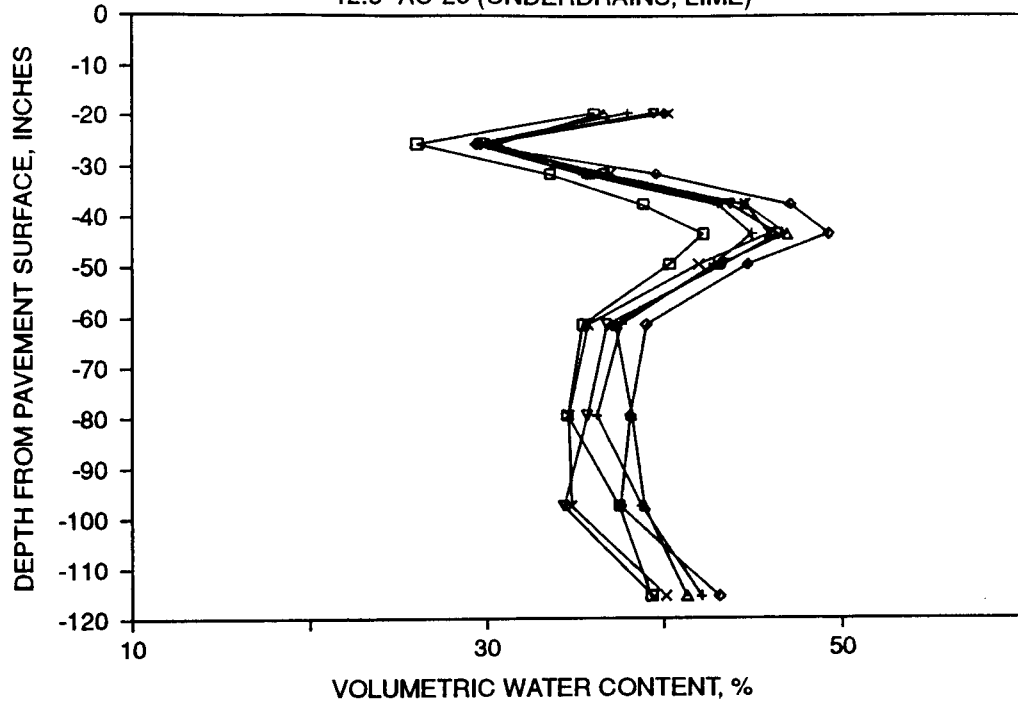


Figure 48D: Shoulder Subgrade Moisture Data for Jointed PCC without Underdrains

### STATION 594+00 IWP

12.5" AC-20 (UNDERDRAINS, LIME)

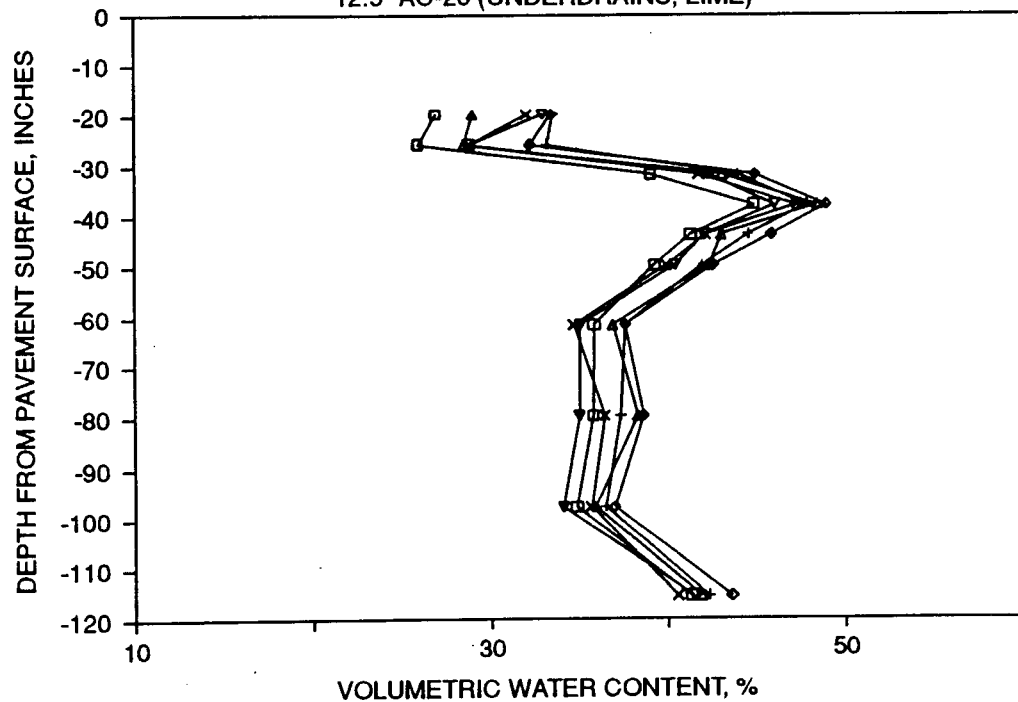


□ 12/86    + 3/87    ◇ 6/87    △ 9/87    × 5/88    ▽ 5/89

Figure 49A: Inner Wheelpath Subgrade Moisture Data for Full-Depth AC with Underdrains

### STATION 594+00 OWP

12.5" AC-20 (UNDERDRAINS, LIME)

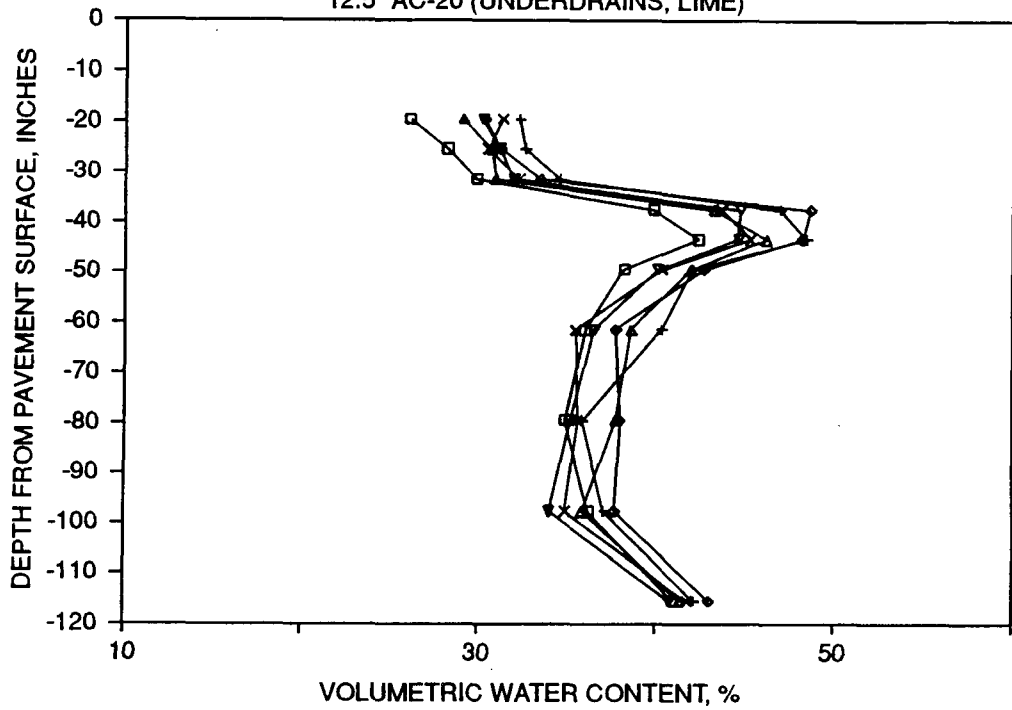


□ 12/86    + 3/87    ◇ 6/87    △ 9/87    × 5/88    ▽ 5/89

Figure 49B: Outer Wheelpath Subgrade Moisture Data for Full-Depth AC with Underdrains

# STATION 594+00 SHOULDER

12.5" AC-20 (UNDERDRAINS, LIME)



□ 12/86      + 3/87      ◊ 6/87      △ 9/87      × 5/88      ▽ 5/89

Figure 49C: Shoulder Subgrade Moisture Data for Full-Depth AC with Underdrains

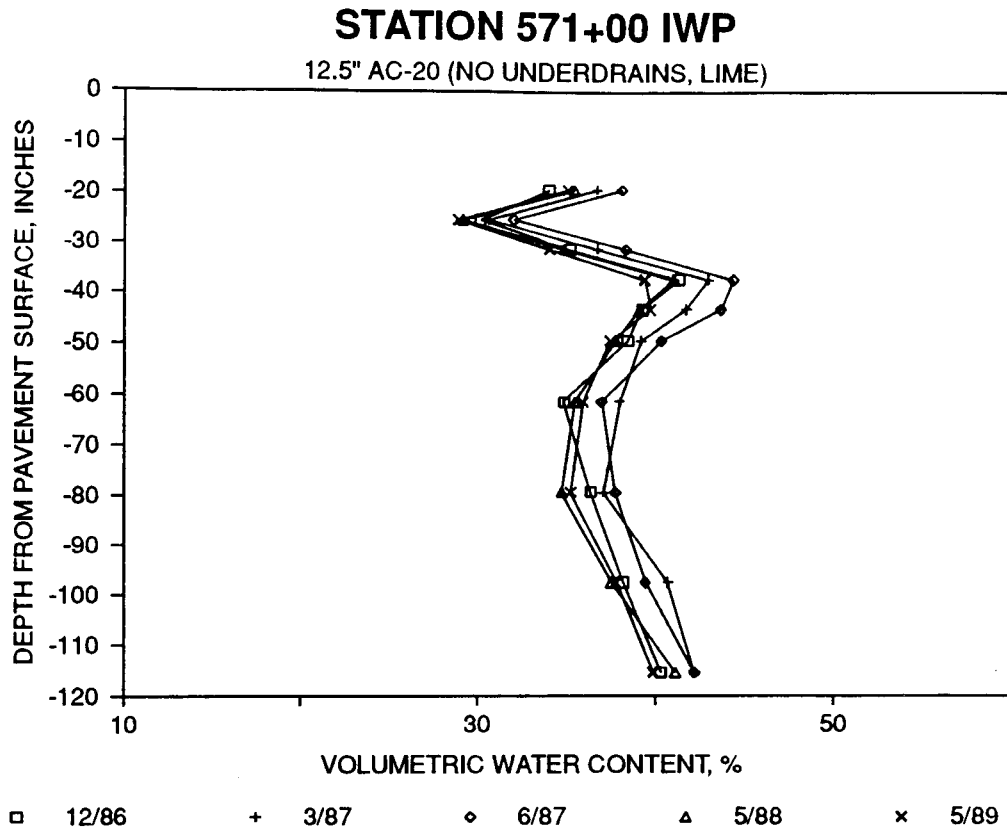


Figure 50A: Inner Wheelpath Subgrade Moisture Data for Full-Depth AC without Underdrains

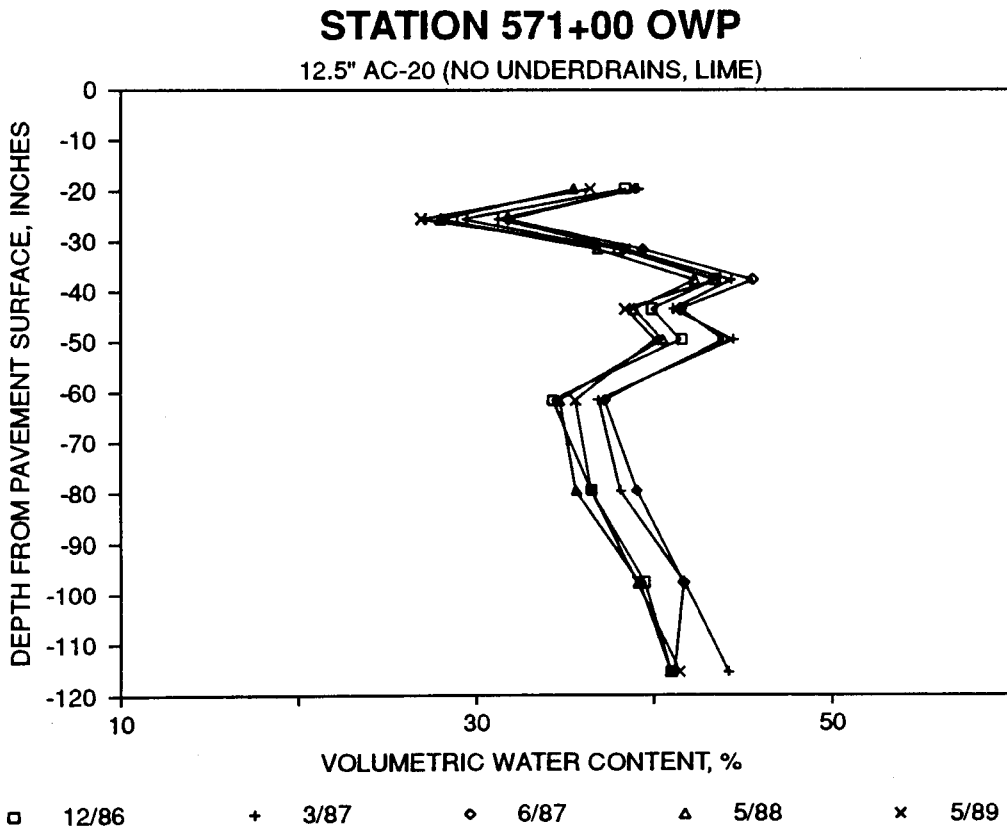


Figure 50B: Outer Wheelpath Subgrade Moisture Data for Full-Depth AC without Underdrains

# STATION 571+00 SHOULDER

12.5" AC-20 (NO UNDERDRAINS, LIME)

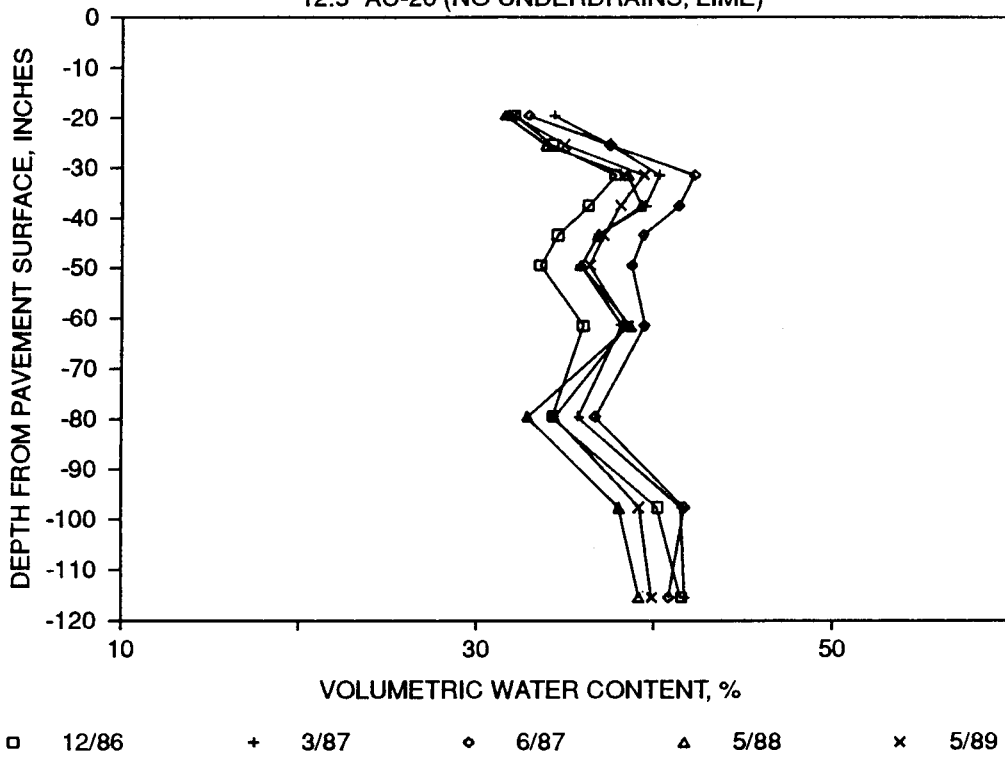


Figure 50C: Shoulder Subgrade Moisture Data for Full-Depth AC without Underdrains

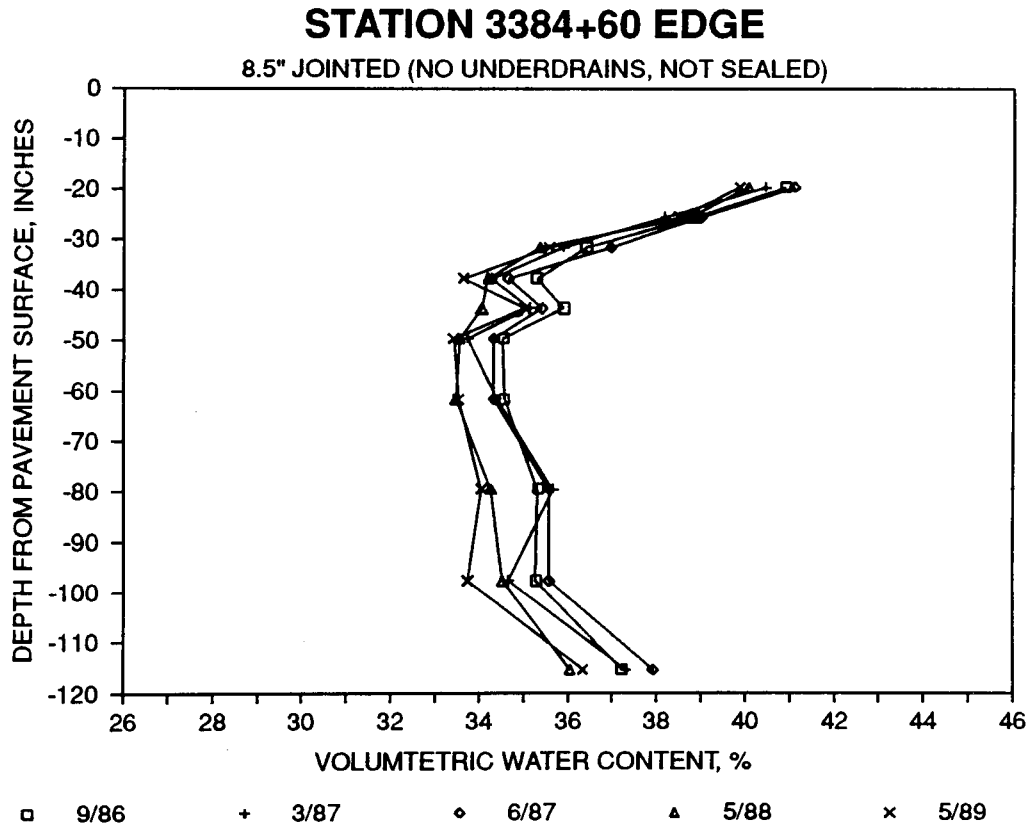
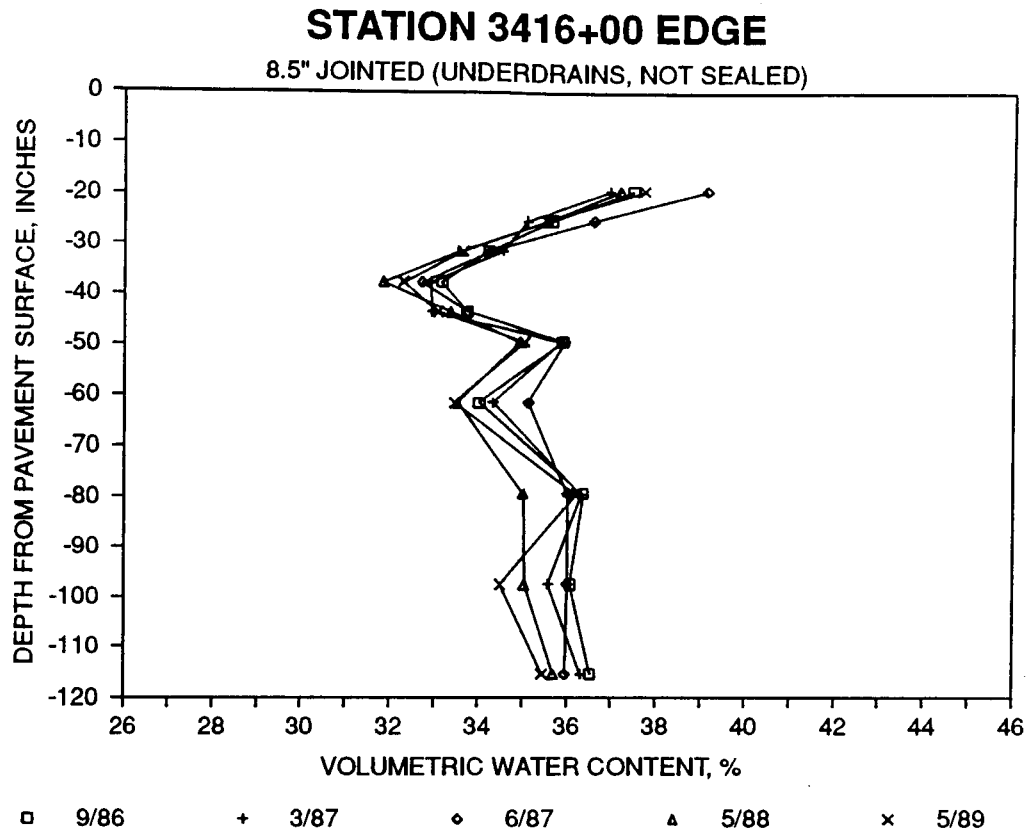
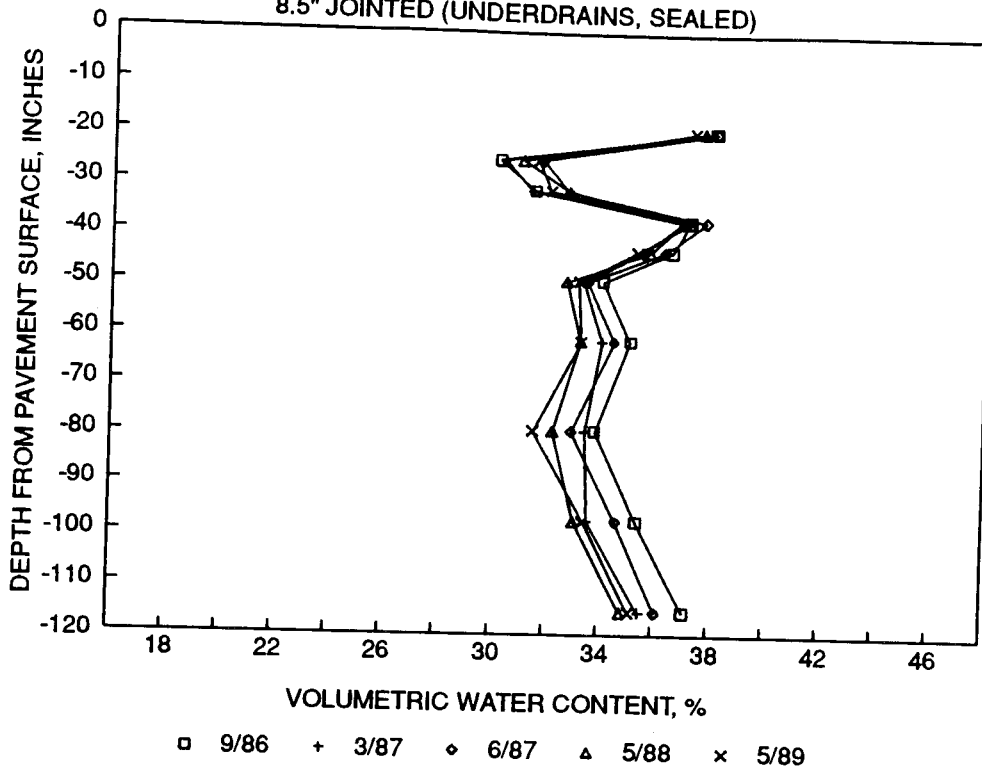


Figure 51: Subgrade Moisture Data Comparison of Unsealed Jointed PCC with and without Underdrain



### STATION 3404+00 EDGE

8.5" JOINTED (UNDERDRAINS, SEALED)



### STATION 3393+00 EDGE

8.5" JOINTED (NO UNDERDRAINS, SEALED)

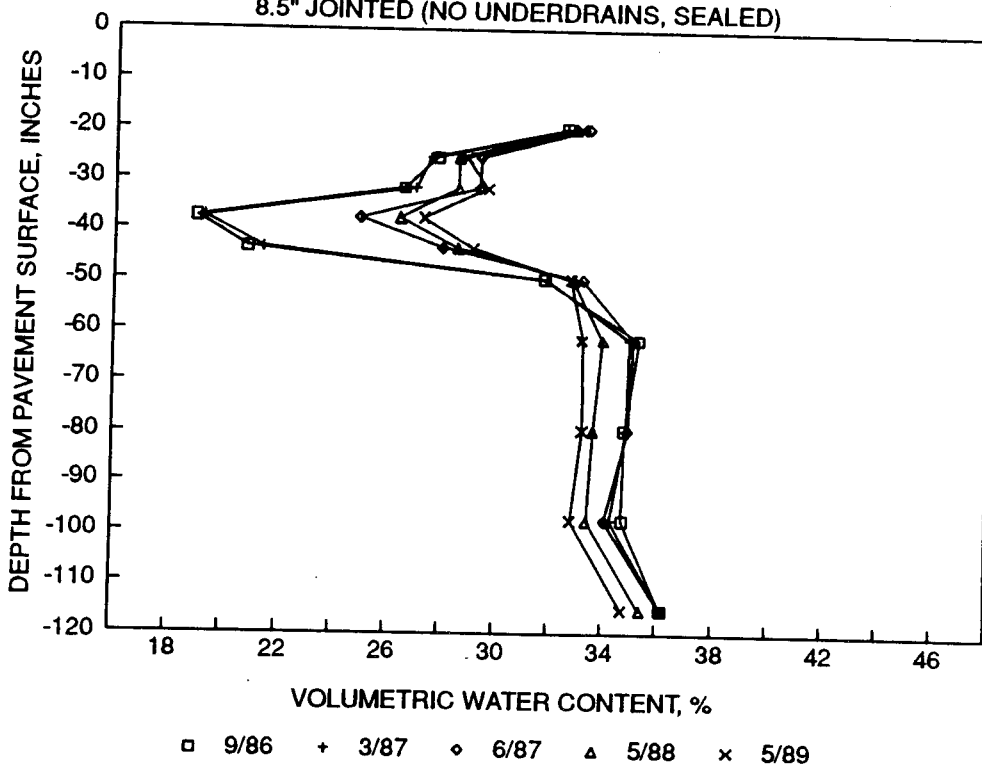
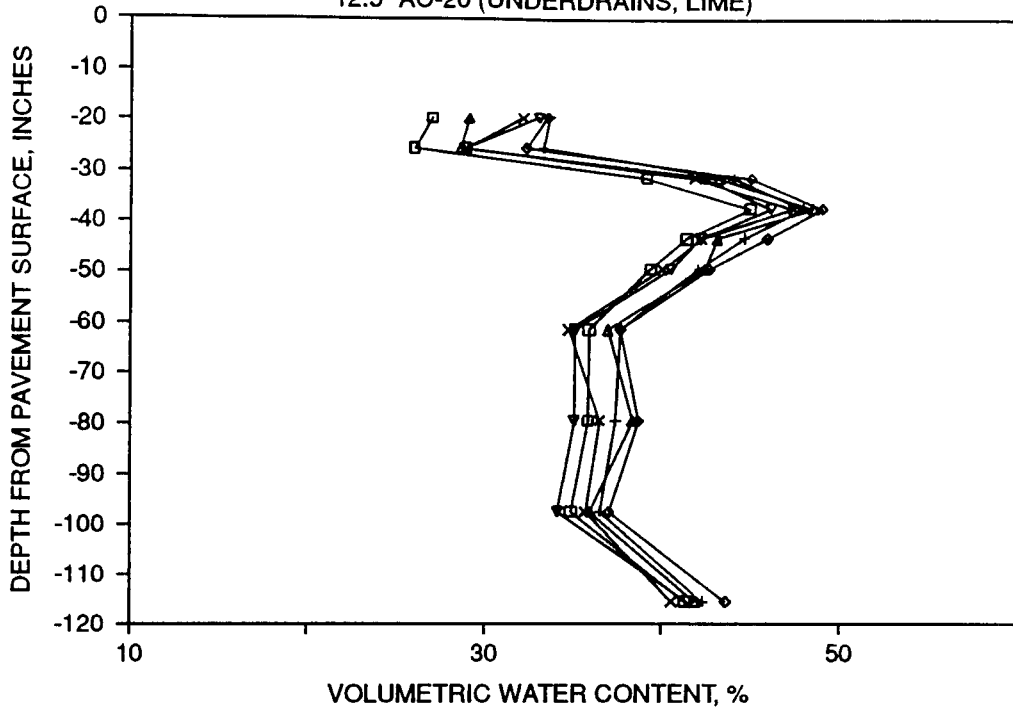


Figure 52: Subgrade Moisture Data Comparison of Sealed Jointed PCC with and without Underdrains

### STATION 594+00 OWP

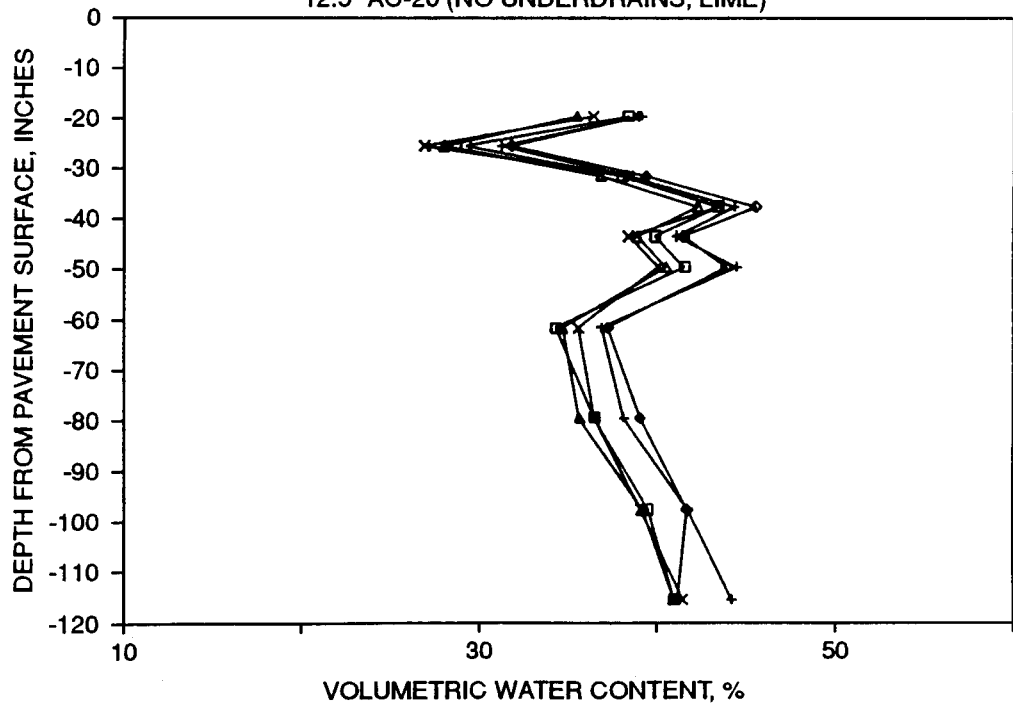
12.5" AC-20 (UNDERDRAINS, LIME)



□ 12/86    + 3/87    ◇ 6/87    △ 9/87    × 5/88    ▽ 5/89

### STATION 571+00 OWP

12.5" AC-20 (NO UNDERDRAINS, LIME)

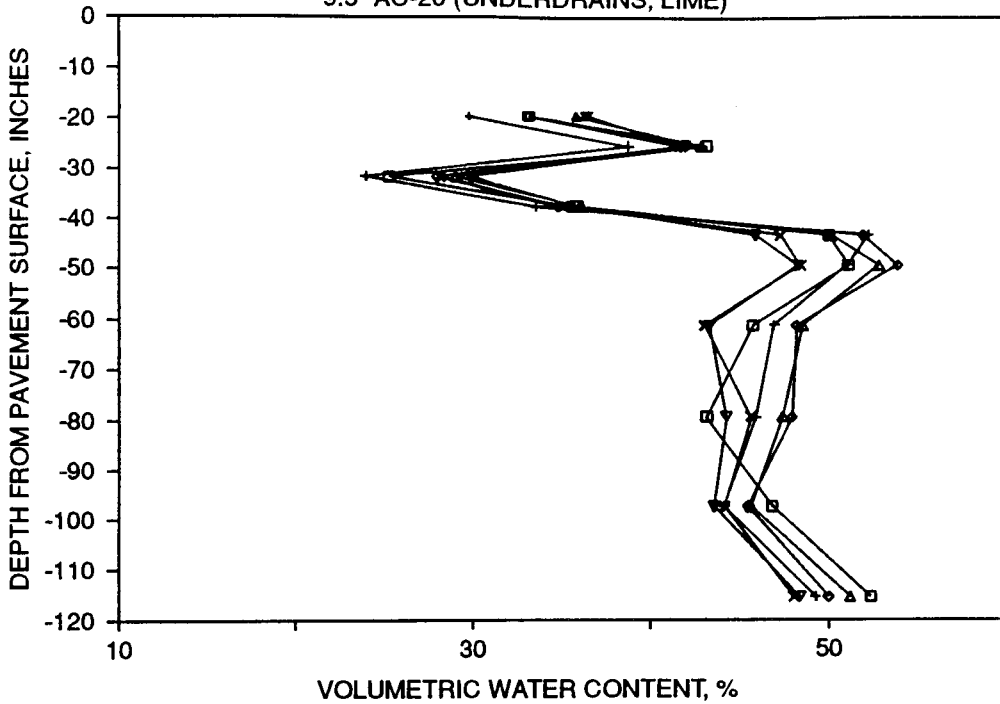


□ 12/86    + 3/87    ◇ 6/87    △ 5/88    × 5/89

Figure 53: Subgrade Moisture Data Comparison for 12.5-inch Full-Depth AC with and without Underdrains

### STATION 2551+00 OWP

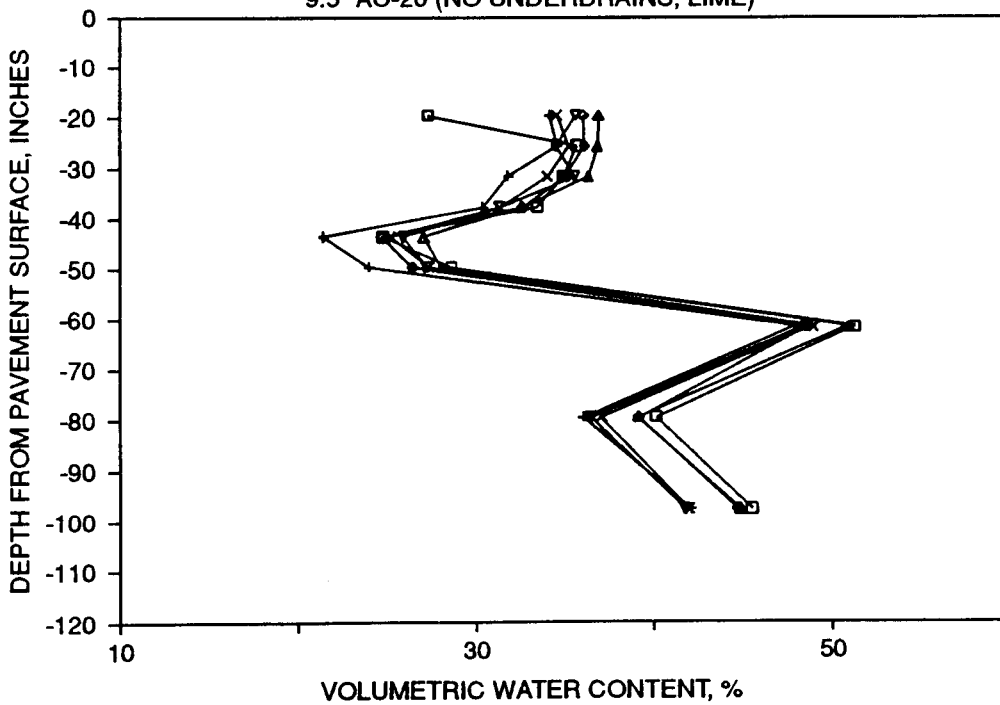
9.5" AC-20 (UNDERDRAINS, LIME)



□ 9/86    + 12/86    ◊ 3/87    △ 6/87    × 5/88    ▽ 5/89

### STATION 2560+00 OWP

9.5" AC-20 (NO UNDERDRAINS, LIME)



□ 9/86    + 12/86    ◊ 3/87    △ 6/87    × 5/88    ▽ 5/89

Figure 54: Subgrade Moisture Data Comparison for 9.5-inch Full-Depth AC with and without Underdrains

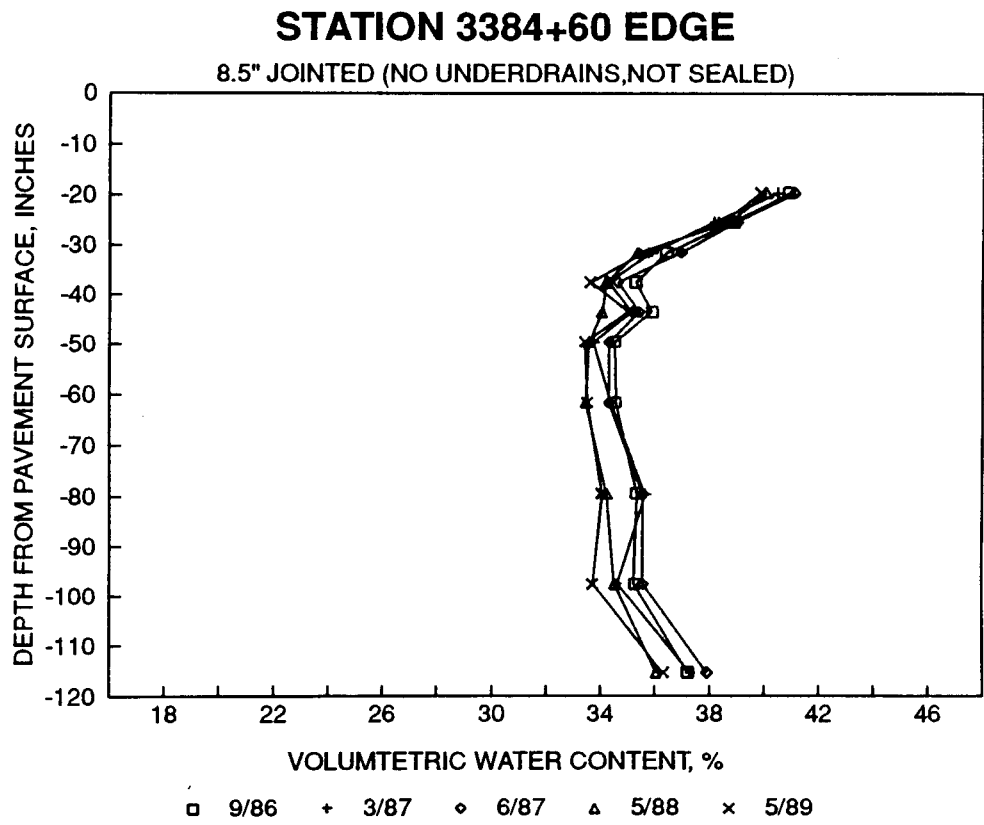
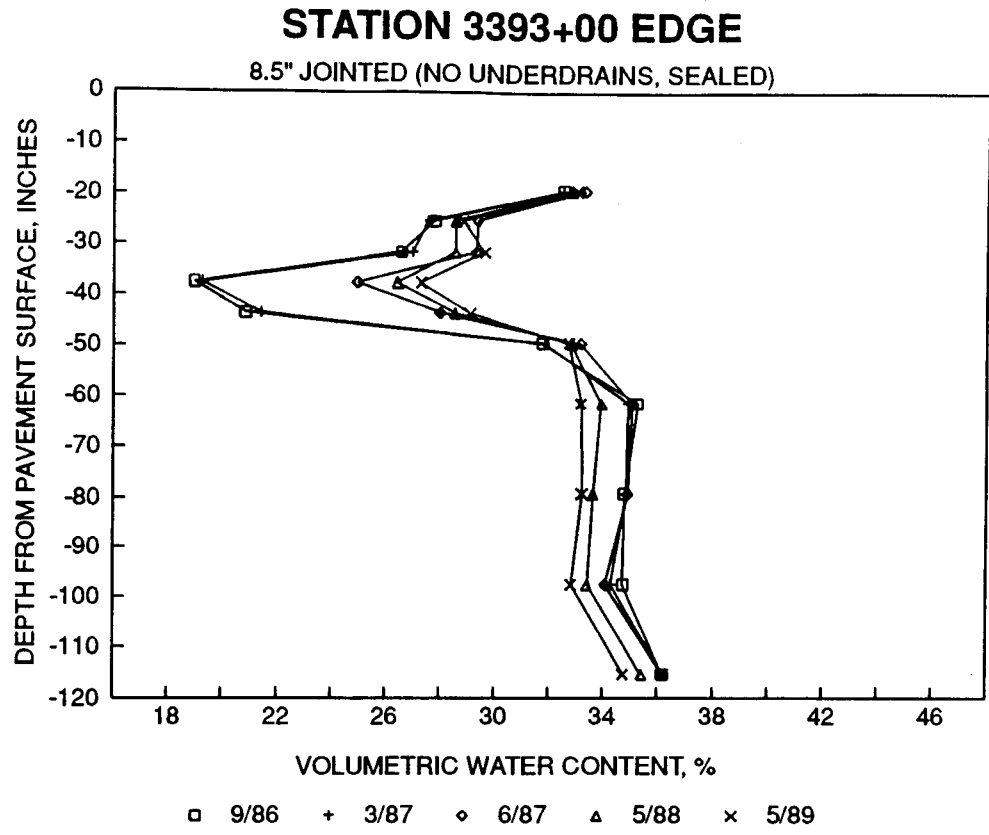


Figure 55: Effect of Sealant on Subgrade Moisture for Jointed PCC without Underdrain

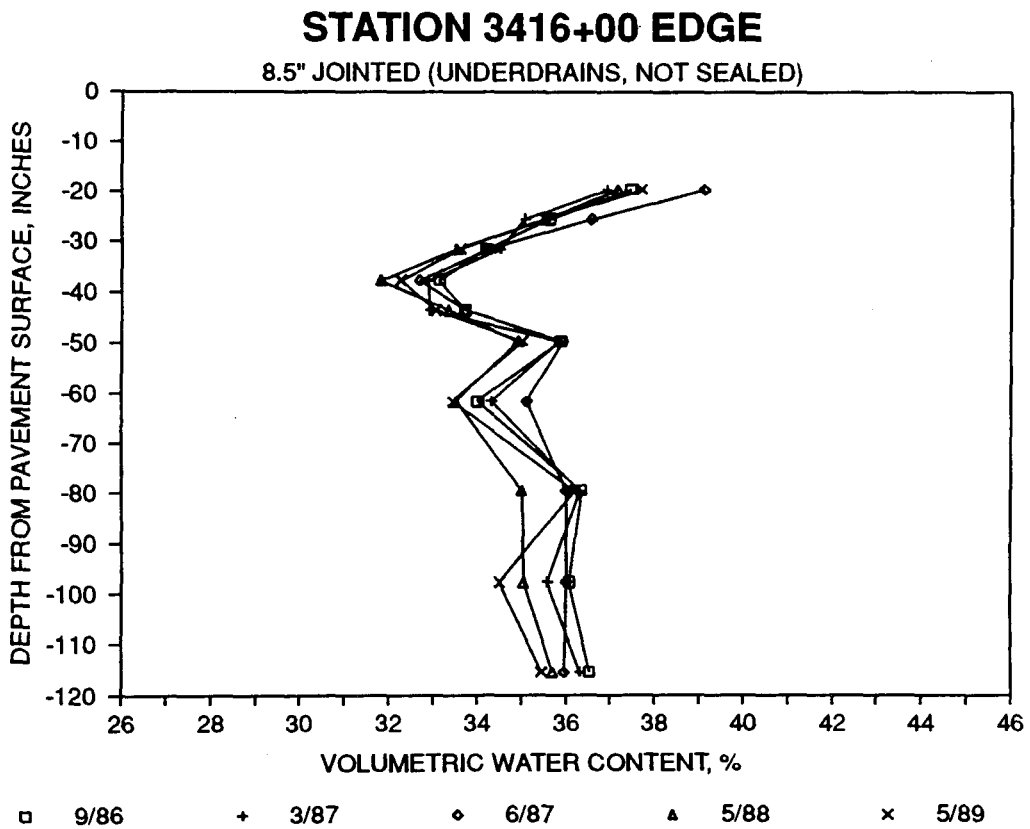
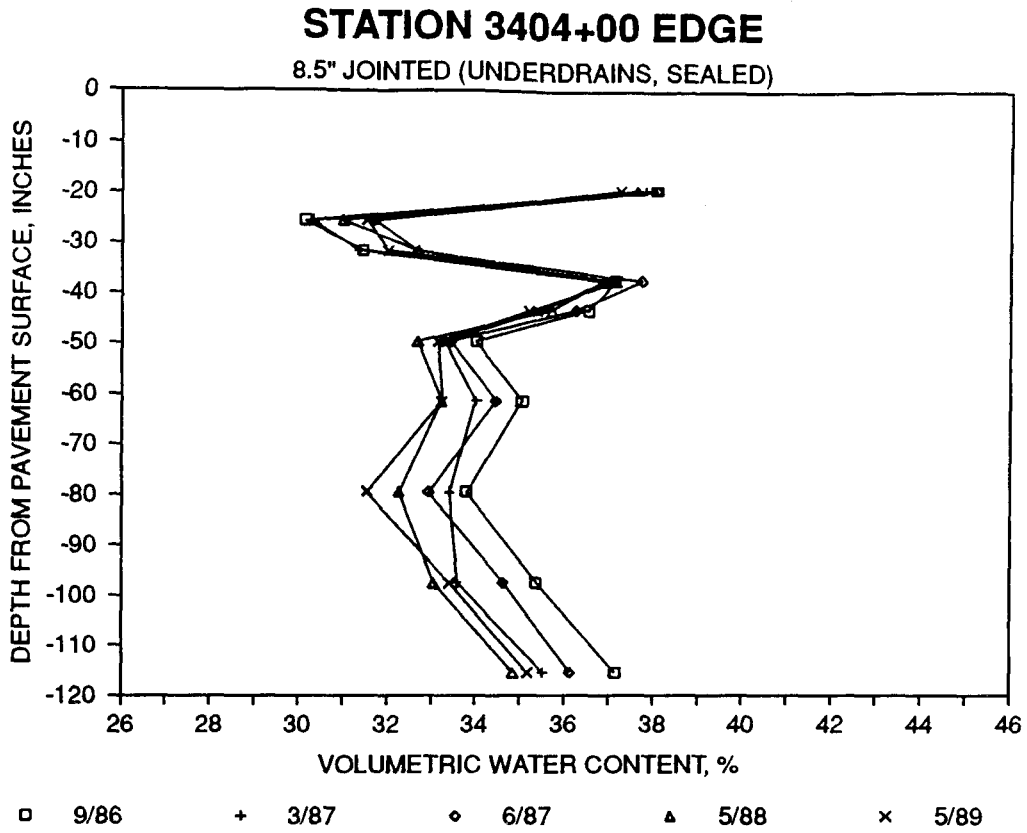


Figure 56: Effects of Sealant on Subgrade Moisture for Jointed PCC with Underdrains

# Frost Gauge Installation

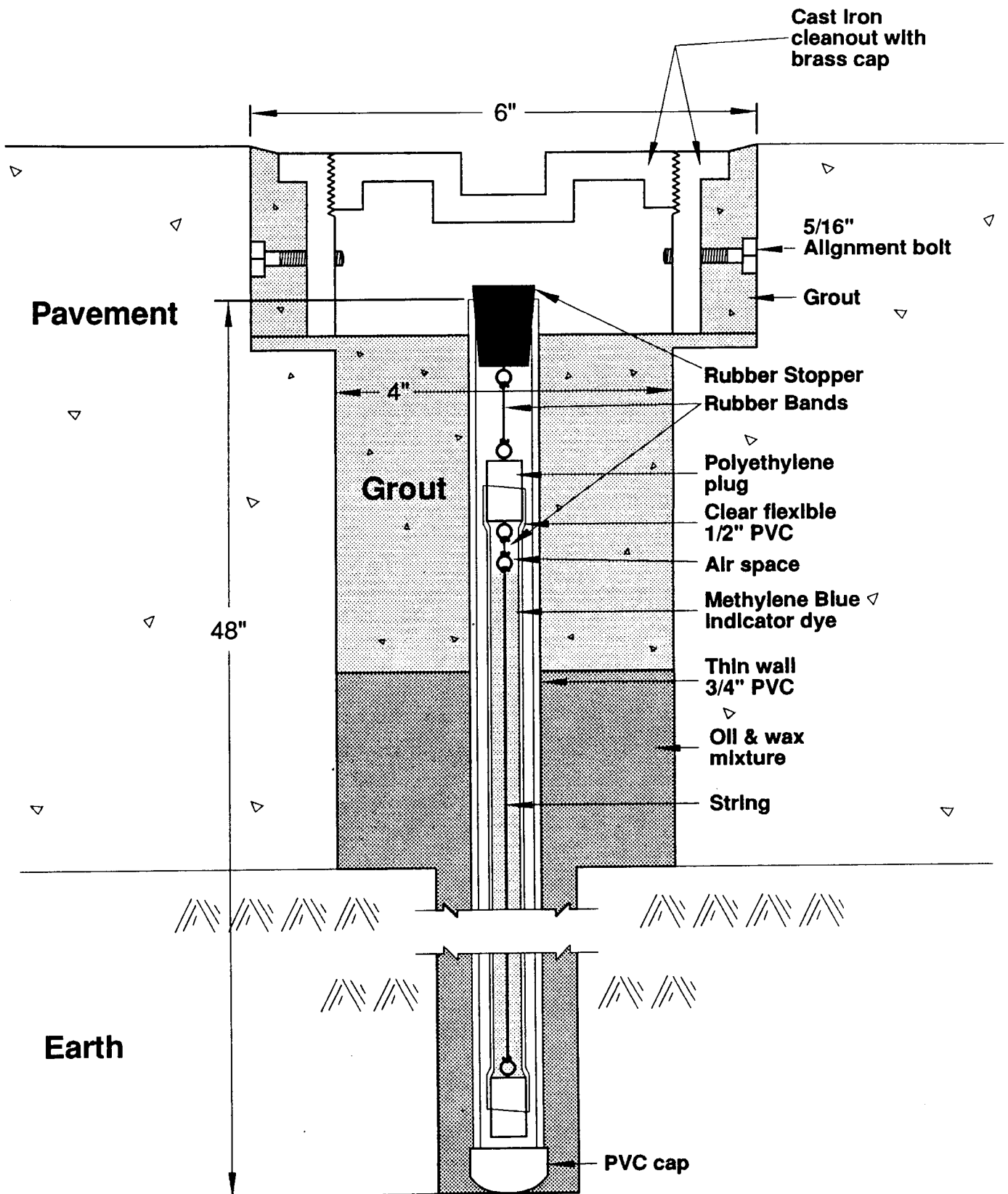


Figure 57: Frost Gauge Installation Diagram